Assessment of Products of Different Thermochemical Processing from Anaerobic Digestion Waste

Nidia Diaz Perez

BSc, MSc

Thesis submitted to the University of Nottingham for the degree of Doctor of Philosophy

February 2022

STORY OF THE PROJECT

Dear reader,

Nidia has asked me to contribute a few words to her thesis explaining some of the journey we have been on whilst she has completed the work you are now reading. I work for Severn Trent Water, we treat c 8 million customers wastewater across the Midlands and into Wales. Our challenges in terms of finding the right balance between cost, environmental improvement and community support are huge and so it is always a pleasure to support any academic work that can help us to deliver on many of these outcomes.

What is much rarer is to get a phone call from a student actively seeking a chance to get involved, and rarer still is for that master's student to engage so much with the process that she goes on to complete a PhD in the same subject area with such passion and engagement.

I still remember the first call I had with Nidia back in 2016. A colleague and I had been asked to come up with a few options for a short master's study that would offer some direct benefit to the way we worked and to see if these fitted with the ambition / intent of the student we would be introduced to. The whole suite of advanced conversion technologies (ACTs) has long been a challenge for the wastewater industry, if we can achieve it, it will be a revolutionary change to the way we work and so I picked a discrete, largely literature-based review of the current ACT market as probably the most complex opportunity we had.

When Nidia came on the call I was immediately impressed by her direct ambition to change things. Very no nonsense and very definitely wanting to change the way things are done for the better. With hindsight, I am not surprised she went for the biggest challenge we had. Her passion and commitment for change were immediately clear and so I had no concerns about offering her the opportunity, the only concerns were about my ability to keep up!

Over the course of that first year, I was impressed with her approach to solving the problem. Keen to get to our sites and understand what we do first-hand and eager to learn from everyone and anyone who was there from operator through to manager. Genuinely interested in the subject matter and passionate about changing the way we work, Nidia was always increasing her knowledge and is willing to share with others.

The outputs of the first year definitely exceeded my expectations, her master's report was thorough and included many areas of the reaction kinetics and engineering science that I had not expected her to complete so quickly. It was clear from our conversations that this wouldn't be the end of her passion for the subject and I was not surprised when she was able to find funding and opportunity to grow the initial subject into this thesis.

I am always impressed by Nidia's approach to her work and the way that she always works and even fights through problems to go after what she wants. Her tenacity and passion are incredible. Where challenge has been put in front of her, she has found ways to move around it, remain focussed and go after her goals.

During her later studies, I have been incredibly impressed by the quality of experimental data, insight and opportunity she has produced. The work contained in this thesis far exceeds my own knowledge in terms of the reaction process, the key parameters for operation and the potential products being recovered. What I do know is that, at each stage, Nidia has kept me involved and engaged as an industrial advisor and it has helped me to grow my own knowledge of this particular subject and why it may or may not work for us in the future. She has an ability to show how the theory applies in practice and how the opportunity for any situation can be grown with the right dedication and drive. This is a very rare skill.

What will not be contained in this thesis, is the personal commitment, challenge and drive to deliver that Nidia has had to find to work in multiple countries on a foreign continent through a pandemic. She has pushed herself incredibly hard to deliver, is her own toughest critic and has had to work through many personal challenges to ensure that she has delivered the high-quality output that you are reading. This is definitely a work of great dedication.

Over the past 5 years I have always enjoyed my trips to the University to discuss the growth of the PhD, the work that is being done and to hear the next challenge that she is going to take on. Her passion for the subject is infectious, and whilst we have not uncovered the revolutionary idea that we may have hoped for originally, my knowledge has grown on how we need to develop the technology. I think the industry will find the outputs incredibly beneficial and I am sure she has created more opportunity for subsequent work to review biorefinery options and products.

I am sure that Nidia will not stop here and will find new opportunities for herself around the engineering industry. It has been my privilege to support her work over the past few years and I can only hope that in some small way I have contributed to her substantial development.

Simon Farris

Bioresources Strategy & Commercial Lead

Severn Trent Water

ACKNOWLEDGMENTS

This thesis represents a dream of mine since 2012, when my experience working with a company that designed wastewater treatment plants in Mexico taught me how waste could be used to produce energy through anaerobic digestion. Since then, my main goal has been to conduct a project to improve this system. However, this project would have never happened without the following people, to whom I would like to express my sincere gratitude:

Dr John Robinson, who became my main supervisor in 2018 and never hesitated to support my research.

A very special thank you to Simon Farris. He was the first person in the United Kingdom who believed in this idea and gave me the opportunity to develop a new research project from scratch at the university. He was always willing to support this project, which allowed me to continue my career in waste valorisation.

Keith Barnes for his support during waste collection and his help in understanding his duties regarding the anaerobic digestion process to keep the system running in the most optimal conditions.

Andrea Garduno and Joseph Meehan for organising and coordinate trips to the sites for safe sample collection.

To Dr Emily Kostas and Dr Daniel Beneroso, who were my main support when I first had this idea and were always there for me.

Dr Ben van den Broek and his colleagues, for all the support during my visit to the Wageningen Research Institute, and the full training to understand more about biomass characterisation and constant discussions on this topic.

Christian Lindfors, Elmeri Pienihäkkinen and Joona Lahtinen, who were the team at the Technical Research Centre of Finland in charge of the fast pyrolysis system, for supporting me during my visit and letting me learn from their experience.

Finally, my beloved parents, who are always there for me, even though we are in different countries. They have always made me feel that it is worth being far from home to achieve new projects in life.

ABSTRACT

Anaerobic digestion (AD) is widely used to treat low-value organic waste to produce a methane-rich biogas for bioenergy generation. Although it has positive sustainability credentials due to its ability to convert waste to energy, only a relatively small amount of waste fed into AD is converted into biogas, resulting in a large amount of residual solid waste known as digestate. This residue can be used as fertiliser, but only if meets strict regulations for spreading on soil. Characterisation of the waste generated in AD systems was carried out in this research, which led to the primary hypothesis that digestate has the potential to produce more valuable bioproducts if pyrolysis technologies are used in conjunction with AD.

Three different pyrolysis were assessed to transform digestate into bio-based products. Fast pyrolysis was studied in collaboration with VTT in Espoo, Finland. Slow pyrolysis and microwave pyrolysis were studied using the available facilities at the University of Nottingham.

Considerable differences were found in pyrolysis products from digestate between these three technologies. Slow pyrolysis at operating temperatures between 355-530ºC resulted in bio-oil yields of 34-46% and with a large amount of water ranging from 13-19% wt. This pyrolytic liquid was a high-acid product where primary compounds from cellulose and hemicellulose, such as levoglucosan and furfural, were not detected. These results revealed that secondary reactions occurred due to the high ash content. Acetic acid was the most prevalent compound quantified with a significant variation between bio-oil samples analysed. This indicated that ash content in digestate was different in each experiment performed, affecting the subsequent chemical composition of the product.

Fast pyrolysis of digestate performed at 460-560ºC produced bio-oils with less water (8-11% wt), but with a high-acid concentration. Sugar production was around 2%, higher than slow pyrolysis, yet a little amount compared with the sugar generation from low-ash biomasses that has been processed in the same system. Due to a high-phenolic concentration in both bio-oils resulting from slow- and fast pyrolysis it was concluded that the presence of ash is likely to be favourable for lignin decomposition.

Experiments with microwave pyrolysis were performed with dry and wet digestate at the same conditions. The highlight was more aldehydes, ketones, phenolics, and even some levoglucosan and furfural were detected with wet biomass using less power input, along with less acid formation. These

results demonstrated that high moisture in digestate could promote lignocellulose depolymerisation with less energy required. However, due to the amount of ash present within digestate any benefit of using this technology appears to be offset by secondary catalytic reactions and further decomposition.

Integration of pyrolysis technologies with AD was the main purpose for this research; however an alternative scenario was evaluated whereby crop waste was pyrolysed directly, without being fed into an AD system. Slow pyrolysis of pre-AD crop produced a large amount of primary holocellulose derivatives, with no acetic acid detected, whereas bio-oil resulting from microwave pyrolysis had a high acetic acid concentration and very small amount of sugars. It was found that not only the presence of ash when biomass is pyrolysed has an effect on chemical composition of the products, but any pre-treatment of feedstock significantly influences in how lignocellulose is thermochemically decomposed.

A kinetic model was developed to predict the conversion of pre- and post-AD waste into pyrolysis products. A scheme of reactions was modified to reduce the activation energy of biochar, water and small-molecule compounds to promote easier generation in a larger range of ash content. The kinetic model shows that high ash content in biomass could impact not only pyrolysis product yields, but also sugar generation. These results agreed with the experimental data obtained from pyrolysis of pre-AD crop and crop digestate.

The high ash content makes pyrolysis of digestate a challenging proposition for a commercial process, irrespective of which technology is used. A third scenario is presented in this project, where digestate from crop- and food waste can be treated in a two-stage process to recover high-value components. Firstly, the aqueous medium resulting directly from post AD can be subjected to a low-temperature treatment with microwave technology to obtain hemicellulose-derived monosaccharides. The second stage consists of an enzymatic processing to depolymerise cellulose into D-glucose to enrich a solution with sugars to be recirculate to the AD system and produce more biogas. Digestate analysed from East Birmingham AD facility (Coleshill) in East Birmingham and Stoke Bardolph in Nottinghamshire in the UK, revealed that every 30g of food-waste digestate has 4g of sugar can be recovered, and every 100g of crop digestate has around 45g of sugar-rich components. This would result in an improvement in biogas production in crop-waste AD systems from 20% to almost 40%, and in food-waste AD from 10% to 20% wt. Final crop digestate would become a lignin-rich biomass and could employed in any thermal technology to obtain a liquid with high phenolic content or to produce other lignin-derived products.

Whilst the primary hypothesis was found not to be a viable approach, this study proposes three different schemes as opportunities to recycle and re-use AD waste to decarbonise and promote the circularity of waste processing.

LIST OF CONTENTS

STORY OF THE PROJECT **1**

ACKNOWLEDGMENTS **4**

ABSTRACT **5**

LIST OF CONTENTS **8**

LIST OF TABLES **11**

LIST OF FIGURES **15**

NOMENCLATURE **18**

CHAPTER 1 .... **19**

- **1.1 INTRODUCTION AND BACKGROUND** **19**
- **1.2 AIM AND OBJECTIVES** **26**
- **1.3 PROJECT OUTLINE** **27**

CHAPTER 2. LITERATURE REVIEW **30**

- **2.1 SUSTAINABLE DEVELOPMENT** **30**
- **2.2 CIRCULAR ECONOMY** **31**
- **2.3 USES OF BIOMASS** **34**
- **2.4 BIOMASS DECOMPOSITION IN PYROLYSIS** **35**
  - 2.4.1 PYROLYSIS REACTORS 37
- **2.5 MECHANISMS OF THERMOCHEMICAL DECOMPOSITION OF LIGNOCELLULOSE AND STARCH** **39**
  - 2.5.1 BIO-OIL COMPOSITION FROM DIFFERENT BIOMASSES 43
  - 2.5.2 STARCH THERMAL DECOMPOSITION 47
- **2.6 SCHEMES OF KINETIC REACTIONS OF BIOMASS DECOMPOSITION DURING PYROLYSIS** **47**
- **2.7 PYROLYSIS OF DIGESTATE** **53**
- **2.8 ROLE OF ASH IN PYROLYSIS OF BIOMASS** **57**
- **2.9 SUMMARY OF LITERATURE FINDINGS AND OPPORTUNITIES FOR FURTHER RESEARCH** **58**

CHAPTER 3. MATERIALS AND METHODS- EXPERIMENTAL WORK **59**

- **3.1 SAMPLE SOURCE AND PREPARATION** **59**
- **3.2 SAMPLE CHARACTERISATION** **60**
  - 3.2.1 PROXIMATE AND ULTIMATE ANALYSIS 60
  - 3.2.2 DETERMINATION OF LIGNOCELLULOSE COMPOSITION AND ASH CONTENT 62
    - *3.2.2.1 ASH CONTENT 62*
    - *3.2.2.2 LIGNOCELLULOSIC MATERIAL 62*
    - *3.2.2.3 HYDROLYSIS - CARBOHYDRATES EXTRACTION 62*
    - *3.2.2.4 STANDARDS PREPARATION 64*
    - *3.2.2.5 CARBOHYDRATES QUANTIFICATION 64*
    - *3.2.2.6 LIGNIN DETERMINATION 66*
    - *3.2.2.7 STARCH DETERMINATION 66*
- **3.3 THERMAL PROCESSING** **66**
  - 3.3.1 PROCESS DESCRIPTION -SLOW PYROLYSIS 66
  - 3.3.2 PROCESS DESCRIPTION - FAST PYROLYSIS SYSTEM 68
  - 3.3.3 PROCESS DESCRIPTION - MICROWAVE PYROLYSIS 71
  - 3.3.4 ANALYSIS OF PYROLYSIS PRODUCTS 72
    - *3.3.4.1 BIOCHAR ANALYSIS PYROLYSIS 72*

3.3.4.2 BIO-OIL ANALYSIS 73
3.3.4.3 STANDARDS PREPARATION 73
3.3.4.4 MASS SPECTROMETER INSTRUMENT-OPERATION 75
3.3.4.5 IDENTIFICATION AND QUANTIFICATION 77
3.3.4.6 WATER DETERMINATION IN BIO-OIL 79
3.3.4.7 GAS ANALYSIS SLOW PYROLYSIS 80

CHAPTER 4. MATERIALS AND METHODS- MODELLING 83
4.1 KINETIC MODEL FOR PYROLYSIS 83
4.1.1 CROP DIGESTATE PSEUDO-LIGNIN COMPOSITION 84
4.2 PYROLYSIS MODEL PRELIMINARY VALIDATION- LITERATURE DATA 88
4.2.1 KINETIC MODEL PRELIMINARY VALIDATION 89

CHAPTER 5. RESULTS AND DISCUSSION 94
5.1 DIGESTATE CHARACTERISATION 94
5.1.1 PROXIMATE AND ULTIMATE ANALYSIS 94
5.1.2 LIGNOCELLULOSE COMPOSITION 96
5.2 SLOW PYROLYSIS 102
5.2.1 ANALYSIS OF SLOW PYROLYSIS PRODUCTS 104
5.2.1.1 BIOCHAR 104
5.2.1.2 BIO-OIL 104
5.2.1.3 GAS 109
5.3 FAST PYROLYSIS 110
5.3.1 ANALYSIS OF FAST PYROLYSIS PRODUCTS 112
5.3.1.1 BIOCHAR 112
5.3.1.2 BIO-OIL 112
5.3.1.3 GAS 116
5.4 MICROWAVE PYROLYSIS 117
5.4.1 BIO-OIL 118
5.5 BIO-OIL COMPARISON BETWEEN BIO-OIL FROM PRE-AD AND DIGESTATE 123
5.5.1 PYROLYSIS OF PRE-AD CROP 123
5.5.1.1 MICROWAVE PYROLYSIS PRE-AD 123
5.5.1.2 SLOW PYROLYSIS PRE-AD 127
5.4 IMPACT OF ASH ON PYROLYSIS PRODUCT COMPOSITION FROM DIGESTATE 132

CHAPTER 6. COMPARISON OF YIELD AND BIO-OIL COMPOSITION FROM DIFFERENT PYROLYSIS TECHNIQUES 135
6.1 LEVOGLUCOSAN DECOMPOSITION 138
6.2 FURFURAL DECOMPOSITION 139
6.3 DECOMPOSITION OF LIGNIN INTO PHENOLICS 140
6.4 SCHEME OF REACTIONS - KINETIC MODEL LIGNOCELLULOSE DECOMPOSITION 141

CHAPTER 7. MODELLING PROJECTIONS - PYROLYSIS OF DIGESTATE 145
7.1 KINETIC MODEL ADJUSTED FOR HEATING RATES 150
7.1.1 PYROLYSIS OF DIGESTATE AT DIFFERENT RATES 154
7.1.2 PYROLYSIS OF PRE-AD CROP AT DIFFERENT RATES 162
7.2 PYROLYSIS OF DIGESTATE AND PRE-AD CROP AT DIFFERENT RATES WITH HIGHER IMPACT OF ASH CONTENT 169

CHAPTER 8. SCENARIOS FOR THERMAL TREATMENT INTEGRATED TO ANAEROBIC DIGESTION SYSTEMS AND POSSIBLE USES OF PYROLYSIS PRODUCTS 177
8.1 SCENARIO 1- POST-AD 179
8.1.1 FAST PYROLYSIS POST-AD 179
8.1.2 SLOW PYROLYSIS POST-AD 182
8.1.3 MICROWAVE PYROLYSIS POST-AD 185

8.2 SCENARIO 2- PRE-AD....187
8.2.1 FAST PYROLYSIS PRE-AD....187
8.2.2 SLOW PYROLYSIS PRE-AD....189
8.2.3 MICROWAVE PYROLYSIS PRE-AD....191
8.3 SCENARIO 3. DEPOLYMERISATION OF CELLULOSE AND HEMICELLULOSE IN DIGESTATE TO INCREASE BIOGAS PRODUCTION....194
8.4 POSSIBLE USES OF PYROLYSIS PRODUCTS....199
8.4.1 BIOCHAR....199
8.4.2 GAS....201
8.4.3 BIO-OIL....203
CHAPTER 9. CONCLUSIONS AND RECOMMENDATIONS....205
APPENDIX A. LIST OF COMPONENTS USED IN MODEL....210
APPENDIX B. THERMOGRAVIMETRIC ANALYSIS DATA....211
APPENDIX C. LIGNIN COMPOSITION OF SEVERAL BIOMASSES....214
APPENDIX D. COMPLEMENTARY DATA - BIO-OIL COMPOSITION....215
REFERENCES....221

LIST OF TABLES

Table 1. Pyrolysis parameters and yield of products [18,19,45,52]. 36

Table 2. Some characteristics of bed reactors used in pyrolysis [19]. 37

Table 3. Ranges of temperatures of lignocellulosic material thermochemical decomposition and key chemicals produced in bio-oil pyrolysis [69,70]. 40

Table 4. Summary of bio-oil generated from woody material through pyrolysis technologies (Data is presented as published by the authors). 45

Table 5. Summary of bio-oil generated from non-woody material through pyrolysis technologies (Data is presented as published by the authors). 46

Table 6. Original scheme of kinetic reactions during pyrolysis proposed by Ranzi et al. [96]. 48

Table 7. Original scheme of kinetic reactions during pyrolysis proposed by Calonaci et al. [97]. 49

Table 8. Model modified with charring factor x, proposed by Anca-Couce et al. [98]. 50

Table 9. Comparison of the results, dry mass % basis, from the model modified by Anca-Couce et al. [98] with original and experimental data. 51

Table 10. Scheme of secondary reactions could take place in slow pyrolysis according to by Park et al. [69] (Scheme is presented as Blondeau et al. [99]). 51

Table 11. Scheme of reactions of lignocellulose decomposition in fast pyrolysis proposed by Ranzi et al. [100]. 53

Table 12. Standards employed to determine sugar composition of pre-AD crop and crop digestate. ... 64

Table 13. Sugars standards and formula. 65

Table 14. Ratios used to prepare calibration standards to a total volume of 1.5 ml. 74

Table 15. Data and outputs from GC-MS analysis. 78

Table 16. Hydrocarbon gas standards to identify and quantify non-condensable pyrolytic gases from digestate. 81

Table 17. Non-hydrocarbon gas standards to identify and quantify non-condensable pyrolytic gases from digestate. 81

Table 18. Characterisation of crop digestate collected in 2016 at Severn Trent site in Stoke Bardolph [145]. 84

Table 19. Cellulose, hemicellulose and lignin proportion in crop digestate adjusted for pseudo-lignin calculation. 84

Table 20. Elemental composition (weight basis) of the main lignocellulosic components in the biomass [147]. 85

Table 21. Lignin composition of different biomass analysed [18,100,147,150]. 86

Table 22. Comparison between pseudo-lignin composition published of some biomasses and projections resulted from correlations [18,147,150]. 87

Table 23. Results of the proportion of the lignin composition (wt %) in the digestate using the model based on the C, H, and O elemental composition. 88

Table 24. Lignocellulose composition in beech and pine presented by Wang et al. [152] and used for the model validation. Data is presented in % wt. 90

Table 25. Comparison between models using different reaction schemes. Empirical data was obtained with beech wood at 500°C from experimental results presented by Wang et al. [152]. 91

Table 26. Comparison between models using different reaction schemes. Empirical data was obtained with pine wood at 500°C from experimental results presented by Wang et al. [152]. 92

Table 27. Proximate and ultimate analysis of 3 batches of digestate collected for thermal treatment, and crop used as starting material to be fed into the AD system. 95

Table 28. Lignocellulose analysis of the 3 batches of crop digestate run in pyrolysis systems performed by Celignis Ltd. 96

Table 29. Lignocellulose analysis of crop digestate of 3 batches collected of digestate to run in pyrolysis systems carried out at WUR. 97

Table 30. Lignocellulose analysis of the crop as starting material of AD, and additional 3 other batches of digestate assays carried out at WUR. 98

Table 31. Summary of pre-AD crop and digestate (3 initial batches) composition values with different measurements methods. Data is the mean weight percentage %. 101

Table 32. Yields of slow pyrolysis products carried out at four different temperatures using crop digestate. 102

Table 33. Ultimate analysis of biochar product collected from slow pyrolysis of crop digestate at different temperatures. 104

Table 34. Proportions of chemical groups in slow pyrolysis bio-oil of digestate. Data is presented in % weight basis, and total represents bio-oil yield. 105

Table 35. Analysed bio-oil product from slow pyrolysis of digestate at two temperatures, 355ºC and 530ºC. Data presented in wt %. 107

Table 36. Composition of non-condensable gases resulting from slow pyrolysis of crop digestate of the gas recovered from the system. Data is presented in weight basis (wt %). 109

Table 37. Overall mass balance (wt %) for dry digestate as raw material of fast pyrolysis system at VTT, Finland. 110

Table 38 Ultimate analysis (wt %) of biochar produced from fast pyrolysis of crop digestate at different temperatures. Analysis performed in VTT, Finland. 112

Table 39. General composition of bio-oil produced from fast pyrolysis of digestate. Data is presented in wt %. 112

Table 40. Fast pyrolysis bio-oil composition produced at four different temperatures. Data presented in wt%. 114

Table 41. Weight basis % of non-condensable gases resulted from fast pyrolysis of crop digestate. This analysis was performed at VTT, Finland. 116

Table 42. Bio-oil composition of microwave pyrolysis of digestate (wt %) at different energy inputs. 118

Table 43. Analysed microwave pyrolysis bio-oil from digestate at three different energy input. Data presented in wt %. 121

Table 44. Bio-oil composition of microwave pyrolysis of pre-AD crop and digestate. Proportions of chemical groups are presented in percentage weight basis (wt %), and the total of bio-oil of each run. 123

Table 45. Analysed microwave pyrolysis bio-oil from pre-AD crop at three different energy input. Data presented in wt %. 125

Table 46. Yields of slow pyrolysis products carried out at four different temperatures using pre-AD crop and digestate. 127

Table 47. Bio-oil composition of slow pyrolysis of pre-AD material. Proportions of chemical groups are presented in % weight basis. 128

Table 48. Analysis of bio-oil from pre-AD material at slow pyrolysis process. Proportions of chemical groups are presented in % weight basis. 130

Table 49. Bio-oil comparison between the three pyrolysis technologies from digestate. Proportions of chemical groups are presented in weight basis % of the total bio-oil of one experiment with equivalent condition: temperature/ specific energy input. 135

Table 50. Bio-oil comparison between the three pyrolysis technologies from digestate. Proportions of chemical groups are presented in percentage weight basis (% wt) of the total bio-oil of one experiment at certain conditions: temperature, or energy input. 137

Table 51. Reactions in scheme of Ranzi et al. [144] non-stoichiometic balanced as they are presented they are presented in the original publication. 143

Table 52. Scheme of reactions proposed for the kinetic model V4b. This is a modification of the scheme presented by Ranzi et al. [144]. The format is shown according to the number of reactions presented in Ranzi et al.'s publication. 144

Table 53. Equivalent composition of lignin and pseudo-lignins in digestate as input for modelling lignocellulose thermal decomposition in fast pyrolysis at different temperature. Data is presented is the average of the 3 batches used in VTT's system. 145

Table 54. Comparison of experimental outputs from fast pyrolysis of digestate performed in VTT with model projections V4b where ash content is included. 146

Table 55. Comparison of experimental outputs from fast pyrolysis of digestate performed in VTT with model projections V4b where ash content is included (cont.). 147

Table 56. Pine composition employed for pyrolysis model at different heating rates. Lignocellulose composition from Wang et al. [152]. Data presented in wt. %. 150

Table 57. Final composition projections of bio-oil at 600ºC at different heating rates. 154

Table 58. Digestate and pre-AD lignocellulose composition employed for pyrolysis model at different heating rates. Data presented in wt. %. 154

Table 59. Final yields (wt %) of pyrolysis products from digestate at different heating rates from 150ºC to 600ºC 156

Table 60. Final composition projections of compounds in bio-oil pyrolysis from digestate, ash and ash-free, at 600ºC with 10ºC/s and 40ºC/s heating rates. 158

Table 61. Final yields (wt %) of compounds in pyrolysis bio-oil from digestate at different heating rates from 150ºC to 600ºC. 160

Table 62. Pre-AD crop composition employed for modelling pyrolysis at different heating rates. Data presented in % wt. 162

Table 63. Final yields of pyrolysis products from pre-AD crop at 600ºC, with different at different heating rates with V-heat. 164

Table 64. Final yields (wt %) of compounds in pyrolysis bio-oil from pre-AD crop at different heating rates at 600ºC. 166

Table 65. Range of yields resulted from projections with model V-heat and experimental measurements using digestate and pre-AD in fast pyrolysis (Data presented in wt %). 166

Table 66. Range of chemical compounds content in bio-oil resulted from projections with model V-heat and experimental measurements using digestate and pre-AD in fast pyrolysis (Data presented in wt %). 168

Table 67. Projections of final yields of pyrolysis products from pre-AD crop at different heating rates from 150ºC to 600ºC, with higher ash impact. 173

Table 68. Range of yields resulted from projections with both models and experimental measurements using digestate and pre-AD in fast pyrolysis (Data presented in wt %). 173

Table 69. Final yields (wt%) of compounds in pyrolysis bio-oil from pre-AD crop at different heating rates from 150ºC to 600ºC, with higher impact of ash. 175

Table 70. Range of chemical compounds content in bio-oil resulted from projections with model V-heat, VAsh10 and experimental measurements using digestate and pre-AD in fast pyrolysis (Data presented in wt %) 175

Table 71. Projection of bio-oil composition produced from digestate at 560ºC with a current scale-up fast pyrolysis technology, Hengelo, the Netherlands. 181

Table 72. Projection of bio-oil composition produced from digestate at around 500ºC with PYREG PX1500 system. 184

Table 73. Projection of bio-oil composition produced from digestate generated on site per day with continuous process of microwave pyrolysis. 186

Table 74. Projection of bio-oil composition produced from pre-AD crop generated on site per day with continuous process of pyrolysis based on Empyro production**.** 188

Table 75. Projection of bio-oil composition produced from pre-AD crop at ~500ºC three units of PYREG PX1500. 190

Table 76. Projection of bio-oil composition produced from pre-AD crop generated on site per day with continuous process of microwave pyrolysis. 192

Table 77. Pre-AD crop composition broken down into total monosaccharides from cellulose, hemicellulose, and starch. 194

Table 78. Sugar composition of food waste digestate collected from Coleshill energy site. 196

Table 79. Kilograms of hydrogen and hydrocarbon gases per day resulted from scaled-up fast pyrolysis from crop digestate. 202

Table 80. Components used of the model employed for fast pyrolysis of digestate [144]. 210

Table 81. Proximate and Ultimate analysis of batch one of digestate collected used in pyrolysis systems. 211

Table 82. Proximate and Ultimate analysis of batch two of digestate collected used in pyrolysis systems. 211

Table 83. Proximate and Ultimate analysis of batch three of digestate collected used in pyrolysis systems. 212

Table 84. Summary of proximate and ultimate analysis of every batch of digestate collected during the 4 seasons to evaluate their variation. 213

Table 85. LigniN composition of different biomass analysed Faravelli et al. [147] 214

Table 86. Other compounds identified in bio-oil from slow pyrolysis of digestate at different temperatures. 215

Table 87. Other compounds identified in bio-oil from fast pyrolysis of digestate at different temperatures. 216

Table 88. Other compounds identified in bio-oil from microwave pyrolysis of digestate at different energy input. 217

Table 89. Other compounds identified in bio-oil from microwave pyrolysis of pre-AD crop at different energy input. 218

Table 90. Bio-oil comparison between the three pyrolysis technologies from digestate. Proportions of chemical groups are presented in weight basis % of the total bio-oil of one experiment at certain conditions: *temperature, or energy input*. 219

Table 91. Bio-oil comparison between the three pyrolysis technologies from digestate. Proportions of chemical groups are presented in weight basis % of the total bio-oil of one experiment at certain conditions: *temperature, or energy input* (Cont.) 220

LIST OF FIGURES

Figure 1. Diagram of a general anaerobic digestion system. 19

Figure 2. Diagram of thermal processing for digestate integrated with an anaerobic digestion system. 23

Figure 3. Range of operating temperatures of conventional pyrolysis [18-20] and product heat value [21,22]. 24

Figure 4. Diagram of the outline of this research project. 29

Figure 5. 17 Sustainable Development Goals (picture source: United Nations). 30

Figure 6. Symbol of circular economy representation (source European Parliament). 32

Figure 7. Diagram of a close loop of waste used to produce green energy through anaerobic digestion and the use of the final co-product, digestate, as fertiliser to amend the soil where this crop is growing. 33

Figure 8. Heating mechanism and temperature distribution in conventional and microwave pyrolysis of wood. Diagram modified from Miura et al. [66]. 38

Figure 9. Structure of lignocellulosic material: cellulose, hemicellulose, and lignin. 39

Figure 10. Pathway of direct cellulose conversion into primary compounds proposed by Shen et al. [43]. 41

Figure 11. Scheme of hemicellulose primary conversions proposed by Patwardhan et al. (Figure as published in Zhou et al. [78]). 41

Figure 12. Pathway proposed by Supriyanto et al. [80] of lignin converted into some phenolics through pyrolysis. 42

Figure 13. Waste collected from Severn Trent sites. 59

Figure 14. Crop digestate samples preparation. 60

Figure 15. Raw and ground crop digestate 60

Figure 16. Thermogravimetric analysis (TGA) of biomass. 61

Figure 17. Difference between two hydrolysis processes implemented to determine carbohydrate levels in crop waste and digestate: (1) strong hydrolysis (2) weak hydrolysis 63

Figure 18. Chromatogram of standard B generated through Chromeleon software from Dionex analysis. 65

Figure 19. Slow pyrolysis system to process crop digestate. 67

Figure 20. Digestate in pellets. 69

Figure 21. Digestate in particles 0.5-0.9 mm 69

Figure 22. Temperature sections across fast pyrolysis reactor. 69

Figure 23. General diagram of fast pyrolysis system in VTT, using crop digestate. 70

Figure 24. Pellets dimension employed in microwave pyrolysis system. 71

Figure 25. Microwave pyrolysis system. 72

Figure 26. GCMS chromatograms of bio-oil from slow pyrolysis experiment at 530ºC: 1) sample with only DCM (2) sample with DCM/MeOH 75

Figure 27. Chromatogram peaks resulted from GC-MS with column 60 m x 250 μm x 0.25 μm of a bio-oil from microwave pyrolysis of pre-AD crop. 76

Figure 28. Chromatogram peaks resulted from GC-MS peaks resulted from GC-MS with column 30 m × 0.25 mm, 0.25 μm. 76

Figure 29. Example of chromatogram resulted from GC-MS analysis of standards. 77

Figure 30. Example of calibration curve. Seven different concentrations of glycolaldehyde dimer. 78

Figure 31. General diagram of Dean-Stark system. 80

Figure 32. Example chromatogram of hydrocarbons detected from the slow pyrolysis system. 82

Figure 33. Base characterisation model to predict the main components in the biomass. 86

Figure 34. C/H, O/C ratios of lignocellulosic material and its distribution of pseudo-lignins due to the ratios. 87

Figure 35. General mass balance of anaerobic digestion considering initial and final starch determined and actual lignocellulose measured from crop waste and its digestate, dry basis. 99
Figure 36. Organic and inorganic material distribution in pre-AD crop and crop digestate, dry basis. 100
Figure 37. General diagram representing the possible ash accumulation and increase in the biomass through the AD process. 101
Figure 38. Yields (wt %) of slow pyrolysis products recovered in slow pyrolysis system. 103
Figure 39. Mass weight distribution of the chemical groups found in bio-oil resulted from slow pyrolysis of digestate at different temperatures. 106
Figure 40. Yields of fast pyrolysis products recovered at different temperature. 111
Figure 41. Mass weight distribution of the chemical groups found in bio-oil resulted from fast pyrolysis of digestate at four different temperatures. 113
Figure 42. Example of experiment performed of microwave pyrolysis with digestate. Curves presented are 500 W power input for 5 minutes, and the power absorbed and reflected. 117
Figure 43. Mass weight (wt %) distribution of the chemical groups found in microwave pyrolysis bio-oil from digestate at different energy input. 120
Figure 44. Mass weight distribution of chemical groups found in bio-oil from microwave pyrolysis of pre-AD material vs digestate at different energy input. 124
Figure 45. Comparison of yields of slow pyrolysis products recovered between using pre-AD crop and digestate as feedstock at same conditions. 128
Figure 46. Mass weight distribution of the chemical groups found in bio-oil from slow pyrolysis of pre-AD material at four different temperatures. 129
Figure 47. Comparison of chromatograms between some compounds identified from pyrolysis of pre-AD crop: (a) microwave pyrolysis with 3.57 kJ/g energy input, and (b) slow pyrolysis at 530ºC. 131
Figure 48. Illustration of possible effect of ash distribution and microwave mechanism through pre-AD crop and digestate pellets utilised in microwave pyrolysis. 133
Figure 49. Mass weight distribution of chemical groups quantified in bio-oil from digestate in all the pyrolysis equivalent conditions. 136
Figure 50. Mechanism of sugar decomposition of hexoses, such as levoglucosan proposed by Shen et al. [43]. 138
Figure 51. Overview of chemical could be derived from Furfural presented by Mariscal et al. [172]. . 139
Figure 52. Mechanism of primary reactions of softwood alkali lignin pyrolysis decomposition proposed by Supriyanto et al. [80]. 140
Figure 53. Scheme of reactions selected to model pyrolysis of digestate. The scheme is presented as published by Ranzi et al. [144]. 142
Figure 54. Comparison of slow and fast pyrolysis of digestate experimental results versus model projections at different temperatures: (a) Yields of fast pyrolysis products at 460ºC, 480ºC, 520ºC and 560ºC. (b) Yields of chemical groups in fast pyrolysis bio-oil, (c) Yields of slow pyrolysis products at different temperatures 355ºC, 425ºC, 485ºC and 530ºC. (d) Yields of chemical groups in slow pyrolysis bio-oil. 149
Figure 55. Model projections (V-heat) of pyrolysis products from pine with ash content at different rates of temperatures. 151
Figure 56. Pyrolysis product formation from pine with ash and ash-free at different heating rates: (a) 5ºC/s and (b) 10ºC/s. 152
Figure 57. V-heat projections of bio-oil compounds formation from pyrolysis of pine at different heating rates 5ºC/s, 10ºC/s and 20ºC/s: (a) sugars. (b) furans, (c) aldehydes & ketones, (d) acids and (e) alcohols and (f) phenolics. 153
Figure 58. V-heat pyrolysis product projection from digestate with ash and ash-free at different heating rates: (a) 5ºC/s and (b) 40ºC/s. 155
Figure 59. V-heat projections of pyrolysis of digestate at 5ºC/s, 10ºC/s, 20ºC/s and 40ºC/s: (a) biomass decomposition. (b) bio-oil, (c) organics, (d) water, (e) biochar, and (f) gas. 157
Figure 60. Sugars, furans and phenolic formation in bio-oil pyrolysis from digestate at different heating rates for ash and ash-free composition: (a) 10ºC/s and (b) 40ºC/s. 158

Figure 61. V-heat projections of bio-oil compounds formation from pyrolysis of digestate at different heating rates 5ºC/s, 10ºC/s, 20ºC/s and 40ºC/s: (a) sugars. (b) furans, (c) aldehydes & ketones, (d) acids and (e) alcohols and (f) phenolics. 159

Figure 62. Pyrolysis products formation from digestate at 360ºC at 20ºC/s heating rate with extended residence time: (a) pyrolysis products and (b) compounds in bio-oil. 161

Figure 63. V-heat projections of pyrolysis of pre-AD crop considering ash content at different heating rates 5ºC/s, 10ºC/s, 20ºC/s and 40ºC/s: (a) biomass decomposition. (b) bio-oil, (c) organics, (d) water, (e) biochar, and (f) gas. 163

Figure 64. V-heat projections of bio-oil compounds formation from pyrolysis of pre-AD crop at different rates 5ºC/s, 10ºC/s, 20ºC/s and 40ºC/s: (a) sugars, (b) furans, (c) aldehydes & ketones, (d) acids and (e) alcohols and (f) phenolics. 165

Figure 65. Projections of pyrolysis of digestate with model VAsh10 at different heating rates: 5ºC/s, 10ºC/s, 20ºC/s and 40ºC/s. (a) biomass decomposition, (b) bio-oil, (c) organics, (d) water, (e) biochar, and (f) gas. 170

Figure 66. Yields of fast pyrolysis products recovered at different temperature and from projections with model VAsh10 using digestate composition. 171

Figure 67. VAsh10 projections of bio-oil compounds formation from pyrolysis of digestate at different heating rates 5ºC/s, 10ºC/s, 20ºC/s and 40ºC/s, with VAsh10 model: (a) sugars. (b) furans, (c) aldehydes & ketones, (d) acids and (e) alcohols and (f) phenolics. 172

Figure 68. Model projections of bio-oil compounds formation from pyrolysis of pre-AD crop at different heating rates 5ºC/s, 10ºC/s, 20ºC/s and 40ºC/s, with higher impact of ash content: (a) sugars. (b) furans, (c) aldehydes & ketones, (d) acids and (e) alcohols and (f) phenolics. 174

Figure 69. Waste collected from Severn Trent sites. 178

Figure 70. Flow diagram of Empyro pyrolysis process (Modified from BTG bioliquids). 180

Figure 71. Flow diagram of fast pyrolysis of digestate integrated to crop AD system. 182

Figure 72. Flow diagram of slow pyrolysis of digestate integrated AD system. 185

Figure 73. Flow diagram of microwave pyrolysis of digestate integrated AD system. 187

Figure 74. Flow diagram of fast pyrolysis of pre-AD. 189

Figure 75. Flow diagram of slow pyrolysis of pre-AD. 191

Figure 76. Flow diagram of microwave pyrolysis of pre-AD crop. 193

Figure 77. General diagram representing pre-AD crop composition and waste crop composition post AD process. 194

Figure 78. General diagram representing composition of pre-AD crop and digestate in monosaccharides content. 195

Figure 79.. Food digestate collected from Coleshill site. 196

Figure 80. General diagram representing crop digestate thermal treated to extract additional sugars from hemicellulose and sugar-rich water recirculation into digester for more biogas production. Residual digestate solids could then be processed in thermal technologies. 197

Figure 81. General diagram representing crop digestate 2-step treatment to extract additional sugars from cellulose and hemicellulose and return sugar-rich liquid into the digester for more biogas production. Residual digestate solids could then be processed in thermal technology to produce pyrolytic lignin derivatives. 198

Figure 82. Alternative uses for biochar. 200

Figure 83. Alternative uses for pyrolytic gas. 201

Figure 84. Alternative uses for pyrolytic bio-oil. 203

NOMENCLATURE

Acronym	Meaning
STW	Severn Trent Water
AD	anaerobic digestion
Pre-AD	previous anaerobic digestion
Post-AD	posterior anaerobic digestion
C	carbon
H	hydrogen
O	oxygen
N	nitrogen
wt %	percentage weight basis
s	seconds
TGA	thermogravimetric analysis
kW_e	kilowatt-electric
kW_{th}	kilowatt-thermal

CHAPTER 1

1.1 INTRODUCTION AND BACKGROUND

Demographic pressures from population growth and economic development are linked to inter-related concerns around waste production, energy market volatility, decreasing safe water supplies and climate change due to the dependency of fossil fuels. Several strategies have been implemented in order to meet these challenges. One of the most successful of these has been sewage treatment. This has become a crucial process in maintenance of the balance between water extraction and effluent discharge to help prevent the pollution of aquifers. In addition, energy production takes place in one of the stages of sewage treatment termed anaerobic digestion (AD). Sludges generated from the system are added to a digester where microorganisms, in the absence of oxygen, break down the organic material to produce biogas. This gas formed is rich in methane and can be used for energy generation (Figure 1).

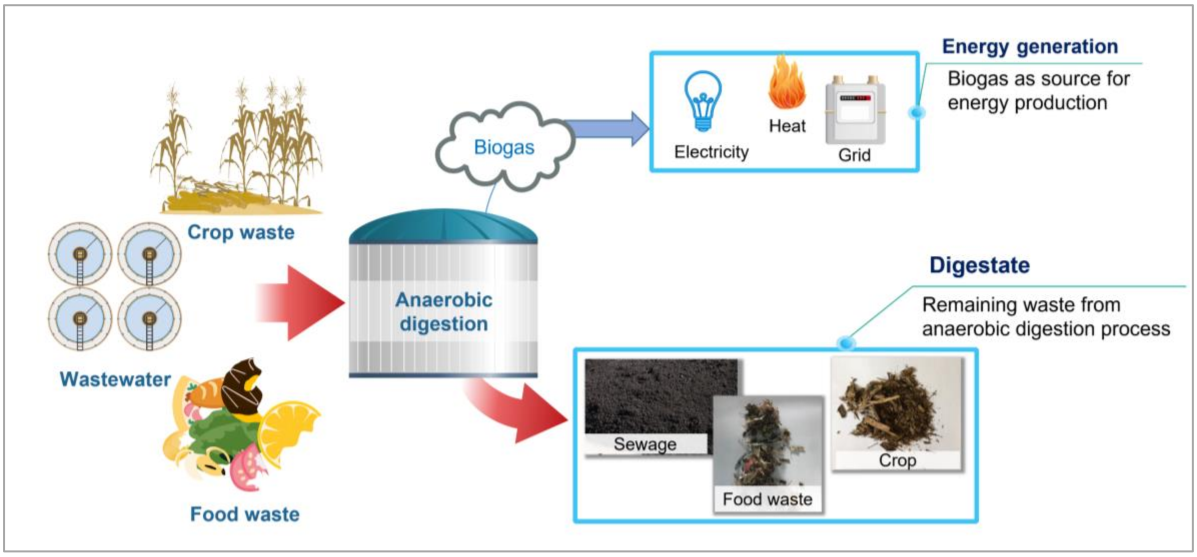
Energy generation
Biogas as source for energy production
Electricity
Heat
Grid
Biogas
Crop waste
Anaerobic digestion
Wastewater
Food waste
Digestate
Remaining waste from anaerobic digestion process
Sewage
Food waste
Crop

Figure 1. Diagram of a general anaerobic digestion system.

AD has a range of different operating conditions. Temperatures vary between 35-40°C and 55-60°C depending on whether mesophilic or thermophilic microorganisms are used. The system can consist of single stage where the conversion of organic material into biogas occurs in only one digester, or multistage which comprises various tanks. Multistage systems can also improve the reactions that take place in each stage of biogas production: hydrolysis, acidogenesis, acetogenesis and methanogenesis [1,2]

AD is used not only during sewage treatment, but also to process other kinds of waste to produce bioenergy. In many countries, the current direct destination of rubbish and waste produced from human activities, including both organic and non-organic material, is landfills or incineration where sometimes there is also heat or electricity production. These techniques are not ideal in solid waste management: not only do they require high capital and operation costs, but there are also difficulties around environment controls, such as air pollution relating to incinerators and the pollution of aquifers or water bodies relating to landfill [2-4]. In addition, landfills and incineration are not as efficient in terms of energy recovery employing an anaerobic digester. AD can be better controlled and can result in higher biofuel production. Furthermore, the implementation of anaerobic digestion systems has impacted positively by reducing the amount that goes to landfill. Some research suggests that treatment of waste through anaerobic digestion has resulted in a reduction of antibiotic resistance genes, which is a positive effect [5,6]. These systems are also considered to provide a continuous source of primary energy with which to generate electricity or heat compared with other sources such as wind or solar which are considered to be intermittent due to weather dependency [7-10].

In order to establish a global perspective on biogas technologies the US Environmental Protection Agency (EPA) worked with the Global Methane Initiative (GMI) to promote the implementation of biogas systems production in several countries. GMI wrote reports which included information from 30 countries about the positive impact of anaerobic digestion systems on their economies and their energy production [11,12]. Although using waste as a sustainable material to produce biofuels could be a potential route for alternative energy generation, there are a number of factors to be considered before this approach can be implemented. These factors include the kind of feedstock needed for production, the economics involved, environmental and social implications, system efficiency and so on. This is the subject of current research, with projects carried out by international organisations focused on bioenergy and renewable resources. The International Energy Agency (IEA) classifies current research into specific Tasks. Task 37, for instance, is focused on anaerobic digestion to be promoted as a multifunctional treatment of waste, which could play an important role as a low-cost feedstock for high-value material generation without using raw resources [13].

In anaerobic digestion processes the main product from the system is biogas but there is also residual waste named digestate. This has characteristics which may allow for further uses or for being converted into other useful products with high value applications. If this waste can be successfully valorised then this could improve the balance of carbon emissions.

There are a number of strategies which might allow enhancement to treat digestate in order to increase its value and use for further processing. The Department of Energy and Climate Change, now part of the Department for Business, Energy & Industrial Strategy (BEIS), made a commitment to what is termed ‘zero waste economy’, and ‘clean growth’ strategies which encourage the use of sustainable systems for energy production, noting the importance of taking advantages of all the products resulting from these processes. These include a waste strategy to improve resource productivity and resource efficiency in the UK. BEIS and the Official Information Portal on Anaerobic Digestion in the UK have mentioned several methods to treat these co-products in order to give them a use: nutrient-stripping, supercritical wet oxidation, gasification, and pyrolysis to produce other high value products. A further option is the use of separated fibre fractions in construction materials [10]. BEIS compared biomasses that could be used as bioenergy feedstocks and their supply in the UK between 2010 and 2030 [14]. This report considered wood, crop and waste as potential resources. Findings reported showed that the price of the biomass to be utilised as a source of energy depends on any possible constraint such as policies, market, technical issues and others. Although anaerobic digestion was considered in this report as a complex process because specific biomass is needed for the conversion, it also highlighted the importance of developing and improving this system for wet-biomass processing where organic fraction can be used to produce biomethane. This report also covered prices of biomass for bioenergy applications. Waste such as mixed solids and wet feedstock for anaerobic digestion (AD) for large electricity sector, for instance, were reported cheaper than other feedstocks used for other facilities. It is considered that AD systems are designed to treat available residues or waste as solid-fuel biomass supply, and these materials can be cheaper than virgin biomass or feedstocks that require pre-treatment such as drying and pelletising. Additionally, gate fees can also be charged for some materials, giving a net negative purchase cost.

Bates (2017) presented an update of this report extending the timeframe to 2050, which includes the comparison of biomass costs for energy production including landfill use for gas production. It was pointed out that if the barriers are overcome, waste food, livestock manures and the renewable fraction of wastes could have a reduction in cost by 45%, around 95% and 35% respectively. However, the results are only based on the cost of biomass that currently can be bought, and it was noted that waste and residues can be even cheaper for bioenergy generation [15].

In November 2021, BEIS released a biomass statement as part of the 'net zero strategy' and to increase the use of biomass to enhance and prioritise bioeconomy to reduce carbon emissions. Some of the incentives consist of supporting the tariff of biomethane resulting from anaerobic digestion using waste and to be injected into the gas grid. Additionally, more investments have been highlighted for further studies to add value to digestate and the possible implementation of other innovative technologies such as gasification to produce different biofuel products resulting from diverse feedstocks [16].

There has been cooperation between different nations in order to promote the concept of the use of biorefineries to reduce environmental damage resulting fossil resource use. One of these strategies is to manage a Circular Economy, where instead of having a linear approach (production, use and then disposal), the value of products must be maintained as long as possible. The European Commission has explained that waste generation and excessive extraction of raw resources needs to be reduced in order to increase the value of materials by extending their use and not disposing until they have reached the end of their usable life. As a result costs can be saved, opportunities for new business can be created and resources are conserved [17].

Severn Trent Water (STW) has used biogas generation from the anaerobic digestion of waste as its main source of renewable energy production at most of its sites. In some cases, biomethane is also exported to the gas grid. Therefore, there is a significant digestate production at STW treatment plants. Some of the digestate that results from food, sewage and crop waste can be introduced into the fertiliser market, although it requires substantial analysis and certification to ensure it meets the quality criteria. The regulations involved include the Quality Protocol and Publicly Available Specification (PAS) 110:2010, which applies in England and Wales, and the Scottish Environment Protection Agency (SEPA) position statement which is employed in Scotland [10]. However, if the digestate comes from sewage then the Biosolids Assurance Scheme, developed by UK water network, needs to be implemented to use this digestate on land. Although some digestate has the quality needed for a biodegradable waste, it has not been profitable to sell it as a product due to the preference for other synthetic fertilisers and the limited market for digestate. Consequently, use of the digestate generates more expenses for STW related to transport and spreading costs for the digestate disposal, and reduces the overall economic and sustainability benefits of using AD.

In order to find more opportunities for use of this ‘waste’, thermal treatments have been considered for further treatment of the digestate. Figure 2 shows a general diagram of how a thermal processing can be integrated with an anaerobic digestion system.

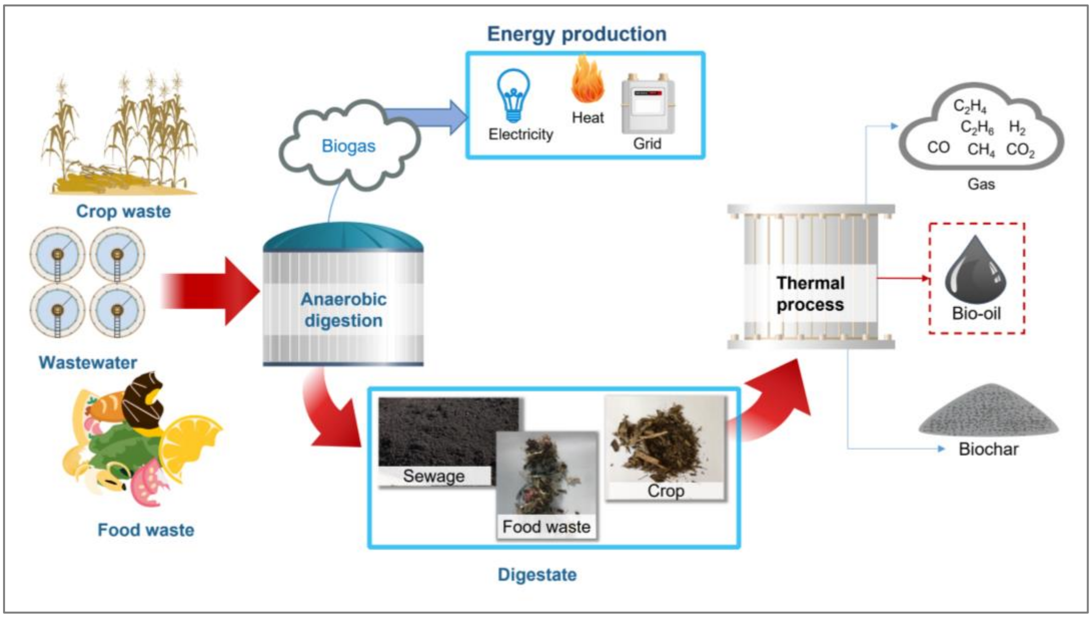
Energy production
Electricity
Heat
Grid
Biogas
Crop waste
Wastewater
Food waste
Anaerobic digestion
Sewage
Food waste
Crop
Digestate
Thermal process
C_2H_4
C_2H_6
H_2
CO
CH_4
CO_2
Gas
Bio-oil
Biochar

Figure 2. Diagram of thermal processing for digestate integrated with an anaerobic digestion system.

Different thermochemical technologies, such as pyrolysis and hydrothermal processing, have been validated through use on several biomass feedstocks, especially wood and other crops. These systems all operate in the absence of oxygen and all of them produce three different products: *gas, bio-oil and biochar*. The energy value and composition of these products vary depending on the feedstock used and the physical conditions employed in these thermal processes. Treating digestate as source with these technologies could reduce the volume by 70%, and the corresponding cost associated with transportation and disposal of the waste [8].

Conventional pyrolysis is a diverse technology which should be analysed as it has been applied at a wide range of operating temperatures in order to obtain different yields of products, as presented in Figure 3.

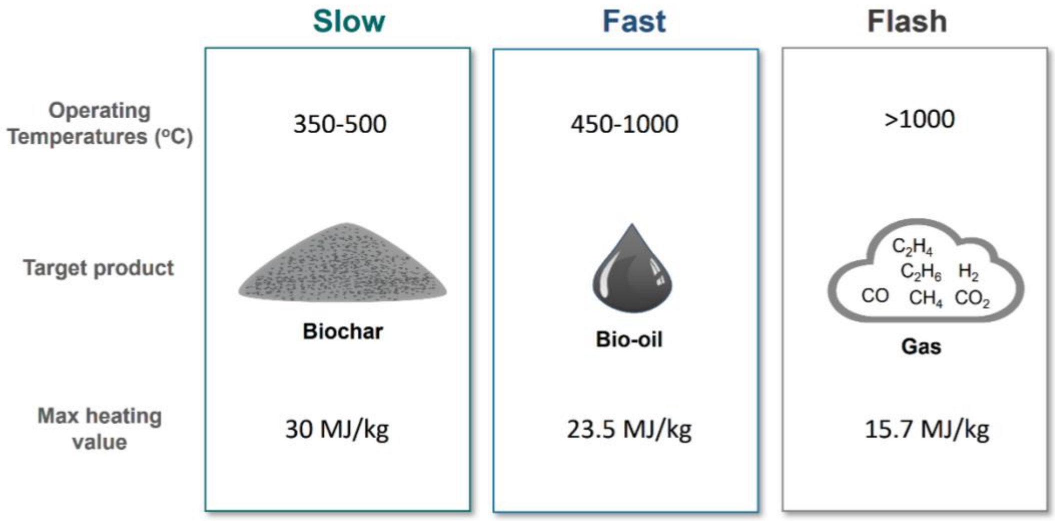

Figure 3. Range of operating temperatures of conventional pyrolysis [18-20] and product heat value [21,22].

Microwave pyrolysis, which differs from conventional pyrolysis due to different heating mechanisms is an alternative technology that has been shown to produce a larger amount of pyrolytic liquid from lignocellulosic waste. Some studies have demonstrated that bio-oil from this technology can be easily obtained while avoiding secondary reactions which can occur in conventional pyrolysis, and can also produce bio-oil with high content of sugars, alkanes, and phenol and its derivatives [23-25].

Hydrothermal processing has the same principle as pyrolysis as energy is applied to decompose biomass to produce hydrochar, bio-oil and gas. In this case the process takes place in an aqueous medium. There are different types of hydrothermal technologies just as there are types of pyrolysis processing, and operating conditions change depending on which product is the target. Hydrothermal processing is based on the critical point of water, this being 374^{o}C and 22.1 MPa [26]. Hydrothermal carbonisation operates under a concept of subcritical water conditions, where temperature is between 180 and 250^{o}C and a pressure is kept a level that results in water staying in liquid state. This results in a higher production of hydrochar [26,27]. Hydrothermal liquefaction needs similar subcritical water conditions: the process is carried out between temperatures of 250 and 370^{o}C, and at pressures between 4 and 20MPa to increase the production of bio-oil. The same pressure conditions, but with an increase in the temperature to 500^{o}C, allows hydrothermal gasification takes place to increase gas production [26,28].

There have been many technologies mentioned in the literature as potential treatments to convert waste into energy; however there is currently very little information about their specific application to digestate, and how this can be used as a feedstock in different thermal technologies. There is also limited information regarding the products than can be generated from this type of treatment, and no detailed composition. Therefore, it is uncertain which process can be suitable to treat this waste, and which other valuable products can be generated from.

Digestate has the potential to be valorised by using it as feedstock with different thermal technologies and by analysing and comparing the products resulting from this. However, it is crucial to know the composition is of this waste to understand its behaviour with each technology. Pyrolysis technologies were selected in this study because they are systems with favourable product separation and accessible product composition analyses. This project is focused on the assessment of using digestate from industry, and analysing its composition in order for it to be processed in different pyrolysis systems, then to examine and compare the products recovered. Therefore, it aims to identify not only the variability between each technology, but also how the pyrolysis products can be useful to generate further valuable chemicals or materials.

1.2 AIM AND OBJECTIVES

The aim is to assess thermal processes as alternative routes to valorise digestate as sustainable biomass in the circular economy and to evaluate the environmental benefits of integrating these technologies with anaerobic digestion. The objectives of this project are focused on evaluating digestate from industry and treating it through different pyrolysis systems:

1. Analyse and compare the liquid, solid and gaseous products from different pyrolysis systems utilising the same digestate as feedstock to evaluate and identify valuable compounds produced in each technology.
2. Develop a pyrolysis model based on thermal decomposition of lignocellulose and validate this by using the empirical data from analyses carried out in the pyrolysis processes.
3. Evaluate the theoretical applications of pyrolysis technologies based on kinetic models already tested with common biomass feedstocks, such as wood, in order to predict the main products from these thermal processing: gas, biochar, bio-oil.
4. Compare and evaluate the final model's results with experimental data to validate whether the model is viable to be used as a tool to obtain the possible outputs using the digestate composition.
5. Validate the kinetic model with experimental data from testing slow and fast pyrolysis processing on digestate feedstock at scale facilities available
6. Analyse and compare the liquid products from different pyrolysis systems in order to differentiate which components can be further employed to produce more valuable materials
7. Investigate process-system level opportunities and limitations for the implementation of the pyrolysis in an anaerobic digestion system

1.3 PROJECT OUTLINE

This project required a theoretical analysis based on understanding the principles of different thermal processing employed for treatment of common biomass. Therefore, it was crucial to identify how these could be implemented using digestate. Direct measurements were needed from experimental work, which consisted of determining digestate composition and testing it as a feedstock for thermal technologies to calculate yields of and examine the composition of the products obtained.

A model was developed in order to simulate pyrolysis of digestate and was evaluated and validated with the information and results from the experiments carried out.

Both sources, experimental data and modelling, have been employed for further evaluation to identify potential components in pyrolysis products that could be used to determine which technology can be the most suitable for the treatment of digestate, and how this can be integrated with an anaerobic digestion system.

The profile of this project is divided into different stages to cover the areas required for this assessment:

Stage 1. Theoretical analysis of thermal technologies

- 1.1 Principles of different pyrolysis systems including operational conditions
- 1.2 Biomass composition and treatment
- 1.3 Mechanism of lignocellulose decomposition

Stage 2. Digestate characterisation

- 2.1 Proximate and ultimate analysis
- 2.2 Lignocellulosic composition: cellulose, hemicellulose and lignin

Stage 3. Digestate as feedstock in pyrolysis facilities

- 3.1 Testing digestate in thermal processes at scale facilities available: slow, fast and microwave pyrolysis
- 3.2 Analysis of yield formation and composition of pyrolysis products
- 3.3 Comparison between products recovered from pyrolysis
- 3.4 Identification of main chemical groups of compounds in bio-oil for further analysis

Stage 4. Thermal process modelling

4.1 Selection of a scheme of reactions suitable for lignocellulosic decomposition in pyrolysis

4.2 Modelling the kinetic reactions selected through use of different compositions of common biomass feedstocks, and data published

4.3 Comparison of projected results with experimental work carried out at the facilities where waste has been pyrolysed

4.4 Adjustments to the kinetic model to be implemented with respect to the most predominant group of compounds in the products

Stage 5. Evaluation of potential uses for pyrolysis products

5.1 Evaluation, comparison and differentiation of components in the liquid products resulting from the same anaerobic digestion waste at equivalent conditions in different thermal technologies: slow, fast and microwave pyrolysis

5.2 Analysis of potential product components for further valuable material, fuel or chemical production

Stage 6. Evaluation of different scenarios to integrate pyrolysis into anaerobic digestion systems

6.1 Identification and selection of scaled-up systems in current operation to pyrolyse the amount of waste produced at Severn Trent sites

6.2 Projections of possible outputs of digestate industrial scale.

This diagram of this outline is shown in Figure 4.

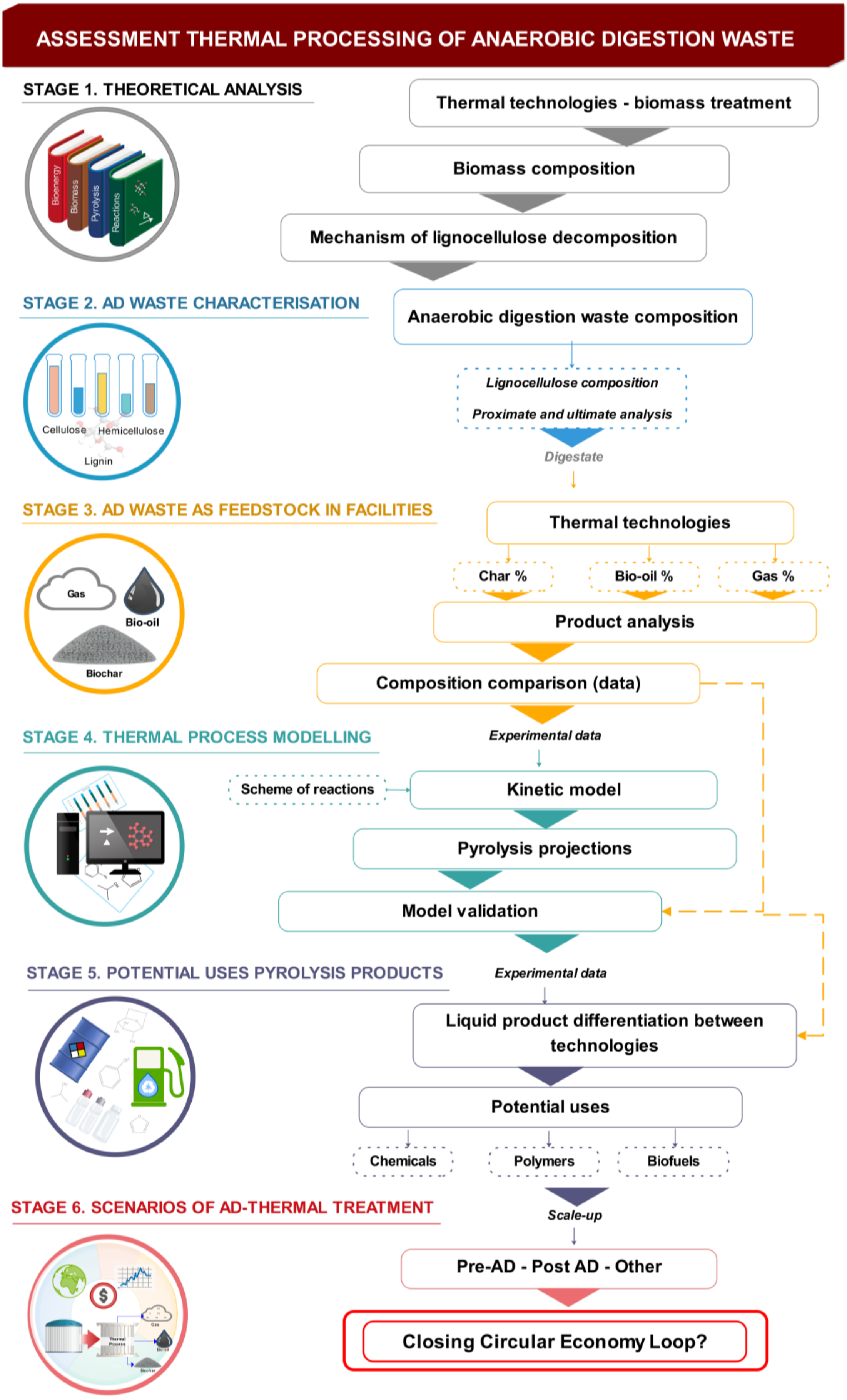
ASSESSMENT THERMAL PROCESSING OF ANAEROBIC DIGESTION WASTE
STAGE 1. THEORETICAL ANALYSIS
Bioenergy
Biomass
Pyrolysis
Reactions
Thermal technologies - biomass treatment
Biomass composition
Mechanism of lignocellulose decomposition
STAGE 2. AD WASTE CHARACTERISATION
Cellulose
Hemicellulose
Lignin
Anaerobic digestion waste composition
Lignocellulose composition
Proximate and ultimate analysis
Digestate
STAGE 3. AD WASTE AS FEEDSTOCK IN FACILITIES
Gas
Bio-oil
Biochar
Thermal technologies
Char %
Bio-oil %
Gas %
Product analysis
Composition comparison (data)
STAGE 4. THERMAL PROCESS MODELLING
Experimental data
Scheme of reactions
Kinetic model
Pyrolysis projections
Model validation
STAGE 5. POTENTIAL USES PYROLYSIS PRODUCTS
Experimental data
Liquid product differentiation between technologies
Potential uses
Chemicals
Polymers
Biofuels
STAGE 6. SCENARIOS OF AD-THERMAL TREATMENT
Scale-up
Pre-AD - Post AD - Other
Closing Circular Economy Loop?

Figure 4. Diagram of the outline of this research project.

CHAPTER 2. LITERATURE REVIEW

2.1 SUSTAINABLE DEVELOPMENT

In 2015 the United Nations recognised the urgency of actions to resolve current challenges the world is facing that have impacted negatively not only on the planet, but on people lives. This includes poverty, hunger, and rapid degradation of the planet due to uncontrollable consumption of natural resources, rapidly and unruly production of goods, and untreated waste resulting from the human activities. This plan is known as the 2030 agenda for sustainable development, and includes 17 sustainable development goals (SDGs), and 69 associated targets. These are represented by the icons shown in Figure 5.

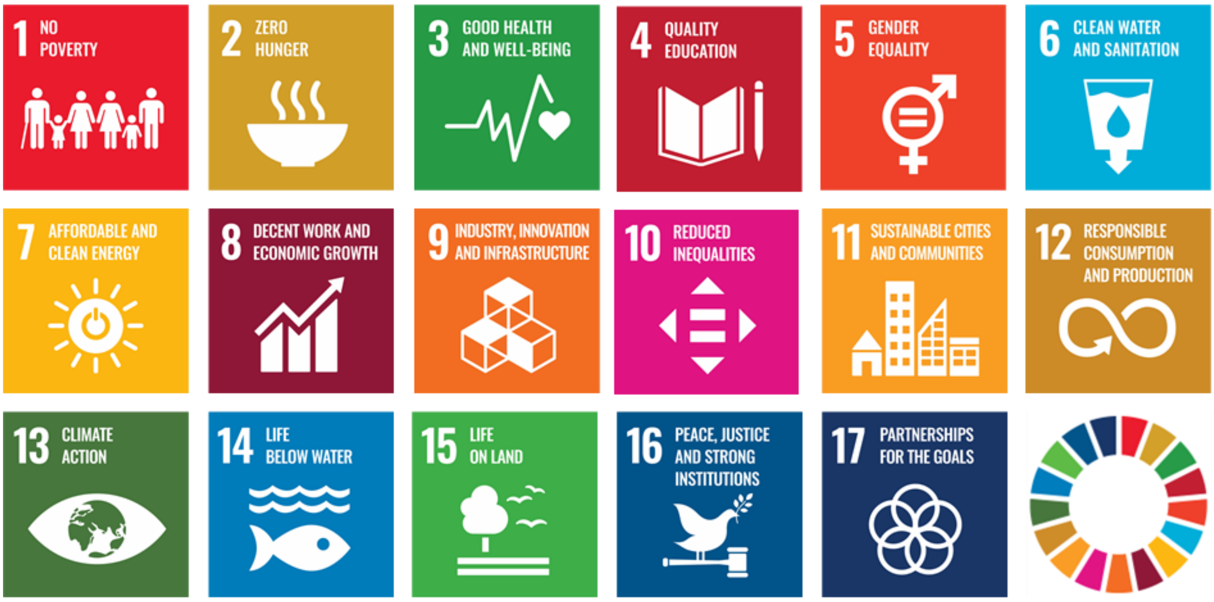
1 NO POVERTY
2 ZERO HUNGER
3 GOOD HEALTH AND WELL-BEING
4 QUALITY EDUCATION
5 GENDER EQUALITY
6 CLEAN WATER AND SANITATION
7 AFFORDABLE AND CLEAN ENERGY
8 DECENT WORK AND ECONOMIC GROWTH
9 INDUSTRY, INNOVATION AND INFRASTRUCTURE
10 REDUCED INEQUALITIES
11 SUSTAINABLE CITIES AND COMMUNITIES
12 RESPONSIBLE CONSUMPTION AND PRODUCTION
13 CLIMATE ACTION
14 LIFE BELOW WATER
15 LIFE ON LAND
16 PEACE, JUSTICE AND STRONG INSTITUTIONS
17 PARTNERSHIPS FOR THE GOALS

Figure 5. 17 Sustainable Development Goals (picture source: United Nations).

Goal 13 has been described as urgent action to tackle climate change and the impacts of this phenomenon [29]. This goal includes as main targets national polices, strategies and planning to mitigate this situation towards to net zero carbon emission.

According to the department for Environment and Food and Rural Affairs in the UK, in 2018 there were a total of 222.2 million tonnes of waste generated in the UK. The final treatment of this total waste was reported as:

- 108.4 million tonnes were recycled and recovered, which mainly included minerals and solids from the construction sector.
- 8.5 million tonnes were incinerated for energy recovery, mainly household waste.

- 7.3 million tonnes were just incinerated, which comprised household waste and other wates from industrial processes and sewage.
- 50.8 million tonnes ended in landfill, which was waste from household, soils and residues from sewage and industry.
- 25.7 tonnes were used as land treatment and released into water bodies, which were mainly from dredging spoils and mineral wastes.

Some of this waste included digestate because anaerobic digestion process was considered as intermediate treatment in this specific UK statistics on waste [30]. Exact information or data is not available on how much of this waste could be still usable for further treatment to generate valuable green products, goods or energy. More detailed information about current waste is needed relating to analysis or characterisation in order to find out which other alternatives routes could be implemented to continue using it.

2.2 CIRCULAR ECONOMY

The circular economy has promoted a different model of how the world could produce and consume in a way that keeps waste generation at the minimum possible. This scheme has been a key global effort to meet the 17 SDGs, and most nations have been working on strategies to analyse how waste production can be decreased. This also has a direct impact on carbon emissions reduction.

The European Commission for instance, released a new circular economy plan which includes a section called *Less waste, more value*. This promotes and enhances relevant requirements and encourages producers through incentives to implement better practices around waste recycling to reduce residual waste generation [31].

The traditional way to use natural resources is described as:

take → produce → consume → dispose

According to the Waste and Resources Action Programme (WRAP) and the European commission, materials and products must be used for as long as possible by sharing, reusing, repairing and recycling. They describe a circular economy as a non-linear linear process which has as a main objective to extend the life cycle of products and resources. This model is graphically represented in Figure 6.

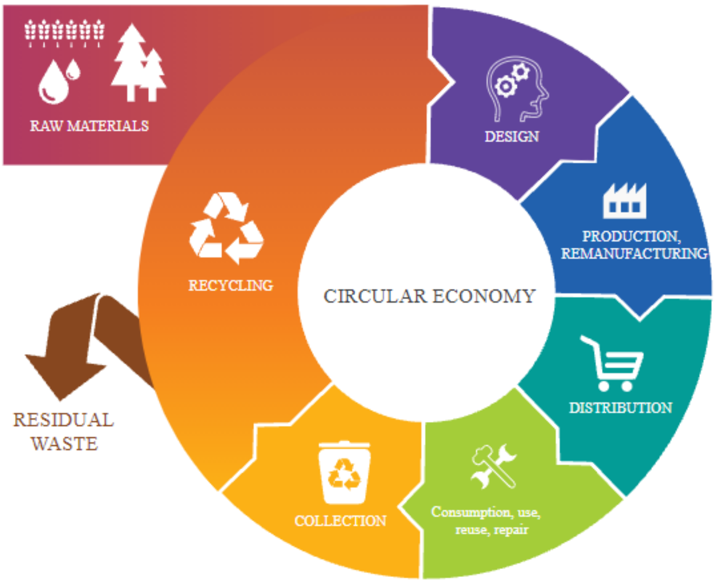
RAW MATERIALS
DESIGN
PRODUCTION, REMANUFACTURING
CIRCULAR ECONOMY
RECYCLING
DISTRIBUTION
Consumption, use, reuse, repair
COLLECTION
RESIDUAL WASTE

Figure 6. Symbol of circular economy representation (source European Parliament).

According to the International Energy Agency (IEA), anaerobic digestion (AD) has been one of the most simple bioprocesses to use waste to produce biogas, and is becoming a ‘green’ energy supply system [13]. Biogas is produced and used in a Combined Heat Power (CHP) system to generate renewable heat and electricity. Alternatively, this gas can be upgraded to be integrated into the gas grid. This system is being considered as a source of natural gas, which can be used to supply electricity to meet some of the current demand for households, industry and transport [32].

AD has been promoted as a key processing technology for green energy production, and digestate has been used mainly as fertiliser due to the nitrogen- and phosphorus-rich material content. This has been considered a net-zero emission system due to reuse of waste: digestate is employed to amend the soil where plants or crops are growing and then these are used for renewable energy generation. Some analysis of this cycle has already been carried out because this system also absorbs carbon dioxide as the vegetation growing in this soil is then improved/amended [33,34]. Since the loop including this waste is closed, it has the potential to form the basis of a genuine circular economy, and it can be represented as shown in Figure 7.

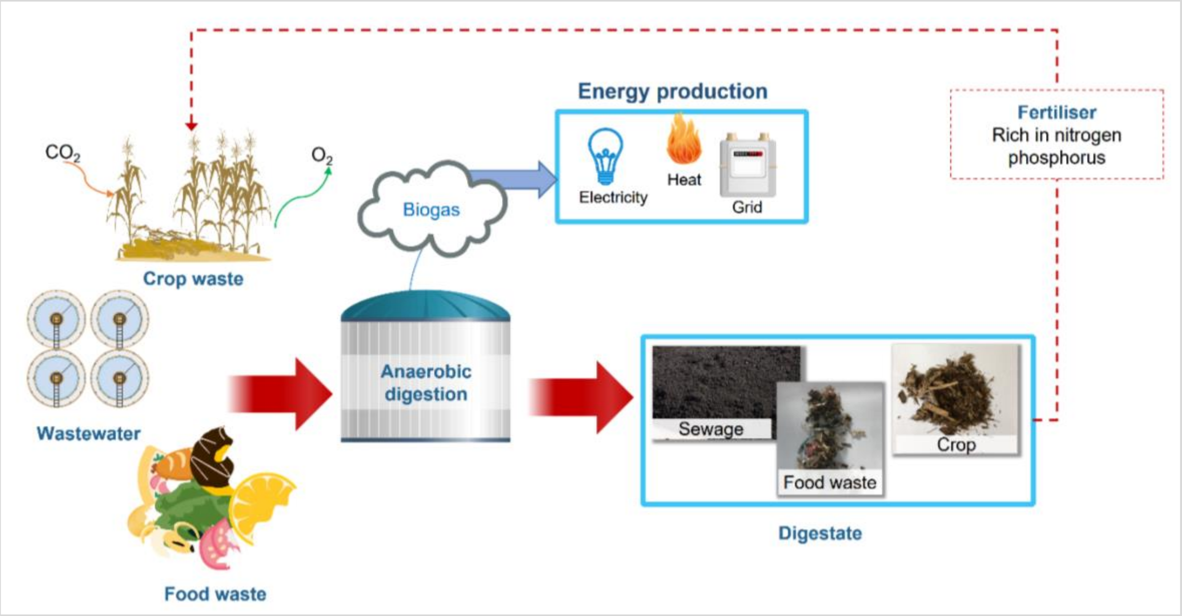

Figure 7. Diagram of a close loop of waste used to produce green energy through anaerobic digestion and the use of the final co-product, digestate, as fertiliser to amend the soil where this crop is growing.

Although this sounds promising, analysis of biobased fertilisers by Kataki et al. [35], mentioned that there are still barriers to implementation of this type of waste due to strict legislation, the lack of incentives for use of this for soil restoration and inadequate investment in research and design to complete a whole cycle of nutrient recovery. Despite the fact that this activity can have a positive impact on the environment due to soil improvement, some of this waste-based fertiliser needs to be transported which results in an additional cost to that of spreading it on the soil, and sometimes then the process has no profit for the producers. These practices also have a negative impact on the digestate effectiveness. Ammonia can arise from digestate, which could lead to emissions and air quality issues in the area where it is utilised [36]. In order to address this, BEIS has released a strategy where more technologies will be analysed to be implemented and reduce the ammonia emissions from digestate utilisation as soil amendment [15].

Changes in the perception of waste as a valuable material for further uses is also needed. According to the United Nations and the 17 SDGs, human education and awareness of climate change is crucial in mitigating and reducing the impact climate change is having. Then, digestate as biomass can be used as a source for additional green processing where alternative products can be obtained, and there is the possibility to reduce the use of fossil and its derivatives. More alternative routes need to be evaluated to exploit this digestate as a main source of raw material for industry revenue. A current disadvantage of this system is the lack of characterisation in all anaerobic digestate waste streams, when it is important to know what is going into the system and what is currently being processes to produce the biogas to identify if there are other components that could be possible recovered.

2.3 USES OF BIOMASS

According to the U.S. Department of Energy, biomass is organic material from plants that can be a source of renewable energy [37]. Due to its diversity and availability, it is considered as supplementary to some fossil fuel derivatives used, for instance in transportation. Examples of biomass are industrial wastes, crop wastes, food waste, municipal solid waste, animal manure and human sewage. Their utilisations depend on their composition, and this can vary between amounts of lipids, starches, lignin, cellulose and hemicellulose. Usually, biomass that contains a large amount of lipids such as oil and wax, commonly non-woody biomass, is suitable for biodiesel production [38]. Shell, for instance has a process called HEFA (hydroprocessed esters and fatty acids) which converts waste and residues such as vegetable oil processing waste, fish fat waste and technical corn oil into renewable diesel and sustainable aviation fuel [39]. Shell is currently working with Neste to increase its production of a biofuel called Neste MY Sustainable Aviation Fuel^{TM}, used currently by Lufthansa and KLM. These companies are continuing research to reuse other waste such plastics and lignocellulosics, and valorisation of municipal solid waste.

Biomass with high cellulose, hemicellulose and lignin content is termed ‘lignocellulosic’ material and it can be utilised to produce different biofuels. Lignocellulose is not soluble in water, but some components can be broken down by hydrolysis into fermentable components. Glucose, which is what cellulose is mainly formed of, once is hydrolysed this can be used to produce bioethanol [38,40,41]. However, lignin is a challenging material to convert into other components to produce biofuels due to its complex structure, requiring a higher energy in order to be depolymerised. Thus, in fermentation processes the whole lignin is found as part of the residue left afterwards [40,41]. Although lignin is not a suitable feedstock for fermentation, thermal processes such as pyrolysis can be potential methods for biofuel production where all the lignocellulosic components can be utilised. Lignin derivatives have been investigated for the production of biobased materials through extraction or thermal processing. Applications such as wastewater treatment, biomedicine, emulsion stabilisers and paint and coatings are also under development for different types of lignin derivatives [42,43].

2.4 BIOMASS DECOMPOSITION IN PYROLYSIS

The principles of pyrolysis have been mainly based on the thermochemical conversion of the lignocellulosic material contained in biomass, resulting in the production bio-oil, biochar and gas. The proportion of each component changes depending on the type of the biomass and its origin. Wood, for instance, is one of the most common materials used in pyrolysis. The ranges of lignocellulose content in woody biomass are 25-30 % lignin, 35-50% cellulose, and 20-30% hemicellulose. This woody biomass can also be classified as hardwoods and softwood depending on the biological origin. Harwoods are those scientifically called angiosperms because they produce leaves and seeds. Softwoods are known as gymnosperms which produce cones [18,40,44].

The yield of products in this process will depend on many factors such as lignocellulose proportion, water and ash content, and operating parameters such as temperature, heating rate, and residence time within the heating system. As highlighted previously there are three different classification of conventional pyrolysis: slow, fast, and flash, which not only vary between the range of temperatures but other operating conditions [18,45,46].

Slow pyrolysis consists of heating the feedstock with a residence time range between 5 and 30 minutes. Due to the large period during which the biomass is subjected to these high temperatures, more reactions take place where the products formed can be cracked resulting in higher formation of biochar and gas. This type of pyrolysis is employed when the main target is biochar generation, and bio-oil formed from slow pyrolysis is generally considered to be a low-quality product [18,45,47]. One of the main drivers of employing this biochar in the market is its potential uses in carbon sequestration; which brings out improvements in the soil structure or bioremediation. However, the main challenge with this approach is the regulations around using biochar in soils [47,48]. A whole analysis of biochar is required to understand more about its chemical composition and avoid possible contaminants. On the other hand, some studies consider biochar as biofuel for energy production in substitution for coal due to its similar composition, and the fact that it can be used in a combustion chamber [48,49]. This could be considered as an appealing option, but must be considered at system-level alongside the alterative of burning the raw biomass.

Fast pyrolysis, in contrast, is employed to produce bio-oil as a main pyrolysis product. It uses a high heating rate and a short processing time, resulting in more condensable product which needs to be recovered to avoid subsequent reactions with the produced biochar. The condensed vapour forms bio-oil once it is cooled down. The typical yields of pyrolysis products (by weight) are 60-75% bio-oil, 15-25% solid biochar and 10-20% non-condensable gases [18,45]. One of the main requirements of this thermal process is that the feedstock particle size is reduced to enable sufficient heat transfer to take place within the required low residence time. This typically means that biomass must be shredded and milled to less than 3mm. Larger particle sizes can result in higher production of biochar and water [50,51].

Finally, flash pyrolysis has a much higher heating rate than other the two processes. It has the specific characteristics of rapid devolatilisation and a requirement of higher temperatures for the reactions. The residence time of the gas is less than one second with a yield of 75% bio-oil. Although this process looks promising because of the bio-oil production, it has the disadvantage of having low thermal stability. In addition, this flash pyrolysis produced bio-oil has highly corrosive properties [18,45,48].

The typical parameters and possible product yields for these pyrolysis processes are shown in Table 1.

Pyrolysis	Residence time (s)	Heating rate (ºC/s)	Particle size (mm)	Product yield (wt %)		
				Bio-oil	Biochar	Gas
Slow	450-550	<10	5 -50	20-40	25-35	25-35
Fast	0.5-5	10-200	<3	60-75	15-20	15-30
Flash	<0.5	450-1000	<0.2	75	12	13

Table 1. Pyrolysis parameters and yield of products [18,19,45,52].

In order to maximise biomass conversion and increase pyrolysis performance, the feedstock typically needs pre-treatment steps such as drying and pelletising. Firstly, moisture content should be in a range of 5% and 10% weight basis because high water amount in biomass is a barrier to obtaining products with greater quality. This moisture has a direct impact on the heat and energy used to decompose the main elements of the biomass. If the amount of water is high, the energy requirements will be increased. Some energy would be needed for pyrolysis of the biomass, but more would be also needed to evaporate this excess water, and that could also lead to losses of organics [53,54]. Secondly, size of particles has an impact on product yield. Small particles, for instance, allow rapid reactions to take place due to high heat transfer [45,55].

2.4.1 PYROLYSIS REACTORS

There are several reactor configurations that can be implemented for these processes. Slow pyrolysis is usually performed in fixed bed or rotary kiln reactors due to high yields of biochar, long residence times and ability to process larger particles sizes [56,57].

Fluidised beds can provide a bubbling and circulating mechanism, and they have been widely evaluated for fast pyrolysis. Implementation of this type of reactors has resulted in reliable data to predict possible yields of the products obtained from this specific process. The thermal reactions occur consistently and can be controlled throughout the reactor, inducing a high yield of bio-oil. In some cases, the liquid yield can reach almost 75% wt [18,19,50]. Bed material is typically sand and the main function of this is to avoid accumulation of the biochar formed across the reactor [58].

According to a study carried out by the International Energy Agency (IEA), where 16 laboratories work in collaboration to evaluate reactors and improve pyrolysis efficiency in order to increase quality of the bio-oil generated, the bubbling Fluidised beds with hot vapour filtration had the best results to be implemented for fast pyrolysis [59]. However, reactor selection to treat biomass depends the target product and application [18,55]. Advantages and disadvantages of some of the reactors mentioned with their range of bio-oil yields are shown in Table 2.

Reactor type	Advantages	Limitations	Bio-oil yield
Fixed bed	Simple design, reliable and biomass size independent	Long solid residence time, difficult to remove biochar	35-50%
Bubbling fluidised bed	Simple design, easy operation and suitable for large scale	Small particle sizes are needed	70-75%
Circulating fluidised bed	Well-understood technology, good control and large particle sizes can be used	Suitable for small scale, but complex hydrodynamics, biochar is finer	70-75%

Table 2. Some characteristics of bed reactors used in pyrolysis [19].

Although the technology that generates these three different products has been described as promising, there is still a great gap in the research about the exact composition of pyrolysis products, primarily of the liquid product. Compounds in bio-oil can change depending on the feedstock utilised, the heating rates employed and the operation temperatures used through pyrolysis systems. In addition, most of the literature about pyrolysis remarks that a high yield of bio-oil can be produced, but that it can have a high content of water [60-64]. In some cases, the liquid product of pyrolysis has been analysed on dry basis to determine its chemical composition, yet it has still not been explained in detail or evaluated as to how the composition of bio-oil could be impacted when this procedure is implemented.

A further challenge associated with circulating or fluidised beds is the need for small and well-controlled particle size. This inevitably required pre-treatments steps and presents an additional challenge in that the solid char needs to be disengaged from the hot pyrolysis vapours before further decomposition occurs. The process flowsheet for a system of this type is much more extensive than a single reactor vessel, and is further complicated by the requirement to supply and pre-heat a high flowrate of inert gas. For this reason, the economics of the process will require high value products in order to offset the relatively high capital cost. The challenges that accompany circulating and fluidised beds have led to the investigation of different technology approaches to carry out pyrolysis.

Microwave pyrolysis is considered as an efficient method to process lignocellulosic material to produce high quality of liquid, with a high organics content due to a different mechanism of heating. According to some research, heat transfer occurs from the centre of the biomass due to molecular interaction with an electric field and, then the gases produced, condensable and non-condensable, go through zones with lower temperatures in the biomass, avoiding these gases taking place in secondary reactions. This is different from conventional pyrolysis where heat travels from the surface into the centre, and the organic compounds generated are in contact with high temperatures. This could cause the products to be converted into additional or other molecules [65,66]. An illustrative representation of heat transfer for both pyrolysis process is shown in Figure 8.

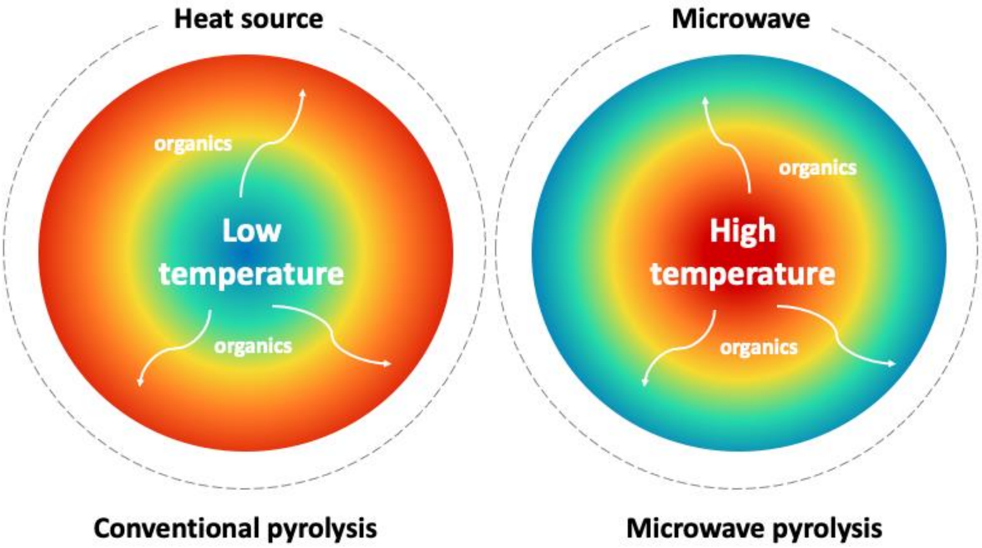

Figure 8. Heating mechanism and temperature distribution in conventional and microwave pyrolysis of wood. Diagram modified from Miura et al. [66].

Due to this microwave mechanism, some organics are produced in higher yields when biomass such as wood is pyrolysed. It is important to consider that these results have been obtained from experiments performed with woody material with a low ash content of around 1-3% wt [67,68]. A major advantage of microwave processing routes over conventional fluidised beds is that the heating is volumetric; that means that there is no heat transfer limitation and therefore high heating rates can be achieved with large particle sizes – far larger than those that can be used in fluidised beds. The logical consequence of this phenomenon is that pre-treatment is not required to the same extent, solid/vapour disengagement is much simpler and the inert gas does not need to be heated or supplied at a high flowrate. As a result, microwave pyrolysis has the potential to transform the product quality, the process flowsheet and the corresponding economics. Although, there is few information about industrial scale, where tonnes of waste could be treated through this technology.

2.5 MECHANISMS OF THERMOCHEMICAL DECOMPOSITION OF LIGNOCELLULOSE AND STARCH

Most of the pyrolysis systems have been studied and employed based on lignocellulose conversion. The thermochemical decomposition of each lignocellulosic compound occurs at different temperatures as they have different structures as shown in Figure 9.

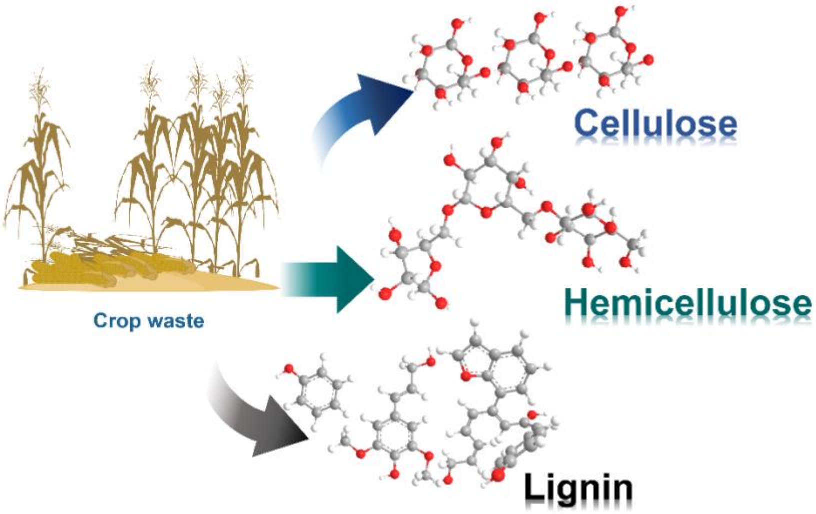

Figure 9. Structure of lignocellulosic material: cellulose, hemicellulose, and lignin.

When this type of biomass is subject to a thermal treatment, the first component to be broken down is hemicellulose, followed by cellulose and finally lignin. The range of temperatures in which each component is decomposed in conventional thermal treatment is shown in Table 3, where some of the key chemicals produced are also presented.

Component	Temperatures of decomposition (ºC)	Chemicals produced
Hemicellulose	200–260	furfural
Cellulose	240–350	levoglucosan
Lignin	280–500	phenolics

Table 3. Ranges of temperatures of lignocellulosic material thermochemical decomposition and key chemicals produced in bio-oil pyrolysis [69,70].

Bio-oil produced from pyrolysis of lignocellulosic material has been studied due to the large amount of chemical compounds formed, and the interest of generating further usable bioproducts under the concept of biorefinery. It has been found that this liquid has chemical groups such as acids, sugars, alcohols, aldehydes, ketones, pyrans, phenolics, and sometimes even hydrocarbons [71-73].

Some pathways have been studied to determine which specific compounds are formed directly from each lignocellulosic compound, without secondary reactions. Cellulose could mainly produce sugars, such as levoglucosan or glucopyranoses. These can be further employed for biofuel production [43]. Furfural has been found as a main product from hemicellulose and it has been used for other chemical formulations [74,75]. Phenolics such as cresols, catechols and guaiacols are formed from lignin [76].

Even though all of these compounds mentioned can be produced in primary reactions during the thermal decomposition of lignocellulose, there are additional small molecules released through the conversion of solid biomass into pyrolysis products; for example, acetic acid, formic acid, water, carbon dioxide and carbon monoxide [74,77]. An illustration of a pathway of cellulose decomposition through pyrolysis is presented in Figure 10, for hemicellulose in Figure 11, and for lignin in Figure 12.

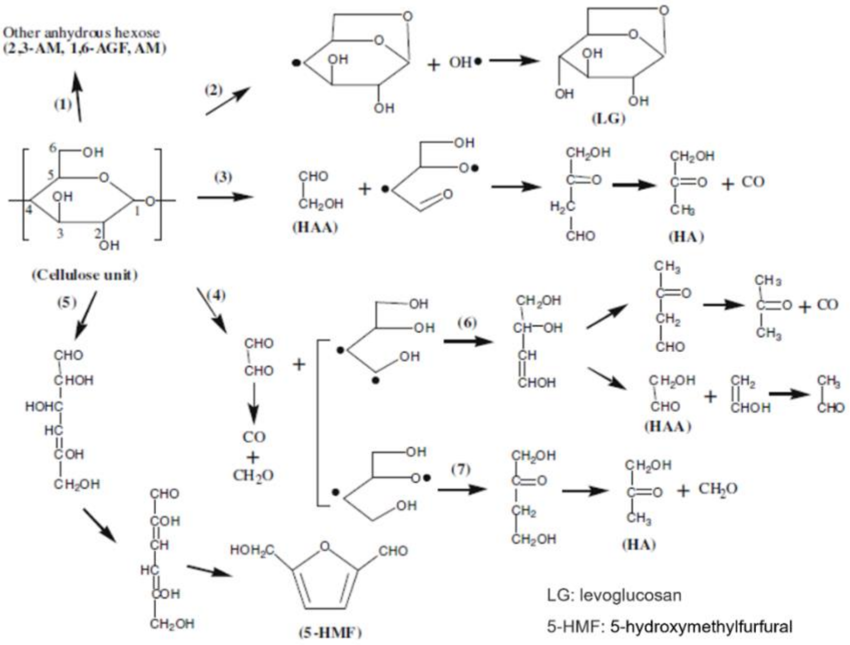
Other anhydrous hexose (2,3-AM, 1,6-AGF, AM)
(1)
(2)
(3)
(4)
(5)
(6)
(7)
(Cellulose unit)
(LG)
(HAA)
(HA)
(5-HMF)

LG: levoglucosan
5-HMF: 5-hydroxymethylfurfural
HAA: Hydroxyacetaldehyde

Figure 10. Pathway of direct cellulose conversion into primary compounds proposed by Shen et al. [43].

According to the scheme proposed by Shen and Gu, cellulose conversion into levoglucosan has four additional reactions that occur at the same time to generate 5-hydroxymethylfurfural, other hexoses, hydroxyacetaldehyde, formaldehyde (CH_2O), and others.

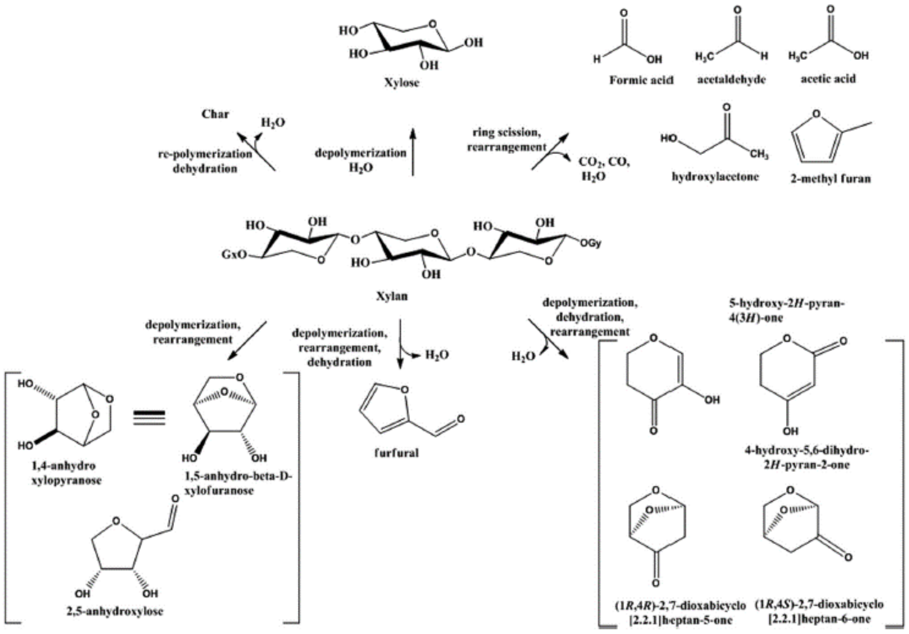
Xylose
Formic acid
acetaldehyde
acetic acid
Char
re-polymerization dehydration
depolymerization H2O
ring scission, rearrangement
CO2, CO, H2O
hydroxylacetone
2-methyl furan
Xylan
depolymerization, rearrangement
depolymerization, rearrangement, dehydration
depolymerization, dehydration, rearrangement
1,4-anhydro xylopyranose
1,5-anhydro-beta-D-xylofuranose
2,5-anhydroxylose
furfural
5-hydroxy-2H-pyran-4(3H)-one
4-hydroxy-5,6-dihydro-2H-pyran-2-one
(1R,4R)-2,7-dioxabicyclo [2.2.1]heptan-5-one
(1R,4S)-2,7-dioxabicyclo [2.2.1]heptan-6-one

Figure 11. Scheme of hemicellulose primary conversions proposed by Patwardhan et al. (Figure as published in Zhou et al. [78]).

The scheme presented by Patwardhan et al. [79], also shows that during hemicellulose conversion there are small molecules produced such as water, acetic acid, formic acid and, gases such as carbon dioxide (CO_2).

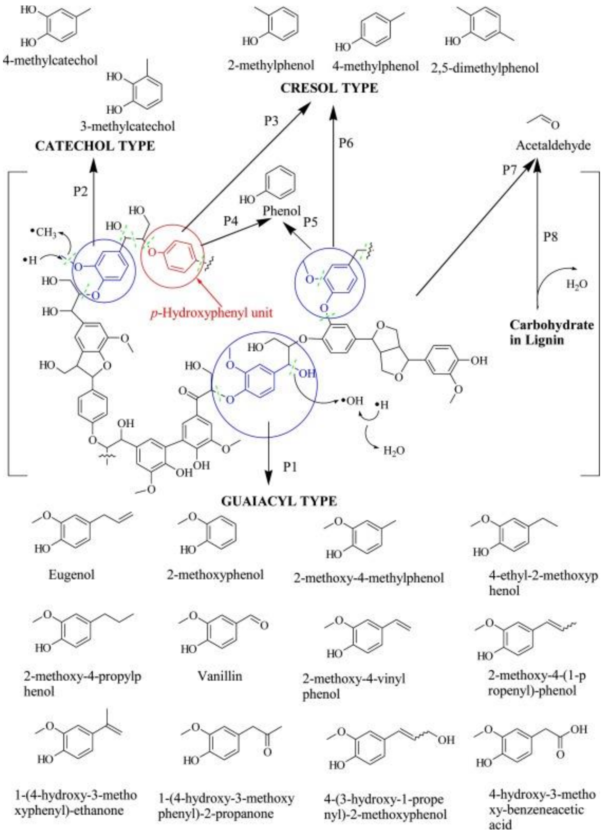
4-methylcatechol
3-methylcatechol
CATECHOL TYPE
2-methylphenol
4-methylphenol
2,5-dimethylphenol
CRESOL TYPE
Acetaldehyde
P2
P3
P4
P5
P6
P7
P8
Phenol
•CH3
•H
p-Hydroxyphenyl unit
H_2O
Carbohydrate in Lignin
•OH
•H
H_2O
P1
GUAIACYL TYPE
Eugenol
2-methoxyphenol
2-methoxy-4-methylphenol
4-ethyl-2-methoxyphenol
2-methoxy-4-propylphenol
Vanillin
2-methoxy-4-vinyl phenol
2-methoxy-4-(1-propenyl)-phenol
1-(4-hydroxy-3-methoxyphenyl)-ethanone
1-(4-hydroxy-3-methoxy phenyl)-2-propanone
4-(3-hydroxy-1-propenyl)-2-methoxyphenol
4-hydroxy-3-methoxy-benzeneacetic acid

Figure 12. Pathway proposed by Supriyanto et al. [80] of lignin converted into some phenolics through pyrolysis.

Supriyanto et al. [80] present some phenolics formed from lignin when thermochemically treated, releasing small molecules such as water and acetaldehyde, similar to what occurs with the conversion of cellulose and hemicellulose.

Identifying exactly where each compound found in bio-oil comes from is challenging given the great variation in biomass composition, and other factors that can have an influence in how the reactions occur. Ash is an inorganic material that can be found in the biomass. This also has a direct impact on some of the chemicals formed during pyrolysis and can effect changes according to the amount which could be present. Ash is a initiator of secondary reactions, and catalytic reactions can take place during pyrolysis when this material is present with the biomass [81].

Ash is one of the reasons an exact pathway for lignocellulose decomposition does not exist. Most of the schemes are based on ash-free and moisture-free biomass, and compounds such as furfural, levoglucosan, and phenolics are key indicators of how lignocellulose can be converted into smaller molecules.

2.5.1 BIO-OIL COMPOSITION FROM DIFFERENT BIOMASSES

Pyrolytic bio-oil composition changes not only between pyrolysis technologies, but among biomasses employed as feedstock. Fast pyrolysis has been the most studied due to a high bio-oil yield, especially that resulting from woody material which has been the most commonly-studied and accessible biomass.

Oasmaa et al. [71] presented experiments with fast pyrolysis systems including the chemical analysis of bio-oil from wood, and other biomass. Pine sawdust, for instance, with a composition of around 40% cellulose, 20% hemicellulose and 30% wt lignin [82] and less than 1% ash, was used in a 1kg/h fast pyrolysis reactor with temperatures ranging from 480-520ºC. The pyrolytic bio-oil containing 10.5% water and 62% organics, and the chemical composition had a distribution of around 5.6% acids, less than 1% alcohols, 45.3% sugars and 20% phenolics [83,84]. Negahdar et al. [85] used pine in a fast pyrolysis system at 500ºC and the produced oil contained 0.27% alcohols, 4.90% acids, 7.05% sugars and just 1.8% wt phenolics. The results are difficult to compare because of the lack information about bio-oil phases by Negahdar et al. [85], and a lack of characterisation of the lignocellulosic make-up of the biomass. However, there are specific groups and compounds that are in close agreement between the two studies. Alcohols and acids were very similar, and levoglucosan was detected in similar amounts in both analyses (between 4% and 6% wt).

Other woody materials have been also processed through pyrolysis technologies which have similar lignocellulose composition. Beech and poplar wood for instance, with cellulose around 45-50%, 25-32% hemicellulose, 22-24% lignin and 0.3-0.9% ash, were employed by Auersvald et al. [86] in a fast pyrolysis apparatus at 550ºC, resulting in a bio-oil yield of 60% with an water of 9.5%. Total organics identified and quantified were around 22% from beech and 20% from poplar with 1.4% and 1.13% alcohols, 10.04% and 4.72% acids, 3% and 4% phenolics, 5.1% and 7.7% aldehydes and ketones, and around 2% wt furans from both biomasses. Levoglucosan was produced in 1.3% from beech and 0.8% from poplar. There was a very low amount of furfural, less than 0.2%, and acetic acid was detected in large amounts from beech (9.63%) compared with the other wood (4.28%).

Studies on microwave pyrolysis with woody material have showed high yields in more primary compounds from lignocellulosic material, such as levoglucosan, furfural and some phenolics. Robinson et al. [25] presented a comparison between bio-oil resulted from experiments carried out with conventional and microwave pyrolysis using European Larch (Larix decidua) woodchips, which according to Bardak et al. [87] this wood has an average lignocellulose composition of 49% cellulose, 19% hemicellulose and 27% lignin and 0.3% wt ash. The conditions were 500ºC as operating temperature for conventional pyrolysis and a range of 2.2−2.5 kJ/g as energy input for microwave pyrolysis. Levoglucosan was produced in around 52 g/kg using microwave pyrolysis, whereas using conventional pyrolysis only around 5 g/kg was obtained, and furfural was produced in 7 g/kg and only 0.6 g/kg respectively. Although acetic acid was formed in high proportion in both pyrolysis in a range between 24-28 g/kg, there were significant differences in phenolic production between these technologies. Catechol, eugenol, and phenol, for instance, were generated in very small amount with conventional pyrolysis, less than 1 g/kg, whereas microwave pyrolysis produced 4.16, 1.42 and 1.39 g/kg respectively.

This woody material mentioned has a similar proportion of lignocellulosic material, however there might be other factors that lead to some variation between bio-oil composition obtained from these thermal technologies such as biomass pre-treatment (drying, pelletising, size particle). Although, some pyrolysis technologies such as microwave could be employed to obtain more primary compounds in bio-oil from wood which has shown higher yields, acid production could indicate there are other compounds could be decomposed during this thermal processing. A summary of pyrolysis treatment of woody material is presented in Table 4.

Biomass	Pine		Beech	Poplar	European Larch	
	Negahdar et al. [85]	Oasmaa et al. [84]	Auersvald et al. [86]		Robinson et al. [25]	
Pyrolysis	Fast 500ºC		Fast 550ºC		Fast 500ºC	Microwave 2.2–2.5 kJ/g
Cellulose (wt %)	-	40	46	51	49	
Hemicellulose (wt %)	-	20	32	25	19	
Lignin (wt%)	25	30	22	24	27	
ash (wt %)	<1	0.2	0.3	0.9	0.3	
Bio-oil key compounds	wt %		wt %		g/kg	
Levoglucosan	6	4.1	1.35	0.76	4.49	52.42
Furfural	0.24	0.22	0.32	0.43	0.59	7.22
Acetic acid	4.58	2.61	9.63	4.28	24	28.32
Guaiacol	0.5	0.24	0.16	0.27	0.53	4.49
Syringol	0.2	0.03	0.23	0.29	-	-
Catechol	0.22	0.02	0.1	0.9	0.7	4.16
Phenol	0.06	0.02	0.1	1.22	0.47	1.39

Table 4. Summary of bio-oil generated from woody material through pyrolysis technologies (Data is presented as published by the authors).

Other non-wood biomasses have been employed in pyrolysis processes to produce bio-oil. These results differ from wood-based material due to the physical structure, lignocellulose proportion and other compounds found in the biomass such as starch and pectin. Fast pyrolysis performed by Guo et al. [88] using rice husk with 37.15% cellulose, 23.87% hemicellulose, 12.84% lignin and 7.55% wt ash with a range of operating temperatures between 450ºC and 550ºC had 46.36% wt. bio-oil yield with 31% of water content. Chemical compounds such as acetic acid, furfural, levoglucosan, phenol and eugenol were found in around 14%, 3%, 6%, 4% and 2% wt respectively. Similar experiments were carried out by Alvarez et al. [89] who also employed rice husk but with an ash content of 12.9% wt, with temperatures in a range of 400-600ºC for fast pyrolysis. The yield of the water was 22-24% at 450-600ºC. The acid concentration was 8.4% at 450ºC and 6% at 600ºC, aldehydes and ketones were 2.18% and 2.08%, phenols 9.31% and almost 12%, furans 4.19% and 3.83% and sugars 1.12% and 1% wt. Both studies showed a very small amount of sugars and high acid production compared with woody material. However, phenolics were found in much higher proportion.

Other analyses have been done in microwave pyrolysis for bio-oil production from non-wood based biomass. Kostas et al. [90] and Rios-Del Toro et al. [91] performed experiments in a similar microwave pyrolysis system using olive pomace and agave tequilana bagasse respectively. The lignocellulose distribution and ash content in olive pomace was 15.9% cellulose, 13.6% hemicellulose and 27% lignin with 1.6% wt ash, and the agave had 55.08% cellulose, 12.44% hemicellulose and

13.12% lignin with 6.9% wt ash. Both biomasses were ground and densified in a pellet press. Although the agave had more cellulose, no levoglucosan was reported, contrary to olive pomace which produced a maximum of 1.3%. Acetic acid production was considerably high, around 70% from olive pomace pyrolysed and around 30-40% from agave. A small amount of furfural was reported by Kostas et al. [90] but none was detected from agave. However, 3.7-4.5% 3-furaldehyde was quantified which could be formed from the decomposition of hemicellulose as furfural (2-furaldehyde). Although olive pomace had more lignin, phenolic generation was lower than agave. The condensed information of these studies is presented in Table 5, which includes some key marker compounds.

Biomass	**Rice husk**		**Olive pomace**	**Agave tequilana bagasse**
	Guo et al. [88]	Alvarez et al. [89]	Kostas et al. [90]	Rios-Del Toro et al. [91]
Pyrolysis	Fast 400-600^{o}C		Microwave 2.3–3.5 kJ/g	Microwave 500- 1000W input
Cellulose (wt %)	37.15	-	15.9	55.08
Hemicellulose (wt %)	23.87	-	13.6	12.44
Lignin (wt%)	12.84	-	27	13.12
Ash (wt %)	7.55	12	1.6	6.9
Bio-oil key compounds	wt %		wt%	
Levoglucosan	5.46	0.4-0.7	0.6-1.3	-
Furfural	3.18	-	0.2-0.5	-
Acetic acid	13.49	0.03-0.8	70-72	32-40
Guaiacol	1.71	-	0.2-0.4	0.9-1.4
Syringol	1.44	-	0.9-1.3	3.3-5.2
Catechol	0.22	1.3-2.3	-	-
Phenol	3.59	1-2.8	0.2-0.4	-

Table 5. Summary of bio-oil generated from non-woody material through pyrolysis technologies (Data is presented as published by the authors).

The significant difference between wood-based and non-wood-based biomass is the amount of ash. Although in all the cases the material is pre-treated before being pyrolysed (grinding, pelletising), wood resulted in more primary compounds such as levoglucosan from cellulose and furfural from hemicellulose. Only Guo et al. [88] reported large amount in bio-oil from rice husk even though this material was ground to get a particle size of 0.45-1 mm.

Ash could therefore influence the pyrolysis product composition, however further analysis and evaluation of biomass with a high ash content is needed. Detailed examination of pyrolysis products is required to validate whether this inorganic material could affect other compounds during lignocellulose decomposition and differentiate which other products could be formed from this.

2.5.2 STARCH THERMAL DECOMPOSITION

Starch can be found in different biomass and can be classified according to its sources, for example maize, corn, rice or potato. It is mainly structured from hexose molecules such as glucose, and it has been found that this can be thermochemically decomposed at temperature of between 200-400°C, the exact level of which depends on the source [92]. When this material is subject to thermal processing compounds such as acetic acid, hydroxyfurans, levoglucosan, methane (CH_4) and carbon dioxide (CO_2) can be formed [93,94]. There are a few studies about the decomposition of this starch in the presence of other composites that biomass could contain. Zong et al. [95] analysed the decomposition of six components at different heating rates: starch, cellulose, hemicellulose, protein, lignin and oil. According to the experiments they performed, these materials produced water, due to dehydration and crosslinking biomass polymers. The first decomposed was hemicellulose, the next starch, followed by oil, cellulose and protein with a similar approach, and with lignin as the final compound. Total conversion of starch in this analysis is at around 400°C and there is a high production of CO_2 and H_2O. Levoglucosan produced from starch, in runs carried out at 550°C with a heating rate of 1°C/s, was much lower than the amount detected with cellulose and this, could indicate that although starch is a glucose-like material, pyrolysing it can lead to formation of smaller molecules, rather than producing more levoglucosan. This could indicate that this type of material could generate more H_2O and CO_2 at higher temperatures and this should be considered when a waste is thermochemically decomposed for product quantification.

2.6 SCHEMES OF KINETIC REACTIONS OF BIOMASS DECOMPOSITION DURING PYROLYSIS

Lignocellulosic decomposition in pyrolysis is a complex process to be analysed, not only because many reactions take place during the thermal decomposition but also temperature, time of residence, lignocellulosic composition, heat transfer, inorganics content, and particle size.

Different schemes of reactions have been developed to demonstrate, in simplified schemes, how biomass is thermochemically decomposed and which possible products could be formed. Through the years, pyrolysis reactions have been evaluated by qualitative means, where experimental work has been carried out based on sample properties, biomass varieties, and at different conditions.

A scheme of reactions has been used for many simulations and projections for pyrolysis. This is based on the three main lignocellulosic components and three pseudo-lignins: lignin rich in carbon (LIG-C), lignin rich in hydrogen (LIG-H), and lignin rich in oxygen (LIG-O). This scheme was proposed in 2008 by Ranzi et al. [96] and, is a multicomponent mechanism based on the volatilisation of the cellulose, hemicellulose and pseudo-lignins. This scheme includes consideration of the parameters of mass transport and resistances during the biomass decomposition. It consists of 18 reactions for fast pyrolysis, and has been employed in fluidised bed reactors. The reactions are shown in Table 7, where A is the frequency or pre-exponential factor, independent on temperature, and E (kJ/mol) is the activation energy.

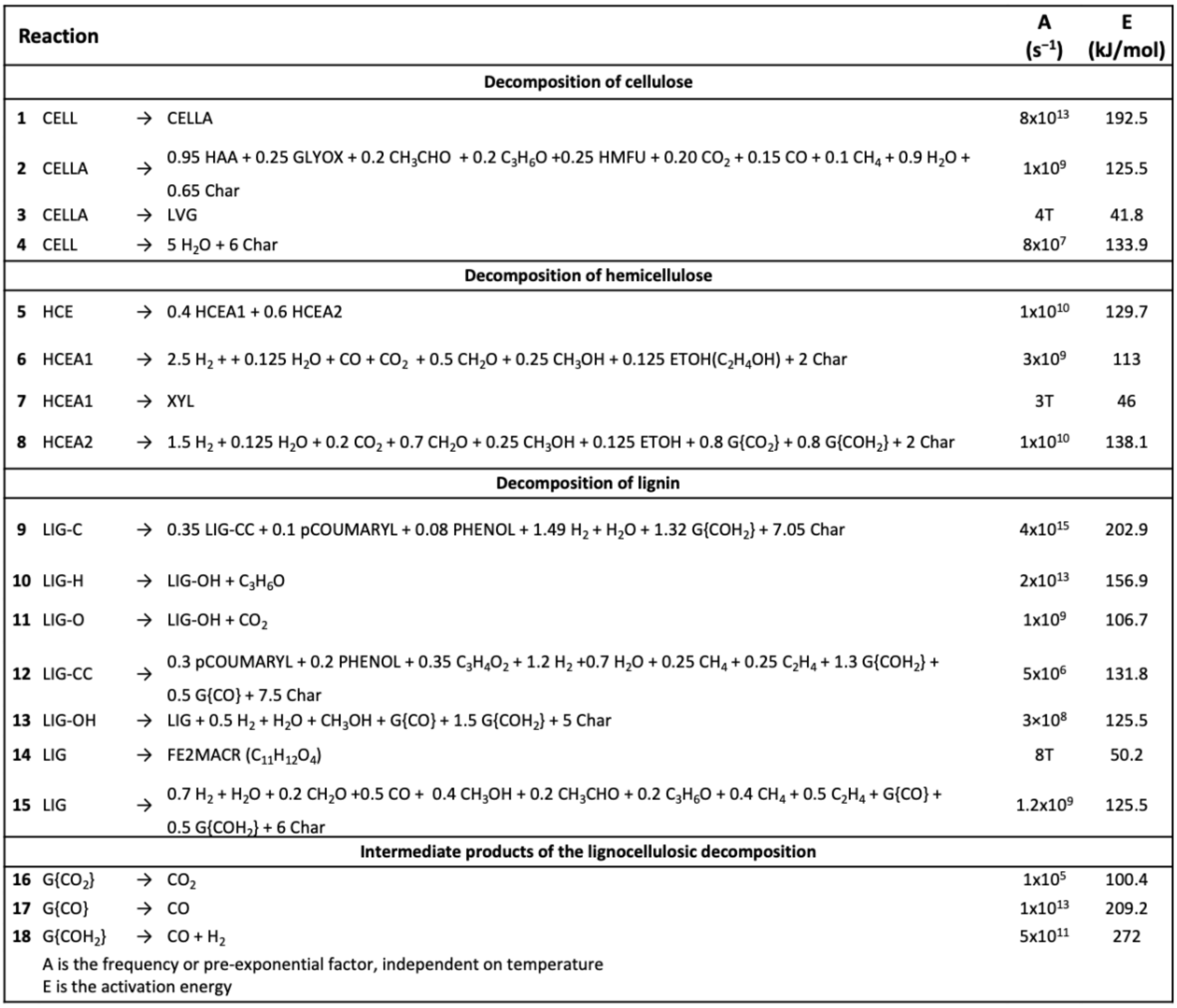

Reaction				**A (s^{-1})**	**E (kJ/mol)**
			Decomposition of cellulose		
1	CELL	→	CELLA	$8x10^{13}$	192.5
2	CELLA	→	0.95 HAA + 0.25 GLYOX + 0.2 CH_3CHO + 0.2 C_3H_6O +0.25 HMFU + 0.20 CO_2 + 0.15 CO + 0.1 CH_4 + 0.9 H_2O + 0.65 Char	$1x10^9$	125.5
3	CELLA	→	LVG	4T	41.8
4	CELL	→	5 H_2O + 6 Char	$8x10^7$	133.9
			Decomposition of hemicellulose		
5	HCE	→	0.4 HCEA1 + 0.6 HCEA2	$1x10^{10}$	129.7
6	HCEA1	→	2.5 H_2 + + 0.125 H_2O + CO + CO_2 + 0.5 CH_2O + 0.25 CH_3OH + 0.125 ETOH(C_2H_4OH) + 2 Char	$3x10^9$	113
7	HCEA1	→	XYL	3T	46
8	HCEA2	→	1.5 H_2 + 0.125 H_2O + 0.2 CO_2 + 0.7 CH_2O + 0.25 CH_3OH + 0.125 ETOH + 0.8 G{CO_2} + 0.8 G{COH_2} + 2 Char	$1x10^{10}$	138.1
			Decomposition of lignin		
9	LIG-C	→	0.35 LIG-CC + 0.1 pCOUMARYL + 0.08 PHENOL + 1.49 H_2 + H_2O + 1.32 G{COH_2} + 7.05 Char	$4x10^{15}$	202.9
10	LIG-H	→	LIG-OH + C_3H_6O	$2x10^{13}$	156.9
11	LIG-O	→	LIG-OH + CO_2	$1x10^9$	106.7
12	LIG-CC	→	0.3 pCOUMARYL + 0.2 PHENOL + 0.35 $C_3H_4O_2$ + 1.2 H_2 +0.7 H_2O + 0.25 CH_4 + 0.25 C_2H_4 + 1.3 G{COH_2} + 0.5 G{CO} + 7.5 Char	$5x10^6$	131.8
13	LIG-OH	→	LIG + 0.5 H_2 + H_2O + CH_3OH + G{CO} + 1.5 G{COH_2} + 5 Char	$3×10^8$	125.5
14	LIG	→	FE2MACR ($C_{11}H_{12}O_4$)	8T	50.2
15	LIG	→	0.7 H_2 + H_2O + 0.2 CH_2O +0.5 CO + 0.4 CH_3OH + 0.2 CH_3CHO + 0.2 C_3H_6O + 0.4 CH_4 + 0.5 C_2H_4 + G{CO} + 0.5 G{COH_2} + 6 Char	$1.2x10^9$	125.5
			Intermediate products of the lignocellulosic decomposition		
16	G{CO_2}	→	CO_2	$1x10^5$	100.4
17	G{CO}	→	CO	$1x10^{13}$	209.2
18	G{COH_2}	→	CO + H_2	$5x10^{11}$	272

A is the frequency or pre-exponential factor, independent on temperature
E is the activation energy

Table 6. Original scheme of kinetic reactions during pyrolysis proposed by Ranzi et al. [96].

These reactions take into account different compounds formed through pyrolysis, summing them up as char, and non-condensable gas and bio-oil. This proposal is limited to 35 compounds in total, whereas in reality at least 200 compounds can be found in pyrolytic bio-oil [71].

This scheme was modified in 2010 and has been presented in different versions in diagrams and tables, but the final is described by Calonaci et al. [97] and in this scheme, compounds are present especially meta-plast or trapped intermediate products such as G{CO_2}, G{CO}, G{COH_2} and G{H_2}. These can be found in gaseous or solid phases, but the information is still uncertain. However, these compounds tend to be released at higher temperatures and become part of incondensable gases. This final scheme is shown in Table 7, and comprises 19 reactions with 36 compounds in total.

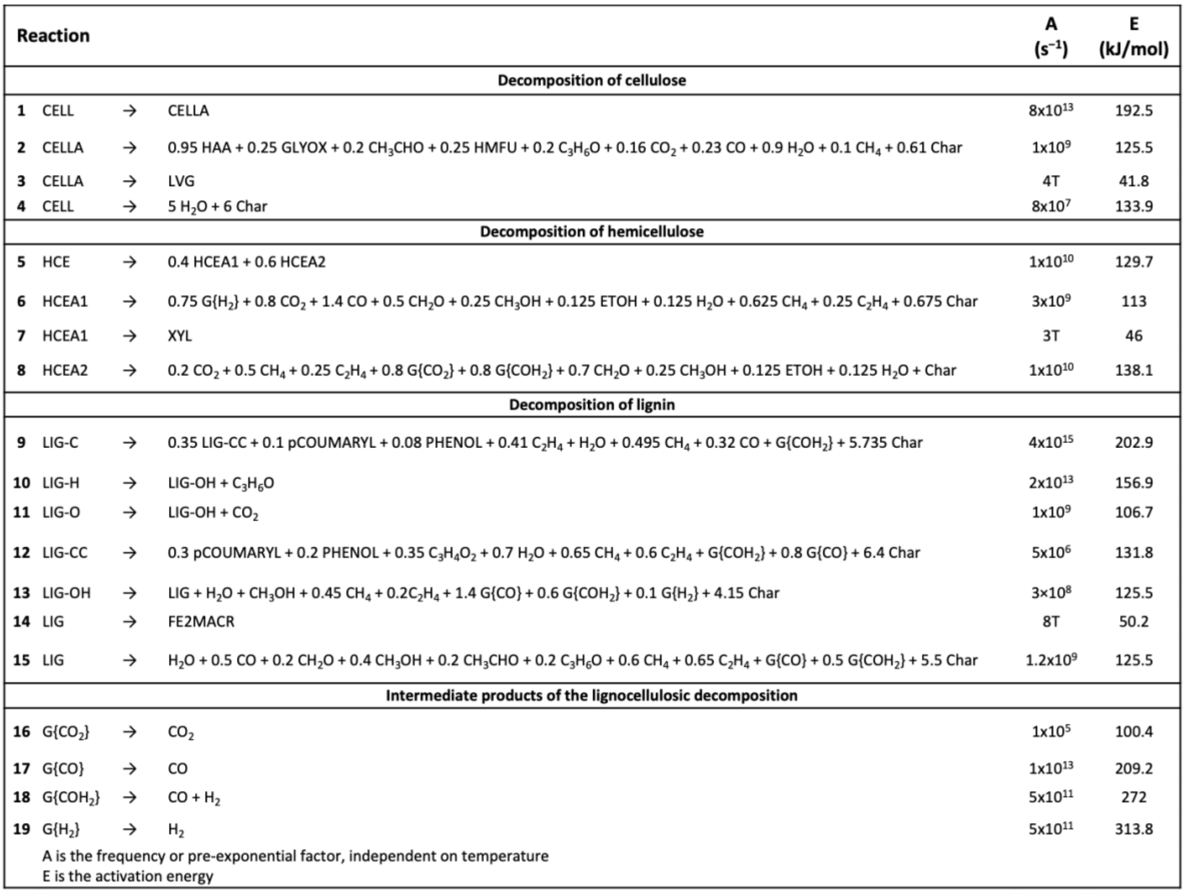

Reaction				**A (s^{-1})**	**E (kJ/mol)**
Decomposition of cellulose					
1	CELL	→	CELLA	$8x10^{13}$	192.5
2	CELLA	→	0.95 HAA + 0.25 GLYOX + 0.2 CH_3CHO + 0.25 HMFU + 0.2 C_3H_6O + 0.16 CO_2 + 0.23 CO + 0.9 H_2O + 0.1 CH_4 + 0.61 Char	$1x10^9$	125.5
3	CELLA	→	LVG	4T	41.8
4	CELL	→	5 H_2O + 6 Char	$8x10^7$	133.9
Decomposition of hemicellulose					
5	HCE	→	0.4 HCEA1 + 0.6 HCEA2	$1x10^{10}$	129.7
6	HCEA1	→	0.75 G{H_2} + 0.8 CO_2 + 1.4 CO + 0.5 CH_2O + 0.25 CH_3OH + 0.125 ETOH + 0.125 H_2O + 0.625 CH_4 + 0.25 C_2H_4 + 0.675 Char	$3x10^9$	113
7	HCEA1	→	XYL	3T	46
8	HCEA2	→	0.2 CO_2 + 0.5 CH_4 + 0.25 C_2H_4 + 0.8 G{CO_2} + 0.8 G{COH_2} + 0.7 CH_2O + 0.25 CH_3OH + 0.125 ETOH + 0.125 H_2O + Char	$1x10^{10}$	138.1
Decomposition of lignin					
9	LIG-C	→	0.35 LIG-CC + 0.1 pCOUMARYL + 0.08 PHENOL + 0.41 C_2H_4 + H_2O + 0.495 CH_4 + 0.32 CO + G{COH_2} + 5.735 Char	$4x10^{15}$	202.9
10	LIG-H	→	LIG-OH + C_3H_6O	$2x10^{13}$	156.9
11	LIG-O	→	LIG-OH + CO_2	$1x10^9$	106.7
12	LIG-CC	→	0.3 pCOUMARYL + 0.2 PHENOL + 0.35 $C_3H_4O_2$ + 0.7 H_2O + 0.65 CH_4 + 0.6 C_2H_4 + G{COH_2} + 0.8 G{CO} + 6.4 Char	$5x10^6$	131.8
13	LIG-OH	→	LIG + H_2O + CH_3OH + 0.45 CH_4 + 0.2C_2H_4 + 1.4 G{CO} + 0.6 G{COH_2} + 0.1 G{H_2} + 4.15 Char	3×10^8	125.5
14	LIG	→	FE2MACR	8T	50.2
15	LIG	→	H_2O + 0.5 CO + 0.2 CH_2O + 0.4 CH_3OH + 0.2 CH_3CHO + 0.2 C_3H_6O + 0.6 CH_4 + 0.65 C_2H_4 + G{CO} + 0.5 G{COH_2} + 5.5 Char	$1.2x10^9$	125.5
Intermediate products of the lignocellulosic decomposition					
16	G{CO_2}	→	CO_2	$1x10^5$	100.4
17	G{CO}	→	CO	$1x10^{13}$	209.2
18	G{COH_2}	→	CO + H_2	$5x10^{11}$	272
19	G{H_2}	→	H_2	$5x10^{11}$	313.8

A is the frequency or pre-exponential factor, independent on temperature
E is the activation energy

Table 7. Original scheme of kinetic reactions during pyrolysis proposed by Calonaci et al. [97].

Although, this mechanism considers the volatilisation of the main components of the lignocellulose where successive reactions take place in a combination of elementary steps, an accurate approximation of the secondary reactions that could occur in presence of ash, for instance, is not found. Some of these steps take into account more biochar formation at low temperatures, which can have a direct impact on the proportions of pyrolysis product formed. For example, reactions 6 and 7 are competing between each other, and xylose (XYL) will be formed more easily at higher temperature due to the lower activation energy.

Anca-Couce et al. [98] have proposed a different kinetic scheme which considers secondary reactions with some adjustments to predict more accurate biochar production. This proposal is a modification of the original scheme of Ranzi's model, but with a modification called 'charring factor', *x*, which has a direct impact on sugar formation. This scheme consists of 13 reactions, but they are enumerated according to the model developed by Ranzi et al. [96]. Although the constants, frequency factor (A) and activation energy (E), are the same as those used by Ranzi, the charring factor adjustment considers possible variations in biochar formation from organic product decomposition. This scheme is shown in Table 8.

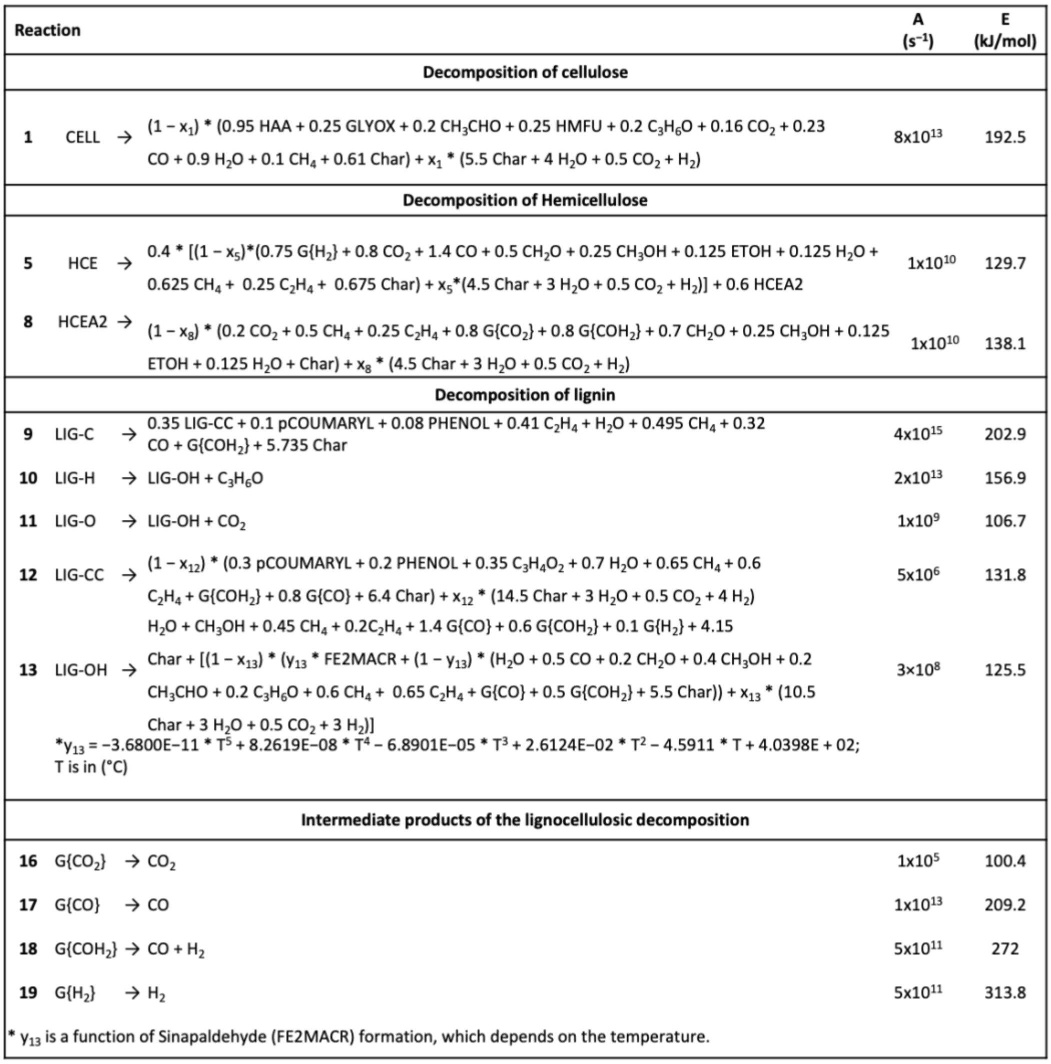

Reaction			**A (s^{-1})**	**E (kJ/mol)**
		Decomposition of cellulose		
1	CELL →	$(1 - x_1) * (0.95\ HAA + 0.25\ GLYOX + 0.2\ CH_3CHO + 0.25\ HMFU + 0.2\ C_3H_6O + 0.16\ CO_2 + 0.23\ CO + 0.9\ H_2O + 0.1\ CH_4 + 0.61\ Char) + x_1 * (5.5\ Char + 4\ H_2O + 0.5\ CO_2 + H_2)$	$8x10^{13}$	192.5
		Decomposition of Hemicellulose		
5	HCE →	$0.4 * [(1 - x_5)*(0.75\ G\{H_2\} + 0.8\ CO_2 + 1.4\ CO + 0.5\ CH_2O + 0.25\ CH_3OH + 0.125\ ETOH + 0.125\ H_2O + 0.625\ CH_4 + 0.25\ C_2H_4 + 0.675\ Char) + x_5*(4.5\ Char + 3\ H_2O + 0.5\ CO_2 + H_2)] + 0.6\ HCEA2$	$1x10^{10}$	129.7
8	HCEA2 →	$(1 - x_8) * (0.2\ CO_2 + 0.5\ CH_4 + 0.25\ C_2H_4 + 0.8\ G\{CO_2\} + 0.8\ G\{COH_2\} + 0.7\ CH_2O + 0.25\ CH_3OH + 0.125\ ETOH + 0.125\ H_2O + Char) + x_8 * (4.5\ Char + 3\ H_2O + 0.5\ CO_2 + H_2)$	$1x10^{10}$	138.1
		Decomposition of lignin		
9	LIG-C →	$0.35\ LIG\text{-}CC + 0.1\ pCOUMARYL + 0.08\ PHENOL + 0.41\ C_2H_4 + H_2O + 0.495\ CH_4 + 0.32\ CO + G\{COH_2\} + 5.735\ Char$	$4x10^{15}$	202.9
10	LIG-H →	$LIG\text{-}OH + C_3H_6O$	$2x10^{13}$	156.9
11	LIG-O →	$LIG\text{-}OH + CO_2$	$1x10^9$	106.7
12	LIG-CC →	$(1 - x_{12}) * (0.3\ pCOUMARYL + 0.2\ PHENOL + 0.35\ C_3H_4O_2 + 0.7\ H_2O + 0.65\ CH_4 + 0.6\ C_2H_4 + G\{COH_2\} + 0.8\ G\{CO\} + 6.4\ Char) + x_{12} * (14.5\ Char + 3\ H_2O + 0.5\ CO_2 + 4\ H_2)$	$5x10^6$	131.8
13	LIG-OH →	$H_2O + CH_3OH + 0.45\ CH_4 + 0.2C_2H_4 + 1.4\ G\{CO\} + 0.6\ G\{COH_2\} + 0.1\ G\{H_2\} + 4.15\ Char + [(1 - x_{13}) * (y_{13} * FE2MACR + (1 - y_{13}) * (H_2O + 0.5\ CO + 0.2\ CH_2O + 0.4\ CH_3OH + 0.2\ CH_3CHO + 0.2\ C_3H_6O + 0.6\ CH_4 + 0.65\ C_2H_4 + G\{CO\} + 0.5\ G\{COH_2\} + 5.5\ Char)) + x_{13} * (10.5\ Char + 3\ H_2O + 0.5\ CO_2 + 3\ H_2)]$	$3{\times}10^8$	125.5
	$*y_{13} = -3.6800E{-}11 * T^5 + 8.2619E{-}08 * T^4 - 6.8901E{-}05 * T^3 + 2.6124E{-}02 * T^2 - 4.5911 * T + 4.0398E + 02;$ T is in (°C)			
		Intermediate products of the lignocellulosic decomposition		
16	$G\{CO_2\}$ →	CO_2	$1x10^5$	100.4
17	$G\{CO\}$ →	CO	$1x10^{13}$	209.2
18	$G\{COH_2\}$ →	$CO + H_2$	$5x10^{11}$	272
19	$G\{H_2\}$ →	H_2	$5x10^{11}$	313.8
* y_{13} is a function of Sinapaldehyde (FE2MACR) formation, which depends on the temperature.				

Table 8. Model modified with charring factor x, proposed by Anca-Couce et al. [98].

The Anca-Couce et al. [98] projections were compared in this paper not only with Ranzi et al. [96] results but also with experimental data. Both considered biomass that was subjected to a slow pyrolysis process*.* The comparison results are shown in Table 9.

Products (% wt)	Experimental data Branca 2003 [64]	Original scheme (Ranzi et al. 2008)	Adapted scheme by Anca-Couce et al.				
			x = 0.1	*x* = 0.2	*x* = 0.3	*x* = 0.4	*x* = 0.5
Biochar	24	13.4	17.3	20.1	22.9	25.8	28.6
Bio-oil	76	86.6	82.7	79.9	77.1	74.2	71.4
Gases	14.5	17.4	24.3	23.5	22.8	22	21.3
Carbonyls and alcohols	21.7	10.9	33.4	30	26.5	23.1	19.7
Furans	6.1	0.5	8.1	7.2	6.3	5.4	4.5
Sugars	0.7	46.1	0	0	0	0	0
Phenolics	12.1	8.3	7.5	6.7	5.9	5.1	4.3
Water	21	3.5	9.4	12.5	15.5	18.6	21.6
Error (%)	0	13.4	6.7	5.1	3.5	2.9	3.6

Table 9. Comparison of the results, dry mass % basis, from the model modified by Anca-Couce et al. [98] with original and experimental data.

According to these results, the best approach for slow pyrolysis is to implement a charring factor of 0.3. These results are more accurate than the original scheme developed by Ranzi (2008), due to secondary reactions where sugars are converted into more biochar. Experimental data shows that biochar yield produced is 24%, whereas with Ranzi et al. [96] model yield of biochar is 13.4% wt. The adapted scheme by Anca-Couce et al. [98] resulted in 22.9% of biochar generated, much closer to the experimental results.

There have been other suggestions about secondary reactions could occur when lignocellulosic material is pyrolysed. An example of this is shown in Table 10.

Reaction				**A (s^{-1})**	**E (kJ/mol)**
			Secondary Reactions		
19	HAA	→	$2\ CO + 2\ H_2$	4.28×10^6	108
20	GLYOX	→	$2\ CO + H_2$	4.28×10^6	108
21	C_3H_6O	→	$0.5\ CO_2 + 0.5\ H_2 + 1.25\ C_2H_4$	4.28×10^6	108
22	$C_3H_4O_2$	→	$CO_2 + C_2H_4$	4.28×10^6	108
23	HMFU	→	$3\ CO + 1.5\ C_2H_4$	4.28×10^6	108
24	LVG	→	$2.5\ CO_2 + 1.5\ H_2 + 1.75\ C_2H_4$	4.28×10^6	108
25	XYL	→	$2\ CO_2 + H_2 + 1.5\ C_2H_4$	4.28×10^6	108
26	pCOUMARYL	→	$CO_2 + 2.5\ C_2H_4$ + 3 Char	4.28×10^6	108
27	PHENOL	→	$0.5\ CO_2 + 1.5\ C_2H_4$ + 2.5 Char	4.28×10^6	108
28	FE2MACR	→	$2\ CO_2 + 3\ C_2H_4$ + 3 Char	4.28×10^6	108

Table 10. Scheme of secondary reactions could take place in slow pyrolysis according to by Park et al. [69] (Scheme is presented as Blondeau et al. [99]).

These reactions proposed by Park et al. [69] were developed based on experiments with dry wood, and considered intermediate compounds formed during pyrolysis could further decompose to form more biochar and gas. However, the same activation energy values are employed to predict this behaviour which can be significantly different to other biomass decomposition during pyrolysis. The scheme is proposed based on spheric wood with specific dimensions.

All the schemes mentioned above are based on ash-free and moisture-free biomass, which can result in a significant deviation in the real biomass conversion through pyrolysis, if compared with experimental data using varieties of biomass. In reality, biomass is not completely dry or ash-free when it is treated, resulting in additional material that could interfere in heat transfer and in lignocellulose decomposition. However, the Anca-Couce et al. [98] approximation can be employed to predict accurate yields for products of slow pyrolysis if biochar production is the main target.

It is uncertain whether there can be a model that can predict exactly the amount of each pyrolysis product through either slow or fast pyrolysis. In addition, most of the projections and models employed to predict the formation and composition of the products have results from pyrolysis of woody biomass; while there are other kinds of biomass that can be suitable as feedstock. There is some information about digestate as biomass and some about its composition, but not enough analysis of how feasible this can be for pyrolysis processes – and about how competitive the market for wood is compared to that for other biofuels or biobased products.

Another scheme of reactions proposed by Ranzi et al. [100] in 2017 includes 29 reactions and consideration of more products. This has been found to be a better approximation for bio-oi composition due to some compounds forming acetic acid and formic acid, usually found in bio-oil. These reactions resulted in 43 compounds. The scheme is represented in Table 11.

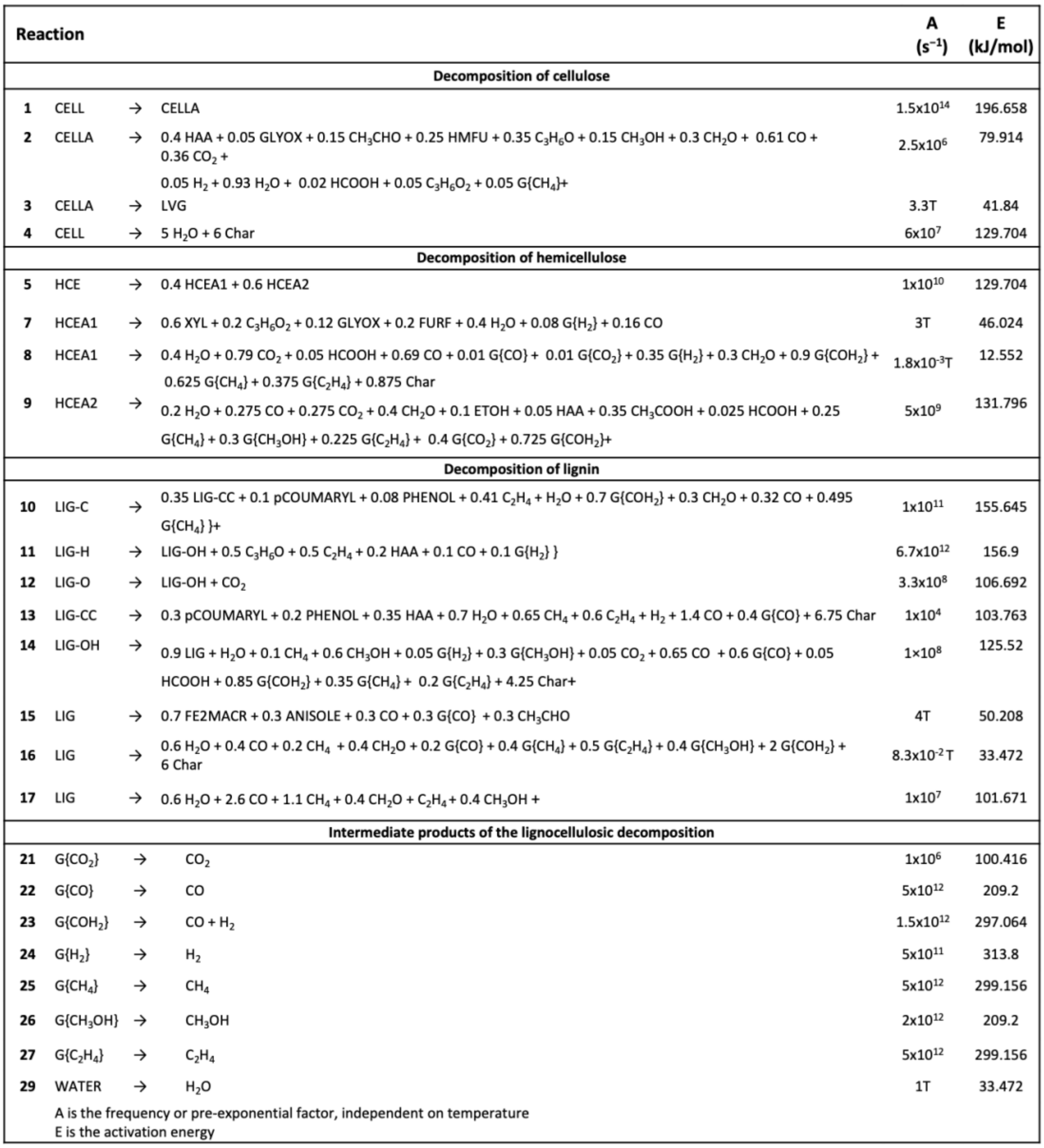

Reaction				A (s^{-1})	E (kJ/mol)
Decomposition of cellulose					
1	CELL	→	CELLA	$1.5x10^{14}$	196.658
2	CELLA	→	0.4 HAA + 0.05 GLYOX + 0.15 CH_3CHO + 0.25 HMFU + 0.35 C_3H_6O + 0.15 CH_3OH + 0.3 CH_2O + 0.61 CO + 0.36 CO_2 + 0.05 H_2 + 0.93 H_2O + 0.02 HCOOH + 0.05 $C_3H_6O_2$ + 0.05 G{CH_4}+	$2.5x10^6$	79.914
3	CELLA	→	LVG	3.3T	41.84
4	CELL	→	5 H_2O + 6 Char	$6x10^7$	129.704
Decomposition of hemicellulose					
5	HCE	→	0.4 HCEA1 + 0.6 HCEA2	$1x10^{10}$	129.704
7	HCEA1	→	0.6 XYL + 0.2 $C_3H_6O_2$ + 0.12 GLYOX + 0.2 FURF + 0.4 H_2O + 0.08 G{H_2} + 0.16 CO	3T	46.024
8	HCEA1	→	0.4 H_2O + 0.79 CO_2 + 0.05 HCOOH + 0.69 CO + 0.01 G{CO} + 0.01 G{CO_2} + 0.35 G{H_2} + 0.3 CH_2O + 0.9 G{COH_2} + 0.625 G{CH_4} + 0.375 G{C_2H_4} + 0.875 Char	$1.8x10^{-3}$T	12.552
9	HCEA2	→	0.2 H_2O + 0.275 CO + 0.275 CO_2 + 0.4 CH_2O + 0.1 ETOH + 0.05 HAA + 0.35 CH_3COOH + 0.025 HCOOH + 0.25 G{CH_4} + 0.3 G{CH_3OH} + 0.225 G{C_2H_4} + 0.4 G{CO_2} + 0.725 G{COH_2}+	$5x10^9$	131.796
Decomposition of lignin					
10	LIG-C	→	0.35 LIG-CC + 0.1 pCOUMARYL + 0.08 PHENOL + 0.41 C_2H_4 + H_2O + 0.7 G{COH_2} + 0.3 CH_2O + 0.32 CO + 0.495 G{CH_4} }+	$1x10^{11}$	155.645
11	LIG-H	→	LIG-OH + 0.5 C_3H_6O + 0.5 C_2H_4 + 0.2 HAA + 0.1 CO + 0.1 G{H_2} }	$6.7x10^{12}$	156.9
12	LIG-O	→	LIG-OH + CO_2	$3.3x10^8$	106.692
13	LIG-CC	→	0.3 pCOUMARYL + 0.2 PHENOL + 0.35 HAA + 0.7 H_2O + 0.65 CH_4 + 0.6 C_2H_4 + H_2 + 1.4 CO + 0.4 G{CO} + 6.75 Char	$1x10^4$	103.763
14	LIG-OH	→	0.9 LIG + H_2O + 0.1 CH_4 + 0.6 CH_3OH + 0.05 G{H_2} + 0.3 G{CH_3OH} + 0.05 CO_2 + 0.65 CO + 0.6 G{CO} + 0.05 HCOOH + 0.85 G{COH_2} + 0.35 G{CH_4} + 0.2 G{C_2H_4} + 4.25 Char+	$1×10^8$	125.52
15	LIG	→	0.7 FE2MACR + 0.3 ANISOLE + 0.3 CO + 0.3 G{CO} + 0.3 CH_3CHO	4T	50.208
16	LIG	→	0.6 H_2O + 0.4 CO + 0.2 CH_4 + 0.4 CH_2O + 0.2 G{CO} + 0.4 G{CH_4} + 0.5 G{C_2H_4} + 0.4 G{CH_3OH} + 2 G{COH_2} + 6 Char	$8.3x10^{-2}$ T	33.472
17	LIG	→	0.6 H_2O + 2.6 CO + 1.1 CH_4 + 0.4 CH_2O + C_2H_4 + 0.4 CH_3OH +	$1x10^7$	101.671
Intermediate products of the lignocellulosic decomposition					
21	G{CO_2}	→	CO_2	$1x10^6$	100.416
22	G{CO}	→	CO	$5x10^{12}$	209.2
23	G{COH_2}	→	CO + H_2	$1.5x10^{12}$	297.064
24	G{H_2}	→	H_2	$5x10^{11}$	313.8
25	G{CH_4}	→	CH_4	$5x10^{12}$	299.156
26	G{CH_3OH}	→	CH_3OH	$2x10^{12}$	209.2
27	G{C_2H_4}	→	C_2H_4	$5x10^{12}$	299.156
29	WATER	→	H_2O	1T	33.472

A is the frequency or pre-exponential factor, independent on temperature
E is the activation energy

Table 11. Scheme of reactions of lignocellulose decomposition in fast pyrolysis proposed by Ranzi et al. [100].

This scheme is one of the most complete schemes for the pyrolysis of lignocellulosic material - ash content is taken into account and the effect of organics formation is considered. However, this scheme is simplified into only 43 components whereas, as it was mentioned previously, pyrolysis products could number more than 200 compounds overall.

2.7 PYROLYSIS OF DIGESTATE

There is some information about digestate treated in pyrolysis reactors; however, there is not enough data about the variability of digestate composition based on lignocellulosic material. Different experimental work has been carried out with digestate from food waste, agricultural residue, manure and municipal solid waste. Experiments performed by Neumann et al. [101] were based on digestate from cattle slurry, pig slurry and corn silage, with the syngas production as the main target of interest. The temperature range of operation was in 500ºC and 750ºC. The yields of the products have been reported at the different temperatures, but there is no information about the relation between lignocellulosic composition and the pyrolysis products. The characterisation of the digestate was based only on proximate and ultimate analysis.

Some experimental information was also presented by Opatokun et al. [22] about the analysis of pyrolysis treatment for food waste and its digestate based on the proximate and ultimate analyses for feedstock characterisation and, some components of the bio-oils produced. These experiments were carried out in a fixed-bed reactor, which is common for slow pyrolysis due to long residence time for the biomass. Pyrolysis was performed with a maximum temperature of 500ºC to produce more bio-oil. Only 32 components were detected and quantified, assuming this paper is a simplified report of bio-oil composition. The yield presented in this work is around 52% liquid, which includes the amount of water produced, but it does not specify the amount of both phases produced: organics and water. Although the information in this work is not based on lignocellulosic composition, there is a further work made by Opatokun et al. [102] where the same food waste digestate was analysed and the lignocellulose components were reported. This also included the energy content of the pyrolysis products, and more details about the composition of the produced bio-oils at different heating rate. However, this composition reported was based on only similar compounds found per experiment performed at certain conditions with each biomass, which was limited to around 16-20 compounds in total.

There is one system proposed by Monlau et al. [21], which includes the energy balances of an integration of pyrolysis reactor with an anaerobic digestion process, and gives promising data about energy recovery from the AD to be used in thermal processing. The pyrolysis products from the digestate, mainly composed of chicken manure, groats, olive oil cake and triticale, are reported at three different temperatures, 400ºC, 500ºC and 600ºC. The study includes mass and energy balances when considering energy recovery from the AD system as an input for feedstock pre-treatment, and some excess to be used into the pyrolysis reactor. It is mentioned which are the best conditions to obtain the higher yield of bio-oil, and the parameters employed to run the experiment are similar to those associated with slow pyrolysis. The reactor employed was a rotary kiln which is considered ideal for slow pyrolysis due to the high production of biochar. This is not only pointed out by Monlau et al. [21] but also for other authors such as Kern et al. [56] and Li et al. [57], and other research studies such as carried out by Brownsort [103]. These conditions have a direct impact on the composition of the bio-oil and outcomes can be different from the bio-oil of fast pyrolysis. However, there is no information about composition of the bio-oil, only energy value to be employed in an oil engine for energy production. It is important that the characterisation of the pyrolysis products from the thermal processing are included in order to evaluate what other potential uses can be for these products. The implementation of pyrolysis to convert digestate into pyrolysis products to then use them in a combustion engine for energy production could result in more expensive processing, considering that digestate could be used for the same purpose and be incinerated to recover the energy produced from it.

There is still further work needed for valuable applications of the pyrolysis products. Some analyses, based on the characterisation of the pyrolysis products, have been done where alternative conversions, by bio-oil refinery for instance, are proposed to produce other commercial products such as synfuel, hydrogen (H_2) or fuel additives [104,105]. Biochar has been used for soil amendment, and also considered as a substitute for coal to produce energy, but it can be used as an additive in AD to increase bio-methane production. One study about returning the water of pyrolysis products into the AD system has been carried on by Hubner et al. [106] to enhance the fermentation and degradation of some pyrolytic compounds. Although the conclusion of this work suggested AD as a promising process to detoxicate pyrolysis liquid, it was also found some inhibition about increasing yield of biomethane in the digester due to the high acid conditions. However, it is mentioned that biochar from the thermal process could overcome this inhibition [107]. As a result, alternative uses of bio-oil need to be analysed in order to valorise its production from waste, and information about the characterisation of the products from pyrolysis or other thermal processing is needed.

González et al. [108] also proposed possible scenarios that could be implemented to increase the value of waste with AD and pyrolysis treatment integration. These scenarios consisted of using swine manure with different AD feedstock alternatives: manure only and manure mixed with other waste. This idea had the aim to improve not only AD biogas generation, but the resulting digestate to use in pyrolysis and increase the energy value of the pyrolysis products. This evaluation was performed by quantifying the amount of energy recovered from using biogas, pyrolytic gas and bio-oil through a combined heat and power (CHP) unit to meet the thermal energy and electricity requirement of the system. However, most of these scenarios were based on anaerobic digestion at laboratory scale, which does not indicate how the composition of these mixtures could affect the microorganism performance to produce biogas at larger scale. Some bacteria could be adaptable to this, but it is not possible to evaluate this without direct measurements. Additionally, the use of pyrolysis to generate a product for combustion could be a more expensive solution for this waste than using a direct combustion of the digestate. Fluidised bed combustion is an alternative solution for a cleaner thermal process where less nitrogen oxides (NOx) and sulphur oxides (SOx) are produced. Additionally, this technology can be employed for energy generation [109].

Ghysels et al. [110] performed an analysis of cocoa waste in different bioprocessing configurations: 1. Pyrolysing raw cocoa pod husks, 2. Pyrolysing digestate from cocoa pods and 3. Pyrolysing co-digestate from a mixture with cocoa pod husk and manure. These three scenarios considered slow pyrolysis as the thermal process. Evaluation was based on digestates generated at lab scale with a lignocellulose composition calculated from elemental analysis, resulting in an empirical chemical formula for waste characterisation. However, this evaluation assumed that carbohydrates contained in raw cocoa were consumed mostly through AD, based on 2-cyclopenten-1-one quantified in the bio-oil. This compound was a key chemical in this assessment due to being a holocellulose (cellulose and hemicellulose) derivative, and it was concluded that biogas produced was from the holocellulose conversion due to the reduction of 2-cyclopenten-1-one in some bio-oil samples. This assumption may not be correct due to the large amount of ash contained within the biomass (higher than 11% wt). Derivatives from cellulose and hemicellulose could be converted into other compounds during pyrolysis and smaller molecules such as carbon dioxide (CO_2) and carbon monoxide (CO) and water could be formed with this amount of ash. The impact of ash on pyrolytic bio-oil composition has been demonstrated through experiments where ash-free biomass and biomass with varied ash content was employed. Yildiz et al. [111] work is an example of a clear description of how the effect of ash on pyrolysis of biomass lead to a reduction in sugars, and higher production of acid and water. In addition, derived-biomass furfural has been studied to form other compounds such as 2-cyclopenten-1-one when it is subjected to catalytic methods [112], which could represent similar path furfural goes through when ash is present in pyrolysis of biomass.

2.8 ROLE OF ASH IN PYROLYSIS OF BIOMASS

Biomass has become an important source of energy production and it is considered a crucial fuel for other green bioproducts. It's properties not only consist of organic material, there is an inorganic phase constituted by mineral components such as silicates, sulphates, phosphates, carbonates, nitrates, and others [113] that can have an effect on the application in which these fuels are employed. Lignocellulosic material has been used in pyrolysis to produce more high-value liquid product, especially with a large amount of anhydro sugars such as levoglucosan. These compounds in pyrolytic bio-oil have been the most studied and analysed as valuable chemicals for further uses. However, these were found in very low yields when the biomass with high content of holocellulose was subjected to pyrolysis due to minerals within the biomass, prompting a reduction of these sugars generated during the thermochemical conversion [114]. According to Shafizadeh et al. [114] pre-treatment to remove this inorganic material from the biomass allowed the conversion of cellulose into higher levoglucosan yields, reaching greater than 50%. Piskorz et al. [115] also presented higher levoglucosan production when poplar wood was pre-treated reducing ash content from 0.46% to only 0.04% wt with yields of this sugar from 3.04% wt to 30.42% wt. Persson et al. [81] also presented how minerals in softwood sawdust increases CO and CO_2 production when this biomass is pyrolysed. Although the amount of ash was only 0.21% wt, it was found a decrease in these gases when this woody material was pre-treated. Using 500ºC as operating temperature with raw sawdust, 6% wt of CO and 7.9% wt CO_2 were generated, whereas by reducing the ash content to 0.05% wt, these gases were formed in 3.3% and 6.3% wt respectively. Bio-oil yield was also impacted by these two conditions of lignocellulosic material employed. Banks et al. [116] studied specific inorganic material, such as potassium, and the effect of this on pyrolysis products from beech wood. This mineral was impregnated in the biomass at different ratios, as the amount of potassium was increased bio-oil yield decreased leading to more production of pyrolytic water and biochar due to cracking of organics. Additionally, the increase of pyrolytic water generation due to ash content can also lead to a phase separation of the bio-oil [83].

2.9 SUMMARY OF LITERATURE FINDINGS AND OPPORTUNITIES FOR FURTHER RESEARCH

Gaps found in the literature associate with the assessment of thermal treatment of digestate are summarised next:

- There are few detailed lignocellulose analyses of biomasses which results difficult to compare digestate with other waste.
- Complete waste characterisation in different AD systems
- There are few schemes of reactions of pyrolysis and other thermal technologies based on decomposition of lignocellulose, but a lack of schemes about thermochemical decomposition of proteins and lipids biomass contains and the compounds that could be formed in pyrolytic bio-oil.
- There is a gap in analysis of pyrolysis products based on utilisation of constant biomass and equivalent characterisation employed through different pyrolysis technologies.
- There are a few studies that present a detailed bio-oil analysis which could include the proportion of chemical groups formed and consistent calculation of total yields of these groups.
- Few analyses of secondary reactions where levoglucosan and furfural take place to form other compounds through pyrolysis at different conditions. These compounds are not converted directly in more biochar, water and gas when secondary reactions occur. There are other composites formed during pyrolysis of lignocellulose in the presence of ash not reported.
- Few analyses of pyrolysis of digestate that includes the whole characterisation of AD systems.

CHAPTER 3. MATERIALS AND METHODS- EXPERIMENTAL WORK

3.1 SAMPLE SOURCE AND PREPARATION

Three different waste biomasses were collected directly from Severn Trent Water anaerobic digestion systems in different sites: pre-anaerobic digestion (pre-AD) crop, crop digestate and sewage digestate from Stoke Bardolph in Nottinghamshire, and food waste digestate from Coleshill in East Birmingham (Figure 13).

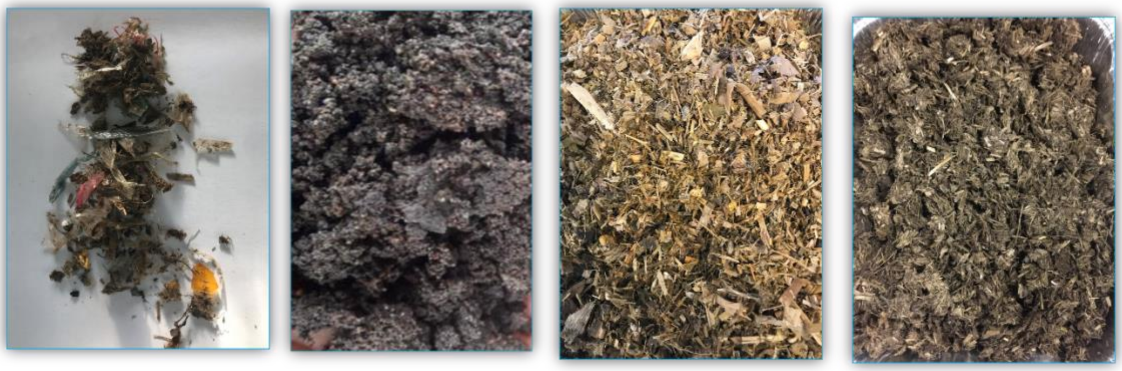

Food waste digestate **Sewage digestate** **Pre-AD crop** **Crop digestate**

Figure 13. Waste collected from Severn Trent sites.

Bioenergy has been controversial due to using land for energy crops versus food crops. However, the land use for this crop was justified for use as an energy source because of soil contamination, with high content of heavy metals that could affect human health if it used for food proposes.

Pre-AD crop and crop digestate were selected for processing through the pyrolysis technologies available. This was based on the possibility to obtain a more complete waste characterisation and to better understand the composition of pyrolysis products arising from the digestate. Food waste and sewage are a very complex waste and difficulties were encountered in management of the pyrolysis experiments and control of product recovery. One was the plastic content in the food waste which had a major bearing on the pyrolytic products. The laboratory facilities available were not able to handle the sewage digestate, so this material was not considered any further during this study.

Crop digestate was collected in a period of 3 to 4 weeks. Each collection was considered as a *batch n* and characterised individually. Due to the higher content of water in this digestate, around 80%, approximately 170 kg of crop digestate were dried to obtain the amount needed for treatment in the fast pyrolysis reactor rig at the Technical Research Centre of Finland, VTT in Espoo Finland, and slow and microwave pyrolysis facilities at the University of Nottingham.

Waste was dried at 105ºC for 24 hours, and then stored in vacuum-sealed packaging to preserve it and ensure that the material can be stored for several months (Figure 14).

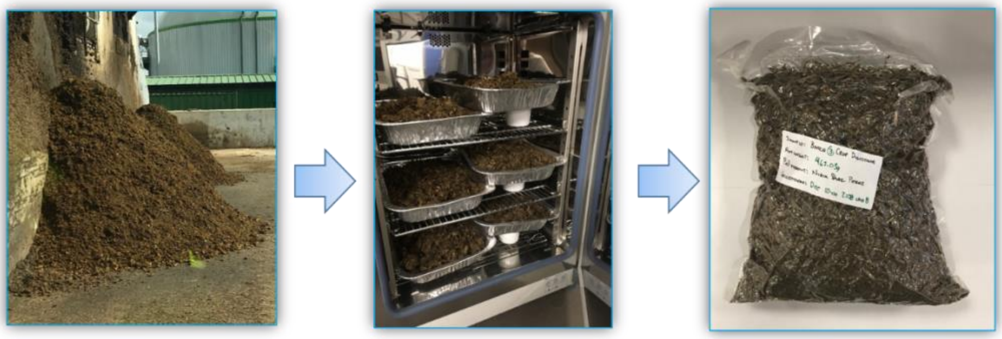

Digestate 80% water

105ºC for 24hrs

Dry digestate in sealed bags

Figure 14. Crop digestate samples preparation.

3.2 SAMPLE CHARACTERISATION

The main characterisation of this digestate and crop waste consisted of proximate, ultimate and lignocellulose analysis. To perform these assays the waste needed to be ground as shown in Figure 15.

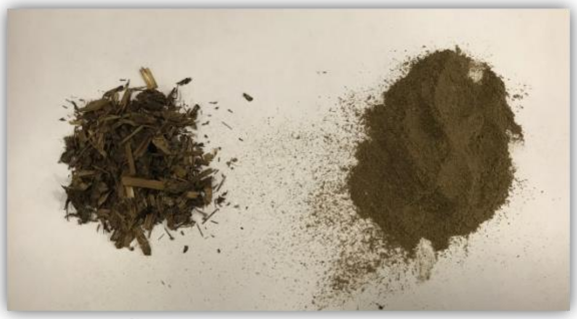

Raw crop digestate

Ground crop digestate

Figure 15. Raw and ground crop digestate

Only determination of monosaccharides content was conducted for food waste digestate due to the high plastics content. Ultimate and proximate analyses were not performed because plastic could decompose and cause contamination in other biomasses processed with the same analyser.

3.2.1 PROXIMATE AND ULTIMATE ANALYSIS

Thermogravimetric analysis (TGA) was conducted to determine the volatile matter and ash content in crop waste and crop digestate. This information will be compared with the lignocellulose composition in order to understand how much of this volatile mass is related to these organic components. The most common method for this analysis is an approach to standard test method ASTM D7348 [117] employed for loss on ignition (LOI) of solid combustion residues performed by Mayoral et al. [118]. The analysis was carried out in a TGA Q600 with a horizontal balance and furnace design. The experiments were conducted with 10-12 mg of sample which was placed in an alumina crucible. Moisture content was determined by heating the biomass up to 110ºC at 20ºC/min with nitrogen (100 ml/min, 1 bar) holding this temperature for 15 minutes. Subsequently, at the same heating rate the temperature was increased to 950ºC and held for 30 minutes to obtain the volatile matter. After this time the sweep gas was switched to air to calculate fixed carbon and ash content by combusting the remaining material for 15 minutes. This analysis was performed at least 3 times per sample. An example of every change of this analysis is shown in Figure 16.

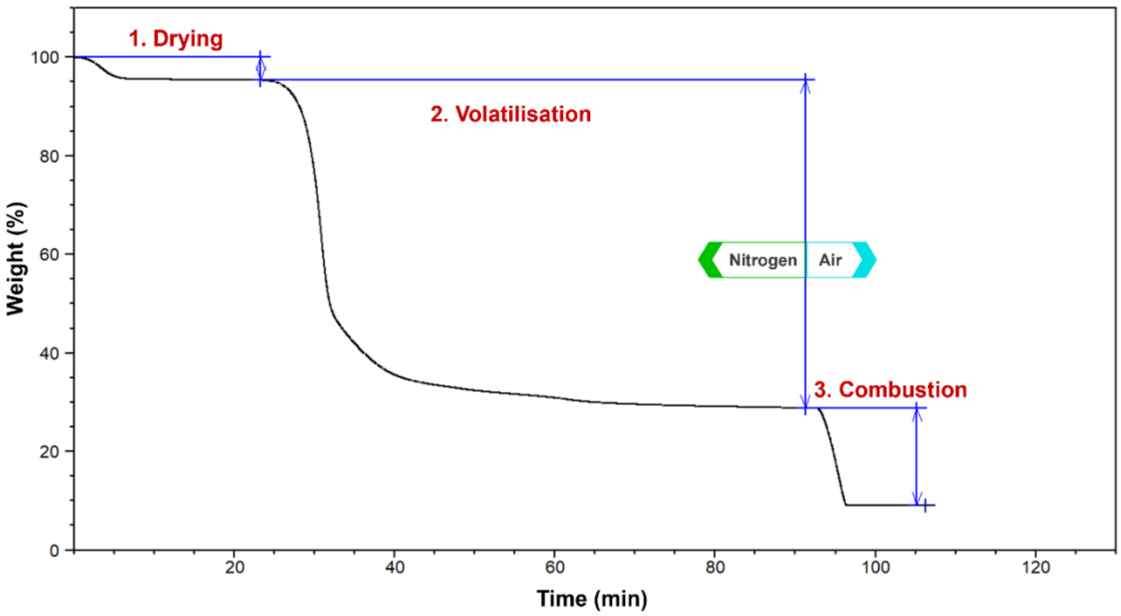

Figure 16. Thermogravimetric analysis (TGA) of biomass.

Ultimate analysis was performed to determine total carbon (C), hydrogen (H), nitrogen (N) and oxygen (O) composition in the waste. This was carried out using a CHN628 elemental analyser, which operates by a complete combustion technique with pure oxygen at temperatures up to 1050°C. This analysis was validated with a certified reference standard BBOT ((2,5-di (5-tert-butylbenzoxazol-2-yl) thiophene) by LECO with specific composition of carbon, nitrogen and hydrogen by processing around 75mg of this standard in the CHN628 analyser before the pre-AD crop and digestate were examined. The main outcomes are the percentage values of carbon, hydrogen, and nitrogen; oxygen content was calculated by difference to sum 100% in total. Ultimate analysis for each sample was carried out with around 60mg of sample and performed in triplicate.

3.2.2 DETERMINATION OF LIGNOCELLULOSE COMPOSITION AND ASH CONTENT

These analyses were carried out at Wageningen University and Research (WUR), Wageningen Food & Biobased Research in Netherlands, funded by BRISK II project: Biofuels Research Infrastructure for Sharing Knowledge II.

3.2.2.1 ASH CONTENT

Additional ash content determination was carried out to validate and compare values between different methods and avoid any discrepancy or possible error.

Ash content analysis was conducted by using a quantitative gravimetric method [119]. A crucible was dried at 105 °C and cooled down in a desiccator. 2 g of the sample was allocated to a tared crucible and heated for 16 hours at 105ºC. After this time, the sample was stored in a desiccator, and cooled down to room temperature before weighing to determine moisture content. Subsequently this dry sample was placed in a muffle furnace and heated to 550ºC within 4 hours, followed for 4 more hours of hold-time at 550ºC to remove any organic matter remaining. The sample was cooled back down to 105ºC and stored in a desiccator to cool it down at room temperature and the sample weight was recorded. Following this, ash content was obtained by placing the sample into the muffle furnace and heating to 900ºC and holding for 4hrs at this temperature. After this the samples were placed in a desiccator to be cooled down and final weight recorded. This analysis was performed in duplicate.

3.2.2.2 LIGNOCELLULOSIC MATERIAL

The method for analysis of cellulose and hemicellulose consists of the hydrolysis, extraction and quantification of the carbohydrates that can be attributed to one particular biopolymer in the source biomass. The remaining material from this extraction is used for lignin determination.

3.2.2.3 HYDROLYSIS - CARBOHYDRATES EXTRACTION

Firstly, the samples were hydrolysed according to Saeman et al. [120] by two different means: strong and weak hydrolysis. Due to the type of material, it was important to identify whether there was any easily broken-down material and differentiate this from lignocellulosic matter, which requires a stronger processing method in order to be depolymerised and quantified. The first assumption was that crop waste might contain starch material. Starch comprises two types of alpha-glucan, which is a polysaccharide of D-glucose monomers: amylose and amylopectin [121,122]. Starches can content around 20-30% of amylose 70-80% of amylopectin [123,124]. Therefore, it was necessary to differentiate these from the D-glucose that is within cellulose’s structure.

Cellulose and starch are decomposed at different temperatures so if these are processed at the same conditions, they will not be converted into the same compounds that could be found in pyrolysis products. Starch could be converted into more water and CO and CO_2 at high temperatures [94,125].

Around 75mg of sample was weighed in a tared screw cap tube for each hydrolysis. Weak hydrolysis consisted of just adding a solution 9% (w/w) sulfuric acid (H_2SO_4) into the tube with the sample and incubated for 1h at 30ºC. Strong hydrolysis comprised two steps. The first was adding a solution of 72% (w/w) H_2SO_4 into the tube with the sample and then incubating at 30ºC for an hour. The second step consisted of adding water to the sample, after the 1h-incubation, to obtain a 9% (w/w) H_2SO_4 solution to which was then incubated for 3 hours at 100ºC.

Differences between both extractions can be seen in Figure 17, where it is noticeable that the solution appearance is darker as a result of the strong hydrolysis due to lignocellulosic material depolymerisation which creates a more saturated solution.

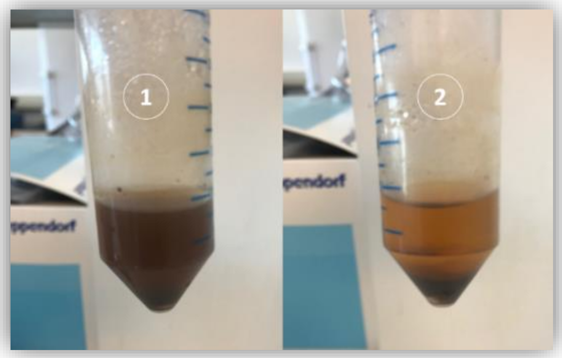

Figure 17. Difference between two hydrolysis processes implemented to determine carbohydrate levels in crop waste and digestate: (1) strong hydrolysis (2) weak hydrolysis

0.1% (w/v) bromophenol blue in ethanol was added to each sample to then adjust the pH with barium carbonate until the solution turned a blue colour. This solution was transferred into a 1.5 ml GC autosampler vial by filtration using a 0.45mm PFTE filter. For this method, 2-deoxy-d-galactose was added to each sample as internal standard (IS).

3.2.2.4 STANDARDS PREPARATION

Wageningen University and Research already has standards prepared for carbohydrates analysis of biomass. Two standard solutions were employed, standard A and standard B, with several monosaccharides at concentrations in a range of 0.1 to 0.02 mg/ml for the calibration curves. Composition of these standards are shown in Table 12.

Standard A		Standard B	
1	Fucose	1	IS-2-deoxy-d-galactose
2	IS-2-deoxy-d-galactose	2	Rhamnose
3	Arabinose	3	Galactosamine HCl
4	Galactose	4	Glucose
5	Glucosamine HCl	5	Mannose
6	Xylose	6	N-Acetyl-d-glucosamine
7	N-Acetyl-d-galactosamine	7	Ribose
8	D-galacturonic acid	8	D-glucoronic acid

Table 12. Standards employed to determine sugar composition of pre-AD crop and crop digestate.

3.2.2.5 CARBOHYDRATES QUANTIFICATION

Carbohydrates were quantified by high performance anion exchange chromatography (HPAEC) using an ICS-5000^{+} ion chromatography system. The system was equipped with a CarboPac PA1 column (2×250 mm) preceded with a CarboPac guard column (2×50 mm), and a pulsed electrochemical detector (Dionex, Sunnyvale, USA). The flow rate employed was 0.3 mL/min, and the temperature in the column was 17^{o}C. The elution in the system was performed next through the following sequence:

- 0-53 min H2O
- 53-63 min 150mM sodium hydroxide (NaOH)
- 63-63.1 min a gradient from 150 mM to 500 mM NaOH
- 63.1-78 min 500 mM NaOH
- 78-83 min a gradient from 500mM NaOH to H_2O
- 83-100 min H_2O

Monosaccharides were detected after the post column addition of 0.5M NaOH at 0.1ml/min.

Peak areas were obtained through Chromeleon 7.2 software, from chromatograms similar to the one shown in Figure 18.

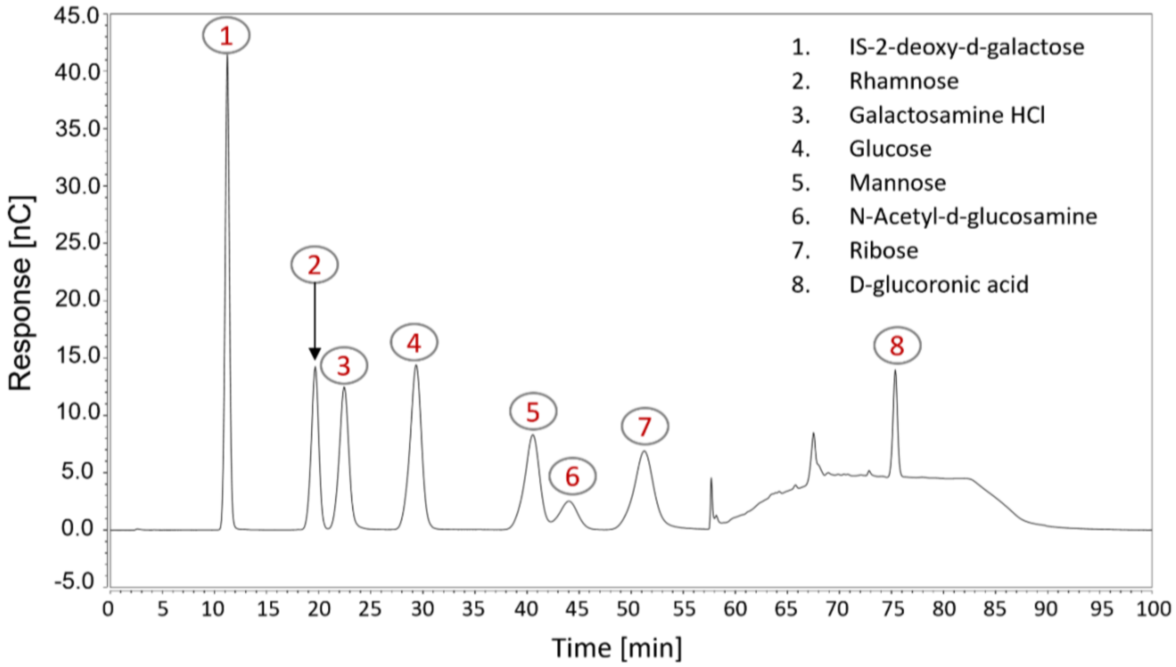

Figure 18. Chromatogram of standard B generated through Chromeleon software from Dionex analysis.

The sugar concentration obtained from this analysis was based on the detection of monomer compounds due to the hydrolysis performed on pre-AD and crop digestate. In order to calculate the concentration on a dry basis of the polysaccharides (cellulose and hemicellulose) in the biomass, anhydro factors were used to apply a correction: a value of 0.88 for C-5 sugars such as xylose and arabinose, and 0.90 for C-6 sugars, such as glucose, galactose, and mannose.

These factors are used depending on the type of sugars present in the samples: pentose or hexose. If the sugars used as standards shown in Table 13 were present in the sample, the final concentration needed to be corrected according to the corresponding factor mentioned.

Monosaccharide	Formula
Fucose	C6 H12 O5
Arabinose	C5 H10 O5
Galactose	C6 H12 O6
Glucosamine HCl	C6 H14 Cl N O5
Xylose	C5 H10 O5
N-Acetyl-d-Galactosamine	C8 H15 N O6
D-galacturonic acid	C6 H10 O7
Rhamnose	C6 H12 O5
Galactosamine HCl	C6 H14 Cl N O5
Glucose	C6 H12 O6
Mannose	C6 H12 O6
N-Acetyl-d-Glucosamine	C8 H15 N O6
Ribose	C5 H10 O5
D-glucuronic acid	C6 H10 O7

Table 13. Sugars standards and formula.

Cellulose content is the amount of glucose minus the starch quantified, and hemicellulose is the sum of arabinose, galactose and xylose.

3.2.2.6 LIGNIN DETERMINATION

A 375 mg of sample was weighed in a tared screw cap tube. The samples were processed with a hydrolysis as described in 3.2.2.3. The insoluble lignin (AIL) in the acid hydrolysate was measured by weight as Klason lignin [126] whereas the soluble lignin (ASL) content was determined spectrophotometrically at 205 nm [127]. For calculation of ASL an extinction coefficient for lignin of 110 L/g.cm at 205 nm was used.

3.2.2.7 STARCH DETERMINATION

Crop waste was subjected to an additional analysis in order to further identify the sugars identified by the weak hydrolysis. Glucose was detected in this material, but it was important to identify if it was starch-like material as, this component could be the main energy-source for the microorganisms in the anaerobic digestion system to produce biogas.

The assay implemented was AOAC Method 996.11AACC Method 76.13 [128], based on the amyloglucosidase/a-amylase method.

3.3 THERMAL PROCESSING

Experimental work has been undertaken in apparatus at the University of Nottingham and at the Technical Research Centre of Finland, VTT, Espoo. Biomass was processed using slow pyrolysis and microwave pyrolysis at the University of Nottingham, and using fast pyrolysis at VTT. Care was taken to ensure that the same samples were used across all three pyrolysis systems, and that comparable analysis was conducted on the bio-oil product.

3.3.1 PROCESS DESCRIPTION -SLOW PYROLYSIS

The experimental work in this system consists of a horizontal single-zone Gray King tube furnace with a Carbolite^{TM} controller. A quartz tube (length: 300 mm, inner diameter: 200 mm) was used as the reactor to hold the biomass during pyrolysis.

5-10g of biomass sample were placed in the quartz tube. The moisture content of the waste was measured before each experiment with a moisture analyser from Adam Equipment Co. Ltd to differentiate this water from that one produced in pyrolysis. Once the system was set, the reactor loaded with sample was flushed with nitrogen to remove traces of air inside the system to enable the experiments to run in absence of oxygen. A thermocouple was introduced into the reactor to determine the difference between the temperature inside of the reactor and the setpoint, which was +/- 5°C. Runs were performed in triplicate at four different temperatures (355°C, 425°C, 485°C and 530°C) with a residence time of 30 minutes. The resulting biochar was contained within the tube. Condensable and non-condensable gases went through a vacuum trap placed in an ice bath in order to recover bio-oil by condensation. Incondensable gas was collected in a sampling bag. The slow pyrolysis apparatus is as shown in Figure 19.

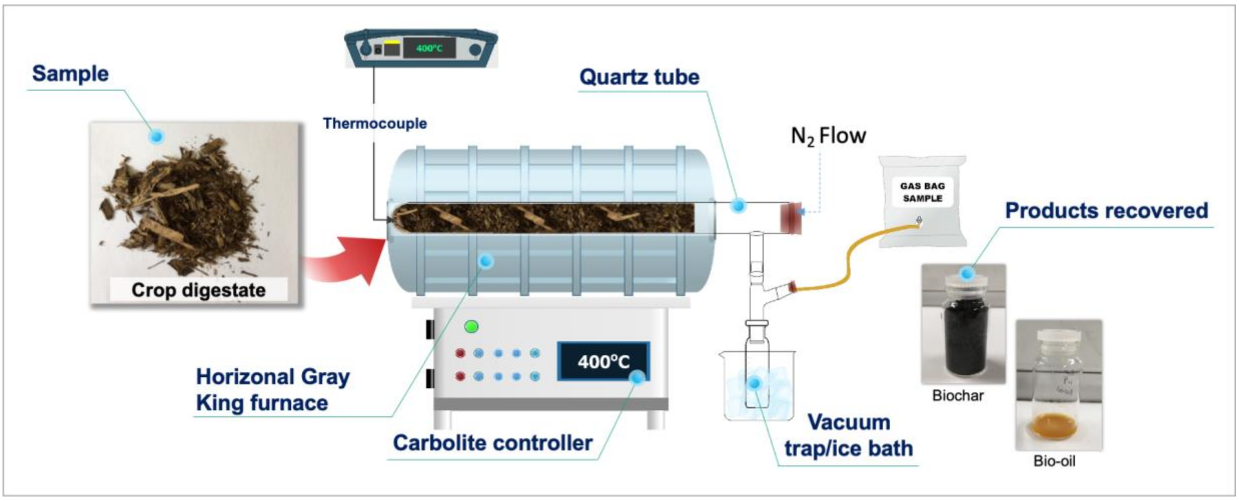
Sample
Crop digestate
400°C
Thermocouple
Quartz tube
N_2 Flow
GAS BAG SAMPLE
Products recovered
Biochar
Bio-oil
Horizonal Gray King furnace
400°C
Carbolite controller
Vacuum trap/ice bath

Figure 19. Slow pyrolysis system to process crop digestate.

Biochar collected from every thermal technology was stored in sealed bags and located in a dry environment until further analysis.

One drop of bio-oil sample was weighed in a tared screw vial to be processed in a mass spectrometer (GC-MS). Methanol (~0.5 ml) was added to preserve the sample before it was stored in a fridge to keep it cold and avoid degradation. This is one of the best methods to preserve bio-oil samples according to studies carried out with different pyrolytic liquid products [129]. The rest of the samples was stored in a glass vial to quantify the water.

SLOW PYROLYSIS MASS BALANCE

Total product recovery was based on the amount of biochar, bio-oil and gas quantified. The general calculations for yield of pyrolysis products consists of the following equations:

Equation 1 $$Y_{biochar}=\frac{(W_Q + W_{biochar})- W_Q}{W_{sample}} x\ 100$$

Equation 2 $$Y_{bio\text{-}oil}=\frac{(W_{trap}+ W_{liquid})\text{-}W_{trap}}{W_{sample}} x\ 100$$

For gas, the volume of the sample collection was measured and converted it into moles with the ideal gas law equation [130]:

Equation 3 $$n_{gas}=\frac{V_{gas}P_{gas}}{RT}$$

Final weight mass was calculated with the quantification determined with gas analyser which is explained more detail in section 3.3.4.7

where:

W_Q is quartz weight mass
W_{trap} is cold trap weight mass
$W_{biochar}$ is biochar recovered, weight mass
W_{sample} sample loaded, weight mass
W_{liquid} liquid recovered, weight mass
$Y_{biochar}$ is the total biochar recovered, weight mass %
Y_{liquid} is the total liquid recovered, weight mass %
n_{gas} is the total moles of gas collected
V_{gas} is total volume of gases collected, m^3
P_{gas} is pressure calculated in the gas sample bag, Pa
T is the temperature in absolute units, K
R is the universal gas constant, 8.314 J/(K-mol)

3.3.2 PROCESS DESCRIPTION - FAST PYROLYSIS SYSTEM

Crop digestate was processed in a 1 kg/h bench scale unit at the Technical Research Centre of Finland, VTT, which has been used successfully for many years to research diverse biomasses and process conditions. The system consists of a fluidised bed reactor, where approximately 0.300 kg of aluminium oxide (Al_2O_3) is used as fluidising agent and nitrogen (N_2) as an inert gas with a flow around 30 L/min. Residence time of the gas phase is less than one second.

The system requires feedstock with low water content, <10%, and particle size less than 1 mm. Crop digestate had to be pre-treated in VTT, where it went from dry raw material into pellets (Figure

20) to be ground, and then it was sieved to get particle sizes between 0.5 and 0.9 mm. The final particles employed in fast pyrolysis are shown Figure 21.

Figure 20. Digestate in pellets.

Figure 21. Digestate in particles 0.5-0.9 mm

The experiments carried out for this project were at four different temperatures: 460ºC, 480ºC, 520ºC and 560ºC. The temperatures across the reactor were measured in 4 sections: on the top, two on the middle and on the bottom. These need to be set around 50ºC above the target temperature the experiments would be run at. This is to stabilise the system because the biomass temperature is colder, and when this is fed it can lower the temperature inside the reactor. An example of the temperatures set up across the reactor for the experiment carried out at 560ºC is shown in Figure 22.

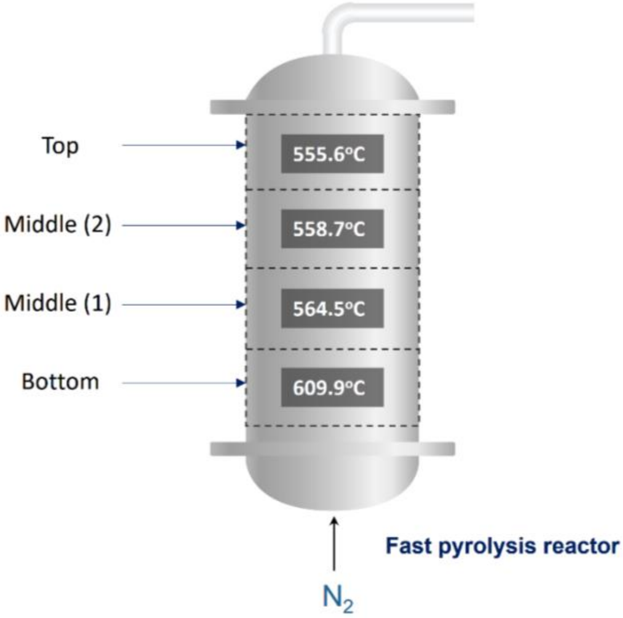

Figure 22. Temperature sections across fast pyrolysis reactor.

Moisture content in digestate was measured before every run to quantify and differentiate it from the water produced in lignocellulose decomposition. Each run duration was 3 hours to allow the system to stabilise and to obtain a reliable overall mass balance for the system.

Biochar was separated from gases and recovered through two cyclones. Hot gases, condensable and non-condensable, went through a liquid recovery section, in which bio-oil was condensed into four fractions. The first section was a water scrubber at around 45ºC where most of the easy condensable gases and water vapour were recovered. The second fraction was for heavier bio-oil compounds which were collected through an electrostatic precipitator. The third and fourth fraction were lighter organics and possible remaining water recovered by glycol coolers.

Non-condensable gases were analysed at the end of the system by directly injecting into a CP-4900 Micro Gas Chromatograph (Varian). Additionally, at the end of the first and the second hour in each experiment permanent gases were collected in sample bags to be analysed in the laboratory.

The general diagram of the process of fast pyrolysis set in VTT is shown in Figure 23. More detail about the system can be found in Oasmaa et al. [82] and other publications from VTT [131].

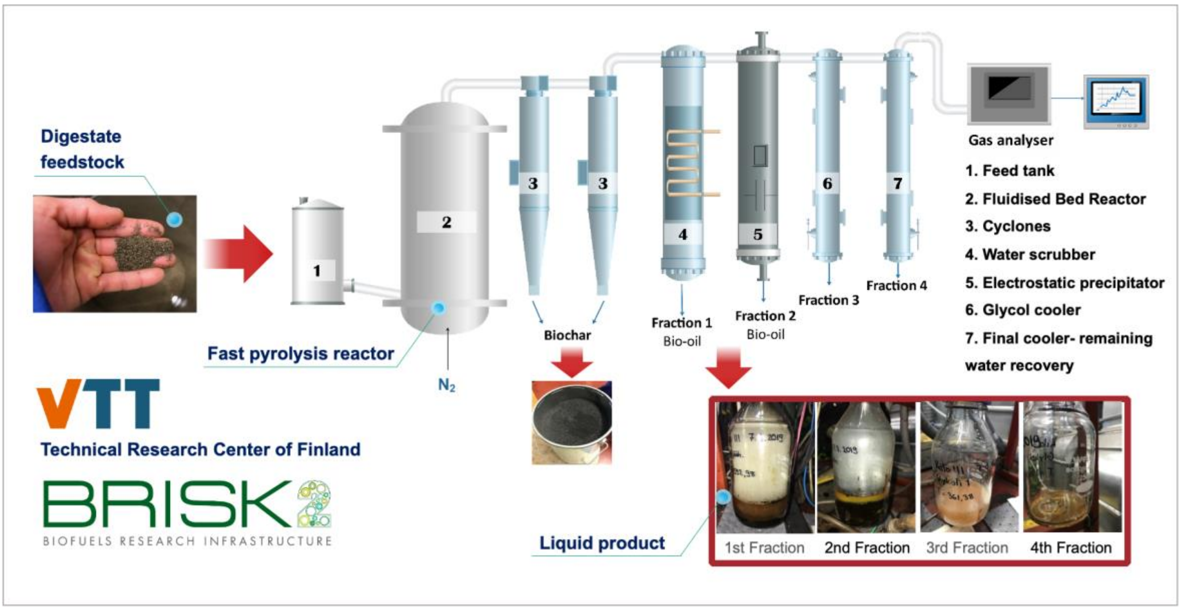
Digestate feedstock
1
2
3
3
4
5
6
7
Gas analyser
1. Feed tank
2. Fluidised Bed Reactor
3. Cyclones
4. Water scrubber
5. Electrostatic precipitator
6. Glycol cooler
7. Final cooler- remaining water recovery
Fraction 1 Bio-oil
Fraction 2 Bio-oil
Fraction 3
Fraction 4
Biochar
Fast pyrolysis reactor
N_2
VTT
Technical Research Center of Finland
BRISK2
BIOFUELS RESEARCH INFRASTRUCTURE
Liquid product
1st Fraction
2nd Fraction
3rd Fraction
4th Fraction

Figure 23. General diagram of fast pyrolysis system in VTT, using crop digestate.

Fast pyrolysis products were collected and labelled to be processed in the laboratory. The results obtained include elemental compositions of bio-oil and biochar and chemical compositions of gas and bio-oil. Water content of the bio-oil was carried out using the Karl Fisher method, which has had already been evaluated with different biomass by Oasmaa et al. [132]. Some bio-oil was sent to the

University of Nottingham to be analysed with the other bio-oil samples from the other technologies, employing the same method to ensure that possible variations in outcomes were not due to the analytical method. Samples were prepared and stored to be quantified by adding methanol and keeping in the fridge at low temperature in order to preserve them and avoid any degradation before being analysed. The same procedure of bio-oil preservation was applied to slow pyrolysis and microwave pyrolysis samples.

3.3.3 PROCESS DESCRIPTION - MICROWAVE PYROLYSIS

Pre-AD crop and crop digestate had a low volumetric density compared with woody biomass. The volume this biomass occupies without pelletising is greater than that occupied by the reactor vessel in the microwave cavity used for this study. As a result, a manual 24 tonne bench top pellet press (Carver Standard) was employed to densify these biomasses. Around 6 g of ground sample was loaded in a 10 mm long and 25 mm diameter pellet die under 10 tons of pressure. This procedure was carried out based on other experiments performed by Kostas et al. [90,133] using non-woody biomass with low volumetric density and with a moisture content lower than 10% in the same apparatus at the University of Nottingham. Pellet dimensions are shown in Figure 24.

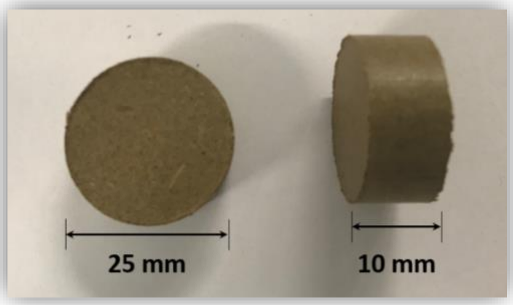

Figure 24. Pellets dimension employed in microwave pyrolysis system.

This system comprises a 2.45-GHz generator (Sairem, Décines-Charpieu, France) with a maximum power input of 2 kW. This power was delivered to the applicator through a standard WR340 waveguide. To improve the microwave power absorption efficiency a sliding short-circuit and a three-stub motorized *Homer* tuner (STHT 2.45 GHz, S-TEAM, Bratislava, Slovakia) were used for impedance matching. The analyser software within the *Homer* tuner processes the microwave power signal to obtain absorbed and reflected power profiles.

A 30 mm internal diameter quartz tube was employed as reactor to hold the biomass pellet and placed in a single-mode cavity. Nitrogen (N_2) was used as inert gas to run the experiments in absence of oxygen with a flow rate around 2 L/min, controlled with a flowmeter. An inlet line was connected on the top of the reactor to recover condensable gases through two vacuum traps in ice bath allocated at the bottom of the system. The set-up of the microwave system is shown in Figure 25.

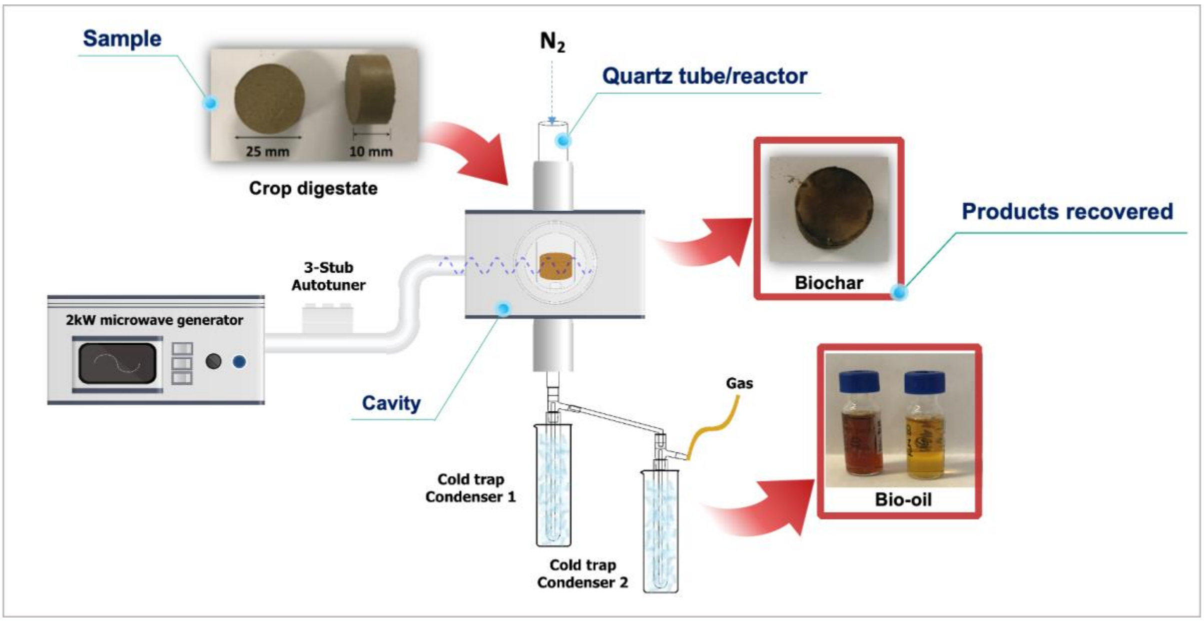
Sample
25 mm
10 mm
Crop digestate
N2
Quartz tube/reactor
Products recovered
Biochar
3-Stub
Autotuner
2kW microwave generator
Cavity
Gas
Bio-oil
Cold trap
Condenser 1
Cold trap
Condenser 2

Figure 25. Microwave pyrolysis system.

3.3.4 ANALYSIS OF PYROLYSIS PRODUCTS

3.3.4.1 BIOCHAR ANALYSIS PYROLYSIS

The same method of ultimate analysis employed for the biomass was implemented to analyse biochar pyrolysis products to determine total carbon (C), hydrogen (H) and nitrogen (N). Oxygen (O) was calculated by difference.

A correlation proposed by Dulong [134], which has been developed for coal, was employed to calculate higher heating value of biochar produced in these pyrolysis technologies, ash-free. This correlation is presented as Equation 4.

Equation 4 $$HHV\left(\frac{MJ}{kg}\right)=33.83\cdot m_c+144\cdot\left(m_H-\left(\frac{m_o}{7.94}\right)\right)$$ [135-137]

where:

m_c is the carbon content in the product.
m_H is the hydrogen content in the product.
m_O is the oxygen content in the product.

3.3.4.2 BIO-OIL ANALYSIS

3.3.4.2.1 BIO-OIL SAMPLE PREPARATION

Bio-oil samples were weighed in a tared 2 ml GC vial. Weight was recorded for quantification purposes. Samples were preserved to avoid exposure to heat and oxygen due to possible bio-oil degradation. 0.5 ml of methanol (MeOH) was added when the samples were collected, and they were then stored in the fridge to keep the samples at low temperature. Graduated vials were employed in order to avoid variation when the samples were prepared for the analysis.

Bio-oil products from pyrolysis have a certain amount of water content and some polar compounds have affinity to this liquid. Consequently, it was crucial not to evaporate this water or to analyse these samples on dry basis due to possible evaporation of irrecoverable organic compounds.

Most of the analytical studies for crude oil or bitumen quantification from fossil fuels are based on extraction with solvents such as dichloromethane (DCM) and being qualified in gas chromatography–mass spectrometry (GC-MS) analysers [138,139]. However, this pyrolytic bio-oil has two main components in the liquid: water and organics, and it cannot be handled similar to a fossil-based solution. In order to have a homogeneous bio-oil mixture, these samples were prepared with 1:1 ratio of MeOH and DCM, where water is miscible in MeOH and bio-crude in DCM.

3.3.4.3 STANDARDS PREPARATION

Standards were employed to obtain reliable quantification of the compound in pyrolysis bio-oil, and based on the analytical procedure developed by the National Renewable Energy Laboratory (NREL) [140]:

- Furfural (Sigma-Aldrich 185914)
- 5-(hydroxymethyl)furfural (Sigma-Aldrich W501808)
- Glycolaldehyde (Sigma-Aldrich G6805)
- Acetic acid (Sigma-Aldrich 320099)
- 1,6-anhidro-β-D-glucosa/levoglucosan (Sigma-Aldrich 316555)
- Trans-3,5-dimethoxy-4- hydroxycinnamaldehyde (Sigma-Aldrich 382159)

Each standard was weighed and allocated into a tared 10 ml volumetric flask to prepare a stock solution. The flask was filled to the graduation mark with 1:1 MeOH and DCM solution. Different dilutions were prepared until the amounts of standards added were similar and representative for pyrolysis bio-oil samples. These were evaluated by comparing the chromatograms of samples injected with standard at different concentrations. Seven dilutions were prepared from the stock for the calibration curves. The ratios of standard preparation are shown in Table 14, where solvent is DCM/MeOH.

Concentration (v/v %)	Solvent (ml)	Stock standard (ml)
90	0.15	1.35
80	0.30	1.2
60	0.60	0.9
50	0.75	0.75
40	0.90	0.6
20	1.20	0.3
10	1.35	0.15

Table 14. Ratios used to prepare calibration standards to a total volume of 1.5 ml.

Trials were also performed to verify whether there were differences between using only DCM as solvent and using a solution of DCM/MeOH in order to validate if the methodology of DCM/MeOH was the best approach for bio-oil analysis. This test was carried out with bio-oil samples and with the standard preparation. Some of the reagents used as standards precipitated when just DCM was added as solvent. The same issue resulted in bio-oil samples when only DCM was used, as some compounds were not detected when the sample was injected into the GC-MS system. An example of these variations resulting from sample preparation is shown in Figure 26, where the same bio-oil was prepared with only DCM and with DCM/MeOH. The sample used was obtained from slow pyrolysis of digestate at 530ºC

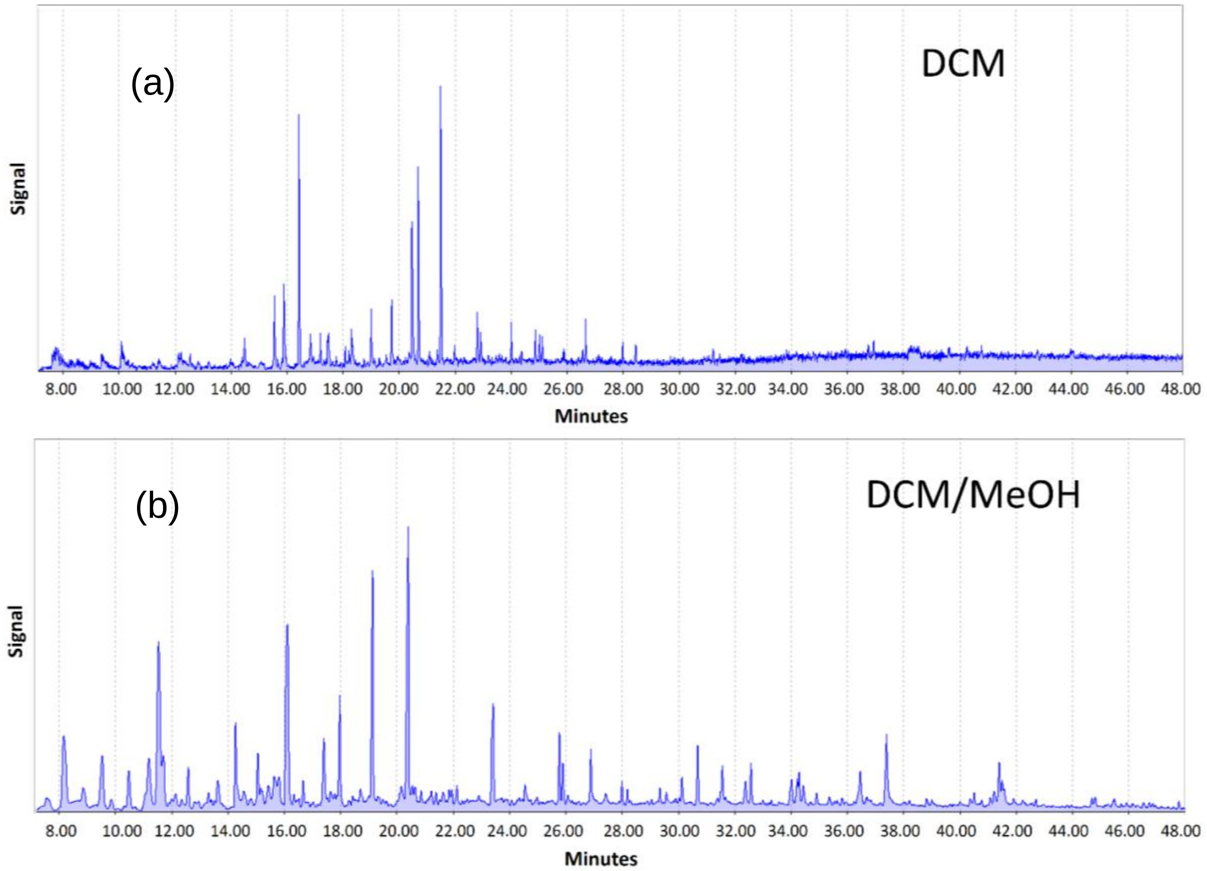

Figure 26. GCMS chromatograms of bio-oil from slow pyrolysis experiment at 530ºC: 1) sample with only DCM (2) sample with DCM/MeOH

Pyrolytic bio-oil was more soluble in a solvent prepared with DCM/MeOH than using DCM alone. The distribution of peaks in Figure 26 (b) is more efficient with less noise around each peak, and more compounds were detected. Chromatograms with this peak distribution facilitated the identification and quantification of compounds in bio-oils, and confirmed that analysis carried out using DCM as the sole solvent would not give a representative outcome.

3.3.4.4 MASS SPECTROMETER INSTRUMENT-OPERATION

The mass spectrometer (GC-MS) employed for this analysis is an Agilent 5977 series single quadrupole mass selective detector (MSD). This MSD processes data according to mass charge ratio (m/z) for small values and increasing to larger values. The range selected to analyse these samples was from m/z 29 to 400. Ionization of samples occurs in the 70 eV ion source and the column employed was DB-1701, a low/mid-polarity with 60 m x 250 μm x 0.25 μm stationary phase thickness. Injection was in splitless mode. Helium was used as carrier gas with a flow 1.2 mL/min. The GC oven was heated from 50ºC to 280ºC at 6°C/min.

Bio-oil resulting from experiments using crop waste (pre-AD) in slow pyrolysis was processed in the same GC-MS but with a different column (30 m × 0.25 mm, 0.25 µm stationary phase thickness). The GC oven was heated from 50ºC to 280ºC at 4°C/min for these measurements.

Standards were injected with these samples for identification and quantification. Additionally, bio-oil samples from microwave pyrolysis of pre-AD crop, already analysed with a 60 m x 250 µm x 0.25 µm column, were also processed with this second column in order to have supplementary solutions as a reference with known compounds. Both standards and bio-oils with known-composition were used to identify and quantify chemicals compounds in bio-oil from slow pyrolysis of pre-AD.

Examples of GC-MS chromatogram with compound identification of a bio-oil sample from microwave pyrolysis of pre-AD crop injected in 30 m and 60 m columns are shown in Figure 27 and Figure 28 respectively.

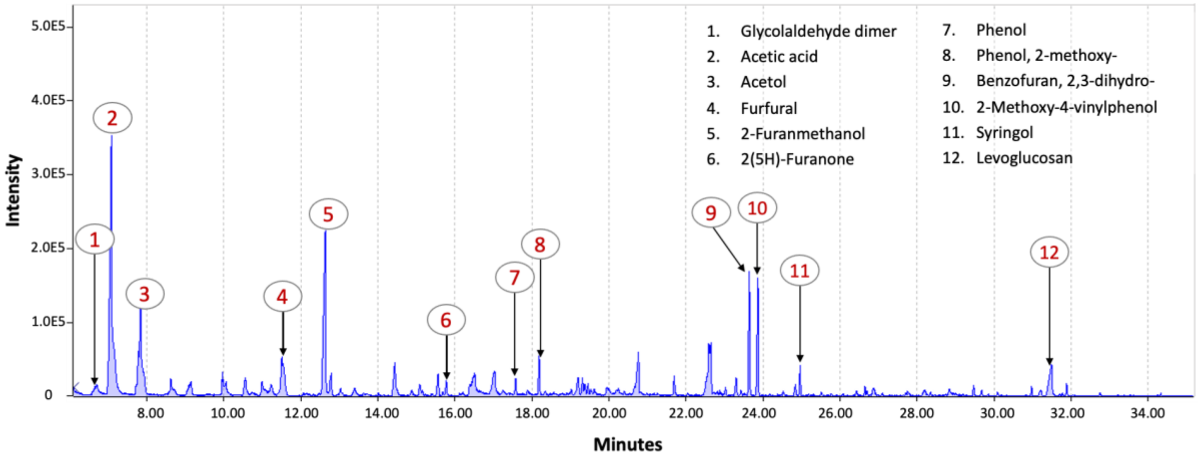

Figure 27. Chromatogram peaks resulted from GC-MS with column 60 m x 250 µm x 0.25 µm of a bio-oil from microwave pyrolysis of pre-AD crop.

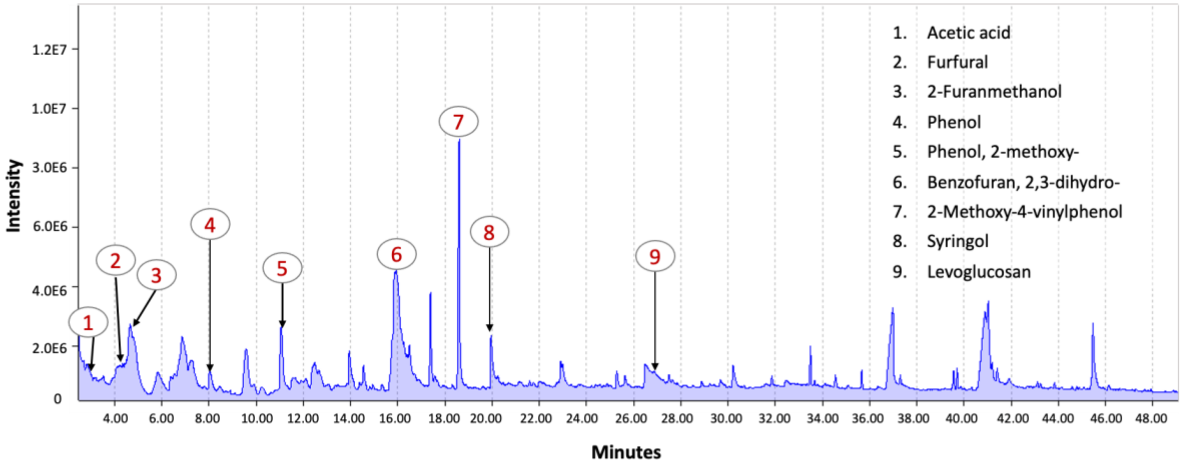

Figure 28. Chromatogram peaks resulted from GC-MS peaks resulted from GC-MS with column 30 m × 0.25 mm, 0.25 µm.

The chromatograms resulted from 60 m column were used as reference to identify key compounds (m/z) and to differentiate their retention time when the bio-oils are processed through 30 m column. This column does not separate some compounds efficiently as the 60 m. However, the quantification of each sample processed was determined according to the standards injected in each column.

3.3.4.5 IDENTIFICATION AND QUANTIFICATION

Standards were injected periodically within the bio-oil sample sequence to account for drift in the peak area and elution times.

Quantification consisted of the area under each peak detected in the chromatogram. This quantification was adjusted according to the standards injected with the samples.

Compound identification was performed by comparing the mass spectrum generated by the GC-MS with the National Institute of Standards and Technology (NIST) library, version 14. Factors considered for this procedure were retention time (RT) and the five greatest m/z values that match between the GC-MS and NIST records.

An example of a chromatogram resulting from a standard solution injected is shown in Figure 29. Table 15 is the summarised data obtained from the chromatogram.

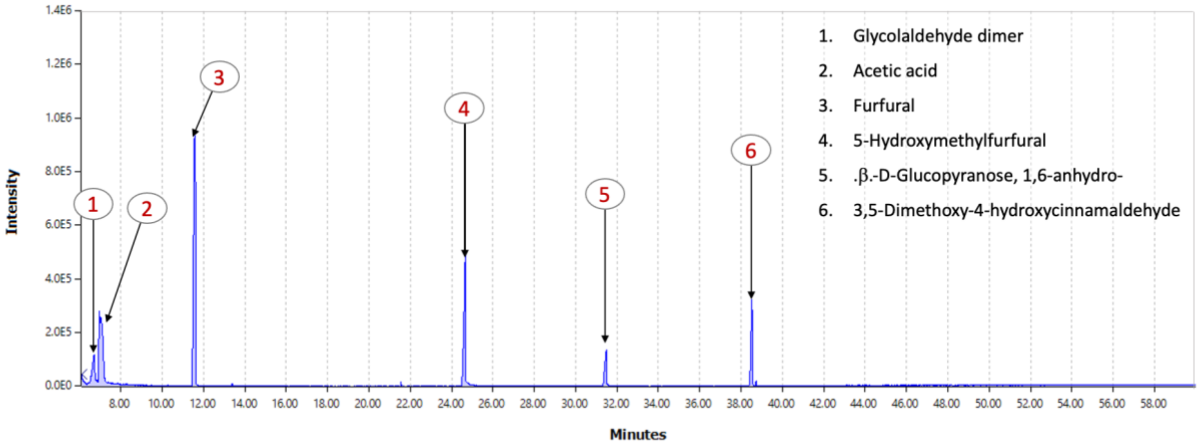

Figure 29. Example of chromatogram resulted from GC-MS analysis of standards.

RT (Min)	Name	MW	Integrated area	% Area	m/z ions
6.73	Glycolaldehyde dimer	120	16868187.94	5.16	31.0 | 32.0 | 60.0 | 42.0 | 30.0
7.09	Acetic acid	60	61680235.51	18.86	43.0 | 45.0 | 60.0 | 42.0 | 31.0
11.63	Furfural	96	143906306.4	44.01	96.0 | 95.0 | 39.0 | 38.0 | 37.0
24.72	5-Hydroxymethylfurfural	126	59039383.64	18.06	97.0 | 126.0 | 41.0 | 39.0 | 69.0
31.52	β.-D-Glucopyranose, 1,6-anhydro-	162	13923873.35	4.26	60.0 | 57.0 | 73.0 | 29.1 | 70.0
38.55	3,5-Dimethoxy-4-hydroxycinnamaldehyde	208	31539367.19	9.65	208.0 | 165.0 | 137.0 | 180.0 | 177.0

Table 15. Data and outputs from GC-MS analysis.

An example of calibration curves resulted from these preparations is shown in Figure 30.

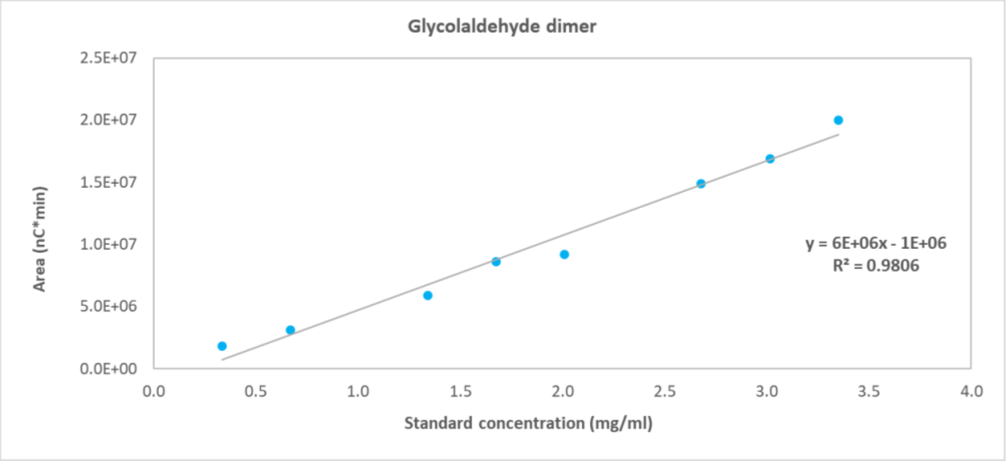

Figure 30. Example of calibration curve. Seven different concentrations of glycolaldehyde dimer.

Bio-oil samples can contain a large number of compounds, sometimes more than 200. This would be the amount of standards needed to get a more precise quantification, and is not practical nor needed for the purposes of this study. However, there are other techniques such as method 8270E, semi-volatile organic compounds by gas chromatography/mass spectrometry, from the United States Environmental Protection Agency (EPA) [141]. This quantification method consists of response factors, which is the ratio between a peak area (response) of specific compound with a known concentration, such as standards, and the response of target compound in a sample.

The calibration curve for this was employed for analytes found in bio-oil samples. However, not all the compounds could be found. The analyte most identified across all the samples injected was acetic acid. This was utilised as the base to calculate the concentration of the other compounds in the bio-oil. Equation 5 and Equation 6 were implemented for this calculation.

Equation 5 $$RF=\frac{PA_1}{C_1}$$

Equation 6 $$C_n=\frac{PA_n}{RF}$$

Where:

RF is response factor
PA_1 is peak area of analyte used as base (acetic acid)
C_1 is concentration of analyte used as base (acetic acid)
PA_n is peak area of *n* compound target to quantify
Cn is concentration of compound *n* target to quantify

The next calculation is an example to obtain acetol concentration in a sample where acetic acid was detected and quantified. Acetic acid had a peak area of 156,645.17 (PA_1) resulting in a concentration of 0.86 mg/mL (C_1), and acetol detected had a peak area of 70,889.92 (PA_2). Using equations Equation 5 and Equation 6 this sample had 0.39 mg/mL (C_2) of acetol:

$$RF=\frac{156{,}645.17}{0.86}=183{,}107.09$$

$$C_2=\frac{70{,}889.92}{183{,}107.09}=0.39\ \left(\frac{mg}{mL}\right)$$

If the case acetic acid was not detected another standard compound identified in the sample was employed for this calculation. Levoglucosan, for instance, was used to adjust the response factors for the bio-oil resulted from pre-AD slow pyrolysis.

3.3.4.6 WATER DETERMINATION IN BIO-OIL

The Dean-Stark method has been employed to determine the amount of water formed in the slow pyrolysis produced bio-oil (ASTM D95). This is a standard test method to determine water in petroleum products by distillation [142].

This assay consisted of adding 150 ml of toluene in a 250-ml round bottom flask with the bio-oil recovered and weighed from the slow pyrolysis system. This flask is connected to a Dean-Stark condenser and heated for around 7 hours until the water has stopped condensing. The water content was measured in using a graduated scale where the difference is between the water (in the bottom) and the toluene (on top). The set-up of this experiment is shown in Figure 31.

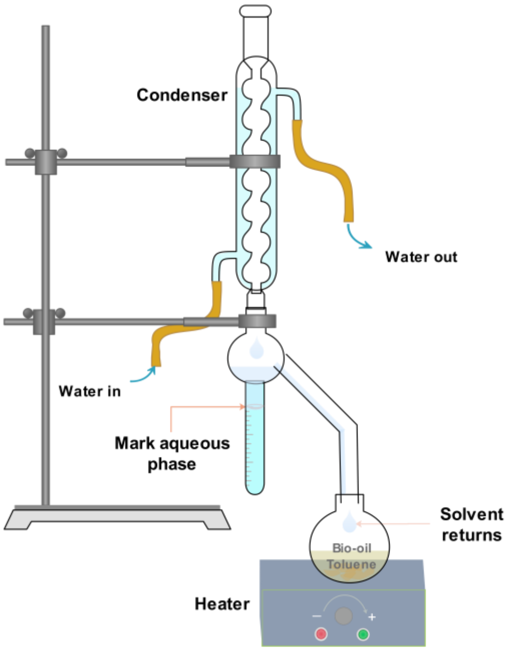

Figure 31. General diagram of Dean-Stark system.

Water in the total bio-oil recovered was calculated with Equation 7, considering water density is 1 g/mL.

Equation 7 $$AP_w = W_{bio\text{-}oil} \times \frac{AP_v \times \rho_{H_2O}}{W_S} \times 100$$

Where:

AP_w is water in mass weight (g)
AP_v is water volume measured in Dean-Stark (ml)
$W_{bio\text{-}oil}$ is the total mass of bio-oil recovered (g)
ρ_{H_2O} is water density (g/ml)
W_S is the weight of the sample tested (g)

The total water formed from the thermochemical decomposition is this value calculated minus the initial mass moisture contained in the biomass pyrolysed.

3.3.4.7 GAS ANALYSIS SLOW PYROLYSIS

The gas samples from slow pyrolysis of digestate were collected directly in Tedlar® PVDF bags, with a Push/Pull Lock Valve (PLV). These specific samples were processed as soon as the experiment was concluded. Gas samples were analysed on a Clarus 580 gas chromatograph (GC) fitted with a flame ionization detector (FID) and thermal conductivity detector (TCD) operating at 200°C. The hydrocarbon gases were analysed by injecting 100 µl of gas in a split ratio of 10:1 onto the FID at 250°C with separation performed on an alumina fused silica 30 m x 0.32 mm x 10 µm column. Helium was used as carrier gas. The oven temperature was programmed to be heated from 60°C, holding for 13 minutes, to 180°C (10 minutes hold), with a heating rate of 10°C/min, for hydrocarbon gases (HC) identification in relation to C1-C5 gases from standard. Non-hydrocarbon (NHC) gas standards, injected individually, were separated through a Haysep N6 packed column (60–80, 7_ ×1/8_sulfinert), using argon as the carrier gas. The oven temperature was programmed from 60°C (13 min hold) to 160°C (2 min hold) at 10°C/min. The non-hydrocarbon (H_2, CO, and CO_2) yields were also identified in relation to their individual gas standards (injected separately) as a mixture of external gas standard.

Gas standards from BOC Ltd consisted of hydrocarbon and non-hydrocarbon. 5 ml of these were injected separately and had have the composition and proportion shown in Table 16 and Table 17.

Components (HC)	Proportion (Vol %)
Methane	20.0%
Ethane	10.0%
Propylene/Propene	0.2%
Ethylene/Propane	5.0%
N-Butane	2.0%
1-Butene	0.2%
N-Pentane	1.0%
1-Pentene	0.2%
Helium	61.2%

Table 16. Hydrocarbon gas standards to identify and quantify non-condensable pyrolytic gases from digestate.

Components (NHC)	Proportion (Vol %)
Hydrogen	10.0%
CO_2	10.0%
H_2S	20.0%
CO	40.0%
Argon	20.0%

Table 17. Non-hydrocarbon gas standards to identify and quantify non-condensable pyrolytic gases from digestate.

The percentage peak area for each compound was determined from the chromatograms resulting from the FID system such as the shown in Figure 32.

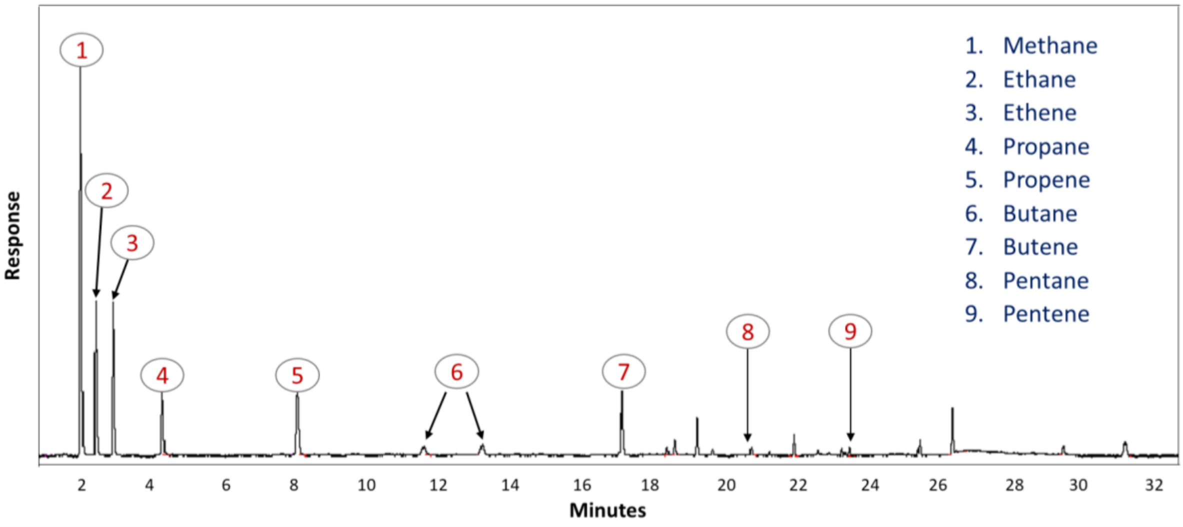

Figure 32. Example chromatogram of hydrocarbons detected from the slow pyrolysis system.

The amount of sample injected was 5 ml. Calculation of the proportion in the gas for each compound was carried out according to the ASTM D7833-14 Standard [143] and Equation 8-10.

Equation 8:

$$\text{HC\% in 5ml} = \frac{A_s}{A_{HC}\ \text{x RF}} \times C_{HC}$$

Equation 9 :

$$\text{NHC\% in 5ml} = \frac{A_s}{A_{NHC}\ \text{x RF}} \times C_{NHC}$$

Where:

RF is response factor

A_S is gas sample area

A_{HC} is the area of hydrocarbon standard

C_{HC} is proportion in % of compound in standard mixture of HC

A_{NHC} is the area of non-hydrocarbon standard

C_{NHC} is proportion in % of compound in standard mixture of NHC

Equation 10:

$$RF_{C6} = RF_{C5AV} \times \frac{72}{93}$$

Where:

RF_i is the response factor for component i

C_i is the known concentration of i

RF_{C5AV} is the average RFs of i-C_5 and n-C_5

CHAPTER 4. MATERIALS AND METHODS- MODELLING

The main driver of choosing a scheme of reactions to model pyrolysis of AD waste was due to the wide variety of biomass feedstocks and subsequently the variation in lignocellulose content of the digestate. Experimental studies can indicate the yield and quality of pyrolysis products for a given feedstock, however this approach cannot be applied universally for all conceivable biomass types. Thus, a model was proposed to predict thermochemical conversion of digestate derived from different material with a different lignocellulosic composition from the biomass studied experimentally. This approach will allow an estimation of the possible characteristics of the pyrolysis products, and subsequently evaluate strategies for the integration of this technology with other process systems across Severn Trent AD sites.

4.1 KINETIC MODEL FOR PYROLYSIS

Three schemes of reactions were selected from those described in the literature in section 2.6 to be compared with published lignocellulose pyrolysis data. These schemes were classified as Versions according to the modelling projections:

- **Version 1:** Ranzi et al. [96] 'Chemical Kinetics of Biomass Pyrolysis'
- **Version 2:** Calonaci et al. [97] 'Comprehensive Kinetic Modeling Study of Bio-oil Formation from Fast Pyrolysis of Biomass'
- **Version 3** (Ash-free): Ranzi et al. [144] 'Mathematical Modeling of Fast Biomass Pyrolysis and Bio-Oil Formation. Note I: Kinetic Mechanism of Biomass Pyrolysis'
- **Version 4 (**Ash content**)**: Ranzi et al. [144] 'Mathematical Modeling of Fast Biomass Pyrolysis and Bio-Oil Formation. Note I: Kinetic Mechanism of Biomass Pyrolysis'

These kinetic schemes were used to predict product yield and composition and to compare with published data. The model employed to simulate pyrolysis of pre-AD and crop digestate was selected according to the best approximation between the modelling results and published data which is described in section 4.2.1.

4.1.1 CROP DIGESTATE PSEUDO-LIGNIN COMPOSITION

One of the primary considerations in each model is the lignocellulosic composition of the biomass. This methodology was implemented in my MSc research project in 2016 [145], and included the analysis of how to predict the distribution of pseudo-lignins. A crop digestate collected and analysed in 2016 was used to exemplify this implementation. The analysis of this specific sample was performed by Dr Emily Kostas based on a method developed by Kostas et al. [146]. The results of this digestate characterisation are shown in Table 18.

Component	Composition
Ash	10.3 ± 0.1
Protein	9.7 ± 0.5
Lipid[a]	3.9 ± 1.1
Lignin[b]	21.8 ± 0.5
Cellulose[c]	20.9 ± 3.9
Hemicellulose[d]	17.5 ± 3.5
Moisture content	5.3 ± 0.2

Data is the mean ± SD of three replicate measurements. Dry weight basis wt %

[a]Solvent extractable lipid

[b]Acetyl bromide soluble lignin

[c]Cellulose is glucose

[d]Hemicellulose of which xylose, arabinose and galactose

Table 18. Characterisation of crop digestate collected in 2016 at Severn Trent site in Stoke Bardolph [145].

In order to employ this information in the model, the data obtained about the lignocellulosic material content in the sample needs to be normalised to a 100% wt as the scheme of reactions is based only on lignocellulose decomposition on a dry weight basis. The distribution of cellulose, hemicellulose and lignin as total content in crop digestate is shown in Table 19.

Crop digestate			
	Cellulose	**Hemicellulose**	**Lignin**
Determined	20.9	17.5	21.8
Normalised	34.7	29.1	36.2

Table 19. Cellulose, hemicellulose and lignin proportion in crop digestate adjusted for pseudo-lignin calculation.

In addition, the kinetic model developed for pyrolysis needs as initial inputs the pseudo-lignins content in digestate, which are: rich in carbon (LIG_C), rich in hydrogen (LIG_H) and rich in oxygen (LIG_O). However, the methodology implemented and equipment employed to analyse the digestate sample to obtain the composition do not deliver this specific information. As a solution, other models and correlations were evaluated to obtain an approximation of all the lignocellulosic components in the digestate.

Most of these models are based on elemental composition such as C, H, O, and C/H ratio. This methodology is based on plotting the lignocellulose components of different biomass samples, which have been already examined, knowing the exact proportion content of each pseudo-lignin.

The initial information needed is the elemental composition of cellulose, hemicellulose, and the pseudo-lignins shown in Table 20.

	Component	Formula	C (wt %)	H (wt %)	O (wt %)	Molecular weight
CELL	Cellulose	$C_6H_{10}O_5$	44.45	6.22	49.34	162.14
HCE	Hemicellulose	$C_5H_8O_5$	45.46	6.10	48.44	132.11
LIG	Lignin	$C_{11}H_{12}O_4$	63.45	5.81	30.74	208.21
LIG_C	Carbon-rich lignin	$C_{15}H_{14}O_4$	69.76	5.46	24.78	258.27
LIG_H	Hydrogen-rich lignin	$C_{20}H_{22}O_{10}$	60.54	6.47	32.99	436.45
LIG_O	Oxygen-rich lignin	$C_{22}H_{28}O_9$	56.87	5.25	37.88	422.38

Table 20. Elemental composition (weight basis) of the main lignocellulosic components in the biomass [147].

Plotting this data results in triangles which represents the limits of the composition range of the biomass, as shown in Figure 33. By using C/H ratios of each component, it is possible to predict the amount of each lignocellulosic component in the biomass. The projections are based on three samples with a known lignocellulosic composition which includes the three lignins. These compounds are shown in Figure 33 as Point 1 (P1), Point 2 (P2), and Point 3 (P3). P1 has a composition of 60% cellulose and 40% hemicellulose with a C/H ratio of 44.8/6.16. P2 has a ratio of 59.0/5.44 and a lignin distribution of 0.8 LIG-O and 0.2 LIG-C, and P3 has a ratio of 61.9/6.4 composed by 0.8 LIG-H and 0.2 LIG-C [148,149].

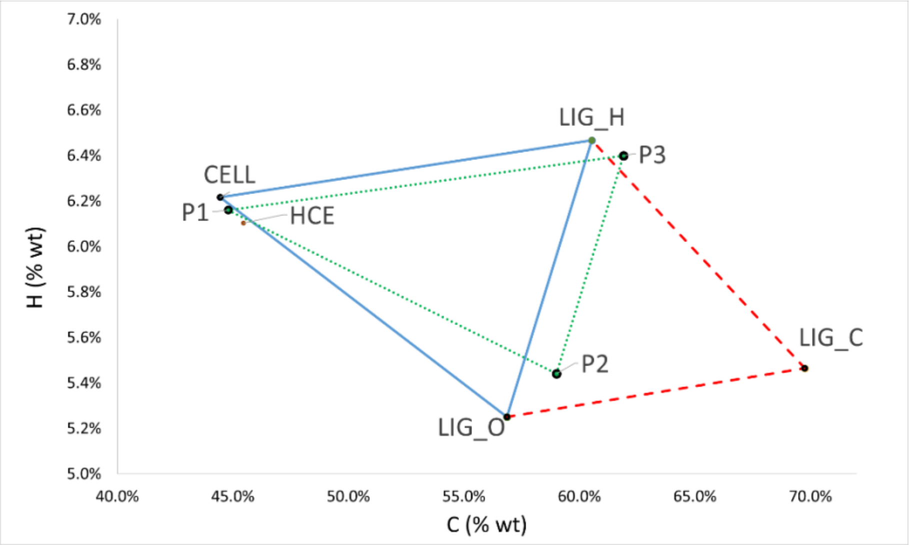

Figure 33. Base characterisation model to predict the main components in the biomass.

The information can be arranged as three equations with three variables:

Equation 11 $$C_{Biomass} = C_{P1} \cdot x_1 + C_{P2} \cdot x_2 + C_{P3} \cdot x_3$$

Equation 12 $$H_{Biomass} = H_{P1} \cdot x_1 + H_{P2} \cdot x_2 + H_{P3} \cdot x_3$$

Equation 13 $$1 = x_1 + x_2 + x_3$$

where every C and H in the equations represent carbon and hydrogen composition, respectively. $C_{Biomass}$ and $H_{Biomass}$ are the composition of the biomass to use as feedstock and need to be considered as ash- and moisture-free content. Examples of pseudo-lignin composition of different biomasses that have been already analysed are shown in Table 21.

Biomass	C (% wt)	H (% wt)	O (% wt)	LIG-C	LIG-H	LIG-O
				% wt	% wt	% wt
Industrial lignin	65.80	6.50	27.70	37.84	37.84	12.93
Almond shell	50.81	42.93	6.26	5.52	28.65	8.37
Beech wood	52.90	5.90	41.20	3.63	10.21	13.85
Poplar wood	50.20	6	43.80	2.14	9.57	13.25
Softwood	53.20	6	40.80	7.07	31.07	16.19
Pinewood	48.30	5.90	43.50	6.6	0	26.2

Table 21. Lignin composition of different biomass analysed [18,100,147,150].

The C/H ratio plotted for each sample is shown in Figure 34 and is essential information for the methodology mentioned before. The C/H and O/C ratios are the base to obtain the composition of the pseudo-lignins.

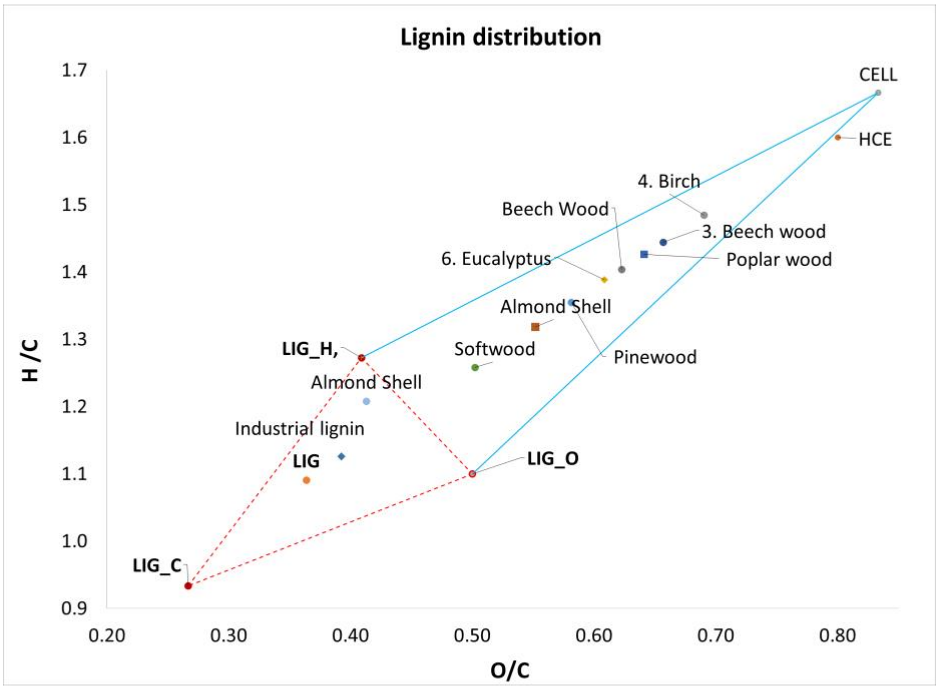

Figure 34. C/H, O/C ratios of lignocellulosic material and its distribution of pseudo-lignins due to the ratios.

There is limited data regarding measurements of pseudo-lignin content in biomasses. However, biomass composition presented in Table 21 could be a reference to validate if these correlations can be employed to determine pseudo-lignin content in crop digestate.

A comparison between biomasses analysed for pseudo-lignins and the calculation using these correlations is presented in Table 22.

Biomass	LIG-C	LIG-H	LIG-O
Beech wood			
Data	3.63	10.21	13.85
Lignin projection	6.09	11.98	12.37
Poplar wood			
Data	2.14	9.57	13.25
Lignin projection	5.17	9.93	10.74
Softwood			
Data	7.07	31.07	16.19
Lignin projection	10.87	20.11	23.36

Table 22. Comparison between pseudo-lignin composition published of some biomasses and projections resulted from correlations [18,147,150].

There is a greater variation between LIG-H and LIG-O in softwood, but beech and poplar wood projections are closer to data from biomass measurements. Considering there are few non-woody biomasses analysed for pseudo-lignins this approximation was considered to be implemented to estimate pseudo-lignin composition in crop digestate. Predictions of pseudo-lignin content in crop digestate are shown in Table 23.

Proportion of lignins in crop digestate			
Total lignin	**Lig-C**	**Lig-H**	**Lig-O**
36.21	**7.24**	**13.48**	**15.49**

Table 23. Results of the proportion of the lignin composition (wt %) in the digestate using the model based on the C, H, and O elemental composition.

This estimation was employed to determine pseudo-lingin in both biomasses employed in this study, pre-AD crop and crop digestate. These results were inputs for the kinetic model.

4.2 PYROLYSIS MODEL PRELIMINARY VALIDATION- LITERATURE DATA

All the schemes of reactions mentioned in Section 4.1 have been used to simulate pyrolysis of digestate based on the information presented of the reactions.

The kinetic model has been developed by using Arrhenius' equation in order to know the rate of lignocellulose decomposition and the formation of the products. This equation is represented in Equation 14.

Equation 14 $$k_n = A_n * e^{(-E_n/R*T)}$$ [151]

where: *n* is related to each reaction of the model

k is the rate coefficient

A is the frequency or pre-exponential factor (s^{-1})

E is the activation energy

R is the universal gas constant, with a value of 8.314×10^{-3} kJ $mol^{-1}K^{-1}$

T is the temperature in kelvin

The principle used to solve the rates of the reactions in each scheme is explained with the next example. When B is decomposed to produce C and D, the expression is:

$$B \rightarrow C + 2D$$

Then, the representation of each component as kinetic rate is:

$\frac{d[B]}{dt}$=-k*[B], the negative sign is due to B decomposition

$\frac{d[C]}{dt}$=k*[B], C is a component generated from B decomposition

$\frac{d[D]}{dt}$=2*k*[B], D is formed from twice the number of moles of B decomposition where the symbol [B] is the concentration of that element.

All the reactions can be considered as first order because there is only one reactant, B, with a stoichiometric coefficient of 1. As a result, this methodology was implemented to quantify the transformation of lignocellulosic material into pyrolysis products. This results in only one reactant per reaction with a stoichiometric coefficient of 1. For example, the decomposition of cellulose and rich-carbon lignin can be exemplified as:

$$\frac{d[CELL]}{dt}=-k^*[CELL] \quad \text{cellulose decomposition}$$

$$\frac{d[LIG\_C]}{dt}=-k^*[LIG\_C] \quad \text{lignin rich in carbon decomposition}$$

where [CELL] and [LIG_C] are the concentration of cellulose and the carbon-rich lignin, respectively.

4.2.1 KINETIC MODEL PRELIMINARY VALIDATION

Based on the scheme of reactions presented in Section 4.1, four versions of the kinetic model were developed with the idea of verifying whether the model could be a reliable way to simulate pyrolysis of digestate.

The outcomes of the four kinetic model versions are the total pyrolysis products and their composition. These are:

- Total solids; the sum of lignin rich in C (LIG-CC), trapped CO_2 (G{CO_2}), trapped CO (G{CO}), trapped COH_2 (G{COH_2}), trapped H_2 (G{H_2}) and biochar (C). Intermediate products such as G{CO_2}, G{CO}, G{COH_2} and G{H_2} are in gas or solid phase. If these components are not completely realised as gas, they are considered as part of the final biochar [96].
- Total gas; hydrogen (H_2), carbon monoxide (CO), carbon dioxide (CO_2), methane (CH_4), ethylene (C_2H_4) and ethane (C_2H_6).
- Total aldehydes and ketones; formaldehyde, acetaldehyde, propanal, hydroxyacetaldehyde, glyoxal, propanedial and acetol.
- Total acids; formic acid and acetic acid.
- Total furans; 5-hydroxymethyl-furfural and furfural.
- Total alcohols; methanol and ethanol.
- Total phenolics; paracoumaryl alcohol, phenol and cinnamaldehyde.

- Total sugars; levoglucosan and xylose.
- Water vapour; the water formed from lignocellulose decomposition.

Preliminary projections of the four versions were carried out in order to select the best approach to simulating pyrolysis of digestate. Data employed to compare these projections is from the literature where experiments were performed with beech and pine by Wang et al. [152]. The mass balance is based on the law of mass conservation, where biomass feed is the equal to mass pyrolysis products. The equations employed were:

Equation 15 $m_{\text{biomass}} = m_{\text{bio-oil}} + m_{\text{gas}} + m_{\text{biochar}} + m_{\text{water}}$
Equation 16 $m_{\text{bio-oil}} = x_{\text{bio-oil}} \cdot m_{\text{biomass}}$
Equation 17 $m_{\text{gas}} = x_{\text{gas}} \cdot m_{\text{biomass}}$
Equation 18 $m_{\text{biochar}} = x_{\text{biochar}} \cdot m_{\text{biomass}}$
Equation 19 $m_{\text{water}} = x_{\text{water}} \cdot m_{\text{biomass}}$

where: m_{biomass}, the total mass of biomass fed into the reactor (wt)
$m_{\text{bio-oil}}$, the total mass of bio-oil produced (wt)
m_{gas}, the total mass of gas produced (wt)
m_{biochar}, the total mass of biochar produced (wt)
m_{water}, the total mass of water produced (wt)
$x_{\text{bio-oil}}$, the mass proportion of bio-oil in the products
x_{gas}, the mass proportion of gas in the products
x_{biochar}, the mass proportion of biochar in the products
x_{water}, the mass proportion of water in the products

Inputs for the model about the biomass composition are presented in Table 24.

Feedstock	Beech wood	Pine wood
Cellulose	43.04	41.71
Hemicellulose	28.66	25.95
Lignin	21.06	25.02
Lignin C	*3.99*	*6.49*
Lignin H	*8.53*	*9.27*
Lignin O	*8.53*	*9.27*
Moisture	6.77	*6.95*
Ash	0.46	*0.37*

Table 24. Lignocellulose composition in beech and pine presented by Wang et al. [152] and used for the model validation. Data is presented in % wt.

Comparison of the models and empirical data are shown for beech in Table 25 and pine in Table 26.

Products	Composition (wt %)				
	Experiment	Projection V1	Projection V2	Projection V3	Projection V4
Total solid	**16.00**	**18.36**	**14.86**	**14.77**	**15.28**
G_CO2		0.00	0.19	0.02	0.02
G_CO		0.00	0.00	0.30	0.30
G_COH2		4.73	5.20	4.57	4.57
G_H2			0.15	0.03	0.03
Biochar (C)		13.63	9.32	6.47	6.97
G_CH4				1.12	1.13
G_C2H4				1.16	1.17
G_CH3OH				1.10	1.10
Total gas	**17.58**	**20.22**	**24.75**	**18.20**	**18.29**
Hydrogen (H2)	0.02	1.04	1.45E-05	0.02	0.02
Carbon monoxide (CO)	4.90	5.76	7.77	8.01	8.05
Carbon dioxide (CO2)	12.0	12.49	11.24	8.29	8.35
Methane (CH4)	0.51	0.46	3.06	0.44	0.43
Ethylene (C2H4)	0.15	0.47	2.69	1.44	1.43
Ethane (C2H6)	0.12				
Total liquid	**57.70**	**60.10**	**59.89**	**58.90**	**54.16**
Water vapor (H_2O)	**12.20**	**4.86**	**4.80**	**6.55**	**5.12**
Total organics	**45.50**	**55.23**	**55.08**	**52.35**	**49.04**
Total aldehydes and ketones		**20.21**	**20.17**	**17.63**	**17.81**
Formaldehyde		4.51	4.51	3.91	3.93
Acetaldehyde		1.58	1.58	1.50	1.52
Propanal		3.31	3.31	4.70	4.76
Hydroxyacetaldehyde		8.50	8.50	5.51	5.58
Glyoxal		2.16	2.16	1.15	1.15
Propanedial		0.15	0.10		
Acetol (C3H6O2)				0.85	0.87
Total alcohols		**4.96**	**4.96**	**3.19**	**3.20**
Methanol		3.62	3.62	2.59	2.60
Ethanol		1.34	1.34	0.60	0.60
Total furans		**4.70**	**4.70**	**8.76**	**8.02**
5-Hydroxymethyl-furfural		4.70	4.70	7.14	6.50
Furfural (C5H4O2)				1.62	1.53
Total sugars		**22.03**	**22.03**	**16.28**	**13.55**
Levoglucosan		21.83	21.83	9.87	9.15
Xylose monomer		0.20	0.20	6.41	4.40
Total phenolics		**3.33**	**3.23**	**3.29**	**3.28**
Paracoumaryl alcohol		0.51	0.44	0.24	0.24
Phenol		0.24	0.20	0.12	0.12
Sinapaldehyde		2.58	2.58	2.54	2.53
Anisol (C7H8O)				0.40	0.39
Total acids		**0.00**	**0.00**	**3.19**	**3.18**
Formic acid (HCOOH)				0.44	0.45
Acetic acid (CH3COOH)				2.75	2.74

Table 25. Comparison between models using different reaction schemes. Empirical data was obtained with beech wood at 500^{o}C from experimental results presented by Wang et al. [152].

Products	Composition (wt %)				
	Experiment	Projection V1	Projection V2	Projection V3	Projection V4
Total solid	**18.40**	**20.45**	**16.75**	**13.54**	**13.92**
G_CO2		0.00	0.03	0.00	0.00
G_CO		0.00	0.00	0.00	0.00
G_COH2		5.09	5.49	4.48	4.48
G_H2			0.14	0.02	0.02
Biochar (C)		15.36	11.09	6.77	7.15
G_CH4				1.15	1.15
G_C2H4				1.07	1.07
G_CH3OH				0.04	0.04
Total gas	**18.00**	**20.27**	**25.37**	**19.25**	**19.28**
Hydrogen (H2)	0.085	1.01	1.20E-04	0.02	0.02
Carbon monoxide (CO)	7.398	6.17	8.39	8.86	8.87
Carbon dioxide (CO2)	8.975	11.91	10.91	8.05	8.07
Methane (CH4)	1.232	0.58	3.18	0.54	0.54
Ethylene (C2H4)	0.310	0.59	2.90	1.78	1.77
Total liquid	**51.40**	**57.72**	**57.65**	**56.72**	**55.62**
Water vapor (H2O)	**10.17**	**5.83**	**5.82**	**6.79**	**6.08**
Total organics	**41.23**	**51.89**	**51.83**	**49.93**	**49.54**
Total aldehydes and ketones		**24.02**	**24.00**	**17.95**	**18.05**
Formaldehyde		4.16	4.16	3.93	3.94
Acetaldehyde		2.01	2.01	1.52	1.53
Propanal		3.98	3.98	4.87	4.90
Hydroxyacetaldehyde		10.86	10.86	5.65	5.69
Glyoxal		2.76	2.76	1.13	1.13
Propanedial		0.24	0.22		
Acetol (C3H6O2)				0.84	0.85
Total alcohols		**4.89**	**4.89**	**4.26**	**4.26**
Methanol		3.67	3.67	3.72	3.71
Ethanol		1.22	1.22	0.55	0.54
Total furans		**6.00**	**6.00**	**8.03**	**8.07**
5-Hydroxymethyl-furfural		6.00	6.00	6.60	6.65
Furfural (C5H4O2)				1.43	1.42
Total sugars		**14.02**	**14.02**	**13.61**	**13.11**
Levoglucosan		13.91	13.91	7.71	7.27
Xylose monomer		0.11	0.11	5.90	5.84
Total phenolics		**2.97**	**2.92**	**3.15**	**3.14**
Paracoumaryl alcohol		0.83	0.80	0.41	0.41
Phenol		0.38	0.37	0.20	0.20
Sinapaldehyde		1.75	1.75	2.19	2.18
Anisol (C7H8O)				0.34	0.34
Total acids		**0.00**	**0.00**	**2.93**	**2.92**
Formic acid (HCOOH)				0.44	0.44
Acetic acid (CH3COOH)				2.49	2.48

Table 26. Comparison between models using different reaction schemes. Empirical data was obtained with pine wood at 500ºC from experimental results presented by Wang et al. [152].

Version 4 was the one with the best approximation to the experimental data for pyrolysis of lignocellulosic material, which also considers the impact of ash on cellulose, hemicellulose and lignin conversion which impacts the bio-oil composition. As a result this version was selected to be implemented and adjusted to simulate pyrolysis of AD waste. Detailed projections and evaluation of this model implementation are presented in CHAPTER 7.

CHAPTER 5. RESULTS AND DISCUSSION

5.1 DIGESTATE CHARACTERISATION

Cellulose, hemicellulose and lignin content of biomass is routinely determined to help understand thermal processing technologies and the subsequent formation of biochar, bio-oil and gas products. However, there are additional components in the biomass such as water and ash that also need to be considered as they can affect the yield and chemical composition of pyrolysis products [53,54,111,153]. Therefore, characterisation of the whole AD system, including the initial crop waste and the resulting digestate is crucial to understand pyrolysis product composition and yields. The crop digestate used as feedstock for the three pyrolysis systems featured in this study was collected over a period of 30 days to control possible variation in composition. Each collection was classified as batch *n*.

The crop waste that is fed into the digester is mixed, and typically comprises of 80% maize and 20% whole crop rye/spot and other cereals. The digestion process involves 60-70 days of retention in the digester, with pH maintained between 6.5 and 8.0, and a mesophilic temperature of 38ºC (+/-2ºC). Once the feedstock is digestated, the sludges have a moisture content of 92-94% and a pH of around 8.2. This slurry goes through a dewatering stage to produce the final solid digestate with around 80% water content.

5.1.1 PROXIMATE AND ULTIMATE ANALYSIS

Proximate analysis was carried out to determine volatile matter, fixed carbon and ash in this material in order to differentiate the organic from the inorganic. Ultimate analysis was carried out to determine elemental composition based on carbon, hydrogen, nitrogen, and oxygen. These results are presented in Table 27, and also include the original moisture content measured when the samples were collected direct from the AD system as part of sample preparation described in Section 3.1.

Parameter	CROP DIGESTATE			PRE-AD CROP	
	19-Nov-18	29-Nov-18	10-Dec-18	17-Jun-19	2-Jul-19
	Batch 1	Batch 2	Batch 3	Batch 1	Batch 2
Initial moisture	80.86 ± 0.164	81.50 ± 0.184	81.97 ± 0.432	66.31 ± 0.008	59.96 ± 0.018
Proximate analysis					
Moisture	5.07 ± 0.27	4.74 ± 0.41	3.80 ± 1.19	2.43 ± 0.09	2.73 ± 0.11
Volatile matter	68.32 ± 1.28	66.96 ± 0.64	65.21 ± 1.64	77.87 ± 0.28	76.35 ± 0.44
Fixed carbon	19.30 ± 0.56	19.83 ± 0.50	19.29 ± 0.79	16.15 ± 0.09	17.45 ± 0.09
Ash	7.32 ± 1.27	8.48 ± 1.47	11.10 ± 2.49	3.54 ± 0.24	3.45 ± 0.63
Ultimate analysis					
C	44.22 ± 0.21	43.86 ± 0.89	44.35 ± 0.66	45.42 ± 0.21	45.89 ± 0.22
H	5.74 ± 0.05	5.68 ± 0.13	5.65 ± 0.07	6.13 ± 0.15	6.27 ± 0.00
N	1.52 ± 0.13	1.70 ± 0.03	1.77 ± 0.22	1.26 ± 0.03	1.28 ± 0.06
O*	48.52 ± 0.16	48.76 ± 1.04	48.24 ± 0.51	47.20 ± 0.19	46.56 ± 0.21

Data is the mean ± SD, % weight basis, with at least three replicate measurements.
* Oxygen was obtained by difference.

Table 27. Proximate and ultimate analysis of 3 batches of digestate collected for thermal treatment, and crop used as starting material to be fed into the AD system.

There is a clear similarity between digestate batches in terms of both volatile matter and fixed carbon content, however, they were found to have a great variation in ash content. This difference was also detected within the same batch when this analysis was carried out, with ash varying from 6% to 13% wt. Therefore, each batch collected was tested around six times to better quantify this uncertainty. Details of the processing of each sample for this analysis can be found in APPENDIX B.

The initial crop waste fed into the AD system (pre-AD crop), was also analysed to confirm whether the large amount of ash found in digestate corresponded to an increase in ash content due to concentration after conversion into biogas.

Information from Severn Trent shows that only around 20-25% of the initial crop waste corresponds to biogas yield. Some additives, such as salts, are added into the system during the process to keep the medium in optimum conditions for the microorganisms. It was also investigated how this crop is fed into the digester in the interests of knowing if there were any further materials going into the AD process. This bioprocess needs to be continuously fed daily with several tonnes of this crop using shovel tractors. The feedstock is kept for three months in a clamp on the floor before being fed into the digester, ending in contact with the ground for a long period of time, and here it could be constantly combined with small stones and dust, after which this material could also enter the AD system. It is also highly likely that larger stones and agglomerated soil matter are present within the harvested biomass, and that this ends up being fed into the digester. This material is likely to be removed from samples prior to analysis, and this could also account for the lower observed ash content in the pre-AD samples.

5.1.2 LIGNOCELLULOSE COMPOSITION

Digestate was firstly sent to Celignis Limited to be analysed using their methodology due to their experience of biomass characterisation. The same digestate was also analysed at Wageningen University and Research (WUR) in Wageningen Food & Biobased Research Institute in The Netherlands, where training for lignocellulose assays was undertaken. It was possible to obtain direct measurements from the samples analysed, and raw data was processed to be able to compare the results from WUR's methodology with values obtained by Celignis Ltd. Cellulose, hemicellulose, lignin and ash contents in the digestate reported by Celignis Ltd. are shown in Table 28, and the outcomes from the analysis performed at WUR are shown in Table 29.

Parameter	CROP DIGESTATE		
	19-Nov-18	29-Nov-18	10-Dec-18
	Batch 1	Batch 2	Batch 3
Cellulose	26.91 ± 0.06	26.32 ± 0.26	24.31 ± 0.05
Hemicellulose	17.97 ± 0.00	17.74 ± 0.17	16.19 ± 0.08
Lignin*	22.40 ± 2.19	22.46 ± 0.21	25.93 ± 0.34
Ash	10.33 ± 0.07	10.66 ± 0.07	10.53 ± 0.24
Total	**77.6**	**77.2**	**77.0**

Data is the mean ± SD, % weight basis, with duplicate measurements, dry basis
Cellulose is glucose
Hemicellulose is the combination of xylose, arabinose and galactose.
*Lignin-remaining content of dry matter after subtraction of carbohydrates.

Table 28. Lignocellulose analysis of the 3 batches of crop digestate run in pyrolysis systems performed by Celignis Ltd.

Parameter	CROP DIGESTATE		
	19-Nov-18	29-Nov-18	10-Dec-18
	Batch 1	Batch 2	Batch 3
Cellulose	24.86 ± 0.06	23.34 ± 0.37	23.06 ± 0.26
Hemicellulose	20.86 ± 0.11	19.38 ± 0.54	19.88 ± 0.15
Lignin*	24.20 ± 2.19	23.80 ± 0.28	24.34 ± 1.38
Ash	9.03 ± 0.07	9.75 ± 0.17	9.42 ± 0.12
Starch	1.51 ± 0.07	1.26 ± 0.01	1.68 ± 0.02
Total	80.45	77.53	78.39

Data is the mean ± SD, % weight basis, with duplicate measurements, dry basis.
Cellulose is glucose.
Hemicellulose is the combination of xylose, arabinose and galactose.
*Lignin remaining content of dry matter after subtraction of carbohydrates.

Table 29. Lignocellulose analysis of crop digestate of 3 batches collected of digestate to run in pyrolysis systems carried out at WUR.

The two characterisation methods are very similar: digestate was subjected to a hydrolysis for sugar determination, and ash content was consistent in both analyses. However, the total cellulose identified in crop digestate could be influences by the starch content, as the measured glucose content could also result from starch.

It was important to identify which components were consumed during anaerobic digestion, and this was done by analysing the pre-AD crop mixture. The first assumption was that pre-AD crop might have contained starch, and this could be the main source from which biogas is produced. This was validated in the study at WUR which performed two types of hydrolysis. The first was a weak hydrolysis that could simulate the first stage of the anaerobic digestion process where the microorganisms consume material which is easy to break down, and then to move into an acidogenesis phase [9]. These easily consumed molecules are represented in Table 29 as starch, a parameter that was not considered in Celignis' report. The other type of hydrolysis performed was a stronger medium to break down non-soluble material such as cellulose and hemicellulose. It was important to differentiate this glucose that derives from starch, from the glucose that forms cellulose. Starch and cellulose are decomposed at different temperatures, and they could be involved in secondary reactions that might lead to the formation of other compounds which could be reflected in the final product composition.

Starch content in the pre-AD crop was confirmed with a complete analysis that included starch quantification by amyloglucosidase/α-amylase method, as explained in Section 3.2.2.7. The data obtained with WUR's method reveals there is around 2% of residual starch in the digestate. Two samples of starting material, and three more of digestate were analysed at WUR. These results are shown in Table 30, and also include ash content determined with a quantitative gravimetric method using a muffle furnace.

Parameter	PRE-AD CROP		CROP DIGESTATE		
	17-Jun-19	2-Jul-19	20-May-19	3-Jun-19	2-Jul-19
	Pre-AD Batch 1	Pre-AD Batch 2	Batch 4	Batch 5	Batch 6
Cellulose	15.78 ± 0.62	16.36 ± 0.75	22.00 ± 0.43	24.42 ± 0.09	23.95 ± 0.39
Hemicellulose	35.28 ± 0.15	35.86 ± 0.58	19.04 ± 0.64	19.84 ± 0.02	19.93 ± 0.28
Lignin*	15.02 ± 0.17	13.14 ± 0.69	21.87 ± 0.24	22.89 ± 0.38	23.12 ± 0.45
Ash	3.53 ± 0.06	3.65 ± 0.11	10.70 ± 0.32	8.99 ± 0.09	9.71 ± 0.21
Starch	27.70 ± 0.42	29.70 ± 0.60	1.57 ± 0.01	1.61 ± 0.96	1.39 ± 0.08
Total	**97.31**	**96.84**	**75.19**	**77.74**	**78.10**

Data is the mean ± SD, % weight basis, with duplicate measurements, dry basis.
Cellulose is glucose
Hemicellulose is the combination of xylose, arabinose and galactose.
*Lignin-remaining content of dry matter after subtraction of carbohydrates.

Table 30. Lignocellulose analysis of the crop as starting material of AD, and additional 3 other batches of digestate assays carried out at WUR.

It was important to measure ash content using other techniques besides TGA to verify the higher ash content in digestate and to rule out any issues with the TGA measurement technique.

The crop waste contained around 30% of starch, and in the digestate, measured in batch 4, 5, and 6, less than 2% remained. It seems that some of the hemicellulose in pre-AD crop was hydrolysed and consumed by the microorganisms due to a decrease in concentration from pre-AD material to the resulting digestate.

This confirms that this anaerobic digestion has microorganisms consuming starch and some hemicellulose as the main source for biogas production and that cellulose content in this crop does not change through anaerobic process. This supports the idea that the conversion of these sugars into biogas is around 20%. However, there is a significant increase in ash content in the digestate, which might be because of the additives and floor traces added during AD operation.

The ash content in digestate emerging from this system indicates that the amount of ash increased in digestate is not in proportion to the enhanced concentration that would result from biogas generation. If it were just the ~20% of conversion from pre-AD crop into biomethane-rich gas, which is mainly the difference between the initial and final starch proportion and some of hemicellulose, the ash in digestate would remain around 5% at the end. This mass balance would be as shown in Figure 35, without any other input.

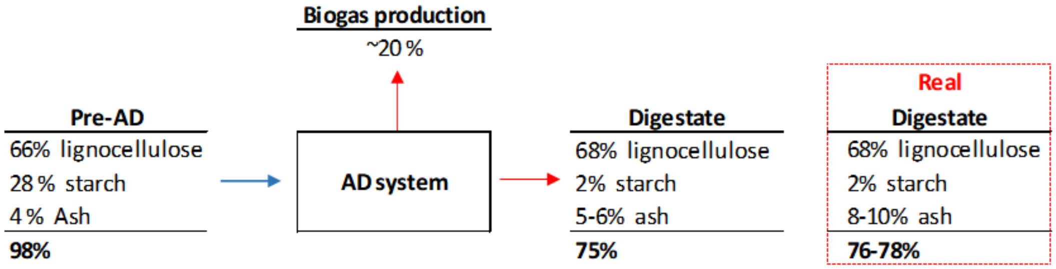

Figure 35. General mass balance of anaerobic digestion considering initial and final starch determined and actual lignocellulose measured from crop waste and its digestate, dry basis.

Pre-AD crop has around 4% wt. ash. This increases in digestate to around 10%, which is more than 50% higher than that in the initial material, considering that most of the lignocellulose does not change though the process and the starch consumed is around 26%, and around 2% of hemicellulose of the total mass. This suggests that the additives going into the system leave with the digestate as part of its inorganic composition rather than in the liquid. Additionally, some of the ash was analysed by Celignis and only around 3% of the ash in this biomass was insoluble, and this might represent the original minerals the crop contains. In general, woody biomass is considered as a low-ash material in comparison with different from others such agriculture or crops [86]. A large range of biomass categorisations in wood, agriculture and other biomasses are presented by Vassilev et al. [150] where ash composition was also considered. Woody material of 28 different variety had an average of 3.5% ash with a minimum of 0.1% and a maximum of 16.5% wt. The biomass with the highest ash (16.5%) reported in this study is land clearing wood which is a residue that could contain not only trees but also a large amount of inorganic material such as soil [154]. However, the wood most used in pyrolysis such as pine, oak and sawdust have lower than 1% ash. Non-woody biomasses such as straws can contain ash in range of the 4.7% and 20.1%, and other material such as sewage, classified as contaminated biomass by Vassilev et al. [150], can reach 40% wt ash.

One explanation for the observed discrepancy in ash content is the sampling methodology. Where stones or soil agglomerates exist in the pre-AD material these will inevitably be removed prior to laboratory analysis, but they will enter the AD system. Within the system the agglomerates will break up due to the mechanical stirring and long residence time, resulting in fine particles being suspended in the liquid medium and mixed with the waste digestate. These solids are impossible to identify and remove prior to subsequent analysis and pyrolysis experiments.

Average distribution of organic and inorganic material identified in pre-AD crop and crop digestate is represented in Figure 36.

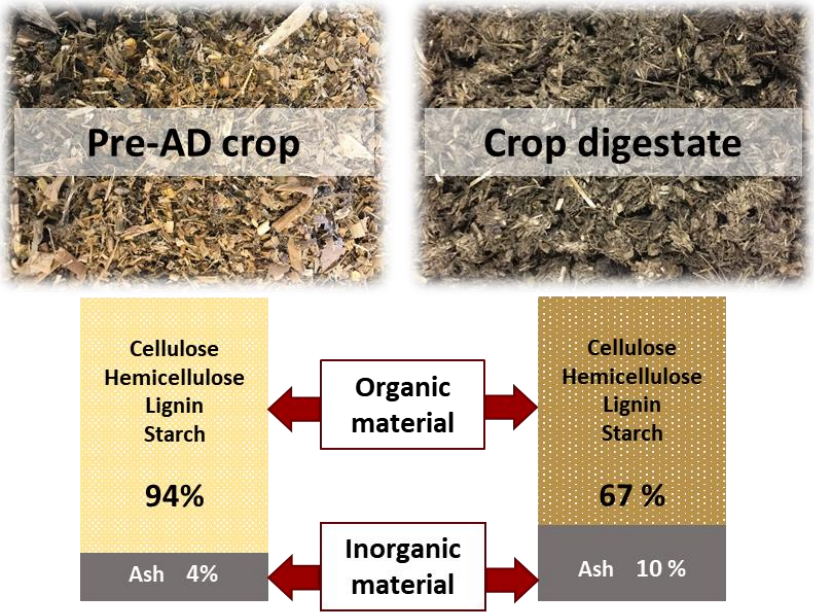
Pre-AD crop
Crop digestate
Cellulose
Hemicellulose
Lignin
Starch
94%
Ash 4%
Organic material
Inorganic material
Cellulose
Hemicellulose
Lignin
Starch
67 %
Ash 10 %

Figure 36. Organic and inorganic material distribution in pre-AD crop and crop digestate, dry basis.

A diagram of the general process of this anaerobic system could be exemplified as in Figure 37, where additives and small stones could be also considered as inputs in this mass balance.

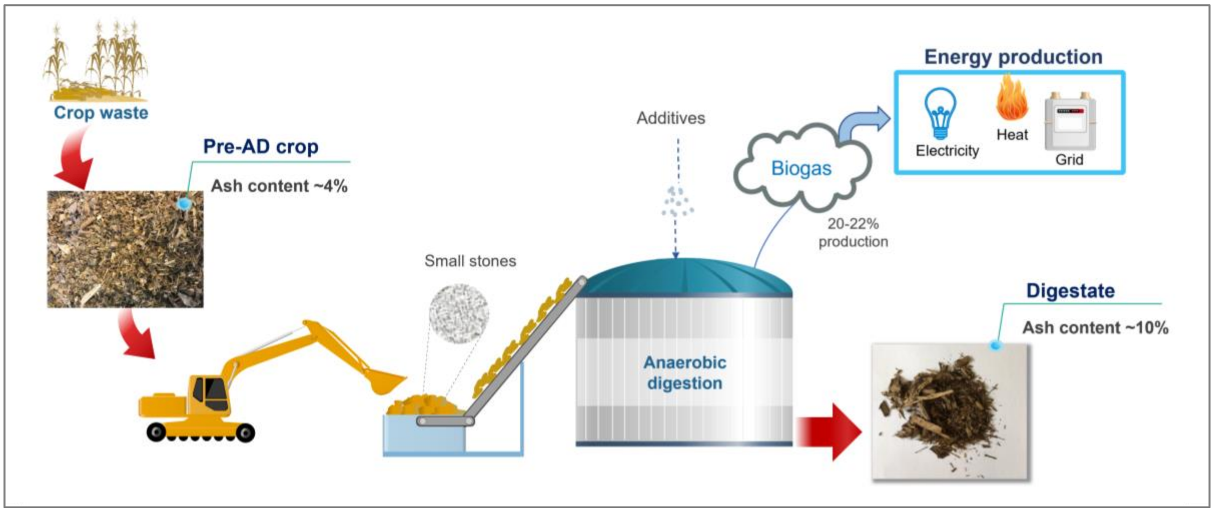
Crop waste
Pre-AD crop
Ash content ~4%
Additives
Small stones
Biogas
20-22% production
Energy production
Electricity
Heat
Grid
Anaerobic digestion
Digestate
Ash content ~10%

Figure 37. General diagram representing the possible ash accumulation and increase in the biomass through the AD process.

With clear information of the whole process of AD from the Severn Trent Crop Energy Plant, it was possible to understand more about the use of digestate as feedstock in the three pyrolysis technologies employed for this project. An overview of the different methodologies applied to characterise the pre-AD crop and digestate of this AD system is presented in Table 31.

Parameter	Methodology	Pre-AD crop	Digestate
Cellulose	Celignis	-	25.85
	WUR	15.85	23.75
Hemicellulose	Celignis	-	17.30
	WUR	35.08	20.04
Lignin	Celignis	-	23.59
	WUR	13.90	24.11
Starch	Celignis	-	-
	WUR	28.70	1.48
Ash	Celignis	-	10.51
	WUR	3.54	9.40
	TGA	3.49	8.36

Table 31. Summary of pre-AD crop and digestate (3 initial batches) composition values with different measurements methods. Data is the mean weight percentage %.

5.2 SLOW PYROLYSIS

Digestate was treated using a lab-scale pyrolysis reactor, and only batch 3 of the digestate collected was employed. Around 6 g of sample was used for each experiment, with a moisture content of around 5% wt. The slow pyrolysis system diagram was presented in Section 3.3.1.

Moisture content was verified before each set of experiments to differentiate it from the water formed during the thermochemical decomposition. These runs were performed at four different temperatures with a variation of +/- 5°C, verified with a thermocouple installed inside the reactor, and in contact with the quartz where the biomass was held.

The yields of products recovered from slow pyrolysis of digestate are shown in Table 32.

Slow Pyrolysis				
Product	**355°C**	**425°C**	**485°C**	**530°C**
Biochar	57.34 ± 3.52	45.30 + 0.72	41.18 + 1.05	39.63 + 1.80
Bio-oil	33.97 ± 3.62	42.19 + 1.94	45.13 + 1.42	46.02 + 1.11
Organics	*18.98 ± 4.72*	*26.26 + 2.61*	*26.68 + 2.13*	*27.02 + 1.58*
Water	*12.47 ± 3.46*	*15.93 + 0.91*	*18.45 + 0.80*	*19.01 + 0.60*
Gas	4.10 + 1.59	5.32 + 1.17	8.30 + 1.06	9.19 + 2.06
Total amount of products	95.41	92.81	94.61	94.84
Data is the mean ± SD, % weight basis, with at least three measurements.				

Table 32. Yields of slow pyrolysis products carried out at four different temperatures using crop digestate.

This data does not consider the initial water content in the biomass. The highest amount of biochar produced is at 355°C with 57.34% wt. of total products. As the temperature increases, biochar yield is reduced. If the aim of thermochemical conversion of biomass is to obtain high biochar yields, slow pyrolysis at temperatures lower than 400°C could be optimum to achieve this. Some of tar formed is cracking due to the ash amount and being deposited on the solid phase inside the reactor leading to more biochar formation [155,156]. The variation in slow pyrolysis product yields between 355°C and the other temperatures is noticeable, especially in the liquid components. The water is proportionally highest at 355°C, almost comprising 50%. This increased by around 30% between 355°C and 425°C and by 14% between 425°C and 485°C. Organics showed a 40% increase from 355°C to 425°C, after which there was little change. The amount of organics produced between 425ºC and 530ºC remained very similar in proportion, with around 27% wt.

Detail of the slow pyrolysis products distribution with the total of product recovered presented in Figure 38.

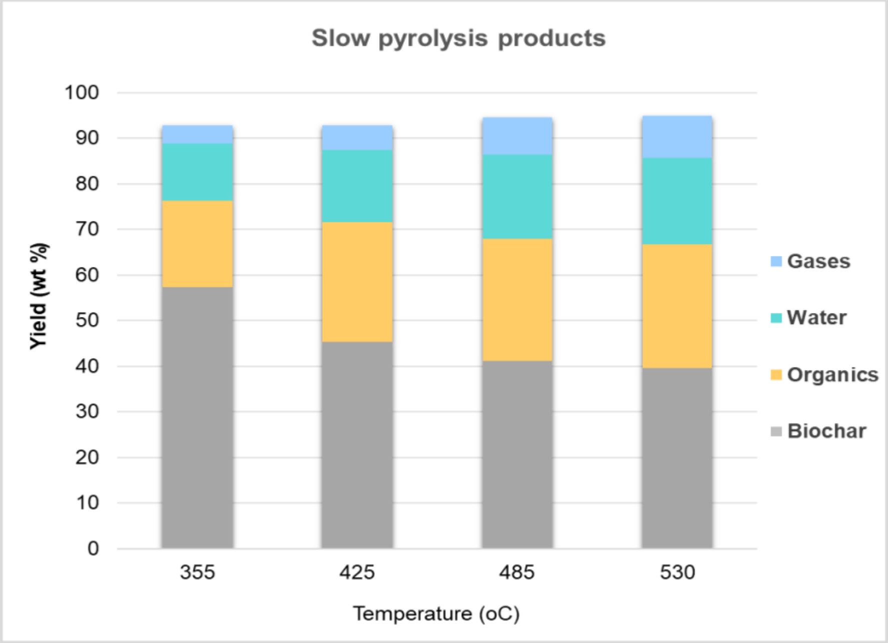

Figure 38. Yields (wt %) of slow pyrolysis products recovered in slow pyrolysis system.

Some of the results at the same conditions show significant variation. For example, at 355ºC the mean of biochar, organics, water, and gas yields were 57.34%, 18.98%, 12.47% and 4.1% wt, respectively, whereas run 1 at these conditions resulted in 59.82% biochar, 8.49% water, 22.15% organics and 5.02% wt gas, and run 2 resulted in 53.31% biochar, 14.16% water, 21.24% organics and 4.36% wt gas. The difference between these two experiments was greater than expected considering the same digestate was used. These differences also emerged at 425ºC, 485ºC and 530ºC.

This could be caused by variation in ash amount within each sample loaded, and similar behaviour was detected in TGA analysis presented in Table 27 in Section 5.1.1. As a result, it is probable that in every experiment carried out with this technology the digestate had different ash content, and that could have a direct impact on pyrolysis product yield and composition. The role of ash will be discussed in Section 5.4.

5.2.1 ANALYSIS OF SLOW PYROLYSIS PRODUCTS

5.2.1.1 BIOCHAR

Biochar composition is based only on elemental quantification (C, H, O, N). These results are shown in Table 33.

Slow pyrolysis biochar				
Element	355°C	425°C	485 °C	530 °C
C	56.28 ± 0.02	57.55 ± 0.73	56.36 ± 0.74	58.28 ± 1.13
H	4.76 ± 0.26	4.11 ± 0.02	3.46 ± 0.11	3.11 ± 0.20
N	2.53 ± 0.09	2.51 ± 0.05	2.44 ± 0.04	2.33 ± 0.01
O*	36.44 ± 0.89	35.82 ± 0.70	37.74 ± 0.72	36.28 ± 1.34
Total biochar	57.34	45.30	41.18	39.63
HHV (MJ/kg)	19.28	18.88	17.19	17.60

Data is the mean ± SD, % weight basis, with duplicate measurements.

* Oxygen was obtained by difference

Table 33. Ultimate analysis of biochar product collected from slow pyrolysis of crop digestate at different temperatures.

Biochar composition is very similar across the results of slow pyrolysis of digestate. It is evident that temperature applied does not have a great impact on the elemental composition of this product. Very small amounts of liquid remained in this biochar, however some organics might have remained at the solid surface. All the biochar recovered from slow pyrolysis test has carbon content of above 50% wt., which is the main valuable factor to be considered in deciding whether it can be utilised as fuel for energy generation.

5.2.1.2 BIO-OIL

All the compounds found in the bio-oil recovered were categorised into seven chemical groups: acids, aldehydes & ketones, alcohols, furans, sugars, phenolics and the rest as ‘others’. Therefore, this information can be used to compare and adjust the kinetic model developed in Section 6.4.

Bio-oil analysis was the key for this study in understanding more about each thermochemical process and the behaviour of the biomass during pyrolysis. Two examples of bio-oil analysed of each set of experiments are shown in Table 34.

Slow pyrolysis bio-oil								
Groups	**Run 1**	**Run 2**	**Run 1**	**Run 2**	**Run 1**	**Run 2**	**Run 1**	**Run 2**
	355ºC	**355ºC**	**425ºC**	**425ºC**	**485ºC**	**485ºC**	**530ºC**	**530ºC**
Acids	9.62	11.18	8.57	6.00	2.67	2.80	8.61	1.80
Aldehydes & ketones	3.13	4.66	4.47	3.95	3.60	3.10	3.62	2.14
Alcohols	2.38	0	0	0.11	0	0	0	0
Furans	3.50	5.37	6.22	7.53	9.78	9.60	6.79	13.12
Sugars	0.14	0.20	0.50	0.46	0.21	0.21	0.55	0.08
Phenolics	9.63	12.32	18.82	21.33	27.01	25.44	22.79	28.37
Others	2.22	1.67	3.02	2.65	3.10	2.44	2.40	0.92
Total bio-oil	**30.63**	**35.40**	**41.59**	**42.04**	**46.36**	**43.58**	**44.77**	**46.43**

Table 34. Proportions of chemical groups in slow pyrolysis bio-oil of digestate. Data is presented in % weight basis, and total represents bio-oil yield.

The analysis presented is based on the whole liquid recovered from pyrolysing digestate, which includes organics and water produced during pyrolysis. The variability in yields highlighted in Section 5.2 also occurred in bio-oil composition.

The lowest yield of bio-oil was at the lowest temperature, in this case 355ºC, but there was a high content of acids. As temperature increased the concentration of acids generally reduced. Total acids not only varied in each bio-oil across temperatures, but in those resulted from experiments carried out at the same conditions. At 355ºC for instance, acid production was 9.62% in run 1 whereas 11.18% of acids were formed in run 2, besides other samples at this temperature resulted with even a larger amount. Another example of a significant variation in acid generation was slow pyrolysis performed at 530ºC, where run 1 resulted with 8.61% acids while run 2 had only 1.80% wt.

Phenolic had a different trend from acids, their concentration increased with increasing temperature. The amount of these compounds produced went from less than 10% at 355ºC to almost 30% wt at 530ºC. This is likely to be associated with lignin decomposition, which requires more energy and higher temperatures to be depolymerised to form these organics in the liquid product [157,158].

An illustration of the distribution and variation of bio-oil composition from slow pyrolysis are shown in Figure 39.

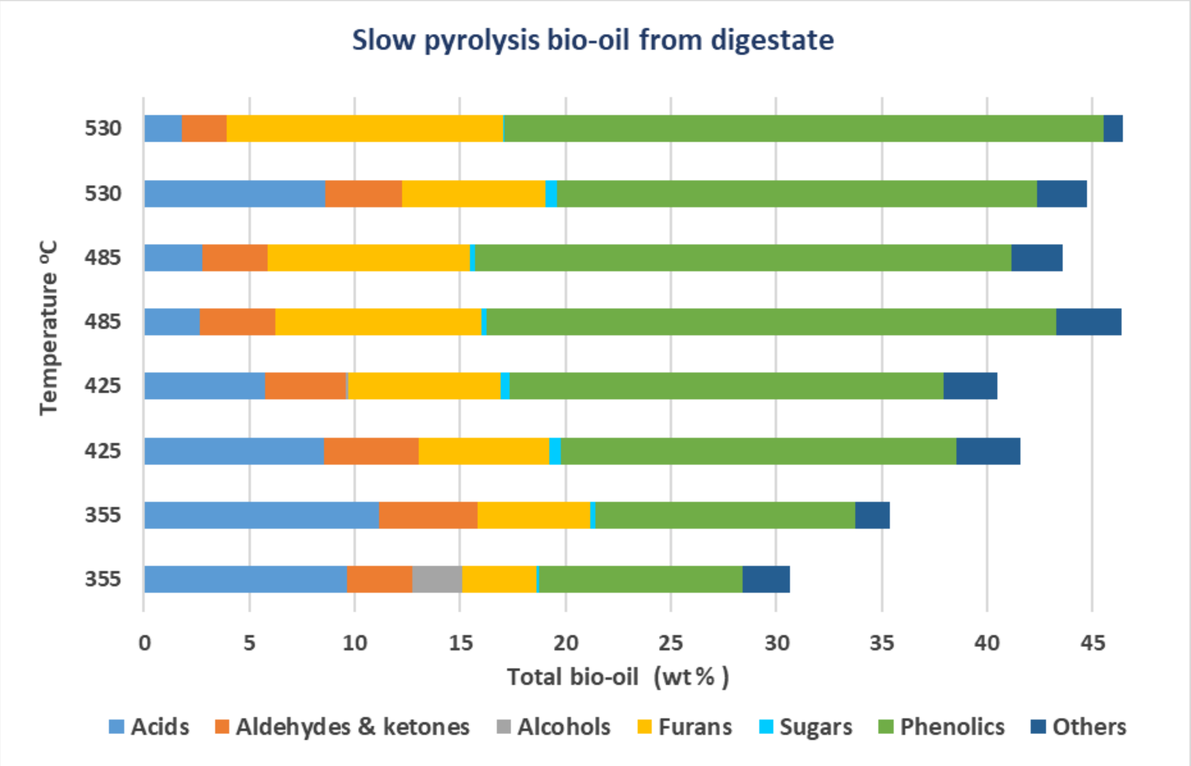

Figure 39. Mass weight distribution of the chemical groups found in bio-oil resulted from slow pyrolysis of digestate at different temperatures.

Alcohols and sugar were barely formed from crop digestate using slow pyrolysis. The maximum alcohol yield was around 2.4% at 355ºC, a very small amount was formed at 425ºC with only 0.11% wt, and no formation was observed at 485ºC and 530ºC. Sugars were detected across the operating temperatures; however, they were at very low concentration. The range of sugar production was only between 0.1% and 0.55% wt.

Aldehydes and ketones were formed almost at the same proportion in most of experiments, between 2% and 5% wt, but furans were at variable concentration among all the slow pyrolysis bio-oils across these temperatures, with the highest quantity at 530ºC.

Full analysis of two bio-oil samples of slow pyrolysis, run 2 at 355ºC and run 1 at 530ºC, is shown in Table 35.

Bio-oil slow pyrolysis								
Compounds	**Run 2 355^{o}C**	**Run1 530^{o}C**	**Compounds**	**Run 2 355^{o}C**	**Run1 530^{o}C**	**Compounds**	**Run 2 355^{o}C**	**Run1 530^{o}C**
Total acids	11.18	8.61	**Total furans**	5.37	6.79	**Total phenolics**	12.32	22.79
Acetic acid	10.08	7.91	2-Furanmethanol	0.00	0.52	Phenol	1.42	2.49
Propanoic acid	1.09	0.71	Ethanone, 1-(2-furanyl)-	0.00	0.00	Phenol, 2-methoxy-	3.95	5.46
Total aldehydes & ketones	4.66	3.62	Butyrolactone	0.57	1.01	Phenol, 2-methyl-	0.00	0.62
2-Cyclopenten-1-one	0.48	0.28	2-Furanmethanol, tetrahydro-	0.00	0.44	p-Cresol	0.19	0.90
2-Propanone, 1-(acetyloxy)-	0.83	0.47	2-Hydroxy-gamma-butyrolactone	1.67	0.13	Phenol, 3-methyl-	0.00	0.00
2-Cyclopenten-1-one, 2-methyl-	0.42	0.34	Benzofuran, 2,3-dihydro-	1.64	4.36	Creosol	1.89	1.60
2,3-Pentanedione	0.10	0.00	5-Hydroxymethyldihydrofuran-2-one	0.12	0.33	Phenol, 4-ethyl-	0.36	0.89
1,2-Cyclopentanedione, 3-methyl-	1.33	1.58				Phenol, 4-ethyl-2-methoxy-	0.64	0.00
Cyclohexanone, 4-ethyl-	0.19	0.00	**Total others**	1.43	2.00	Phenol, 2-ethyl-5-methyl-	0.00	0.38
2-Cyclopenten-1-one, 3-ethyl-2-hydroxy-	0.54	0.53	Propanoic acid, 2-oxo-, methyl ester	0.28	0.00	2-Methoxy-4-vinylphenol	0.61	2.32
4-Hexen-3-one, 4,5-dimethyl-	0.25	0.19	Pyridine	0.21	0.19	Phenol, 2,6-dimethoxy- / Syringol	2.74	5.84
Butanal, 3-hydroxy-	0.38	0	Acetamide	0.40	0.21	trans-Isoeugenol	0.13	0.55
Butanal, 2-ethyl-	0	0.23	Butanoic acid, methyl ester	0.00	0.25	3,5-Dimethoxy-4-hydroxytoluene	0.23	0.54
3-Decanone	0.16	0	Butanoic acid, propyl ester	0.36	1.12	3',5'-Dimethoxyacetophenone	0.00	0.19
Total sugars	0.21	0.55	Benzene, 1,2,3-trimethoxy-5-methyl-	0.18	0	2-Propanone, 1-(4-hydroxy-3-methoxyphenyl)-	0.18	0.34
1,4:3,6-Dianhydro-.alpha.-d-glucopyranose	0.21	0.19	Pyridine, 3-(2,4,6-trimethylphenyl)-	0.00	0.22	Methyl 3-(4-hydroxy-3-methoxyphenyl)propanoate	0.00	0.17
DL-Xylose	0	0.36	Propanoic acid, 2-oxo-, methyl ester	1.43	0	Ethanone, 1-(4-hydroxy-3,5-dimethoxyphenyl)-	0.00	0.27
Total Alcohols	0	0				2-Pentanone, 1-(2,4,6-trihydroxyphenyl)	0.00	0.21

Table 35. Analysed bio-oil product from slow pyrolysis of digestate at two temperatures, 355^{o}C and 530^{o}C. Data presented in wt %.

Acetic acid is the most predominant compound in these samples. There is a great variation in this acid formation between these two temperatures. Almost 12% wt of the total bio-oil was acetic acid at 355ºC while only around 9% wt was formed at 530ºC.This compound is formed from the decomposition of hemicellulose, yet secondary reactions can also lead to producing small molecules during the conversion.

Ketones are mainly comprised by cyclopentanones and butanones. Butyrolactone and benzofuran are the most prevalent compounds in group of furans, at 355ºC and 530ºC respectively. Butyrolactone concentration decreased with temperature in these samples. This went from 1.70% at 355ºC to 1.01% wt at 530ºC, whereas benzofuran had a significant increase from only 1.17% to 4.36% wt. Although benzofuran is an aromatic chemical, it has been categorised as furan. Studies have found that benzofurans formed from lignin depolymerisation and additional polycyclic aromatic hydrocarbons (PAHs), such as naphthalenes and benzenes, could be formed in their presence when they are subjected to catalytic processing, [159,160]. Some of these aromatic hydrocarbons were detected in one bio-oil experiment at 355ºC in around 1%. There were some traces in other samples but with very low concentrations which were difficult to quantify. Benzene, 1,2,3-trimethoxy-5-methyl- was one compound detected in most of these bio-oils at all temperatures, and some nitrogen chemicals also were identified, such as amides and pyridines which can result from proteins [95]. Digestate was analysed previously for proteins [145] which might come from the maize in the original feedstock. This amount of protein might result in the nitrogen compound detected in the pyrolytic bio-oil.

Phenolics were in less concentration at 355ºC than results at 530ºC where these were the highest proportion of total bio-oil. Some such as phenol, phenol, 2-methoxy- and phenol, 2,6-dimethoxy- (syringol) had an evident increase in production from a low concentration at 355ºC with 1.44%, 4.03 % and 2.79% wt. to a 2.49%, 5.46% and almost 6% at 530ºC respectively. Most of these compounds can be used for further valuable products for chemical applications.

More details of other compounds detected in bio-oil from every experiment can be found in APPENDIX D.

5.2.1.3 GAS

The dentification and quantification of non-condensable gases are shown in Table 36.

Slow pyrolysis gas

Compound	**355^{o}C**		**425^{o}C**		**485^{o}C**		**530^{o}C**	
	Run 1	**Run 2**	**Run 1**	**Run 2**	**Run 1**	**Run 2**	**Run 1**	**Run 2**
Hydrogen, H_2	0.0004	0.000	0.012	0.011	0.002	0.002	0.01	0.01
Methane, CH_4	0.009	0.009	0.025	0.023	0.091	0.101	0.24	0.15
Carbon monoxide, CO	1.502	0.802	1.681	2.000	1.828	2.963	1.58	1.46
Carbon dioxide, CO_2	3.484	3.529	3.777	3.474	6.225	7.258	10.16	5.97
Ethane, C_2H_6	0.003	0.003	0.009	0.008	0.036	0.040	0.10	0.06
Ethylene, C_2H_4	0.003	0.003	0.006	0.005	0.016	0.019	0.04	0.02
Propane, C_3H_8	0.002	0.002	0.005	0.004	0.017	0.019	0.04	0.03
Propylene, C_3H_6	0.003	0.003	0.005	0.005	0.016	0.018	0.04	0.02
Butane, C_4H_{10}	0.001	0.002	0.002	0.003	0.007	0.009	0.02	0.03
Butene, C_4H_8	0.003	0.004	0.007	0.007	0.012	0.022	0.03	0.02
Pentane, C_5H_{12}	0.002	0.001	0.004	0.004	0.011	0.007	0.03	0.01
Pentene, C_5H_{10}	0.001	0.000	0.002	0.002	0.005	0.007	0.02	0.01
C-6+	0.004	0.005	0.008	0.007	0.016	0.017	0.03	0.02
Total gas	**5.02**	**4.36**	**5.54**	**5.55**	**8.28**	**10.48**	**12.34**	**7.80**

Data is presented in wt % (weight basis)

Table 36. Composition of non-condensable gases resulting from slow pyrolysis of crop digestate of the gas recovered from the system. Data is presented in weight basis (wt %).

Pyrolysis gases comprise mainly carbon dioxide (CO_2) and carbon monoxide (CO). CO_2 production increased at higher temperature, equivalent to what occurred with C2+ gases yields, yet the opposite is true of CO generation, which was in lower concentration at 530^{o}C in these experiments. Very low concentrations of hydrogen (H_2) and methane (CH_4) were observed, which are the valuable target compounds for energy generation.

CO and CO_2 concentrations were much higher than the other gases. There was also a variation between concentration in gas samples at the same conditions. These differences could be due to ash content in each set of experiments where some degradation or further reactions might occur and some of the larger compounds could break down into gases with small molecules. 1.50 % CO was formed at 355^{o}C in run 1, and there was a decrease at the same conditions in run 2 with 0.82 %. On the contrary, CO_2 generation increased from run 1 to run 2 at 355ºC, from 1.09 % to 3.77% wt.

5.3 FAST PYROLYSIS

The general diagram of the fast pyrolysis system at the Technical Research Centre of Finland, VTT was presented in section 3.3.2. The main analysis of products was performed by VTT in Finland, and then bio-oil was sent to the UK to be analysed with the same method as for slow and microwave pyrolysis bio-oil to compare outcomes.

The mass balance for the fast pyrolysis system is shown in Table 37 for different operating temperatures. The data comprises water and organics, similar to the data presented for slow pyrolysis.

Fast pyrolysis				
Product	**460°C**	**480°C**	**520°C**	**560°C**
Cyclone biochar	34.22	34.65	31.77	30.45
Pyrolysis gases (CO, CO_2, CH_4, H_2, C_2-C_5 hydrocarbons)	18.49	17.84	20.92	21.37
Bio-oil	36.03	43.50	39.48	40.15
Organics	27.81	36.98	29.67	29.47
Water	8.22	6.52	9.81	10.67
Total amount of products	88.74	95.99	92.17	91.96

Table 37. Overall mass balance (wt %) for dry digestate as raw material of fast pyrolysis system at VTT, Finland.

Due to the larger mass of biomass tested in this system the products were collected after three hours of operation. The water was determined with Karl Fischer titration with a more precise method developed by VTT. More details of this method employed and approved by VTT can be found at Oasmaa et al. [132]. Fast pyrolysis of digestate produced between 8% and 11% of water as product, which increased at the highest operating temperatures. The maximum amount of water quantified from this system is much less than that produced in slow pyrolysis. Organics, however, were relatively constant through the experiments. There was an increase observed at 480ºC, whereas at 460ºC, 520ºC and 560ºC organics were produced at around 30%. The lowest gas generation was 17.84% at 480ºC, with a slight increase through other conditions to reach a maximum production of just above 21% at 560ºC. Biochar product from digestate in this pyrolysis was less than 35% in all the experiments. This was different to the biochar generated in slow pyrolysis, where it was at least 40% wt of the total products.

The general distribution of fast pyrolysis products recovered from digestate at different temperatures are shown in Figure 40.

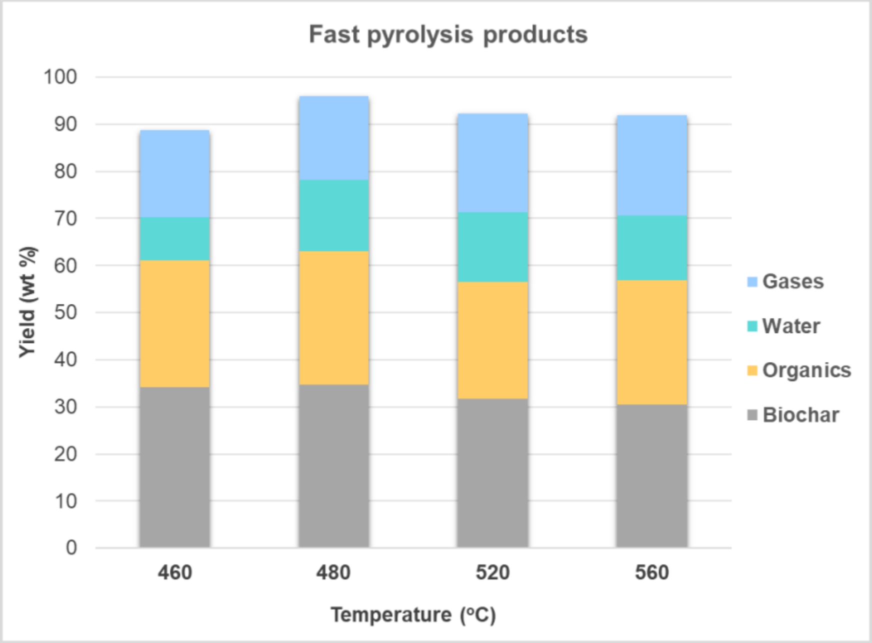

Figure 40. Yields of fast pyrolysis products recovered at different temperature.

Fast pyrolysis products resulted in similar compositions in each experiment. The mass balance of this system does not add up 100% due to losses during product recovery. Product recovery of this system has been tested with several biomasses and optimised to obtain consistent yields. Information about the system product recovery is presented by Oasmaa et al. [82], and by Lindfors et al. [73] who describes in more detail different operating conditions through liquid recovery section that could change bio-oil composition.

Although most of the products were generated at similar proportions in each processing condition, it was important to identify any possible variation in product composition and the differences between them occurring with temperature changes. Then, it was necessary to evaluate the quality of the products for further uses.

5.3.1 ANALYSIS OF FAST PYROLYSIS PRODUCTS

5.3.1.1 BIOCHAR

Elemental quantification of carbon (C), hydrogen (H), oxygen (O) and nitrogen (N) was determined for each biochar as shown in Table 38 , using the same method used for characterisation of the biochar resulting from slow pyrolysis.

Fast pyrolysis biochar				
Element	**460°C**	**480°C**	**520°C**	**560°C**
C	60	60.40	59.50	58.10
H	3	2.8	2.4	2.2
N	1.80	1.80	1.70	1.60
O*	35.2	35.0	36.4	38.1
Total biochar	34.22	34.65	31.77	30.45
HHV (MJ/kg)	18.22	18.11	16.63	15.9

* Oxygen was obtained by difference.

Table 38 Ultimate analysis (wt %) of biochar produced from fast pyrolysis of crop digestate at different temperatures. Analysis performed in VTT, Finland.

Carbon content of this biochar reached 60%, higher than that for biochar produced from slow pyrolysis. There was not a significant variation in elemental composition across temperatures. This biochar was recovered almost dry, with less than 0.1% of moisture content.

5.3.1.2 BIO-OIL

Bio-oil resulting from the fast pyrolysis system was examined with the same method by which slow pyrolysis bio-oil was processed. The summary of this analysis is shown in Table 39 and, which shows bio-oil quantification by chemical groups at different temperatures.

Fast pyrolysis bio-oil				
Groups	**460°C**	**480°C**	**520°C**	**560°C**
Acids	6.20	23.49	13.45	6.64
Aldehydes & ketones	4.03	4.25	3.76	4.41
Alcohols	0.17	0.68	0.44	0.43
Furans	3.46	2.54	3.41	6.31
Sugars	1.28	3.31	2.12	1.86
Phenolics	19.00	7.53	14.43	17.62
Others	1.90	1.70	1.85	2.88
Total bio-oil	**36.03**	**43.50**	**39.48**	**40.15**

Table 39. General composition of bio-oil produced from fast pyrolysis of digestate. Data is presented in wt %.

Sugars were identified in these bio-oil samples at around 1-3 % wt, and very small amount of alcohols, less than 1%. Additionally, there was less acid production at the lowest and highest temperature. Phenolics were formed at relative high proportion in most of the temperatures at 14-19% wt, but at 480ºC it was much lower. These phenolics at 480ºC could be decomposed into other smaller molecules because the biomass had to be grounded for pellets preparation. This could lead to lignin to being decomposed easier, and the amount of energy employed could result in a surplus which was then able to break down phenolics into smaller molecules. These compounds might then have gone through an additional reaction, to be decomposed into other chemicals and form more acids. Aldehydes and ketones were at low concentration in most of these conditions, very similar to slow pyrolysis yields. Furans, however, are at smaller amounts with a maximum of approximately 6% wt, whereas in slow pyrolysis they reached to around 13% at 530ºC.

The graphic distribution of fast pyrolysis bio-oil composition is shown in Figure 41.

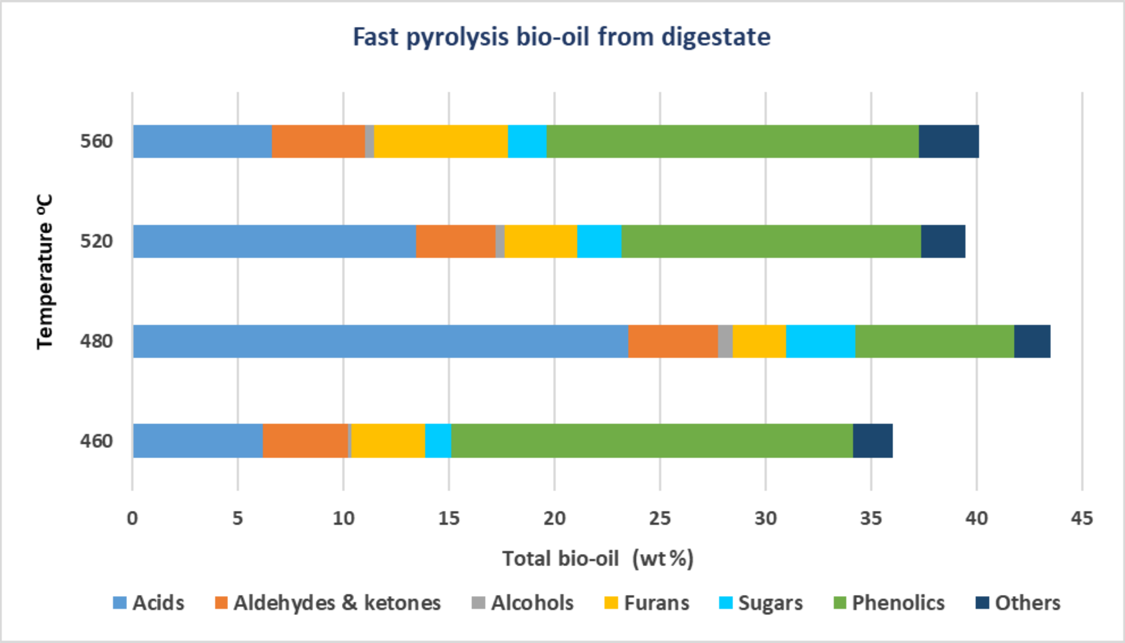

Figure 41. Mass weight distribution of the chemical groups found in bio-oil resulted from fast pyrolysis of digestate at four different temperatures.

Sugars were found in a greater amount in fast pyrolysis bio-oil, whereas in slow bio-oil they did not even reach 1% wt. Alcohols also are noticeable, something not found in slow pyrolysis bio-oil. It is evident that the composition and distribution of these chemical groups varied between slow pyrolysis and fast pyrolysis bio-oil. Detailed composition of fast pyrolysis biooil is presented in Table 40.

Bio-oil Fast pyrolysis									
Compounds	**460°C**	**480°C**	**520°C**	**560°C**	**Compounds**	**460°C**	**480°C**	**520°C**	**560°C**
Total acids	6.2	23.5	13.5	6.6	**Total phenolics**	19.00	7.53	14.18	17.62
Acetic acid	5.70	22.79	12.96	6.07	Phenol	1.68	0.55	2.13	4.03
Propanoic acid	0.50	0.11	0.49	0.57	Phenol, 2-methoxy-	2.90	1.11	2.08	1.78
Butanoic acid	0	0.59	0	0	Phenol, 2-methyl-	0.54	0.17	0.64	1.03
Total aldehydes & ketones	4.03	4.25	3.76	4.41	Phenol, 2,5-dimethyl-	0.00	0.00	0.10	0.15
2-Propanone, 1-hydroxy-/Acetol	0	1.17	0	0	p-Cresol	0.90	0.11	0.55	0.95
1-Hydroxy-2-butanone	0	0.49	0	0	Creosol	0.86	0	0.64	0.49
2-Cyclopenten-1-one	0.18	0.07	0.13	0	Phenol, 3,5-dimethyl-	0	0	0.27	0.48
2-Propanone, 1-(acetyloxy)-	0.34	0.39	0.35	0.30	Phenol, 2,3-dimethyl-	0.32	1.32	0.07	0.12
2-Cyclopenten-1-one, 2-methyl-	0.36	0.13	0.30	0.56	Phenol, 4-ethyl-	2.21	0.26	1.64	2.79
2-Cyclopenten-1-one, 3-methyl-	0.71	0	0.72	1.00	Phenol, 4-ethyl-2-methoxy-	1.15	1.25	0.61	0.43
1,2-Cyclopentanedione, 3-methyl-	0	1.45	1.63	1.77	Phenol, 4-ethyl-3-methyl-	0.13	0	0	0.24
2-Cyclopenten-1-one, 2-hydroxy-3-methyl-	1.76	0	0	0	Phenol, 2-ethyl-5-methyl-	0	0	0.12	0
1,3-Cyclopentanedione, 2,4-dimethyl-	0.18	0.09	0.17	0.24	2-Methoxy-4-vinylphenol	1.58	0.35	0.91	0.88
2-Cyclopenten-1-one, 3-ethyl-	0	0	0.10	0.25	Eugenol	0.21	0.00	0.18	0.30
2-Cyclopenten-1-one, 3-ethyl-2-hydroxy-	0.49	0.47	0.36	0.29	Phenol, 2,6-dimethoxy- / Syringol	3.01	1.66	1.79	0.98
Total alcohols	0.17	0.68	0.44	0.43	Phenol, 4-ethyl-2-methoxy-	0.19	0	0.18	0.62
1,2-Ethanediol	0.17	0.61	0.44	0.43	2-Hydroxy-3-methoxybenzyl alcohol, di(methyl) ether	0	0	0	0.45
Isopropyl Alcohol	0	0.07	0	0	Phenol, 2-methoxy-4-(1-propenyl)-/Isoeugenol	0.24	0	0.11	0.00
Total furans	3.46	2.54	3.41	6.31	Phenol, 4-(2-propenyl)-	0.16	0	0.22	0.41
Furan, 3-methyl-	0	0	0	0.24	trans-Isoeugenol	0.84	0	0.52	0.46
2-Furanmethanol	0.38	1.04	0.30	0.40	3,5-Dimethoxy-4-hydroxytoluene	0.52	0	0.34	0.27
Ethanone, 1-(2-furanyl)-	0	0.05	0	0	Phenol, 4-methoxy-3-(methoxymethyl)-	0	0.14	0	0
Butyrolactone	0	0.54	0	0	Hydroquinone	0	0.16	0	0
2-Furanmethanol, tetrahydro-	0	0.06	0	0	Ethanone, 1-(2-hydroxy-4-methoxyphenyl)-	0.10	0	0.20	0
2(5H)-Furanone	0	0.16	0	0	Ethanone, 1-(3,4-dimethoxyphenyl)-	0.31	0	0	0.23
Benzofuran, 2,3-dihydro-	2.86	0.45	2.88	5.48	2-Propanone, 1-(4-hydroxy-3-methoxyphenyl)-	0.25	0.17	0.17	0
5-Hydroxymethyldihydrofuran-2-one	0.22	0.24	0.23	0.18	Phenol, 2,6-dimethoxy-4-(2-propenyl)-	0	0	0.15	0.19
Total sugars	1.28	3.31	2.12	1.86	Phenol, 4-(1-methyl-1-phenylethyl)-	0.23	0	0.17	0.18
1,4:3,6-Dianhydro-.alpha.-d-glucopyranose	0.16	0.32	0.29	0.31	(E)-2,6-Dimethoxy-4-(prop-1-en-1-yl)phenol	0.28	0	0.17	0
DL-Xylose	0.34	0.72	0.38	0.36	Ethanone, 1-(4-hydroxy-3,5-dimethoxyphenyl)-	0.25	0.17	0.23	0
d-Mannose	0.24	0.47	0.44	0.35	2-Pentanone, 1-(2,4,6-trihydroxyphenyl)	0.14	0.11	0	0.16
β.-D-Glucopyranose, 1,6-anhydro-/ Levoglucosan	0.54	1.80	1.01	0.84					

Table 40. Fast pyrolysis bio-oil composition produced at four different temperatures. Data presented in wt%.

Acetic acid was also the main compound in these bio-oils, and aside from propanoic acid also found in bio-oil from slow pyrolysis, butanoic acid was only detected at 480ºC in very low concentration. Acetol, mainly formed from cellulose and hemicellulose [161], was detected with 1.7% at 480ºC. 1,2-cyclopentanedione, 3-methyl- was found in higher proportion than other compounds in the aldehydes & ketones group.

Furans in this case consist mainly of 2-furanmethanol and benzofuran, with the highest concentration at 560ºC reaching almost 6% wt. Furan,3-methyl was also found, which is one compound derived from furfural. Both furfural and this derivative came out at the same retention time in the GC-MS analysis of the bio-oil. However, the NIST library would give as the first option the compound in greater concentration in the bio-oil. This was considered to select the most likely compounds, although, it seems furfural and some of its derivatives could be co-eluted.

Levoglucosan (LVG) is the most prevalent of the sugars in the composition which means some of the cellulose was directly converted into this compound [162]. The highest yield of this sugar was at 480ºC with almost 2%. This fast pyrolysis bio-oil had also benzofuran, which could have been formed in greater proportion due to ash presence which might easily enhance decomposition of lignin. This compound went from around 3% to approximately 6% at 460ºC and 560ºC respectively. Syringol was formed at around 1-3%, which was in less amount than bio-oils produced from slow pyrolysis. This phenolic was produced in slow pyrolysis with a minimum of 3.5% wt, and just above 7% as the highest amount at 530ºC. This was different from production of phenol, which reached just above 4% wt. at 560ºC in fast pyrolysis.

Bio-oil resulting from fast pyrolysis processing was analysed in VTT to determine if any ash residues could be found within the liquid. This could lead to bio-oil compounds continuing to react, resulting in further decomposition. However, the analysis obtained showed ash content in bio-oil is 0.07%, 0.13%, 0.12% and 0.04% wt at 480ºC, 460ºC, 520ºC and 560ºC respectively.

In CHAPTER 6 more descriptive information will be explained about additional compounds which could be products resulting from secondary reactions that are taking place within pyrolysis of digestate because of the large amount of ash.

Other compounds identified in this bio-oil can be found in APPENDIX D.

5.3.1.3 GAS

The VTT fast pyrolysis system has an analyser attached to the system and additional bags with gas samples were sent to VTT's laboratory for quantification and validation of the data. This analysis resulted in more compounds identified within the total gas. Non-condensable gas composition is detailed in Table 41.

Fast pyrolysis gas				
Compound	**460°C**	**480 °C**	**520 °C**	**560 °C**
Hydrogen, H_2	0.016	0.022	0.076	0.116
Methane, CH_4	0.432	0.895	1.209	1.199
Carbon monoxide, CO	4.178	4.417	5.181	5.747
Carbon dioxide, CO_2	13.57	11.83	12.89	12.92
Ethane, C_2H_6	0.133	0.154	0.253	0.301
Ethylene, C_2H_4	0.073	0.079	0.156	0.227
Propane, C_3H_8	0.026	0.061	0.083	0.091
Propylene, C_3H_6	0.055	0.098	0.178	0.248
Acetylene, C_2H_2	0	0.007	0.007	0.008
Iso-Butane, I-C_4H_{10}	0	0.005	0.006	0.007
Propadiene, C_3H_4	0	0	0.001	0.001
N-butane, N-C_4H_{10}	0	0.015	0.018	0.018
Trans-2-Butene, Trans-2-C_4H_8	0	0.011	0.017	0.022
Isobutene, I-C_4H_8	0	0.023	0.033	0.042
Isopentane, I-C_5H_{12}	0	0.004	0.004	0.004
Pentane, N-C_5H_{12}	0	0.004	0.004	0.005
1.3-Butadiene, 1.3-C_4H_6	0	0.010	0.026	0.046
1-Pentene, 1-C_5H_{10}	0	0.008	0.013	0.015
Benzene, C_6H_6	0	0.019	0.416	0.001
Toluene, C_7H_8	0	0.024	0.097	0.020
C-4	0	0.030	0.052	0.073
C-5	0	0.018	0.031	0.046
C-6	0	0.090	0.152	0.194
C-7	0	0.009	0.015	0.018
Total gas	**18.49**	**17.84**	**20.92**	**21.37**

Table 41. Weight basis % of non-condensable gases resulted from fast pyrolysis of crop digestate. This analysis was performed at VTT, Finland.

These gases consist of large amounts of carbon monoxide (CO) and carbon dioxide (CO_2), almost 60% of the total gas produced. For this technology, there was some production of hydrogen (H_2) and methane (CH_4) reached a concentration just above 1% at the highest temperatures. Some aromatic hydrocarbons were formed in this processing such as benzene and toluene, both in smaller amounts at the highest temperature. Aromatic hydrocarbons (AHs) were also found in very small amounts in some bio-oils from digestate, which supports the idea that catalytic reactions are happening during the pyrolysis process.

Several studies have been undertaken into the reactivity of the inorganic material during pyrolysis, and the effect on the final products. Persson et al. [81] shows how the minerals in biomass act as catalytic material that supress production of levoglucosan and other primary compounds from lignocellulose and higher amounts of pyrolytic water and gas are generated. These experiments performed by Persson et al. [81] include additional catalytic upgrading of bio-oil formed with the raw material with ash, resulting in higher amounts of aromatic hydrocarbons with more CO_2 and CO production, which could be assumed as similar behaviour within digestate during the pyrolysis process.

5.4 MICROWAVE PYROLYSIS

Digestate was employed on a dry basis during microwave pyrolysis with the purpose of comparing this technology with conventional pyrolysis. Samples were ground then pelletised in order to give a consistent structure and geometry of biomass through all the runs. The microwave pyrolysis system set to treat digestate was shown in Section 3.3.3.

For these experiments the power delivered by the microwave generator was set at 500 W and 700 W. The output power was absorbed by the biomass or was reflected, with reflected power logged over the duration of each experiment and used to calculate the net energy input. A graphic representation of the power data obtained from microwave pyrolysis system is shown in Figure 42.

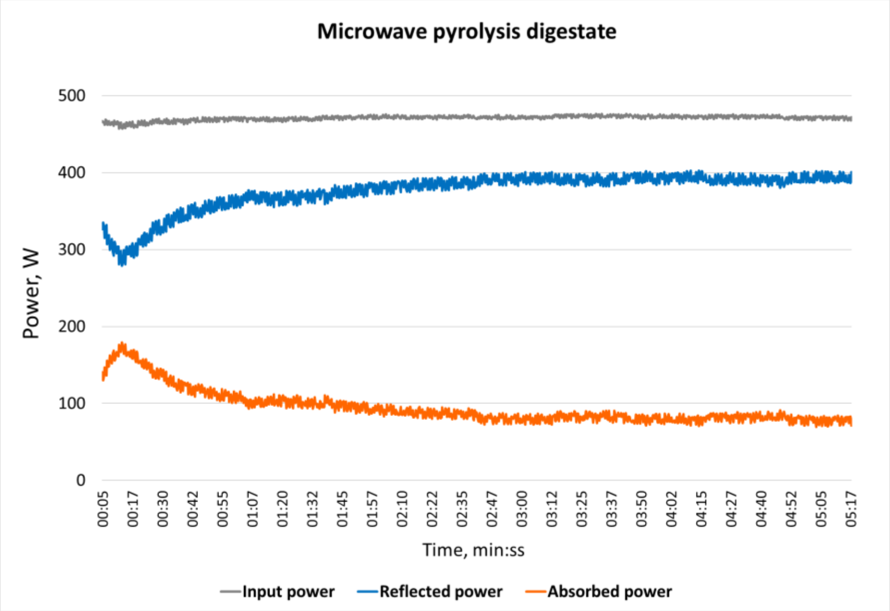

Figure 42. Example of experiment performed of microwave pyrolysis with digestate. Curves presented are 500 W power input for 5 minutes, and the power absorbed and reflected.

This dry digestate is not a good absorbent microwave material. Energy absorbed in each experiment was only around 100 W out of 500 W, and 700 W. Due to the difficulty of measuring the exact temperature inside the system and the biomass, energy input was instead used to present the results of microwave pyrolysis of digestate. This energy is the average power absorbed divided by the time for which digestate was pyrolysed.

5.4.1 BIO-OIL

Due to limited time the product characterisation was focused solely on bio-oil analysis. The system was set up with two condensers in series, and the total amount recovered from both was considered for bio-oil chemical analysis. Six examples of bio-oils recovered from this technology are presented in Table 42.

Microwave pyrolysis bio-oil						
Groups	1.27 kJ/g	1.88 kJ/g	4.07 kJ/g	4.07 kJ/g	5.08 kJ/g	6.85 kJ/g
	Dry	Dry	Wet	Dry	Wet	Dry
Acids	3.48	4.70	3.51	7.89	3.90	6.27
Aldehydes & ketones	3.37	5.95	3.72	5.33	1.20	1.69
Alcohols	0.05	0.00	0	0	0.02	0.02
Furans	2.98	2.44	3.50	2.76	0.70	3.13
Sugars	0.06	0.02	0	0	0.07	0
Phenolics	5.43	6.85	6.90	4.28	6.10	3.90
Others	0.94	0.70	0.73	0.60	2.41	1.07
Total bio-oil	**16.30**	**20.65**	**18.35**	**20.86**	**14.40**	**16.08**

Table 42. Bio-oil composition of microwave pyrolysis of digestate (wt %) at different energy inputs.

There is considerable variation in these compounds between experiments. Grinding and pelletising the material might have given an ash distribution more consistent between samples, however it is likely that every sample used in each microwave experiment contained different amount of ash, which could have had similar impact on bio-oil composition with slow pyrolysis tests.

Experiments with energy input of 1.27 kJ/g and 1.88 kJ/g, for instance, were performed at the same power input, 700 W, and bio-oil yields and compositions were different. Production of aldehydes and ketones and phenolics was higher at 1.88 kJ/g with almost 6% and 7% respectively, but with a lower concentration of furans. Bio-oil resulting from 1.27 kJ/g energy input contained some alcohols and sugars, whereas these were not detected at 1.88 kJ/g. Additionally, grinding of digestate could have caused a higher ash surface area to be distributed through the samples due to small stones found in digestate. It was also expected that more sugars could be formed from cellulose and hemicellulose using microwaves compared with conventional pyrolysis. Both could be converted into sugars and furans, such as furfural, when subjected to a thermochemical process, yet this was not the case. Large amounts of levoglucosan, product from cellulose, have found when biomass such as wood is thermal treated with microwave pyrolysis [25], different from these microwave experiments using digestate.

Biomass conditions in two runs, 4.07 kJ/g and 5.08 kJ/g, were modified to tune the system to promote better power absorption. Dielectric properties of these samples were increased by adding water, which increases microwave interaction with digestate. This was also important to perform in order to evaluate whether there were some differences between dry and wet conditions. Digestate considered as ‘dry’ contained approximately 4% wt water, and samples with additional water reached around 8% wt moisture. Previous research shows that water content in biomass could lead to more bio-oil and gas production [163-165] which was important to consider for this analysis.

The first comparison between bio-oils from dry and wet biomass was samples with an energy input of 4.07 kJ/g (Table 42). Although this number is the same in both cases, the tests were performed at different power input. The experiment which resulting in a yield of about 18% was performed using a digestate sample with a moisture content of 7.34% wt, and power input of 500 W. The other test with bio-oil yield resulting in around 20% wt was conducted with a sample with approximately 4% wt of moisture and using a power input of 700 W. Due to the amount of phenolics formed it is noticeable that digestate was easily microwave pyrolysed with higher moisture content. The amount of produced phenolics indicates that larger amount of lignin could be depolymerised because of that additional water. Lignin is one composite of lignocellulosic material that requires more energy to be decomposed. Therefore, more phenolics were obtained with a power of 500 W, almost 7%, in contrast to around 4% wt obtained using 700 W.

The second comparison is for samples with an energy input of 5.08 kJ/g and 6.85 kJ/g, utilising digestate with almost 10% and 4% wt of moisture and conducted at different power input, 500 W and 700 W respectively.

The digestate with greater amount of water resulted in a bio-oil product with higher proportion of phenolics and less acids produced. Both cases of wet conditions show similar digestate pyrolysis behaviour.

More examples of how bio-oils are comprised by each chemical group in microwave pyrolysis are illustrated in Figure 43, where the difference between each run, aside from the two examples mentioned before, is evident with higher moisture content in biomass.

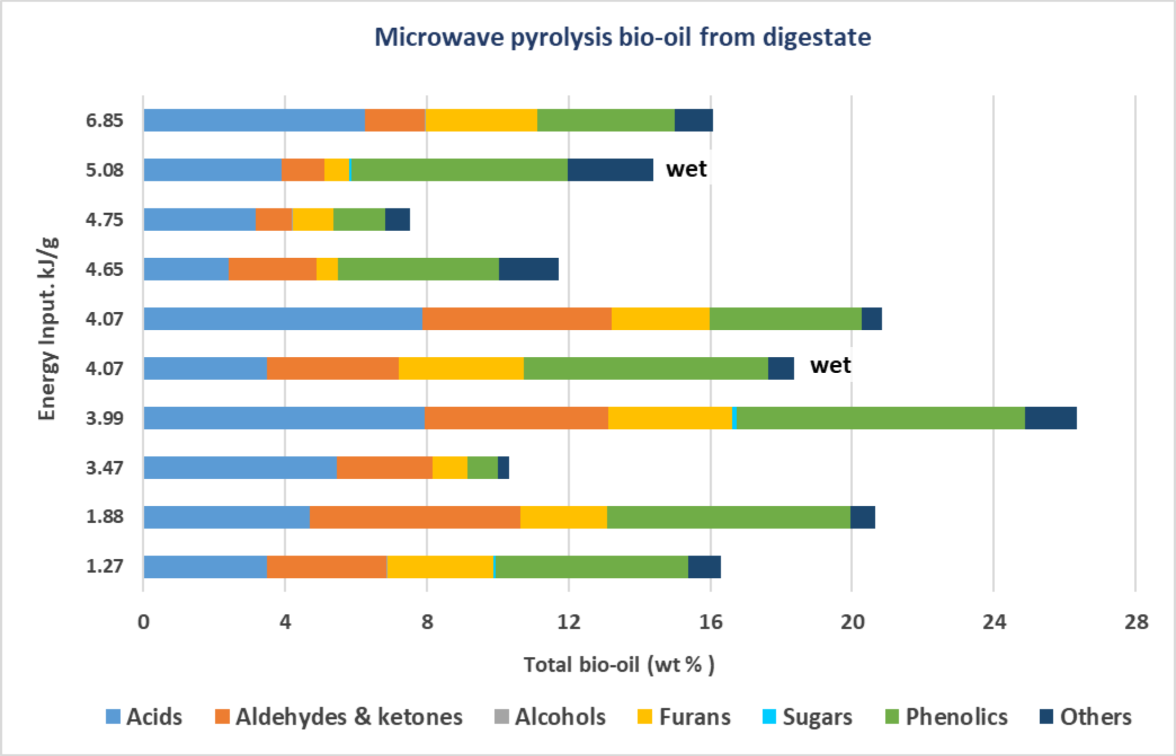

Figure 43. Mass weight (wt %) distribution of the chemical groups found in microwave pyrolysis bio-oil from digestate at different energy input.

Acid content was high in most of microwave pyrolysis bio-oils. Sugars and alcohols were detected in low concentration in few samples with less than 1% wt. Aldehydes and ketones in some cases reached yields considerably higher than those from slow and fast pyrolysis, where the highest amount was under 5% wt. This technology produced in a few bio-oil samples almost 6% of these compounds; digestate pyrolysed with 1.88 kJ/g energy input for instance.

Detailed bio-oil composition of three samples from microwave pyrolysis is presented in Table 43.

Microwave pyrolysis							
Compounds	1.88 kJ/g Dry	3.99 kJ/g Dry	5.08 kJ/g Wet	Compounds	1.88 kJ/g Dry	3.99 kJ/g Dry	5.08 kJ/g Wet
Total acids	4.7	7.9	3.9	**Total sugars**	0.02	0.10	0.07
Acetic acid	4.49	7.43	3.74	1,4:3,6-Dianhydro-.alpha.-d-glucopyranose	0.02	0.02	0.02
Propanoic acid	0.21	0.50	0.16	DL-Xylose	0	0.08	0.03
Total aldehydes & ketones	5.95	5.19	1.20	d-Mannose	0	0	0.02
2-Propanone, 1-hydroxy-/Acetol	3.18	2.71	0.26	β.-D-Glucopyranose, 1,6-anhydro-/LVG	0	0	0.05
Acetoin	0.09	0	0	**Total phenolics**	6.85	8.13	6.10
1-Hydroxy-2-butanone	0.48	0.61	0.08	Phenol	0.71	0.63	0.35
2-Cyclopenten-1-one	0.66	0.58	0	Phenol, 2-methoxy-	1.49	1.74	1.33
2-Propanone, 1-(acetyloxy)-	0.26	0.27	0.08	Phenol, 2-methyl-	0.17	0.10	0.08
2-Cyclopenten-1-one, 2-methyl-	0.23	0.18	0.09	Benzene, 1-ethenyl-4-methoxy-	0	0	0
2-Cyclopenten-1-one, 2-hydroxy-	0.02	0	0	p-Cresol	0.16	0.04	0.05
2-Butanone, 3,3-dimethyl-	0	0	0.05	Phenol, 3-methyl-	0	0.08	0.02
2-Cyclopenten-1-one, 3-methyl-	0.19	0	0	Creosol	0.52	0.44	0.14
Cyclopentanone, 2-methyl-	0	0	0.09	Phenol, 3,5-dimethyl-	0.04	0	0
1,2-Cyclopentanedione, 3-methyl-	0.61	0.58	0.38	Phenol, 4-ethyl-	0.34	0.37	0.23
2-Cyclopenten-1-one, 2-hydroxy-3,4-dimethyl-	0.03	0.04	0	Phenol, 4-ethyl-2-methoxy-	0.58	1.12	1.06
1,3-Cyclopentanedione, 2,4-dimethyl-	0	0	0.04	2-Methoxy-4-vinylphenol	0.90	1.29	1.15
Cyclohexanone, 4-ethyl-	0	0.04	0.02	Eugenol	0	0	0.01
2-Cyclopenten-1-one, 3-ethyl-	0	0	0.02	Ethyl Vanillin	0	0	0.02
2-Cyclopenten-1-one, 3-ethyl-2-hydroxy-	0.16	0.18	0.11	Phenol, 2,6-dimethoxy- / Syringol	0.98	1.21	0.98
4-Hexen-3-one, 4,5-dimethyl-	0.04	0	0	Phenol, 2-methoxy-4-(1-propenyl)-/Isoeugenol	0	0.02	0.03
Total alcohols	0	0	0.02	Phenol, 4-(2-propenyl)-	0	0	0.02
1-Butanol	0	0	0.02	trans-Isoeugenol	0.16	0.17	0.12
Total furans	2.44	3.51	0.70	3,5-Dimethoxy-4-hydroxytoluene	0.15	0.17	0.10
Furfural	0	0	0.35	Vanillin	0	0.03	0.03
2-Furanmethanol	0.51	0.87	0.02	Apocynin / Acetoguaiacone	0	0	0.02
Ethanone, 1-(2-furanyl)-	0.03	0.09	0.25	Ethanone, 1-(3,4-dimethoxyphenyl)-	0	0	0.06
Butyrolactone	0.19	0.53	0	2',4'-Dimethoxyacetophenone	0	0.08	0
2-Furanmethanol, tetrahydro-	0.08	0.17	0	3',5'-Dimethoxyacetophenone	0.28	0.19	0
2(5H)-Furanone	0.04	0	0.02	2-Propanone, 1-(4-hydroxy-3-methoxyphenyl)-	0.10	0.12	0.08
2-Furanone, 2,5-dihydro-3,5-dimethyl	0	0.03	0	Phenol, 2,6-dimethoxy-4-(2-propenyl)-	0	0.05	0.05
2-Hydroxy-gamma-butyrolactone	0.03	0	0	Methyl 3-(4-hydroxy-3-methoxyphenyl)propanoate	0	0	0.03
Benzofuran, 2,3-dihydro-	1.47	1.74	0	(E)-2,6-Dimethoxy-4-(prop-1-en-1-yl)phenol	0.20	0.23	0.02
5-Hydroxymethyldihydrofuran-2-one	0.07	0.08	0	Benzaldehyde, 4-hydroxy-3,5-dimethoxy-	0	0	0.03
				Ethanone, 1-(4-hydroxy-3,5-dimethoxyphenyl)-	0.04	0.04	0.05
				2-Pentanone, 1-(2,4,6-trihydroxyphenyl)	0.04	0.04	0.05

Table 43. Analysed microwave pyrolysis bio-oil from digestate at three different energy input. Data presented in wt %.

The first two results presented at 1.88 kJ/g and 3.99 kJ/g are from dry biomass test. The noticeable difference between these results and the composition of the bio-oil resulting from 5.08 kJ/g energy input, which had additional water in the sample, is some furfural and levoglucosan generation. This suggests that the extra moisture content enables products to be obtained without going through secondary reactions, with hemicellulose and cellulose decomposed into primary compounds. An equivalent situation occurs with acetic acid - there was less production from wet biomass, 3.7% wt at 5.08 kJ/kg, comparing with dry digestate which gave 4.7% wt and 7.43% wt at 1.88 kJ/kg and 3.99 kJ/kg respectively. Although wet-basis experiments had a low bio-oil yield, phenolics were a highlight due to their formation in almost equal amounts to those in dry-digestate experiments, all of them with a production higher than 6% wt. Bio-oil generated at 5.08 kJ/g energy input was exclusive of benzofuran formation. Other compounds were also detected, different from these categories presented in Table 43, and can be found in detail in APPENDIX D.

Bio-oils from digestate with additional moisture contained more larger molecules such as phenolics and this is an evident difference with the other two bio-oils from dry digestate. Robinson et al. [166] presented studies of cellulose and hemicellulose decomposition using microwave pyrolysis, where one of the variables studied was water content. These results revealed that higher moisture content can lead to the depolymerisation of cellulose and hemicellulose to form larger amount of levoglucosan and furfural at lower temperatures. This mechanism has similarities to what occurs during hydrothermal decomposition of lignocellulosic material, and the same outcomes could have arisen when digestate was subjected to microwave pyrolysis due to the amount of cellulose and hemicellulose within this material. However, ash content in this biomass led to lower yields of these products in the liquid, although the energy input and ash could have enhanced the depolymerisation of lignin.

It has not been possible to make a direct and meticulous comparison between these three pyrolysis technologies due to some operating parameters, for instance energy input and temperature. It is complicated to measure the temperature in the microwave system to interpret how the lignocellulose is decomposed in this specific waste, and how other compounds can be formed by secondary reactions taking place. It was crucial to understand why during the thermochemical decomposition of lignocellulosic material furfural and sugar were not formed as expected. There have been studies of this technology in pyrolysing woody material and due to microwave mechanism high yield of furfural and levoglucosan has resulted, yet with cleaner wood than digestate with under 1% wt of ash [23,25],

5.5 BIO-OIL COMPARISON BETWEEN BIO-OIL FROM PRE-AD AND DIGESTATE

Experiments were carried out using the pre-AD material to evaluate the corresponding pyrolysis products and to differentiate them from those that result from digestate. The technologies available for this comparison were microwave pyrolysis and slow pyrolysis.

5.5.1 PYROLYSIS OF PRE-AD CROP

5.5.1.1 MICROWAVE PYROLYSIS PRE-AD

Pre-AD crop was treated using microwave pyrolysis with the same conditions to which the digestate was subjected. The material was ground and pelletised, and experiments were performed only on dry biomass due to limited access to the lab (COVID-19). It was not possible to carry out experiments on wet biomass with pre-AD crop. Bio-oil analysis of these experiments and from digestate are shown in Table 44.

Microwave pyrolysis bio-oil						
Groups	**Pre-AD 1.83 kJ/kg**	**Digestate 1.88 kJ/kg**	**Pre-AD 3.57 kJ/kg**	**Digestate 3.99 kJ/kg**	**Pre-AD 5.89 kJ/kg**	**Digestate 6.85 kJ/kg**
Acids	5.53	4.70	11.53	7.93	7.63	6.27
Aldehydes & ketones	4.17	5.95	3.54	5.19	3.71	1.69
Alcohols	0.31	0.00	0.63	0.00	0.28	0.02
Furans	4.58	2.44	4.95	3.51	6.68	3.13
Sugars	0.54	0.02	0.45	0.10	0.69	0.00
Phenolics	0.84	6.85	1.14	8.13	1.31	3.90
Others	1.06	0.70	1.25	1.47	1.61	1.07
Total bio-oil	**17.04**	**20.65**	**23.49**	**26.34**	**21.91**	**16.08**

Table 44. Bio-oil composition of microwave pyrolysis of pre-AD crop and digestate. Proportions of chemical groups are presented in percentage weight basis (wt %), and the total of bio-oil of each run.

Sugars and alcohols were barely formed in final bio-oil resulting from digestate, with a maximum of 0.1% wt. Although pyrolytic bio-oil from pre-AD had more sugars and alcohols the concentration was lower than 1% wt. Acid production was expected to be less using pre-AD as feedstock, however samples had higher yields of acids than digestate. Microwave pyrolysis of digestate produced a maximum acid yield of around 8% wt, whereas using pre-AD material acid production was in a range of around 6-18% wt. On the contrary, phenolics were produced in small amounts from pre-AD tests, less than 3% wt, when these reached an amount higher than 8% wt from digestate.

A visual proportion of these chemical groups formed with microwave pyrolysis of pre-AD material, and some of digestate at comparable energy input, is shown in Figure 44.

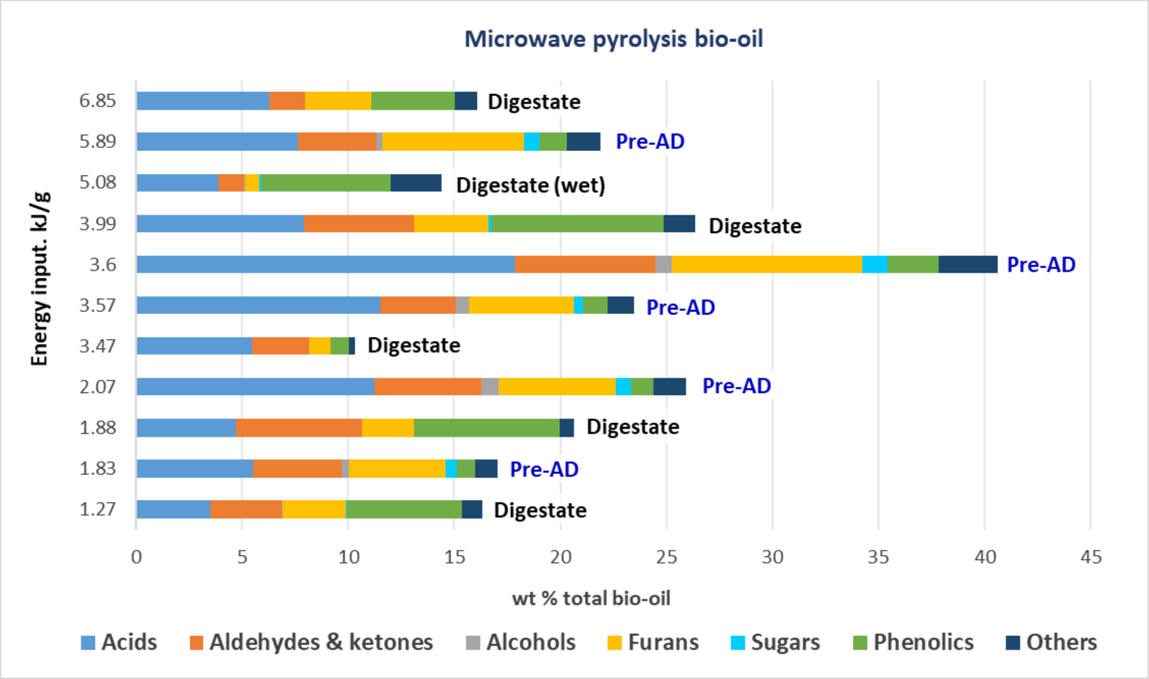

Figure 44. Mass weight distribution of chemical groups found in bio-oil from microwave pyrolysis of pre-AD material vs digestate at different energy input.

Using pre-AD crop resulted in an increase of bio-oil yields, from 17% wt as the lowest, to approximately 40% wt. It is clear in this illustrative distribution that there is difference in composition between both bio-oils, where with lower energy input it is possible to get more product from pre-AD material. However, the small amount of phenolics formed at these conditions indicates that more energy (or time) was needed to decompose lignin due to more organic material in pre-AD crop than digestate. The difference was around 30% in form of starch and hemicellulose, which was what microorganisms consumed during the AD process. Performing these experiments at the same period of time might cause only the conversion of starch, hemicellulose, cellulose and a small fraction of the lignin. The evidence of this is the highest bio-oil yield from pre-AD (~40% wt) at 3.6 kJ/g. This specific experiment was performed with around 10-15 additional seconds which allowed more biomass conversion than all the rest.

Detailed bio-oil analysis of some samples is presented in Table 45.

	Microwave pyrolysis								
Compounds	**1.83 kJ/g**	**3.57 kJ/g**	**3.6 kJ/g**	**5.89 kJ/g**	**Compounds**	**1.83 kJ/g**	**3.6 kJ/g**	**3.57 kJ/g**	**5.89 kJ/g**
Total acids	5.53	11.53	17.86	7.63	**Total furans**	4.58	8.97	4.95	6.68
Formic acid	0.11	0.12	0.21	0.24	Furfural	0.99	1.46	1.56	1.77
Acetic acid	5.17	11.12	17.11	6.94	2-Furanmethanol	0.99	2.98	2.05	1.98
Propanoic acid	0.13	0.18	0.30	0.24	Ethanone, 1-(2-furanyl)-	0.04	0.14	0.07	0.05
2-Propenoic acid	0	0	0.14	0	2-Furancarboxaldehyde, 5-methyl-	0.06	0.10	0.09	0.11
Butanoic acid	0.11	0.12	0	0.20	Butyrolactone	0.12	0.30	0.18	0.08
Butanoic acid, 2-oxo-	0.01	0	0.11	0	2(5H)-Furanone	0.10	0.20	0.12	0.13
Total aldehydes & ketones	4.17	3.54	6.63	3.71	2(5H)-Furanone, 5-methyl-	0	0	0	0.05
Glycolaldehyde dimer	0.89	0	1.35	0	2-Furanone, 2,5-dihydro-3,5-dimethyl	0	0.06	0	0
2-Propanone, 1-hydroxy-/Acetol	2.11	2.21	3.01	1.96	Furaneol	0	0.04	0	0.03
1-Hydroxy-2-butanone	0.30	0.13	0.57	0.67	2(3H)-Furanone, dihydro-4-hydroxy-	0.23	0.54	0.31	0.37
1-Hydroxy-3-methyl-2-butanone	0.12	0.12	0.25	0.03	Benzofuran, 2,3-dihydro-	0.39	0.94	0.59	0.75
2-Cyclopenten-1-one	0	0	0.04	0	5-Hydroxymethylfurfural	1.62	2.13	0	1.34
2-Propanone, 1-(acetyloxy)-	0.17	0.16	0.22	0.27	5-Hydroxymethyldihydrofuran-2-one	0.04	0.09	0	0.03
2-Cyclopenten-1-one, 2-methyl-	0	0	0.12	0	**Total Sugars**	0.54	1.17	0.45	0.69
2-Butanone	0	0.02	0	0.03	2,3-Anhydro-d-galactosan	0.02	0.04	0	0
3-Penten-2-one	0.01	0	0	0	2,3-Anhydro-d-mannosan	0	0.08	0	0
2-Cyclopenten-1-one, 2-hydroxy-	0	0.36	0.7	0.33	1,4:3,6-Dianhydro-.alpha.-d-glucopyranose	0.05	0.15	0.05	0.04
Cyclohexanone, 2-ethyl-	0	0.03	0	0	DL-Xylose	0.02	0.08	0	0.02
3-Pentanone, 1,5-dimethoxy-	0	0.24	0	0.18	d-Mannitol, 1,4-anhydro-	0	0.03	0	0
1,2-Cyclopentanedione, 3-methyl-	0.21	0.22	0.13	0.17	d-Mannose	0.02	0.04	0	0
2-Cyclohexen-1-one, 4,5-dimethyl-	0	0	0.05	0	β.-D-Glucopyranose, 1,6-anhydro-/LVG	0.43	0.75	0.40	0.50
2-Cyclopenten-1-one, 3-ethyl-2-hydroxy-	0.07	0.04	0.23	0.08	**Total phenolics**	0.84	2.42	1.14	1.31
4-Ethyl-2-hydroxycyclopent-2-en-1-one	0	0	0	0	Phenol	0.05	0.17	0.08	0.08
Total alcohols	0.31	0.63	0.78	0.28	Phenol, 2-methoxy-	0.13	0.36	0.22	0.18
Ethanol, 2-ethoxy-	0.09	0	0.26	0	Phenol, 3-methyl-	0	0.07	0	0
Propylene Glycol	0.16	0.31	0.21	0.28	Creosol	0	0.04	0	0
2-Hexanol	0	0	0.04	0	Phenol, 4-ethyl-	0	0.16	0.06	0.06
2-Cyclohexen-1-ol	0.04	0	0.06	0	Phenol, 2-ethyl-	0.04	0	0	0
2-Propanol, 1,3-dimethoxy-	0.01	0.25	0	0	Phenol, 4-ethyl-2-methoxy-	0	0.03	0	0
2,4-Pentanediol	0	0.07	0.04	0	2-Methoxy-4-vinylphenol	0.42	0.94	0.59	0.73
Cyclopentanol	0	0	0.16	0	Phenol, 2,6-dimethoxy-	0.08	0.25	0.10	0.08
Others	0.9	1.0	1.2	1.5	trans-Isoeugenol	0.04	0.06	0.03	0.05
Hydrazine, (2-methylpropyl)-	0.06	0.15	0.10	0.23	3,5-Dimethoxy-4-hydroxytoluene	0	0.10	0	0
Butanoic acid, propyl ester	0.11	0.54	0.55	0.37	Vanillin	0	0.01	0	0.01
9-Octadecenamide, (Z)-	0.07	0.31	0.06	0.05	Orcinol	0	0.04	0	0
					3',5'-Dimethoxyacetophenone	0.04	0.08	0.02	0.04

Table 45. Analysed microwave pyrolysis bio-oil from pre-AD crop at three different energy input. Data presented in wt %.

Alcohols were detected in pre-AD bio-oil in very minute amounts, between 0.3% and 0.8% wt; whereas from digestate these were barely found, less than 0.05% wt. The obvious difference in these pre-AD microwave results was that compounds such as 5-hydroxymethylfurfural was quantified at around 1-2% wt, but not detected at all in bio-oil from digestate. It is also noticeable that there was a low production of benzofuran. While bio-oil from digestate contained almost 2% wt benzofuran, the maximum amount produced with pre-AD material was under 1% wt. This suggests that there might be less decomposition of lignin in the pre-AD material.

Considering that this biomass had much less ash than digestate, yields of sugars were lower than expected, just above 1% in some cases. It seems that the ash level of 4% in the crop had a negative impact on sugar formation, and led to more acid generation. Acetic acid was in higher proportion from pre-AD than the amount formed from digestate in microwave pyrolysis. The range of this chemical produced with digestate was round 3-8% whereas with pre-AD crop the production was around 5-17% wt.

Despite this, there were additional compounds formed as expected from lignocellulose contained in pre-AD crop, especially those which have been studied when biomass is treated with conventional pyrolysis such as glycolaldehyde dimer, acetol, levoglucosan and furfural, but at a relatively low concentration.

Formic acid is also a small molecule which resulted from lignocellulose decomposition, and it was only detected in these microwave experiments with pre-AD crop. 2-cyclopenten-1-one is another highlighted. This compound was found in one bio-oil sample from pre-AD crop at very low concentration, differently from those bio-oils produced from digestate where it was found in most of the samples. Previous studies have shown that microwave pyrolysis can produce a high yield of primary compounds such as levoglucosan and furfural [23,68,166], however this did not occur during microwave pyrolysis of pre-AD crop using the conditions employed in this study.

More compounds were detected and quantified classified as others; these are shown in APPENDIX D.

5.5.1.2 SLOW PYROLYSIS PRE-AD

Slow pyrolysis pre-AD crop processing was performed under the same conditions as the digestate was processed. The general mass balance from slow pyrolysis is presented in Table 46.

Product	Slow pyrolysis							
	355ºC		425 ºC		485 ºC		530 ºC	
	Pre-AD	Digestate	Pre-AD	Digestate	Pre-AD	Digestate	Pre-AD	Digestate
Biochar	41.47	57.34	35.26	45.30	30.46	41.18	27.50	39.63
Bio-oil	49.18	33.97	54.17	42.19	57.05	45.13	58.99	46.02
Organics	*38.16*	*18.98*	*44.06*	*26.26*	*46.54*	*26.68*	*50.39*	*27.02*
Water	*11.02*	*12.47*	*10.11*	*15.93*	*10.52*	*18.45*	*8.59*	*19.01*
Gas	4.57	4.10	6.88	5.32	8.34	8.30	9.13	9.19
Total products recovered	**95.22**	**95.41**	**96.31**	**92.81**	**95.85**	**94.61**	**95.62**	**94.84**

Table 46. Yields of slow pyrolysis products carried out at four different temperatures using pre-AD crop and digestate.

Biochar formation from pre-AD crop at the lowest temperature is higher than for any other condition, similar to findings in slow pyrolysis of digestate but with a larger amount of liquid product. This crop waste has a larger organic matter content, material usually consumed by AD microorganisms for biogas production. This material is around 20% of the total pre-AD crop composition and it can be more easily converted into other products when subjected to a thermochemical treatment. This is reflected in bio-oil composition and in final pyrolytic liquid formed, because gas generation was consistent between both biomasses pyrolysed at 4-9% wt. Biochar production with digestate at 530ºC was almost 40% of the total products, whereas with pre-AD crop at the same temperature biochar was under 30%, with the highest amount of organics in bio-oil at approximately 50% wt. Less water was formed with pre-AD crop. These yields vary in a range of 13-19% and 8-11% wt using digestate and pre-AD material respectively in slow pyrolysis.

There is a significant difference between yields of products with pre-AD material as feedstock and yields from pyrolysed digestate. This difference in pyrolysis product from both biomasses is shown in Figure 45.

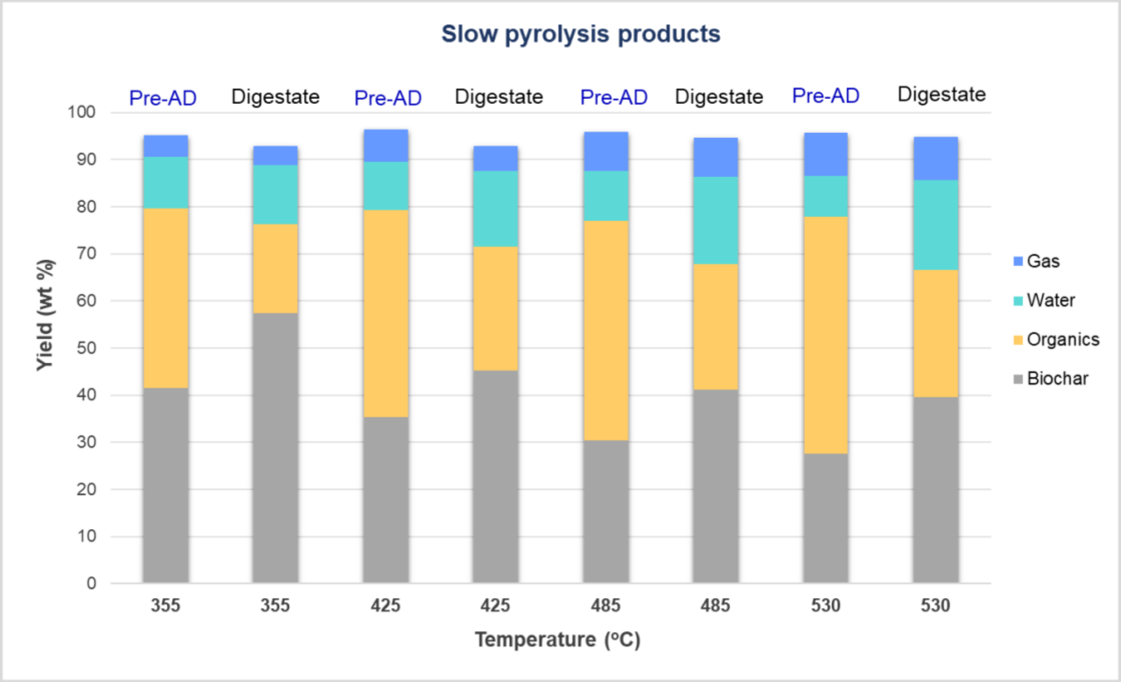

Figure 45. Comparison of yields of slow pyrolysis products recovered between using pre-AD crop and digestate as feedstock at same conditions.

Biochar and water generation is greater with digestate than with pre-AD crop across the entire temperature range, and organics production is nearly doubled from pre-AD crop to that produced from digestate. The composition of chemical groups in bio-oils from pre-AD crop are shown in Table 47.

Slow pyrolysis pre-AD Bio-oil								
GROUPS	**355 °C**		**425 °C**		**485 °C**		**530 °C**	
	Pre-AD	**Digestate**	**Pre-AD**	**Digestate**	**Pre-AD**	**Digestate**	**Pre-AD**	**Digestate**
Acids	1.13	9.78	0.00	8.57	0.00	2.80	0.00	8.61
Aldehydes & ketones	13.99	3.18	15.13	4.47	10.85	3.10	18.55	3.62
Alcohols	1.35	2.42	0.67	0.00	0.60	0.00	0.00	0.00
Furans	19.22	3.56	14.57	6.22	20.85	9.60	8.69	6.79
Sugars	0.55	0.15	7.43	0.50	5.89	0.21	8.72	0.55
Phenolics	12.62	9.79	15.98	18.82	18.86	25.44	23.03	22.79
Others	0.31	2.26	0.39	3.02	0.00	2.44	0.00	2.40
Total bio-oil	**49.2**	**31.13**	**54.17**	**41.59**	**57.05**	**43.58**	**58.99**	**44.77**

Table 47. Bio-oil composition of slow pyrolysis of pre-AD material. Proportions of chemical groups are presented in % weight basis.

Acids were not formed from pre-AD in significant amounts compared with other pyrolysis experiments. At 425-520°C no acids were produced from pre-AD material, whereas from digestate these compouds were found at 3-10% wt at the same temperatures. Furans were generated in larger amounts, between 14% and

20% wt at 355ºC, 425ºC and 485ºC; yet in lower proportion at 530ºC. This is contrary to the amount formed from digestate where the maximum was 10% at the same conditions.

It seems most of the lignocellulose material was converted into aldheydes, alcohols, furans, sugars and phenolics, and there was almost negligible formation of other compounds. Illustrative representation of the chemical group distribution in bio-oils formed from pyrolysis of pre-AD crop, and digestate is shown in Figure 46.

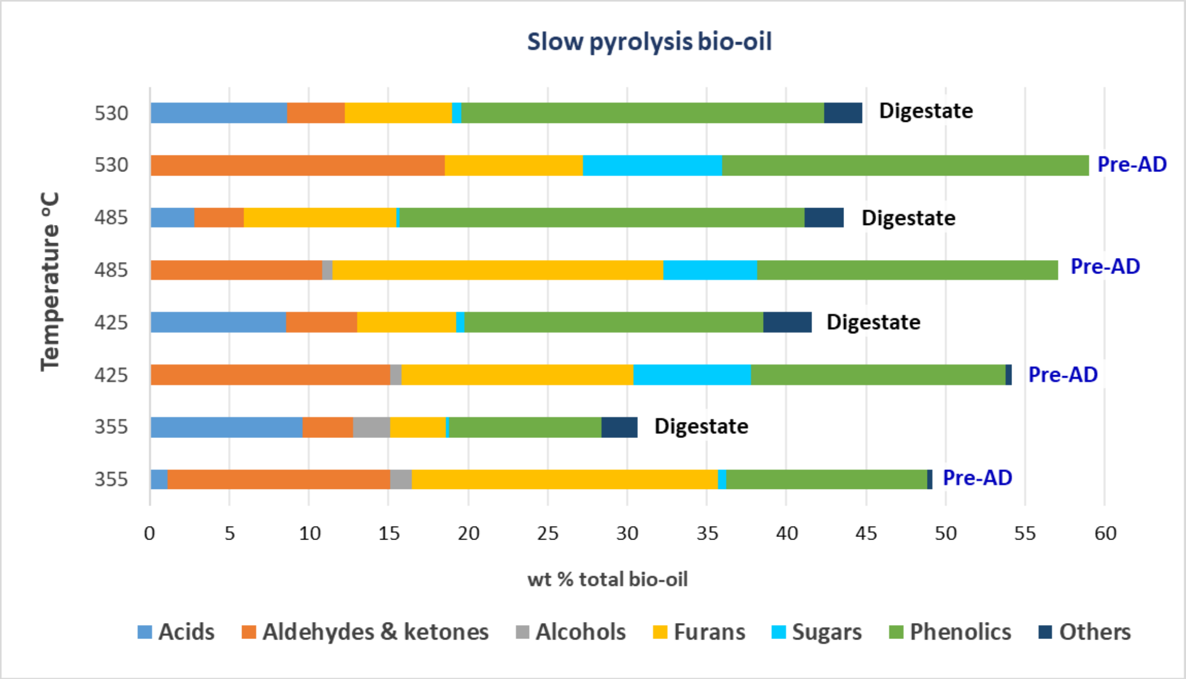

Figure 46. Mass weight distribution of the chemical groups found in bio-oil from slow pyrolysis of pre-AD material at four different temperatures.

The only acid produced and detected in this pre-AD pyrolysis bio-oil has a molecular weight of 74 g/mol at 355ºC, which is a lager molecule than acetic acid (60 g/mol), which was not formed in slow pyrolysis of pre-AD. In experiments at the highest temperatures the first compound identified had a larger molecular weight of approximately 90 g/mol. This could indicate that the depolymerisation of lignocellulosic material forms larger molecules during thermal conversion of pre-AD material. This can also be evaluated through comparison with chemical composition of these bio-oils. The detailed chemical analysis of these is presented in Table 48.

Slow pyrolysis pre-AD io-oil				
Compounds	**355°C**	**425°C**	**485°C**	**530°C**
Total acids	**1.13**	**0**	**0**	**0**
Propanoic acid	1.13	0	0	0
Total aldehydes & ketones	**13.99**	**15.13**	**10.85**	**18.55**
2-Butanone, 4-hydroxy-3-methyl-	0.11	0.08	0.27	2.75
1,2-Cyclopentanedione	4.18	3.67	1.70	0.21
4-Heptanone	1.74	1.56	0	0
2-Cyclopenten-1-one, 2-hydroxy-3-methyl-	2.92	4.24	4.06	6.85
Butanal, 3-hydroxy-	4.12	4.36	3.78	6.93
2-Cyclopenten-1-one, 3-ethyl-2-hydroxy-	0.92	1.22	1.04	1.81
Total alcohols	**1.35**	**0.67**	**0.60**	**0**
2-Propanol, 1-propoxy-	1.35	0.67	0.60	0
Total furans	**19.22**	**14.57**	**20.85**	**8.69**
Furfural	3.48	1.84	2.96	1.99
2-Furanmethanol	8.24	1.91	5.47	1.77
Ethanone, 1-(2-furanyl)-	1.99	3.10	3.31	0.88
2-Furancarboxaldehyde, 5-methyl-	1.38	1.70	1.36	0
2(3H)-Furanone, 3-butyldihydro-	2.40	2.63	2.31	2.37
Benzofuran, 2,3-dihydro-	1.73	3.39	5.44	1.68
Total sugars	**0.55**	**7.43**	**5.89**	**8.72**
β.-D-Glucopyranose, 1,6-anhydro-	0.55	7.43	5.89	8.72
Total phenolics	**12.62**	**15.98**	**18.86**	**23.03**
Phenol	0.73	0.96	1.08	1.86
Phenol, 2-methoxy-	2.24	2.79	3.70	5.37
Phenol, 3-methyl-	0	0	0.57	0
Creosol	0.49	1.32	0.72	0.64
Phenol, 2-ethyl-	0.65	0.48	0.89	1.02
Phenol, 4-ethyl-2-methoxy-	1.02	2.18	2.34	0.84
2-Methoxy-4-vinylphenol	3.90	3.96	4.57	7.28
Phenol, 2,6-dimethoxy-	1.63	2.76	2.20	2.53
trans-Isoeugenol	0.60	0.72	1.07	1.36
2-Propanone, 1-(4-hydroxy-3-methoxyphenyl)-	0.26	0.31	0.36	0.20
(E)-2,6-Dimethoxy-4-(prop-1-en-1-yl)phenol	0	0	0.35	0

Table 48. Analysis of bio-oil from pre-AD material at slow pyrolysis process. Proportions of chemical groups are presented in % weight basis.

Furfural and levoglucosan are formed in larger amounts in these bio-oils from pre-AD material; something that did not arise with the other experiments with digestate. It is possible this occurred due to the amount of starch content in the starting crop. However, there are studies which show that this can be decomposed into CO_2 and H_2O instead of levoglucosan if it is processed at temperatures higher than 300°C

[92,125]. Benzofuran was still produced in considerable amount in these bio-oils, although this pre-AD material had around 4% wt of ash, and the residence time of biomass in the reactor was 30 minutes which could lead lignin to being decomposed into more benzofuran.

In order to verify that acetic acid was not formed in these experiments, bio-oil samples from pre-AD crop subjected to microwave pyrolysis were also analysed in GC-MS at the same time. These samples had acetic acid in large amounts, and were used to validate that acetic acid was not detected in bio-oils from slow pyrolysis of pre-AD crop. This evaluation is shown Figure 47.

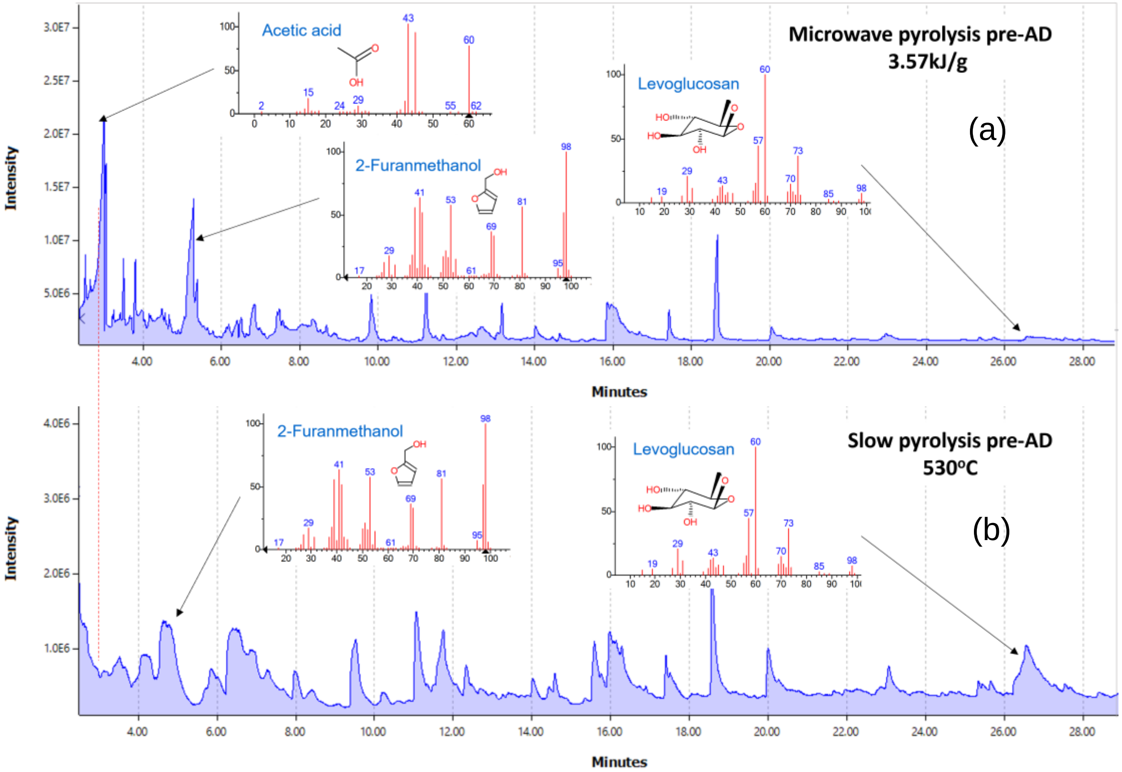

Figure 47. Comparison of chromatograms between some compounds identified from pyrolysis of pre-AD crop: (a) microwave pyrolysis with 3.57 kJ/g energy input, and (b) slow pyrolysis at 530ºC.

Chromatogram (a) shows a sample of bio-oil from pre-AD crop with acetic acid, 2-furanmethanol and levoglucosan detected. In chromatogram (b) at around 2.5 minutes there should be a peak that represents acetic acid, as the 2-furanmethanol peak emerges at minute 4, which indicates that this compound was not formed. The only difference between the pre-AD crop used in these two processing technologies was that for microwave pyroysis this material was ground to make pellets, and for slow pyrolysis this crop was added as was dried, preserving its original form. Grinding this material might have an impact on how lignocellulose was thermochemically decomposed due to the alteration of biomass structure. It is also possible the ash content could be distributed in different ways, with a higher surface area from the grinding and pelletising process.

5.4 IMPACT OF ASH ON PYROLYSIS PRODUCT COMPOSITION FROM DIGESTATE

It is noticeable how the results between pyrolysis products change, not only between technologies, but also between set of runs at the same conditions. It was mentioned previously that due to the ash content in both biomasses the amount of this inorganic material could be different in each sample loaded into the reactors used for slow and microwave pyrolysis. These pyrolysis reactors only needed samples of around 6g, and there might be significant variation between these, in similar way to the results obtained when ash content was determined with TGA.

Ash is assumed to be an initiator for secondary reactions, due to its properties as a catalyst, and it can lead to more water and CO_2 formation. Persson et al. [81], for instance, presented some tests which revealed that by demineralising biomass more stable polymers can resulted when this biomass is thermochemically processed to form larger molecules in pyrolytic bio-oil.

The main pyrolysis products from cellulose and hemicellulose, such as sugars and furfural, might be further decomposed into sub-compounds at high temperatures and especially in the presence of the large amounts of ash this biomass contains [81,111]. Some cases have been presented where larger amounts of levoglucosan are formed when lignocellulosic material is pre-treated to reduce the ash content, resulting also in very low yields of small-molecule compounds such as acetic acid, acetol, formic acid, water and gas. These last two went from 12.2% to 0.9%wt and from 10.8% to 6.4% wt respectively. This indicates that primary compounds are not going through further decomposition when the inorganic ash is removed.

However, lignin derivatives such as phenolics can be more stable and be formed at high temperatures without further decomposition. Research has been carried out where catalytic reactions are performed by adding inorganic material to convert lignin material into phenolics. Thus, ash could enhance this transformation at high temperatures, and even some hydrocarbons could be formed [167-169].

Ash content and grinding of biomass seem to be factors with a negative impact on sugar production in pyrolysis. In microwave pyrolysis, for instance, biomass being pre-treated might have led to a surplus energy input for cellulose and hemicellulose conversion into sugars, and secondary reactions could have occurred during pyrolysis to form these other compounds derived from levoglucosan and xylose. Additionally, ash distribution in pellets might be different from that in the original material due to being ground. Results between pre-AD crop and crop digestate in slow and microwave pyrolysis could demonstrate this theory. Slow pyrolysis of pre-AD material produced more sugars and very small amounts of acids. Similar results were expected for microwave pyrolysis when the same material was processed: more primary compounds, such as levoglucosan and furfural due to less amount of ash content.

The heating mechanism in microwave and the ash distribution could also lead to breaking down some primary organics formed from lignocellulose. This can be represented in Figure 48.

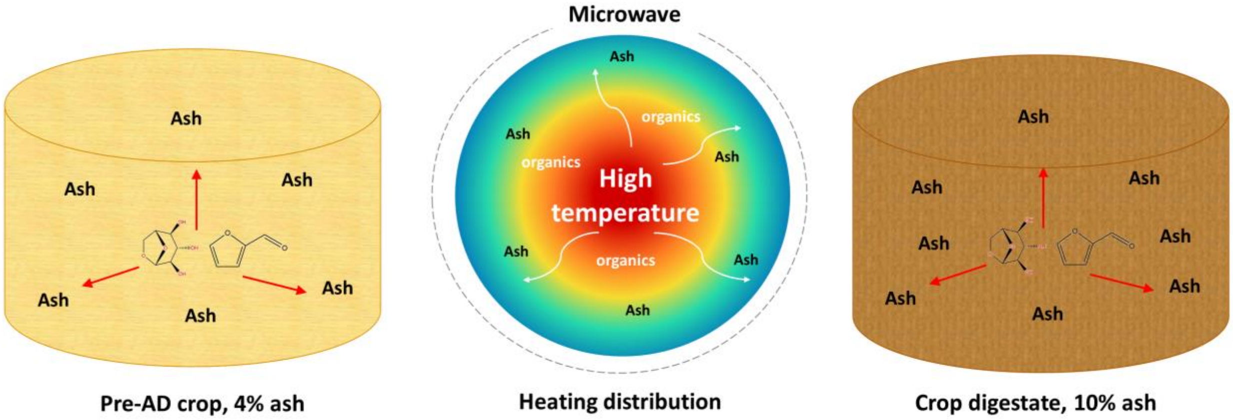

Figure 48. Illustration of possible effect of ash distribution and microwave mechanism through pre-AD crop and digestate pellets utilised in microwave pyrolysis.

Results from microwave pyrolysis of digestate, where the experiments were carried on wet biomass, were favourable for lignin when it is decomposed in presence of ash. It seems that the combination of water and ash enhance easier depolymerisation of lignin to from phenolics with this technology.

In contrast, data from slow pyrolysis of digestate shows that phenolics and acids were in high proportion. This was at temperatures around 355ºC, where more char was produced. These results could support the hypothesis that phenolics would be broken down into smaller molecules due to ash presence and larger residence time. A similar situation occurred with fast pyrolysis, at 480ºC, where acids were in greater proportion than phenolics and this, could also be influenced by the sample preparation as digestate was ground to make pellets. This and ash content could lead to the conversion of these lignin-derived products into others compounds, producing smaller molecules such as acetic acid, and CO_2.

The digestate is analysed regularly at the AD plant by Schmack Biogas Service to determine nutrients within the material and to determine it is suitability for use as a fertiliser. Some of the inorganic compounds found are calcium, phosphorus, magnesium and potassium, and these are the main compounds considered as nutrients for soil amendment. There also some metals such as copper and zinc in very low concentration. These tests are carried out under DIN EN ISO 11885 2009-09 methods. All these inorganic compounds are considered as catalysts in biomass thermochemical processing. Some have analysed their effect on pyrolysis products formation and composition, where reactions can result in dehydration and lead to more water generation. [111,116,170].

This ash could also enhance specific secondary reactions where compounds such as levoglucosan and furfural are converted into other compounds found in bio-oil pyrolysis of digestate. These are explained in more detail in the next chapter.

CHAPTER 6. COMPARISON OF YIELD AND BIO-OIL COMPOSITION FROM DIFFERENT PYROLYSIS TECHNIQUES

Pyrolytic bio-oil was selected as a main target to compare the results of pyrolysing digestate through the three technologies. Bio-oil is one of the products that has specific compounds formed directly from cellulose, hemicellulose and lignin and could give indications about how the decomposition of this lignocellulosic material in digestate occurs through these systems. Samples obtained under equivalent conditions of temperature or energy input were selected to be evaluated, and based only on experiments performed with dry biomass. In the range of conditions implemented to pyrolyse digestate, medium and high values of energy input and temperature were considered for this analysis.

These bio-oils and estimation of their distribution of chemicals groups are shown in Table 49 and, graphically presented in Figure 49.

GROUPS	**Medium**			**High**		
	Slow	**Fast**	**Microwave**	**Slow**	**Fast**	**Microwave**
	425°C	**460°C**	**1.88 kJ/g**	**530°C**	**560°C**	**3.99 kJ/kg**
Acids	8.57	6.20	4.70	8.61	6.64	7.93
Aldehydes & ketones	4.47	4.03	5.95	3.62	4.41	5.19
Alcohols	0.00	0.17	0	0.00	0.43	0
Furans	6.22	3.46	2.44	6.79	6.31	3.51
Sugars	0.50	1.28	0.02	0.55	1.86	0.10
Phenolics	18.82	19.00	6.85	22.79	17.82	8.13
Others	3.02	1.90	0.70	2.40	2.69	1.47
Total bio-oil	41.59	36.03	20.65	44.77	40.15	26.34

Table 49. Bio-oil comparison between the three pyrolysis technologies from digestate. Proportions of chemical groups are presented in weight basis % of the total bio-oil of one experiment with equivalent condition: temperature/ specific energy input.

The first highlight is that production of sugars in fast pyrolysis was 1.28% wt at 460°C, and almost 2% at 560°C; this is different from slow and microwave pyrolysis which resulted in a very small amount of sugars formed. In addition, levoglucosan is the only sugar compound generated in fast pyrolysis. Acids are also produced in all these samples, yet it is possible that microwave pyrolysis could have led to more acid formation, considering that bio-oil recovery was lower than for other technologies. The amount of furans is consistent across these systems, with the lowest amount of 2.44% wt from microwave pyrolysis at 1.88kJ/kg energy input, 3.46% from fast pyrolysis at 460°C and 6.22% wt from slow pyrolysis at 425°C. These also increased when temperature and energy input were higher. The opposite was found with aldehydes and ketones, which decreased in content with slow and microwave pyrolysis at higher temperature and energy input. There is just a minor increase with fast pyrolysis from 4.03% to 4.41% wt. Phenolics were formed in the highest proportion across these technologies. However, phenolic compounds increased in slow and microwave pyrolysis from around 19% to almost 23%, and 6.85% to 8.13% wt respectively. Contrastingly, they were slightly less generated in fast pyrolysis, reduced from 19% at 460ºC to 17.82% at 560ºC.

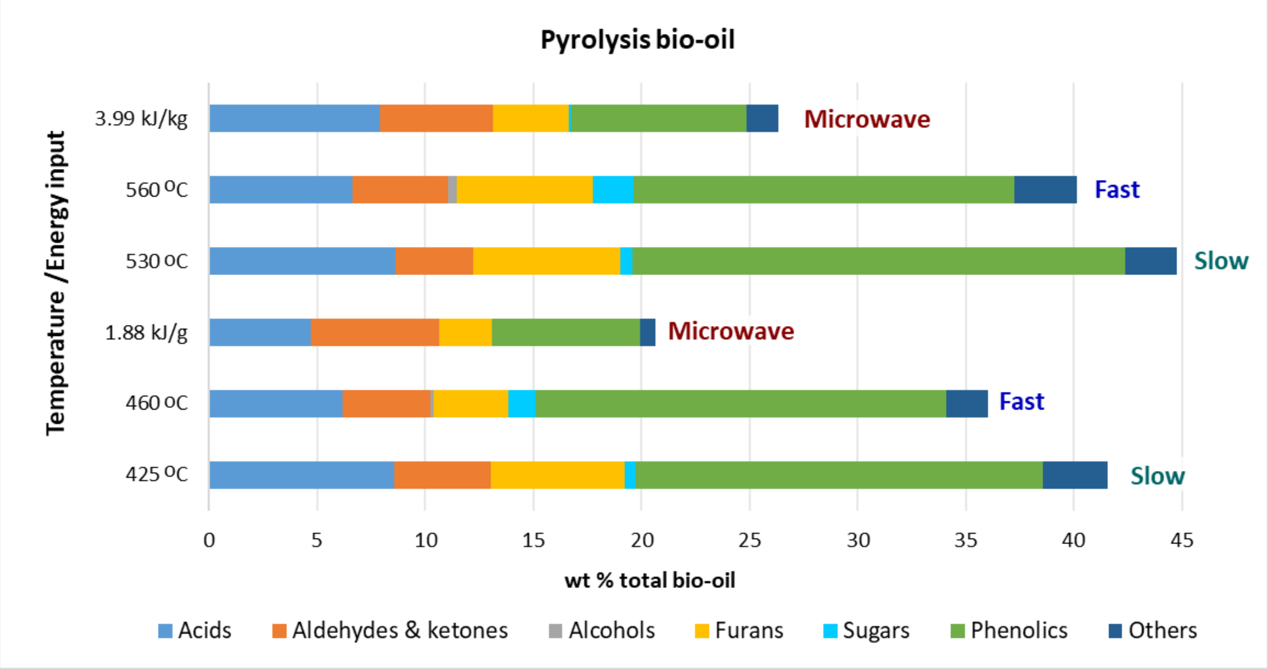

Figure 49. Mass weight distribution of chemical groups quantified in bio-oil from digestate in all the pyrolysis equivalent conditions.

Phenolics are the most noticeable and predominant compounds in this comparison. Fast and slow pyrolysis produced more of these compounds whereas microwave pyrolysis enhanced aldehyde and ketone generation. Sugars were detected at low concentrations in all bio-oils, with the largest amounts from fast pyrolysis. Analytical details of these bio-oils are presented in Table 50.

GROUPS	Medium			High		
	Slow 425°C	Fast 460°C	Microwave 1.88 kJ/g	Slow 530°C	Fast 560°C	Microwave 3.99 kJ/g
Acids						
Acetic acid	7.81	5.70	4.49	7.91	6.07	7.43
Propanoic acid	0.76	0.50	0.21	0.71	0.57	0.50
Aldehydes & ketones						
2-Propanone, 1-hydroxy-/Acetol	0	0	3.18	0	0	2.71
2-Cyclopenten-1-one	0.42	0.18	0.66	0.28	0	0.58
2-Cyclopenten-1-one, 3-methyl-	0	0.71	0.19	0	1.00	0
1,2-Cyclopentanedione, 3-methyl-	1.60	0	0.61	1.58	1.77	0.58
Furans						
Furfural	0	0	0	0	0	0
Furan, 3-methyl-	0	0	0	0	0.24	0
2-Furanmethanol	0.73	0.38	0.51	0.52	0.40	0.87
Butyrolactone	1.21	0	0.19	1.01	0	0.53
2-Furanmethanol, tetrahydro-	0.68	0	0.08	0.44	0	0.17
Benzofuran, 2,3-dihydro-	3.08	2.86	1.47	4.36	5.48	1.74
Sugars						
1,4:3,6-Dianhydro-.alpha.-d-glucopyranose	0.26	0.16	0.02	0.19	0.31	0.02
DL-Xylose	0.24	0.34	0	0.36	0.36	0.08
β.-D-Glucopyranose, 1,6-anhydro-/LVG	0	0.54	0	0	0.84	0
Phenolics						
Phenol	1.84	1.68	0.71	2.49	4.03	0.63
Phenol, 2-methoxy-	5.51	2.90	1.49	5.46	1.78	1.74
Creosol	1.82	0.86	0.52	1.6	0.49	0.44
Phenol, 4-ethyl-	0.63	2.21	0.34	0.89	2.79	0.37
Phenol, 2,6-dimethoxy- / Syringol	4.52	3.01	0.98	5.84	0.98	1.21

Table 50. Bio-oil comparison between the three pyrolysis technologies from digestate. Proportions of chemical groups are presented in percentage weight basis (% wt) of the total bio-oil of one experiment at certain conditions: temperature, or energy input.

Differences were observed not only in the bio-oil generated from each pyrolysis technology, but between each bio-oil produced in every run of each set of experiments at the same conditions. Some of the primary compounds formed from lignocellulosic material, such as acetol, acetic acid, furfural, levoglucosan and phenol could have been generated, but transformed into other molecules because very low concentration or just traces, in some cases, were found in bio-oil samples. According to mechanisms in the literature, bio-oil compounds expected might have been decomposed into smaller molecules such as acetic acid. Furfural could form compounds such as furan,3-methyl-, 2-furanmethanol, butyrolactone, 2-furanmethanol, tetrahydro- and 2-cyclopenten-1-one, if secondary reactions take place, and the presence of these in most of the bio-oils recovered suggests that this might have occurred during pyrolysis of digestate. This and other possible reactions are explained in more detail in the next section.

6.1 LEVOGLUCOSAN DECOMPOSITION

The decomposition of levoglucosan (LVG) is one example of why small molecules could be found in pyrolysis products due to secondary reactions. If cellulose content in digestate is around 25%, LVG should be formed in larger amount than just around 2%, which was the highest proportion found across these pyrolysis treatments. An illustrative conversion of how LVG could be broken down into smaller molecules is shown in Figure 50, where Shen et al. [43] suggested that this sugar would be decomposed through several steps, including a dehydration where water, furans and ketones are formed, but this step might also comprise the generation of small fragments to form compounds such as CO, CO_2, formaldehyde (CH_2O) and acetic acid.

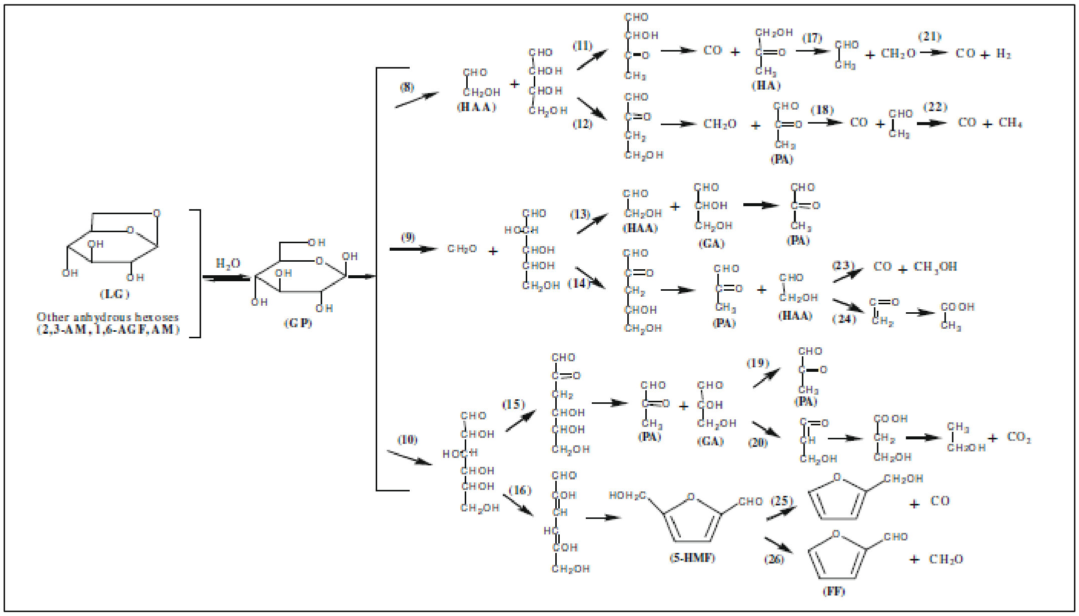

Figure 50. Mechanism of sugar decomposition of hexoses, such as levoglucosan proposed by Shen et al. [43].

This could be one reason CO_2 and acetic acid is in high proportion in most of the gas and bio-oil products. Furthermore, 5-hydroxymethyl-furfural is expected to be formed from LVG, but this compound was not identified in any of the digestate pyrolysed, it was only found in some pre-AD produced bio-oil. LVG was detected in less than 1 wt % with fast pyrolysis of digestate at 460ºC and 560ºC. Studies have less sugar formation when catalytic material is contained in the pyrolysis of biomass, such as in comparisons made by Yildiz et al. [111], where levoglucosan yield is reduced in the presence of ash and more acetic acid and acetol are formed. Other experiments were carried out by Banks et al. [116] who showed how ash-free wood, and biomass impregnated with potassium and with phosphorus had a direct impact on levoglucosan detection in bio-oil produced, and it was found a significant amount of smaller molecules such acetic acid and other compounds categorised as furans such as 2(5H)-furanone.

6.2 FURFURAL DECOMPOSITION

Furfural was not detected in the analysis of bio-oil from slow, fast and microwave pyrolysis of digestate (Table 50). However, there are some compounds identified that might come from the decomposition of furfural: 2-furanmethanol, butyrolactone and 2-cyclopenten-1-one. Furfural, which results from hemicellulose [77], can be subject to catalytic treatment to obtain these as products [171] and these provide clear indications that secondary reactions were taking place during pyrolysis of this digestate. An example of the possible chemicals derived from the decomposition of furfural are shown in Figure 51.

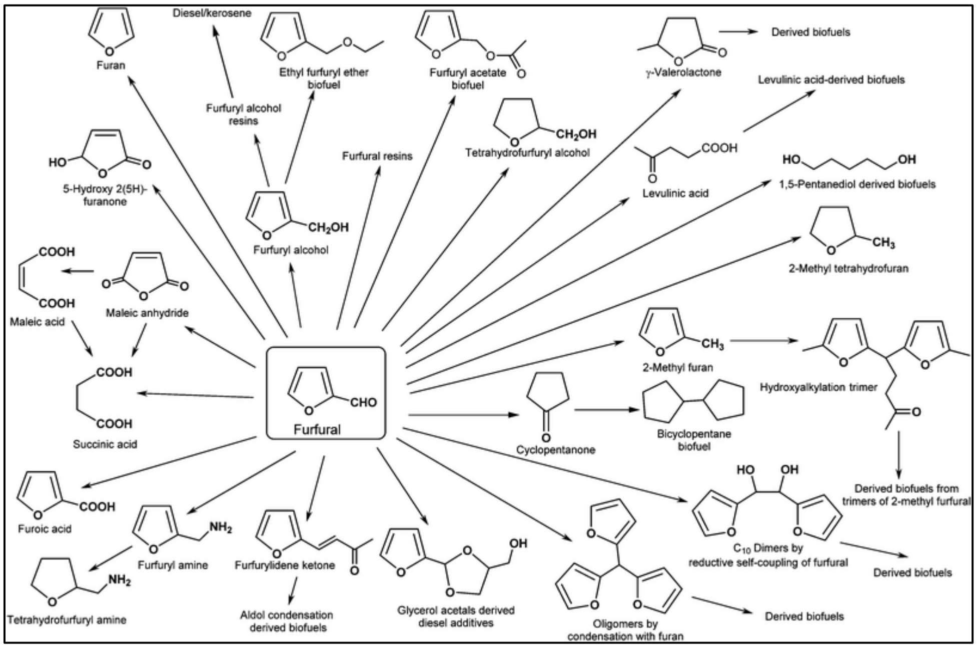
Furan
Diesel/kerosene
Ethyl furfuryl ether biofuel
Furfuryl acetate biofuel
γ-Valerolactone
Derived biofuels
Levulinic acid-derived biofuels
Furfuryl alcohol resins
Furfural resins
CH₂OH
Tetrahydrofurfuryl alcohol
COOH
Levulinic acid
HO
OH
1,5-Pentanediol derived biofuels
5-Hydroxy 2(5H)-furanone
Furfuryl alcohol
CH₃
2-Methyl tetrahydrofuran
Maleic acid
Maleic anhydride
2-Methyl furan
Hydroxyalkylation trimer
CHO
Furfural
Succinic acid
Cyclopentanone
Bicyclopentane biofuel
Derived biofuels from trimers of 2-methyl furfural
Furoic acid
NH₂
Furfuryl amine
Furfurylidene ketone
C₁₀ Dimers by reductive self-coupling of furfural
Derived biofuels
Tetrahydrofurfuryl amine
Aldol condensation derived biofuels
Glycerol acetals derived diesel additives
Oligomers by condensation with furan
Derived biofuels

Figure 51. Overview of chemical could be derived from Furfural presented by Mariscal et al. [172].

2-furanmethanol was found at a slightly higher proportion in microwave pyrolysis at 3.99 kJ/kg energy input, and less than 0.4% in fast pyrolysis. 2-cyclopenten-1-one was also found in most of the bio-oils, but in more quantity with microwave pyrolysis of digestate. Aside from this, butyrolactone and 2-furanmethanol,tetrahydro-, were in greater proportion (approximately 1% and around 0.5% respectively) following slow pyrolysis, lower after microwave pyrolysis and not formed during fast pyrolysis.

6.3 DECOMPOSITION OF LIGNIN INTO PHENOLICS

High acid production could result from additional decomposition of lignin to form phenolics, and subsequent conversion of those phenolics if ash has a catalytic effect on them [173] . There have been many studies about this decomposition which show that to form phenolics the lignin polymer goes through reaction paths where there are low-molecular weight compounds realised such as H_2O, carboxyl compounds, and CO_2 [157,174]. Thus, as experimental data obtained from thermochemical treatment of digestate shows that water and gas result not just from secondary reactions due to the large amount of ash, but due to dehydration stages in the primary decomposition reactions as shown in Figure 52. This adds to the water formed from the decomposition of cellulose and hemicellulose discussed in Section 6.1 and 6.2.

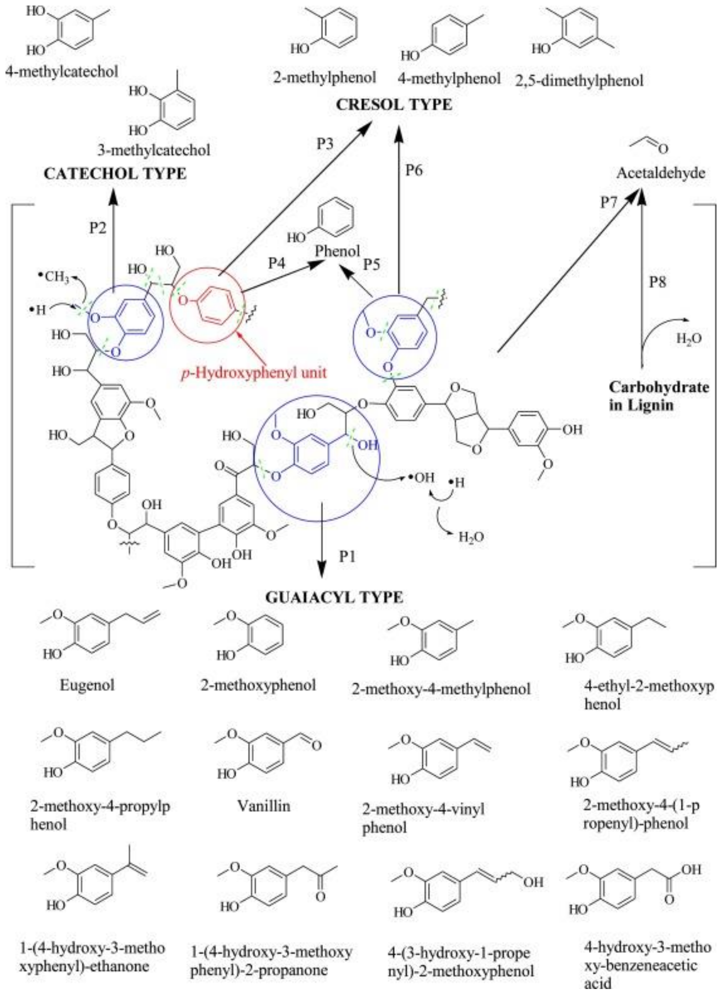
4-methylcatechol
3-methylcatechol
CATECHOL TYPE
2-methylphenol
4-methylphenol
2,5-dimethylphenol
CRESOL TYPE
P3
P6
Acetaldehyde
P7
P2
P4
Phenol
P5
P8
•CH3
•H
H2O
p-Hydroxyphenyl unit
Carbohydrate in Lignin
•OH
•H
H2O
P1
GUAIACYL TYPE
Eugenol
2-methoxyphenol
2-methoxy-4-methylphenol
4-ethyl-2-methoxyp henol
2-methoxy-4-propylp henol
Vanillin
2-methoxy-4-vinyl phenol
2-methoxy-4-(1-p ropenyl)-phenol
1-(4-hydroxy-3-metho xyphenyl)-ethanone
1-(4-hydroxy-3-methoxy phenyl)-2-propanone
4-(3-hydroxy-1-prope nyl)-2-methoxyphenol
4-hydroxy-3-metho xy-benzeneacetic acid

Figure 52. Mechanism of primary reactions of softwood alkali lignin pyrolysis decomposition proposed by Supriyanto et al. [80].

For lignocellulose quantification the biomass needed to be ground into fine particles in order to enable extraction of the monosaccharides that form cellulose and hemicellulose, but also for lignin qualification. However, in this assay, biomass was exposed just to 100ºC. If these sugars are subjected to higher temperatures, such as those used in pyrolysis, they could be converted into other compounds as has been presented before. Grinding of the material can be a factor to produce more acids in any pyrolysis technology.

6.4 SCHEME OF REACTIONS - KINETIC MODEL LIGNOCELLULOSE DECOMPOSITION

Most of the schemes of reactions in the literature do not consider the amount of ash a biomass could contain, and this increases the complexity when attempting to make a precise projection of how biomass could behave when it is processed through pyrolysis.

After the evaluation of different schemes in Section 4.2.1 the multistep kinetic scheme selected was the one proposed by Ranzi et al. [144] where acids are included and ash is a factor contemplated in the reactions, highlighting that a biomass with higher than 5% wt. of ash content could lead to a catalytic effect. This scheme of reactions, classified in this project as version 4 (V4) is presented in Figure 53.

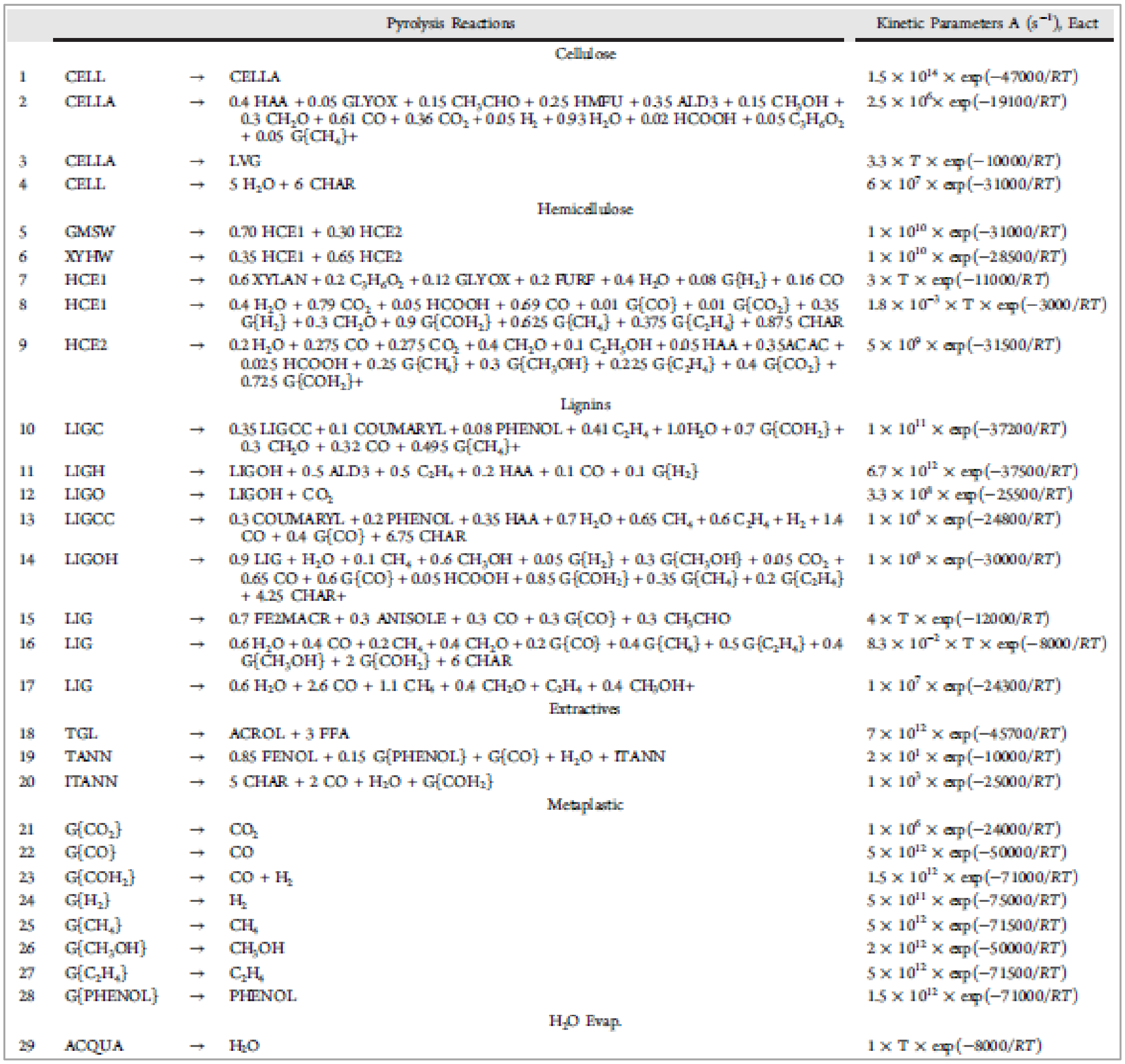

	Pyrolysis Reactions			Kinetic Parameters A (s^{-1}), Eact
			Cellulose	
1	CELL	→	CELLA	$1.5 \times 10^{14} \times \exp(-47000/RT)$
2	CELLA	→	0.4 HAA + 0.05 GLYOX + 0.15 CH_3CHO + 0.25 HMFU + 0.35 ALD3 + 0.15 CH_3OH + 0.3 CH_2O + 0.61 CO + 0.36 CO_2 + 0.05 H_2 + 0.93 H_2O + 0.02 HCOOH + 0.05 $C_3H_6O_2$ + 0.05 G{CH_4}+	$2.5 \times 10^{6} \times \exp(-19100/RT)$
3	CELLA	→	LVG	$3.3 \times T \times \exp(-10000/RT)$
4	CELL	→	5 H_2O + 6 CHAR	$6 \times 10^{7} \times \exp(-31000/RT)$
			Hemicellulose	
5	GMSW	→	0.70 HCE1 + 0.30 HCE2	$1 \times 10^{10} \times \exp(-31000/RT)$
6	XYHW	→	0.35 HCE1 + 0.65 HCE2	$1 \times 10^{10} \times \exp(-28500/RT)$
7	HCE1	→	0.6 XYLAN + 0.2 $C_3H_6O_2$ + 0.12 GLYOX + 0.2 FURF + 0.4 H_2O + 0.08 G{H_2} + 0.16 CO	$3 \times T \times \exp(-11000/RT)$
8	HCE1	→	0.4 H_2O + 0.79 CO_2 + 0.05 HCOOH + 0.69 CO + 0.01 G{CO} + 0.01 G{CO_2} + 0.35 G{H_2} + 0.3 CH_2O + 0.9 G{COH_2} + 0.625 G{CH_4} + 0.375 G{C_2H_4} + 0.875 CHAR	$1.8 \times 10^{-3} \times T \times \exp(-3000/RT)$
9	HCE2	→	0.2 H_2O + 0.275 CO + 0.275 CO_2 + 0.4 CH_2O + 0.1 C_2H_5OH + 0.05 HAA + 0.35ACAC + 0.025 HCOOH + 0.25 G{CH_4} + 0.3 G{CH_3OH} + 0.225 G{C_2H_4} + 0.4 G{CO_2} + 0.725 G{COH_2}+	$5 \times 10^{9} \times \exp(-31500/RT)$
			Lignins	
10	LIGC	→	0.35 LIGCC + 0.1 COUMARYL + 0.08 PHENOL + 0.41 C_2H_4 + 1.0 H_2O + 0.7 G{COH_2} + 0.3 CH_2O + 0.32 CO + 0.495 G{CH_4}+	$1 \times 10^{11} \times \exp(-37200/RT)$
11	LIGH	→	LIGOH + 0.5 ALD3 + 0.5 C_2H_4 + 0.2 HAA + 0.1 CO + 0.1 G{H_2}	$6.7 \times 10^{12} \times \exp(-37500/RT)$
12	LIGO	→	LIGOH + CO_2	$3.3 \times 10^{8} \times \exp(-25500/RT)$
13	LIGCC	→	0.3 COUMARYL + 0.2 PHENOL + 0.35 HAA + 0.7 H_2O + 0.65 CH_4 + 0.6 C_2H_4 + H_2 + 1.4 CO + 0.4 G{CO} + 6.75 CHAR	$1 \times 10^{6} \times \exp(-24800/RT)$
14	LIGOH	→	0.9 LIG + H_2O + 0.1 CH_4 + 0.6 CH_3OH + 0.05 G{H_2} + 0.3 G{CH_3OH} + 0.05 CO_2 + 0.65 CO + 0.6 G{CO} + 0.05 HCOOH + 0.85 G{COH_2} + 0.35 G{CH_4} + 0.2 G{C_2H_4} + 4.25 CHAR+	$1 \times 10^{8} \times \exp(-30000/RT)$
15	LIG	→	0.7 FE2MACR + 0.3 ANISOLE + 0.3 CO + 0.3 G{CO} + 0.3 CH_3CHO	$4 \times T \times \exp(-12000/RT)$
16	LIG	→	0.6 H_2O + 0.4 CO + 0.2 CH_4 + 0.4 CH_2O + 0.2 G{CO} + 0.4 G{CH_4} + 0.5 G{C_2H_4} + 0.4 G{CH_3OH} + 2 G{COH_2} + 6 CHAR	$8.3 \times 10^{-2} \times T \times \exp(-8000/RT)$
17	LIG	→	0.6 H_2O + 2.6 CO + 1.1 CH_4 + 0.4 CH_2O + C_2H_4 + 0.4 CH_3OH+	$1 \times 10^{7} \times \exp(-24300/RT)$
			Extractives	
18	TGL	→	ACROL + 3 FFA	$7 \times 10^{12} \times \exp(-45700/RT)$
19	TANN	→	0.85 FENOL + 0.15 G{PHENOL} + G{CO} + H_2O + ITANN	$2 \times 10^{1} \times \exp(-10000/RT)$
20	ITANN	→	5 CHAR + 2 CO + H_2O + G{COH_2}	$1 \times 10^{3} \times \exp(-25000/RT)$
			Metaplastic	
21	G{CO_2}	→	CO_2	$1 \times 10^{6} \times \exp(-24000/RT)$
22	G{CO}	→	CO	$5 \times 10^{12} \times \exp(-50000/RT)$
23	G{COH_2}	→	CO + H_2	$1.5 \times 10^{12} \times \exp(-71000/RT)$
24	G{H_2}	→	H_2	$5 \times 10^{11} \times \exp(-75000/RT)$
25	G{CH_4}	→	CH_4	$5 \times 10^{12} \times \exp(-71500/RT)$
26	G{CH_3OH}	→	CH_3OH	$2 \times 10^{12} \times \exp(-50000/RT)$
27	G{C_2H_4}	→	C_2H_4	$5 \times 10^{12} \times \exp(-71500/RT)$
28	G{PHENOL}	→	PHENOL	$1.5 \times 10^{12} \times \exp(-71000/RT)$
			H_2O Evap.	
29	ACQUA	→	H_2O	$1 \times T \times \exp(-8000/RT)$

Figure 53. Scheme of reactions selected to model pyrolysis of digestate. The scheme is presented as published by Ranzi et al. [144].

All the components of the scheme mentioned in Section 4.2.1 were broken down into elemental distribution of carbon (C), hydrogen (H) and oxygen (O) in order to have an elemental balance of lignocellulosic material and products. Some reactions were completed in the last scheme proposed by Ranzi et al. [144] due a non-stoichiometric balance in the published article. A few adjustments were made to have this stoichiometrically balanced, and these are demonstrated in Table 51.

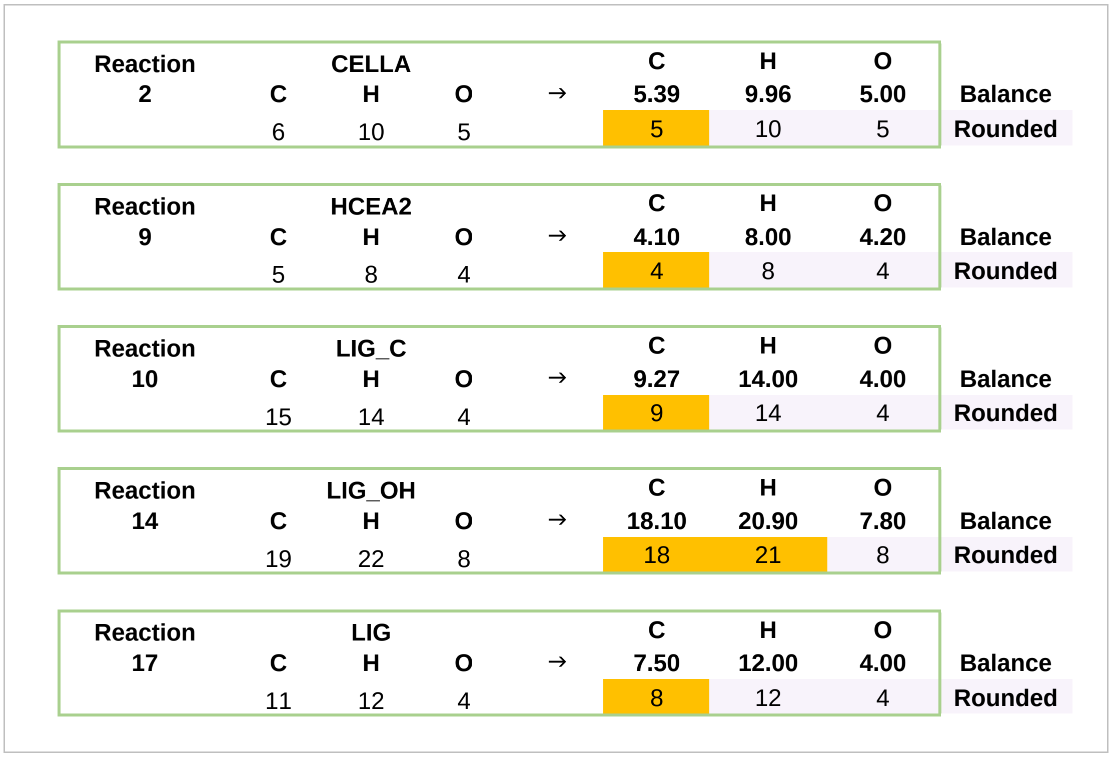

Reaction		CELLA			C	H	O	
2	C	H	O	→	5.39	9.96	5.00	Balance
	6	10	5		5	10	5	Rounded

Reaction		HCEA2			C	H	O	
9	C	H	O	→	4.10	8.00	4.20	Balance
	5	8	4		4	8	4	Rounded

Reaction		LIG_C			C	H	O	
10	C	H	O	→	9.27	14.00	4.00	Balance
	15	14	4		9	14	4	Rounded

Reaction		LIG_OH			C	H	O	
14	C	H	O	→	18.10	20.90	7.80	Balance
	19	22	8		18	21	8	Rounded

Reaction		LIG			C	H	O	
17	C	H	O	→	7.50	12.00	4.00	Balance
	11	12	4		8	12	4	Rounded

Table 51. Reactions in scheme of Ranzi et al. [144] non-stoichiometric balanced as they are presented they are presented in the original publication.

Additionally, not all the reactions presented in Ranzi et al. [144] were considered due to the type of biomass which has been used for this project. Some of these reactions, such as 5 and 6 are specifically for hardwood (XYHW) and softwood (GMSW) respectively, and the digestate used was not a woody material. However, in other schemes, also suggested from the original scheme by Ranzi et al. [96] hemicellulose (HCE), is presented as a reaction to be converted into active hemicellulose (HCEA). This approach is shown in the scheme proposed by Calonaci et al. [97] and has been used for the propose of this project to compare in general how hemicellulose is thermally decomposed. The final scheme of reactions balanced is shown in Table 52, and it would be named V4b (version 4 balanced).

	Reaction			A (s^{-1})	E (kJ/mol)
Decomposition of cellulose					
1	CELL	→	CELLA	$1.5x10^{14}$	196.658
2	CELLA	→	0.4 HAA + 0.05 GLYOX + 0.15 CH_3CHO + 0.25 HMFU + 0.35 C_3H_6O + 0.15 CH_3OH + 0.3 CH_2O + 0.61 CO + 0.36 CO_2 + 0.05 H_2 + 0.93 H_2O + 0.02 HCOOH + 0.05 $C_3H_6O_2$ + 0.05 G{CH_4} + 0.61 Char	$2.5x10^{6}$	79.914
3	CELLA	→	LVG	3.3T	41.84
4	CELL	→	5 H_2O + 6 Char	$6x10^{7}$	129.704
Decomposition of hemicellulose					
5	HCE	→	0.4 HCEA1 + 0.6 HCEA2	$1x10^{10}$	129.704
7	HCEA1	→	0.6 XYL + 0.2 $C_3H_6O_2$ + 0.12 GLYOX + 0.2 FURF + 0.4 H_2O + 0.08 G{H_2} + 0.16 CO	3T	46.024
8	HCEA1	→	0.4 H_2O + 0.79 CO_2 + 0.05 HCOOH + 0.69 CO + 0.01 G{CO} + 0.01 G{CO_2} + 0.35 G{H_2} + 0.3 CH_2O + 0.9 G{COH_2} + 0.625 G{CH_4} + 0.375 G{C_2H_4} + 0.875 Char	$1.8x10^{-3}T$	12.552
9	HCEA2	→	0.2 H_2O + 0.275 CO + 0.275 CO_2 + 0.4 CH_2O + 0.1 ETOH + 0.05 HAA + 0.35 CH_3COOH + 0.025 HCOOH + 0.25 G{CH_4} + 0.3 G{CH_3OH} + 0.225 G{C_2H_4} + 0.4 G{CO_2} + 0.725 G{COH_2} + 0.9 Char	$5x10^{9}$	131.796
Decomposition of lignins					
10	LIG-C	→	0.35 LIG-CC + 0.1 pCOUMARYL + 0.08 PHENOL + 0.41 C_2H_4 + H_2O + 0.7 G{COH_2} + 0.3 CH_2O + 0.32 CO + 0.495 G{CH_4} } + 0.9 Char	$1x10^{11}$	155.645
11	LIG-H	→	LIG-OH + 0.5 C_3H_6O + 0.5 C_2H_4 + 0.2 HAA + 0.1 CO + 0.1 G{H_2}	$6.7x10^{12}$	156.9
12	LIG-O	→	LIG-OH + CO_2	$3.3x10^{8}$	106.692
13	LIG-CC	→	0.3 pCOUMARYL + 0.2 PHENOL + 0.35 HAA + 0.7 H_2O + 0.65 CH_4 + 0.6 C_2H_4 + H_2 + 1.4 CO + 0.4 G{CO} + 6.75 Char	$1x10^{4}$	103.763
14	LIG-OH	→	0.9 LIG + H_2O + 0.1 CH_4 + 0.6 CH_3OH + 0.05 G{H_2} + 0.3 G{CH_3OH} + 0.05 CO_2 + 0.65 CO + 0.6 G{CO} + 0.05 HCOOH + 0.85 G{COH_2} + 0.35 G{CH_4} + 0.2 G{C_2H_4} + 0.37 C_2H_4 + 4.25 Char	1×10^{8}	125.52
15	LIG	→	0.7 FE2MACR + 0.3 ANISOLE + 0.3 CO + 0.3 G{CO} + 0.3 CH_3CHO	4T	50.208
16	LIG	→	0.6 H_2O + 0.4 CO + 0.2 CH_4 + 0.4 CH_2O + 0.2 G{CO} + 0.4 G{CH_4} + 0.5 G{C_2H_4} + 0.4 G{CH_3OH} + 2 G{COH_2} + 6 Char	$8.3x10^{-2}$ T	33.472
17	LIG	→	0.6 H_2O + 2.6 CO + 1.1 CH_4 + 0.4 CH_2O + C_2H_4 + 0.4 CH_3OH + 3.5 Char	$1x10^{7}$	101.671
Intermediate products of the lignocellulosic decomposition					
21	G{CO_2}	→	CO_2	$1x10^{6}$	100.416
22	G{CO}	→	CO	$5x10^{12}$	209.2
23	G{COH_2}	→	CO + H_2	$1.5x10^{12}$	297.064
24	G{H_2}	→	H_2	$5x10^{11}$	313.8
25	G{CH_4}	→	CH_4	$5x10^{12}$	299.156
26	G{CH_3OH}	→	CH_3OH	$2x10^{12}$	209.2
27	G{C_2H_4}	→	C_2H_4	$5x10^{12}$	299.156

A is a constant, which is independent on temperature.

E is the activation energy

Table 52. Scheme of reactions proposed for the kinetic model V4b. This is a modification of the scheme presented by Ranzi et al. [144]. The format is shown according to the number of reactions presented in Ranzi et al.'s publication.

CHAPTER 7. MODELLING PROJECTIONS - PYROLYSIS OF DIGESTATE

Ranzi et al.'s scheme of reactions was developed for fast pyrolysis of biomass. These reactions consider pseudo-lignins: rich in carbon, hydrogen, and oxygen; and require calculation according to amount of the lignocellulosic material in biomass. This method is described in Section 4.1.1.

The main inputs for these models are the proportion of lignocellulosic material, ash and moisture in the biomass. Initial data employed for the next projections are shown in Table 53.

Feedstock	Digestate
Cellulose	33.63
Hemicellulose	22.51
Lignin	30.71
Lignin C	*6.14*
Lignin H	*13.15*
Lignin O	*11.42*
Moisture	4.99
Ash	8.16

Table 53. Equivalent composition of lignin and pseudo-lignins in digestate as input for modelling lignocellulose thermal decomposition in fast pyrolysis at different temperature. Data is presented is the average of the 3 batches used in VTT's system.

Ash content as input was considered the minimum average quantified in in the three digestate batches collected, which is around 8%. This and lignocellulose composition was used to predict product yield and composition at the same temperatures that digestate was treated during experiments: 460ºC, 480ºC, 520ºC and 560ºC. The outcomes of modelling the pyrolysis of digestate versus pyrolysis products analysis from experimental work are shown in Table 54 and Table 55.

Products	Composition							
	460^{o}C		480^{o}C		520^{o}C		560^{o}C	
	Exp. 1	Projection V4b	Exp. 2	Projection V4b	Exp. 3	Projection V4b	Exp. 4	Projection V4b
Total biochar	**34.22**	**25.00**	**34.65**	**24.22**	**31.77**	**24.14**	**30.45**	**24.05**
Total gas	**18.49**	**17.69**	**17.84**	**19.85**	**20.92**	**20.69**	**21.37**	**21.28**
Hydrogen (H2)	0.016	0.02	0.022	0.03	0.076	0.03	0.116	0.04
Carbon monoxide (CO)	4.18	7.86	4.42	9.47	5.18	9.97	5.75	10.31
Carbon dioxide (CO2)	13.57	7.29	11.83	7.23	12.90	7.28	12.92	7.31
Methane (CH4)	0.43	0.54	0.89	0.72	1.21	0.83	1.20	0.91
Ethylene (C2H4)	0.07	1.97	0.08	2.40	0.16	2.58	0.23	2.72
Ethane (C2H6)	0.13		0.15		0.25		0.30	
Acetylene (C2H2)	0.00		0.01		0.01		0.01	
C3-7	0.08		0.43		1.15		0.85	
Total liquid	**36.02**	**49.19**	**43.50**	**50.63**	**39.48**	**50.09**	**40.14**	**49.44**
Water vapor (H2O)	**8.22**	**5.89**	**6.52**	**6.03**	**9.81**	**6.04**	**10.67**	**6.07**
Total organics	**27.80**	**43.31**	**36.98**	**44.61**	**29.67**	**44.05**	**29.47**	**43.37**
Total aldehydes and ketones	**4.03**	**14.99**	**4.25**	**15.18**	**3.76**	**15.69**	**4.41**	**16.03**
Formaldehyde	0	3.40	0	3.41	0	3.49	0	3.55
Acetaldehyde	0	1.33	0	1.33	0	1.34	0	1.33
Propanal	0	4.13	0	4.21	0	4.37	0	4.48
Hydroxyacetaldehyde*	0	4.52	0	4.65	0	4.88	0	5.03
Glyoxal	0	0.86	0	0.85	0	0.88	0	0.91
Acetol (C3H6O2)	0	0.76	1.17	0.73	0	0.73	0	0.73
Others	4.03		3.08		3.76		4.41	

* Standard utilised to identified and quantified markers in bio-oil as reference.
Experimental data (Exp)

Table 54. Comparison of experimental outputs from fast pyrolysis of digestate performed in VTT with model projections V4b where ash content is included.

Products	Composition							
	460ºC		480ºC		520ºC		560ºC	
	Exp. 1	Projection V4b	Exp. 2	Projection V4b	Exp. 3	Projection V4b	Exp. 4	Projection V4b
Total alcohols	**0.17**	**2.99**	**0.68**	**4.47**	**0.44**	**4.55**	**0.43**	**4.62**
Methanol	0	2.52	0	4.02	0	4.10	0	4.17
Ethanol	0	0.47	0	0.45	0	0.45	00	0.45
Others	0.17		0.68		0.44		0.43	
Total furans	**3.46**	**6.13**	**2.54**	**6.07**	**3.41**	**6.35**	**6.31**	**6.56**
5-Hydroxymethyl-furfural *	0	5.04	0	5.00	0	5.24	0	5.42
Furfural (C5H4O2)*	0	1.09	0	1.07	0	1.11	0	1.14
Others	3.46		2.54		3.41		6.31	
Total sugars	**1.28**	**11.10**	**3.30**	**10.24**	**2.12**	**9.50**	**1.86**	**8.89**
Levoglucosan*	0.54	6.62	1.80	5.84	1.01	4.93	0.84	4.20
Xylose monomer	0.34	4.48	0.72	4.40	0.38	4.57	0.36	4.69
Other	0.40		0.78		0.73		0.66	
Total phenolic	**19.00**	**5.52**	**8.08**	**6.16**	**14.18**	**5.48**	**17.62**	**4.78**
Paracoumaryl alcohol	0	0.37	**0**	0.70	0	0.80	0	0.82
Phenol	1.68	0.19	0.55	0.32	2.13	0.37	4.03	0.38
Sinapaldehyde*	0	4.30	0	4.45	0	3.73	0	3.10
Anisol (C7H8O)	0	0.67	0	0.69	0	0.58	0	0.48
Others	17.32		7.53		12.05		13.59	
Total acids	**6.20**	**2.57**	**23.50**	**2.49**	**13.50**	**2.49**	**6.60**	**2.49**
Formic Acid (HCOOH)	0	0.42	**0**	0.43	0	0.43	0	0.43
Acetic Acid (CH3COOH)*	5.70	2.15	22.79	2.06	12.96	2.06	6.07	2.06
Others	0.50		0.71		0.54		0.53	

* Standard utilised to identified and quantified markers in bio-oil as reference.
Experimental data (Exp)

Table 55. Comparison of experimental outputs from fast pyrolysis of digestate performed in VTT with model projections V4b where ash content is included (cont.).

These projections are based on accumulation of the product after a certain time. It is important to emphasise that it is only the proportion of lignocellulosic material content in the biomass converted into just 32 compounds in total, when a real conversion of biomass through pyrolysis the number of analytes could reach 300.

Specific compounds considered in this scheme of reactions do not match with fast pyrolysis products that result from experimental work, especially compounds in the bio-oil. Paracoumaryl alcohol and sinapaldehyde, for instance, were not identified despite a standard being employed to identify the second one. The distribution of compounds in each pyrolysis product varies between experimental figures and model outputs. Phenolics, for instance, were produced in large amounts while the model's yield result is just under 10% wt. However, total yields of bio-oil and gas are close to experimental data at temperatures higher than 460ºC. Biochar yield is very low compared with data obtained from the fast pyrolysis system.

Illustrative representation of experimental data and model projections are in Figure 54. Projections were performed using actual composition of digestate, and experimental data is from the analysis of pyrolysis of digestate.

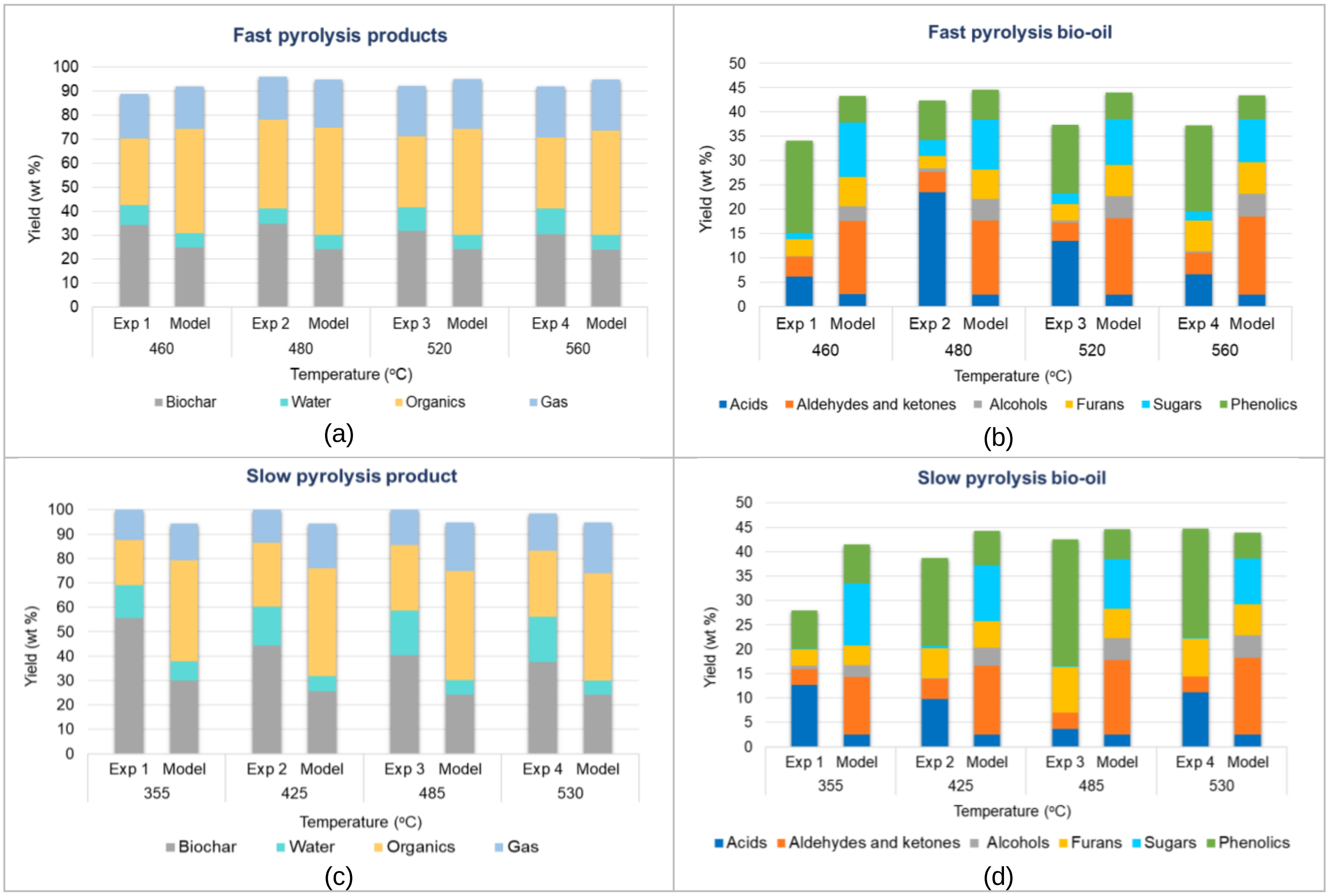

Figure 54. Comparison of slow and fast pyrolysis of digestate experimental results versus model projections at different temperatures: (a) Yields of fast pyrolysis products at 460ºC, 480ºC, 520ºC and 560ºC. (b) Yields of chemical groups in fast pyrolysis bio-oil, (c) Yields of slow pyrolysis products at different temperatures 355ºC, 425ºC, 485ºC and 530ºC. (d) Yields of chemical groups in slow pyrolysis bio-oil.

Projections using the model developed in this work consists of only two parameters with direct impact on lignocellulose thermal decomposition: temperature and ash content. Modelling outputs are presented without considering the water content in biomass in the final amount of water.

This water is one of the main sources of difference between experimental data and model results for total pyrolysis products. However, there is a large discrepancy in bio-oil composition between experimental data and the projections.

This model adjusted (V4b) from Ranzi et al. [144], was computed to simulate isothermal behaviour, which differs from the experimental cases where the output products are cumulative from the heat-up phase and the target temperature. Additionally, the scheme of reactions just considers some of the compounds in bio-oil out of more than 100 possible found [64,70,71,73,85]. As a result of the low number of individual compounds in bio-oil composition, the outcomes from the model projections are focussed on just the total of chemical groups in the bio-oil, total char and total gas formed from pyrolysis of lignocellulosic material.

7.1 KINETIC MODEL ADJUSTED FOR HEATING RATES

The model has been improved by adding variability in heating rates, which has been termed as V-heat, with the possibility of projecting how lignocellulosic biomass decomposition could change in the presence of ash. Some initial validation with low-ash biomass, such as pine, has been employed to verify these variations in pyrolysis product formation. Composition of the pine used as initial output is presented in Table 56, which includes a case where pine would be ash-free biomass.

Feedstock	Pine	Pine (ash-free)
Cellulose	41.71	41.86
Hemicellulose	25.95	26.05
Lignin	25.02	25.12
Lignin C	*6.49*	*6.51*
Lignin H	*9.27*	*9.30*
Lignin O	*9.27*	*9.30*
Moisture	6.95	6.98
Ash	0.37	0

Table 56. Pine composition employed for pyrolysis model at different heating rates. Lignocellulose composition from Wang et al. [152]. Data presented in wt. %.

Projections were run from 100ºC to 600ºC at different heating rates - 5ºC/s, 10ºC/s and 20ºC/s. Below 100ºC the results represent water evaporation. Pyrolysis product formation from pine decomposition at different heating rates is shown in Figure 55, for both pine composition types.

Note: Any label presented on the profiles and plots as '(ash)' is a reference to imply these results are from using biomass with ash content.

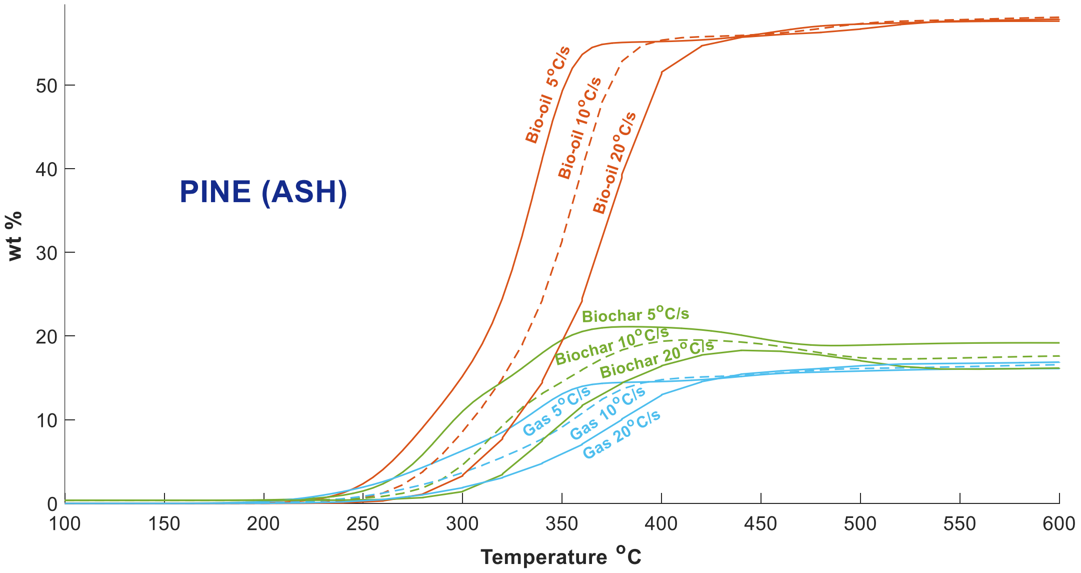

Figure 55. Model projections (V-heat) of pyrolysis products from pine with ash content at different rates of temperatures.

Yield of final products seems to be equal at these rates for bio-oil and gas, where final values are 58% wt. and 16.5% respectively. There is a slight difference in biochar production, where at 5ºC/s biochar reached approximately 19% weight mass, and at 20ºC/s around 16%. According to these projections with different rates, there would be greater variation between yields of pyrolysis products when temperature is less than 450ºC.The lower the rate, the higher the yield.

In order to verify whether there could be any variation in how ash affects pyrolysis product formation, some projections at 5ºC/s and 10ºC/s, with ash and ash-free composition, were carried out. These results are shown in Figure 56.

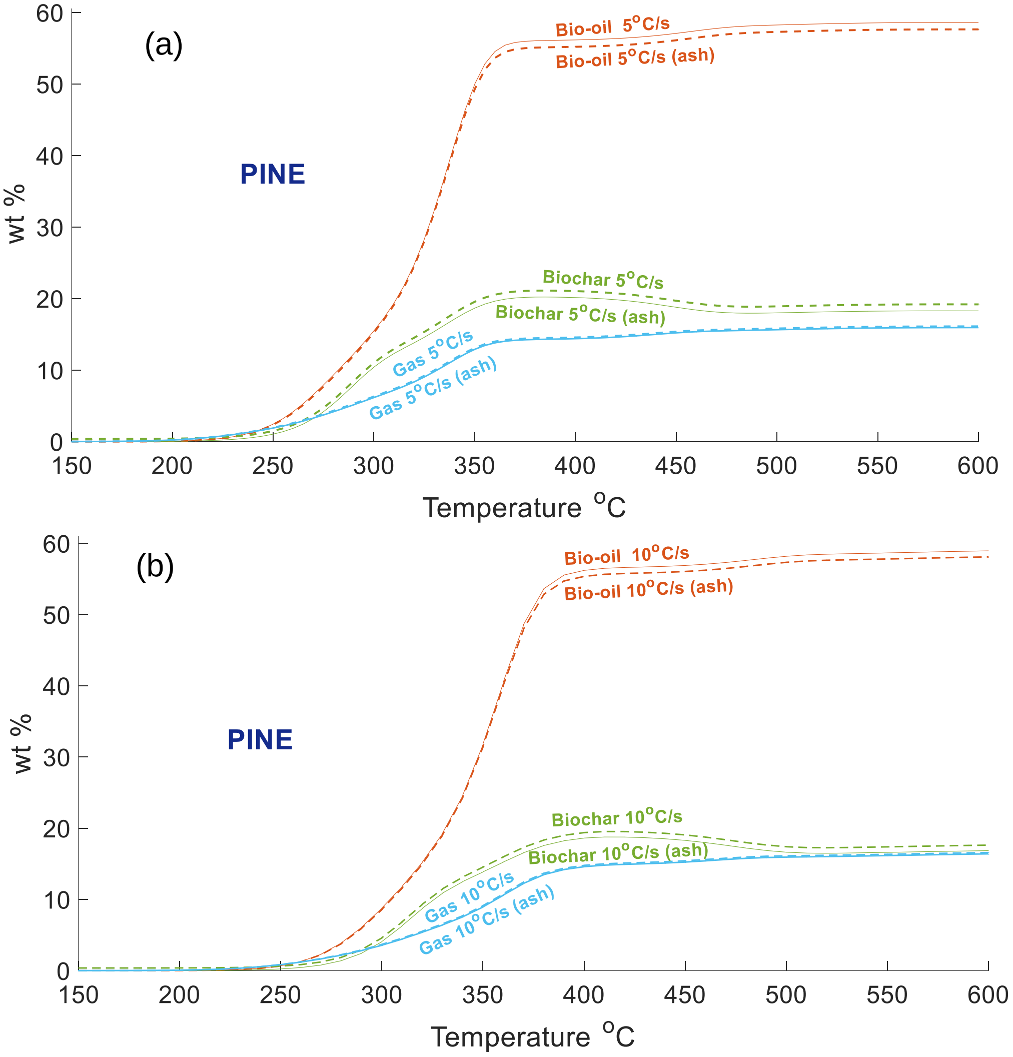

Figure 56. Pyrolysis product formation from pine with ash and ash-free at different heating rates: (a) 5ºC/s and (b) 10ºC/s.

Due to lack of decomposition before 150ºC, plots were adjusted from this temperature to 600ºC. Additionally, with V-heat it was possible to analyse the biochar profile in more detail. This reached the highest amount at around 380ºC and 410ºC with 5ºC/s and 10ºC/s respectively, followed by a decrease right after these temperatures. This is the stage where trapped intermediate products such as G{CH_4}, G{CO_2}, G{CO} and G{H_2} went from solid to gas phase (described in Section 2.6). There was a slight increase in gas production at the temperature corresponding to the phase change of these intermediate compounds.

These profiles shown no difference pyrolysis product generation in the presence of this amount of ash. However, there are some variations with heating rate. The same conditions were employed for bio-oil compound formation, and there are changes between different heating rates. These outlines of chemical groups in bio-oil are shown in Figure 57.

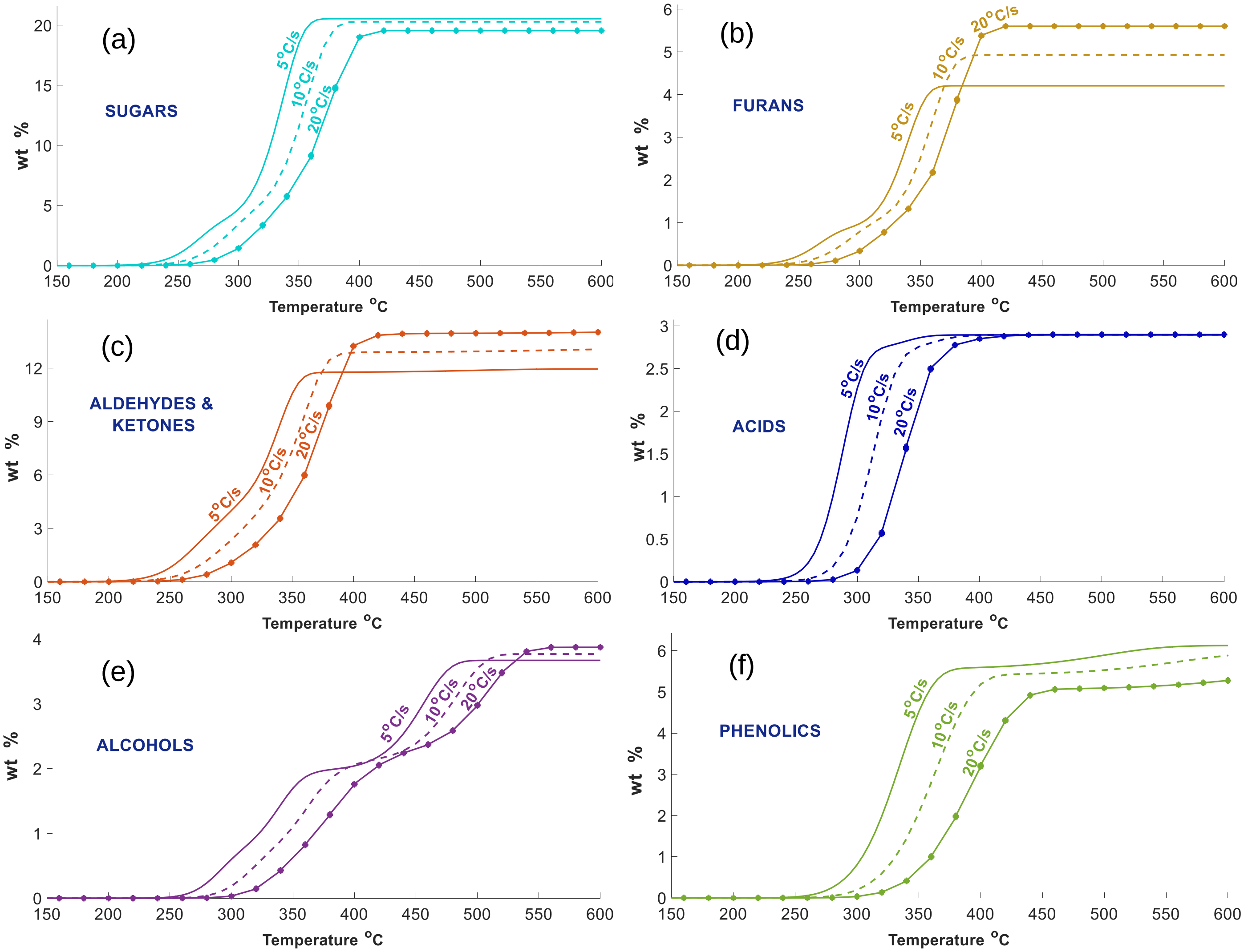

Figure 57. V-heat projections of bio-oil compounds formation from pyrolysis of pine at different heating rates 5ºC/s, 10ºC/s and 20ºC/s: (a) sugars. (b) furans, (c) aldehydes & ketones, (d) acids and (e) alcohols and (f) phenolics.

Some groups such as acids end with the same yield at the final temperature, in this case 350°C. However, furans, aldehydes & ketones have greater final yield at higher heating rates. In contrast with sugars and phenolics which are produced in larger amounts when heating rates are lower. Final yields based on these model projections are shown in Table 57.

Compounds	5ºC/s	10ºC/s	20ºC/s
Sugars	20.55	20.30	19.56
Furans	4.21	4.93	5.60
Aldehydes and ketones	11.95	13.06	14.02
Acids	2.89	2.90	2.90
Alcohols	3.67	3.77	3.87
Phenolics	6.13	5.89	5.28

Table 57. Final composition projections of bio-oil at 600ºC at different heating rates.

Due to pine having a low ash content it was used as a feedstock for these preliminary projections with the kinetic model. This type of biomass has been one of the most commonly used for pyrolysis processing. Results from this modelling show only a slight difference between bio-oil composition at different rate. The most noticeable difference is for aldehyde and ketone generation, which goes from 11.95% to 14.02% wt as heating rate increases. Although the model considers ash content, the amount this biomass has is almost neglected by the model and has no effect on the final yield of pyrolysis products.

The next projections employing this kinetic model are with digestate and pre-AD crop to identify how the formation of bio-oil, biochar and gas is affected by higher levels of ash, and then to compare this estimation with the experimental data obtained from experimental data from pyrolysing digestate.

7.1.1 PYROLYSIS OF DIGESTATE AT DIFFERENT RATES

Although pre-AD crop contains less ash than digestate, this amount is still higher than common wood used in pyrolysis. Lignocellulose compositions used as inputs for the kinetic model are shown in Table 58.

Feedstock Composition	Digestate	Digestate (ash-free)	Pre-AD crop
Cellulose	33.63	36.23	23.32
Hemicellulose	22.51	24.25	50.87
Lignin	30.71	33.1	20.13
Lignin C	*6.14*	*6.62*	*4.03*
Lignin H	*13.15*	*12.31*	*6.86*
Lignin O	*11.42*	*14.17*	*9.24*
Moisture	4.99	6.26	2.29
Ash	8.16	0	3.39

Table 58. Digestate and pre-AD lignocellulose composition employed for pyrolysis model at different heating rates. Data presented in wt. %.

The first projections were run at 5ºC/s, 10ºC/s, 20ºC/s and 40ºC/s for digestate with the original ash content and also assuming hypothetically that the digestate was ash-free. In pyrolysis processes the ash ends up within the biochar product, and consequently in this projection the biochar yield starts with the amount of ash contained in the biomass, which is around 8% for digestate. Figure 58 illustrates two examples of pyrolysis product formation from digestate with ash and ash-free at the same heating rate.

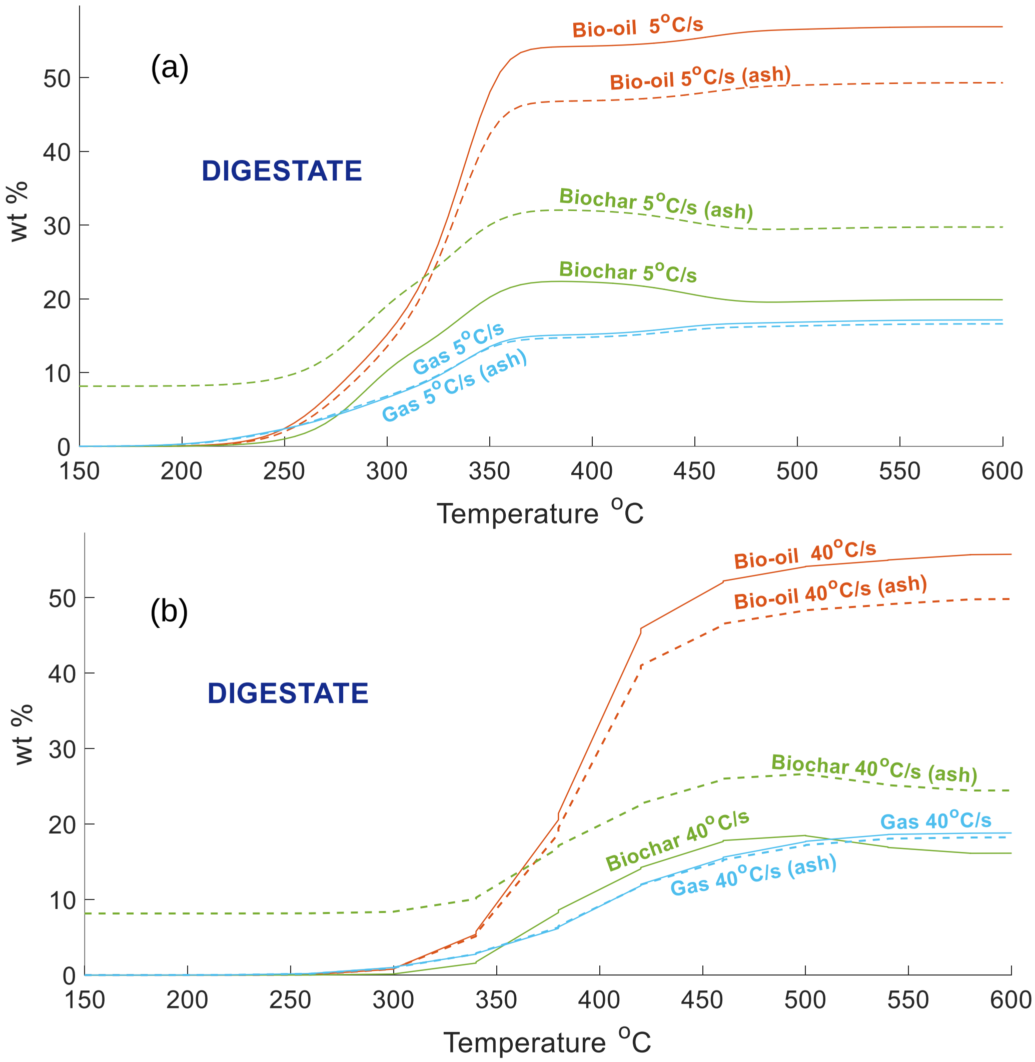

Figure 58. V-heat pyrolysis product projection from digestate with ash and ash-free at different heating rates: (a) 5ºC/s and (b) 40ºC/s.

Digestate decomposition at 5ºC/s shows a steady product formation after 350ºC, and a large difference in bio-oil yield between biomass with ash and ash-free biomass. In contrast, with 40ºC/s, pyrolysis products reach almost the highest production around 450ºC, but with different final yields between the two types of digestate. Gas generation has no difference in distribution from both feedstocks; these patterns, with ash and ash-free digestate, are very similar through the thermal processing. However, there is a higher final yield of this product when the projection is conducted at 40ºC/s. Biochar has a similar behaviour, yet there is a greater gap between each profile in both heating rates, mainly due to ash content. Final yields of these simulations are presented in Table 59.

Product	5ºC/s		40ºC/s	
	Ash	Ash-free	Ash	Ash-free
Biochar	29.74	19.89	24.47	16.16
Bio-oil	49.31	56.91	49.86	55.78
Organics	*39.62*	*49.51*	*43.33*	*49.79*
Water	*9.69*	*7.40*	*6.53*	*6.00*
Gas	16.61	17.15	18.28	18.85

Table 59. Final yields (wt %) of pyrolysis products from digestate at different heating rates from 150ºC to 600ºC

Bio-oil is produced in lower amount in the presence of ash at both heating rates, but with a higher level of water generated at 5ºC/s. Biochar production is higher due to ash content in both cases: at 40ºC/s the difference is just because of the amount of ash in the digestate, 8.31% wt, while at 5ºC/s there is higher biochar production mainly because of the low heating rate. Final yield of gas is very similar between both biomasses, and between these conditions. Comparing this with experimental data the water produced is between 13-19% in slow pyrolysis, and 8-10% wt in fast pyrolysis. In these simulations, on the other hand, the maximum amount of water produced is less than 10% wt.

Profiles of the thermochemical decomposition of this digestate and of pyrolysis product generation have been projected with this model at four different heating rates to identify if these projections agree with experimental data obtained. These are represented as shown in Figure 59.

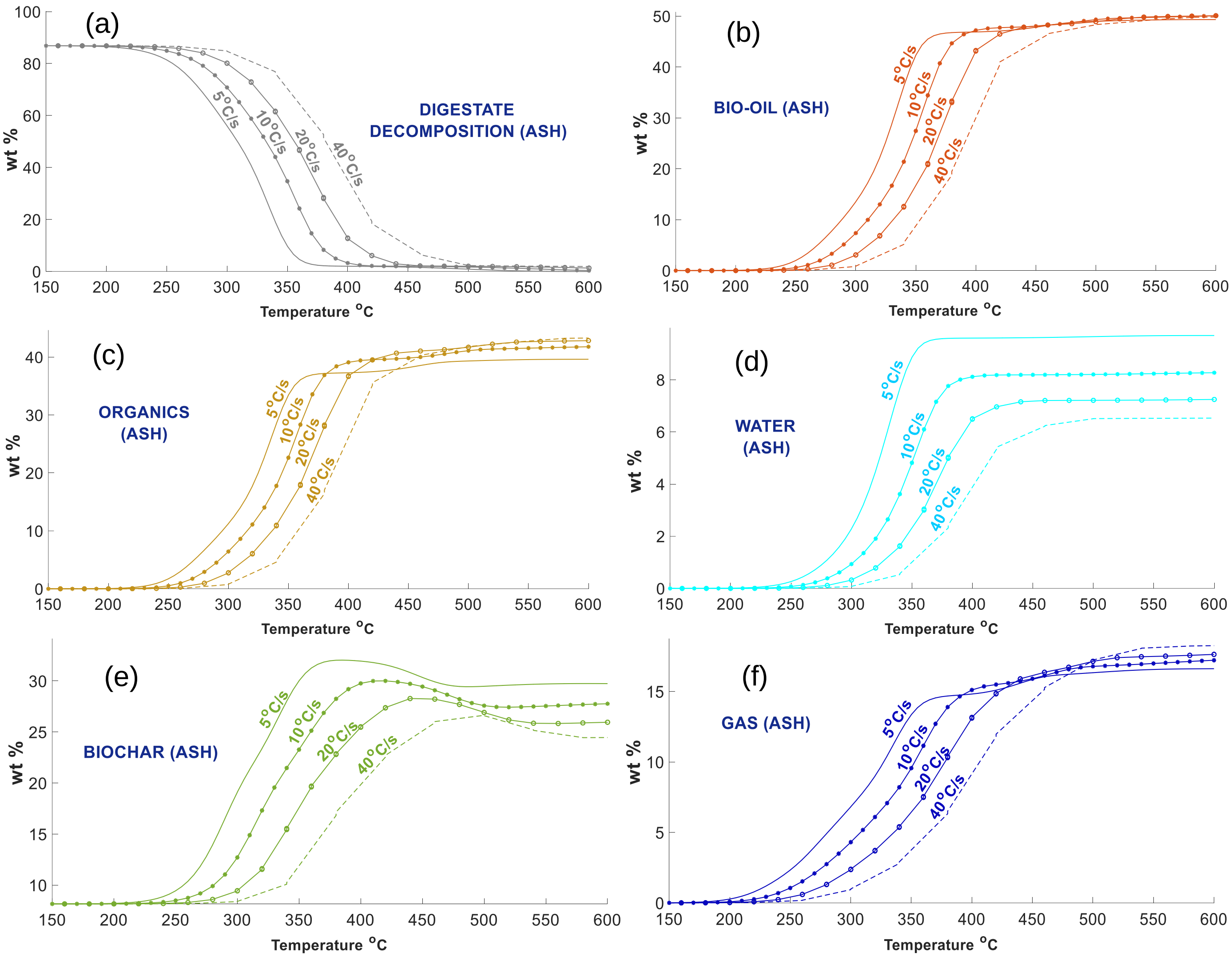

Figure 59. V-heat projections of pyrolysis of digestate at 5ºC/s, 10ºC/s, 20ºC/s and 40ºC/s: (a) biomass decomposition. (b) bio-oil, (c) organics, (d) water, (e) biochar, and (f) gas.

Biochar yield from digestate reached the highest amount at around 385ºC, 420ºC, 440ºC and 500ºC with 5ºC/s, 10ºC/s, 20ºC/s and 40ºC/s respectively. This product and bio-oil generation is not only affected by ash content, but by heating rate changes. Water and biochar are produced in larger amount at 5ºC/s, opposite to the behaviour of organics and gas production which have higher yields at 40ºC/s. Gas has a steady production with close values for final yields, approximately 16-18% wt. The main variation in yields for any pyrolysis product presented would be at temperatures under 400ºC. A number of specific compounds in bio-oil were selected in order to model their profiles through pyrolysis processing and to illustrate how ash content and heating rate variation influence in their formation. These outlines are shown in Figure 60 for digestate and ash-free material for comparison.

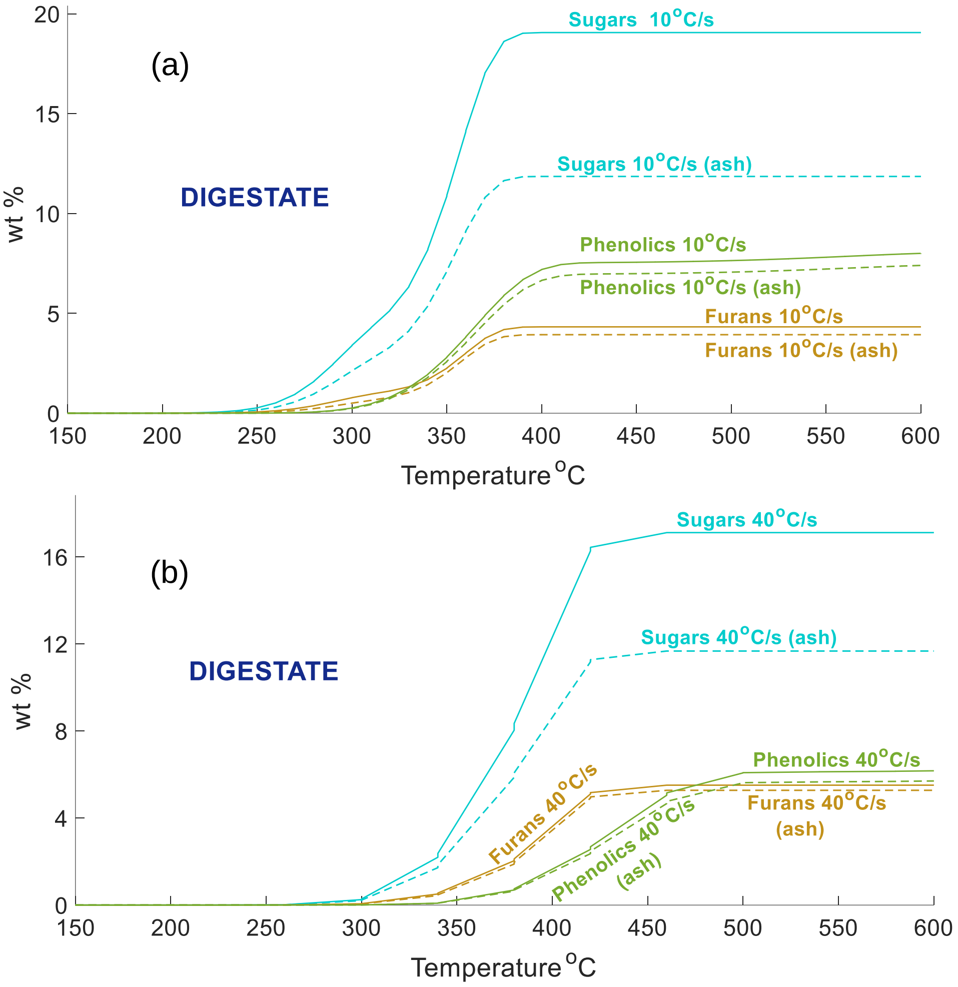

Figure 60. Sugars, furans and phenolic formation in bio-oil pyrolysis from digestate at different heating rates for ash and ash-free composition: (a) 10ºC/s and (b) 40ºC/s.

Both factors, ash content and heating rates, have a considerable impact on bio-oil production and composition. These profiles show that formation of sugars is the most affected due to these conditions, resulting in a difference higher than 6% wt. between each type of biomass. The summary of the total yields of these compounds in these projections is show in Table 60.

Compounds	10ºC/s		40ºC/s	
	Ash	Ash-free	Ash	Ash-free
Sugars	11.85	19.06	11.67	17.11
Furans	3.93	4.32	5.27	5.51
Aldehydes and ketones	12.08	12.11	13.91	13.79
Acids	2.58	2.75	2.58	2.75
Alcohols	3.93	4.21	4.16	4.44
Phenolics	7.40	8.00	5.73	6.19

Table 60. Final composition projections of compounds in bio-oil pyrolysis from digestate, ash and ash-free, at 600ºC with 10ºC/s and 40ºC/s heating rates.

Phenolics are mainly impacted by heating rate changes rather than ash content. Sugar content shows a reduction of 30% and 40% at 10ºC/s and 40ºC/s respectively due to the high ash content. However, according to the experimental data sugar concentration is less than 1% in slow pyrolysis, and between 2-3% wt in fast pyrolysis of the total products. This suggests that in this case, with higher concentrations of ash the effect should be greater than just a 40% of sugars reduction.

Clear representation of effect of heating rate on each bio-oil chemical group formation from digestate is shown in Figure 61.

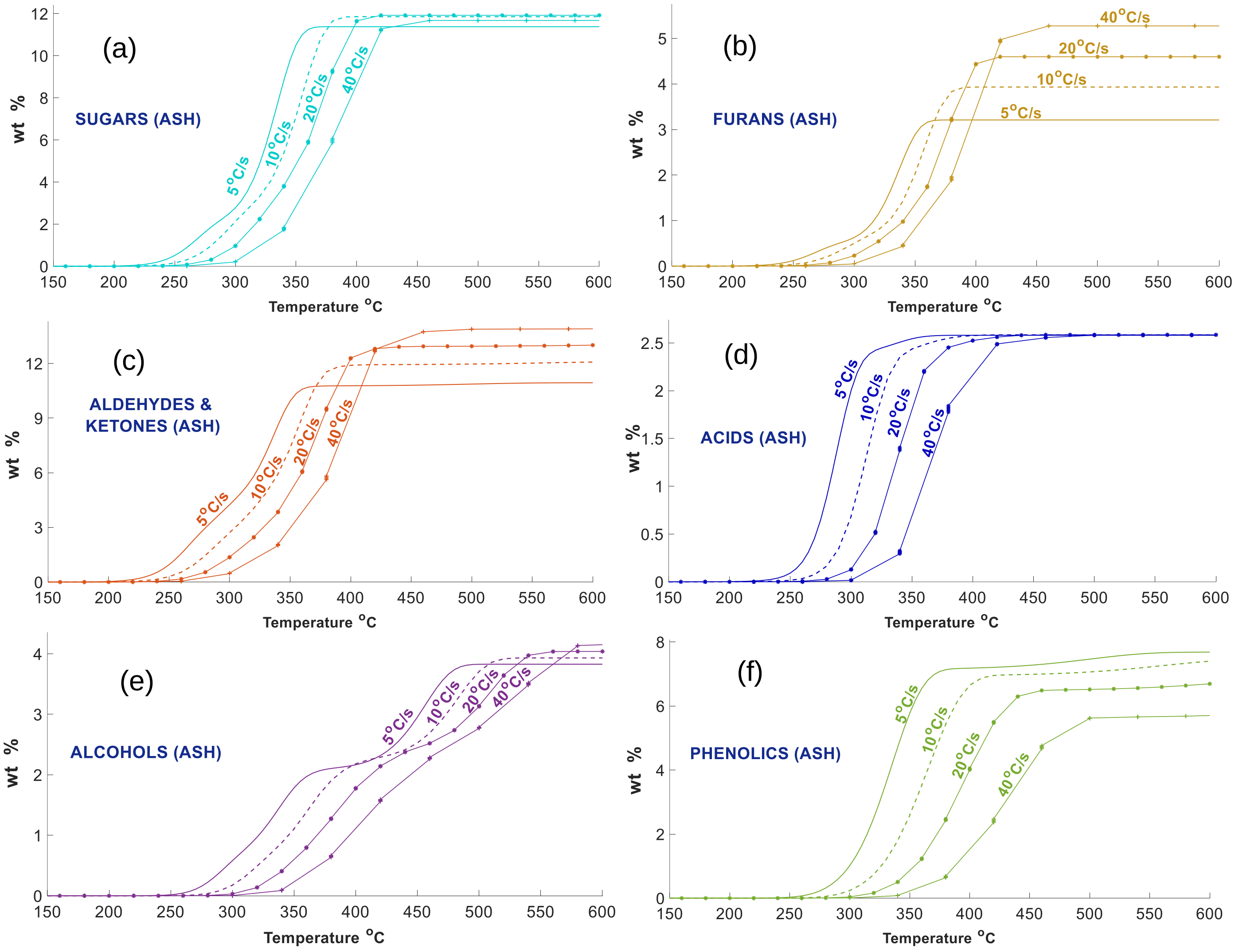

Figure 61. V-heat projections of bio-oil compounds formation from pyrolysis of digestate at different heating rates 5ºC/s, 10ºC/s, 20ºC/s and 40ºC/s: (a) sugars. (b) furans, (c) aldehydes & ketones, (d) acids and (e) alcohols and (f) phenolics.

Acids, alcohols, and sugars do not show a difference in final yields, although their production could change if the process is run under 400ºC-450ºC. Aldehydes and ketones (A&K), phenolics and furan yields are affected by heating rate variations. Less furans and A&K are produced at low heating rates, which is opposite to phenolic, which are in greater proportion at low heating rates. The final cumulative yields of these bio-oil components with these simulations are shown in Table 61.

Compound	5ºC/s	10ºC/s	20ºC/s	40ºC/s
Sugars	11.38	11.85	11.92	11.67
Furans	3.21	3.93	4.60	5.27
Aldehydes and ketones	10.94	12.08	13.01	13.91
Acids	2.58	2.58	2.58	2.58
Alcohols	3.83	3.93	4.04	4.16
Phenolics	7.68	7.40	6.69	5.73

Table 61. Final yields (wt %) of compounds in pyrolysis bio-oil from digestate at different heating rates from 150ºC to 600ºC.

Most of these groups remain within similar range of yields despite changes in heating rate. It was expected that there would be more acid production due to secondary reactions, and less sugars produced. Experimental results from slow and fast pyrolysis of digestate, for instance, indicated that phenolics were produced at around 10% wt at the lowest temperature (350ºC), and around 18% wt at 425°C, whereas projections from the kinetic model show than the highest production of phenolic compounds is about 8%. This suggests that lignin decomposition is not inclined to phenolic formation as temperature rises, and that other reactions may be competing to produce more aldehydes and ketones.

If the model is employed to simulate pyrolysis with longer resident time of the biomass, once the target temperature is reached digestate is decomposed for a prolonged period of time, longer than the fast pyrolysis system requires to process the biomass. This can be graphically represented in Figure 62, which consists of a projection performed at 360ºC.

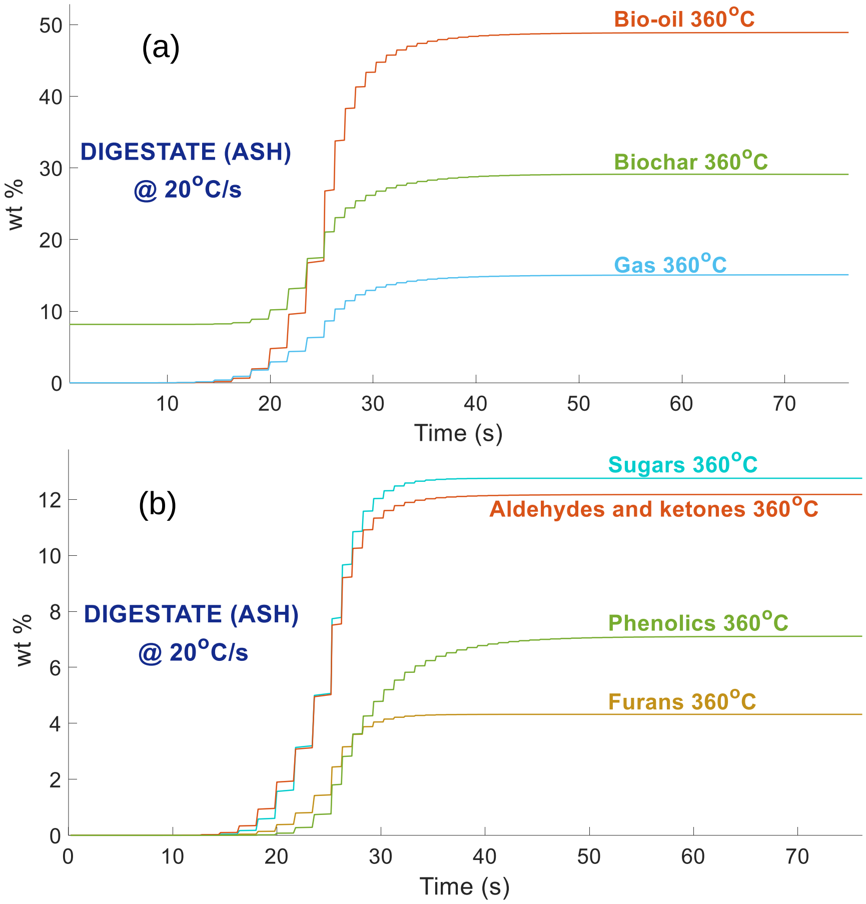

Figure 62. Pyrolysis products formation from digestate at 360ºC at 20ºC/s heating rate with extended residence time: (a) pyrolysis products and (b) compounds in bio-oil.

Final yields for these simulations are 48.91% bio-oil with and water of 7.69%, organics 41.22%, biochar 29.10% and gas 15.09% wt. A high sugar content is produced, at around 13%. Comparing these results with experiments of slow pyrolysis at 355ºC, water resulted around 13%, biochar generated was higher than 50%, and the amount of sugar recorded was less than 2% wt.

This scheme of reactions of pyrolysis was developed based on a comparison with biomasses with different amounts of ash, and an analysis made by Oasmaa et al. [83] is also included where over two years of analysing pyrolytic bio-oils produced in VTT have demonstrated how bio-oils from ash-high biomasses result in more water production and higher gas yield. The scheme proposed by Ranzi et al. [144] results in predictions that show 10% difference between samples containing ash and ash-free biomass. However, the impact of this inorganic material in digestate has a major effect. Considerations in the experimental work of Ranzi et al. [144] and Oasmaa et al. [83] does not include biomass with a higher ash content than 5%. The ash factor, introduced in Section 6.4, is integral to these models and takes a value between 0-1, and for low ash biomass the value is 0.5 and for ash contents of more than 4-5% wt the value of this factor is close to 1. The main effect of these values is on the activation energy of some reaction, but only in those where cellulose and hemicellulose are decomposed.

According to the experimental data obtained from pyrolysis of digestate, the impact of ash on sugar production could be 10 times higher than this scheme of proposed reactions. Additionally, this amount of ash has also led to production of more phenolics, explained in more detail in Section 6.3. It seems this inorganic material could also enhance lignin decomposition, something not considered in these reaction schemes

7.1.2 PYROLYSIS OF PRE-AD CROP AT DIFFERENT RATES

Projections were performed with pre-AD crop, which contains around 4% ash. The main input for the simulation of pre-AD crop was only the lignocellulose material without considering starch content because this material can be converted into other compounds such as levoglucosan, methane (CH_4) or furans at temperatures around 200ºC, higher temperatures could lead to more carbon dioxide (CO_2) and water production [93,125], and starch is not considered in the scheme of reactions. Composition of pre-AD crop employed for the kinetic model is shown in Table 62.

Feedstock composition	Pre-AD crop
Cellulose	23.32
Hemicellulose	50.87
Lignin	20.13
Lignin C	*4.03*
Lignin H	*6.86*
Lignin O	*9.24*
Moisture	2.29
Ash	3.39

Table 62. Pre-AD crop composition employed for modelling pyrolysis at different heating rates. Data presented in % wt.

The same heating rates used for digestate projections were applied to simulate profiles of how pre-AD crop is decomposed, and how pyrolysis products were generated. These simulations are shown in Figure 63.

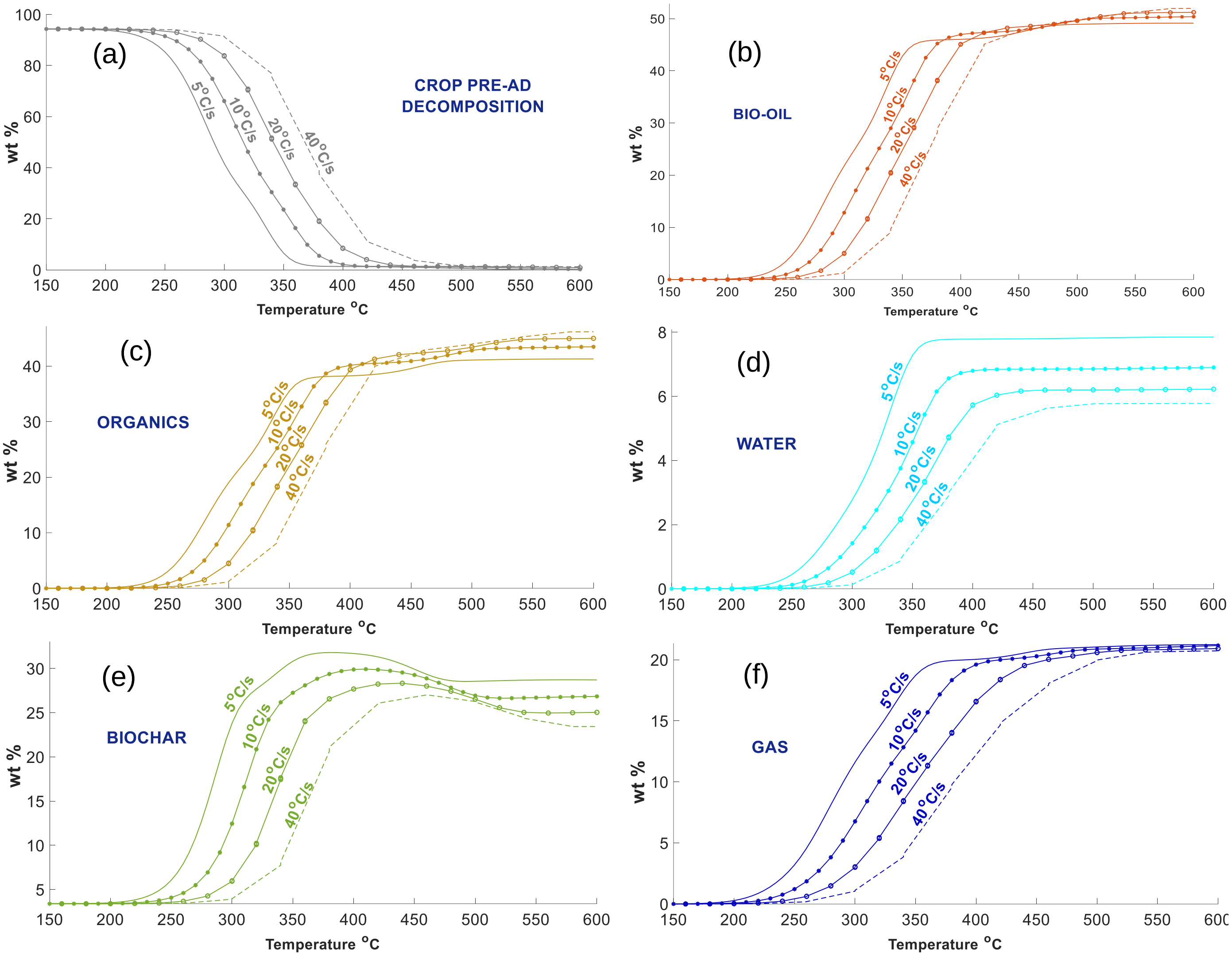

Figure 63. V-heat projections of pyrolysis of pre-AD crop considering ash content at different heating rates 5ºC/s, 10ºC/s, 20ºC/s and 40ºC/s: (a) biomass decomposition. (b) bio-oil, (c) organics, (d) water, (e) biochar, and (f) gas.

Water profile shows the highest yield at 5ºC/s reached around 8% wt, and the lowest at 40ºC/s with just below 6% wt which is less amount than the formed using digestate composition. Water yield resulting from digestate at 5ºC/s was almost 10% and 6.5% wt at 40ºC/s.

In this case with pre-AD crop, biochar yield reached a maximum amount at around 380ºC, 410ºC, 440ºC and 460ºC with 5ºC/s, 10ºC/s, 20ºC/s and 40ºC/s respectively. From the analysis of measurements obtained between slow and fast pyrolysis with digestate, biochar production with this biomass can be higher by around 20-30% using slow pyrolysis. These projections presented in Figure 63 could be closer to those yields of fast pyrolysis products. Experiments in slow pyrolysis of pre-AD crop demonstrated that biochar was generated as minimum 27.5% wt at 530ºC. Biochar then could be produced using fast pyrolysis in around 22% wt at similar temperatures.

Projections of final yields of biochar, bio-oil and gas using this kinetic model (V-heat) from pre-AD crop are shown in Table 63.

Product	5ºC/s	10 ºC/s	20 ºC/s	40 ºC/s
Biochar	28.71	26.85	25.04	23.44
Bio-oil	49.14	50.38	51.23	52.01
Organics	*41.29*	*43.48*	*45.00*	*46.23*
Water	*7.85*	*6.90*	*6.22*	*5.78*
Gas	21.24	21.16	20.92	20.74

Table 63. Final yields of pyrolysis products from pre-AD crop at 600ºC, with different at different heating rates with V-heat.

Simulation of bio-oil production from pre-AD is close to final yields from data estimated for fast pyrolysis from experimental results, where bio-oil yield could be produced between 48% and 57%, and the prediction with the model is around 49-52% wt. However, for this waste valorisation and other similar biomass, it is crucial to make an appropriate approximation of chemical composition of these products.

The simulation of chemical group profiles of production in bio-oil during pyrolysis of pre-AD crop are shown in Figure 64.

.

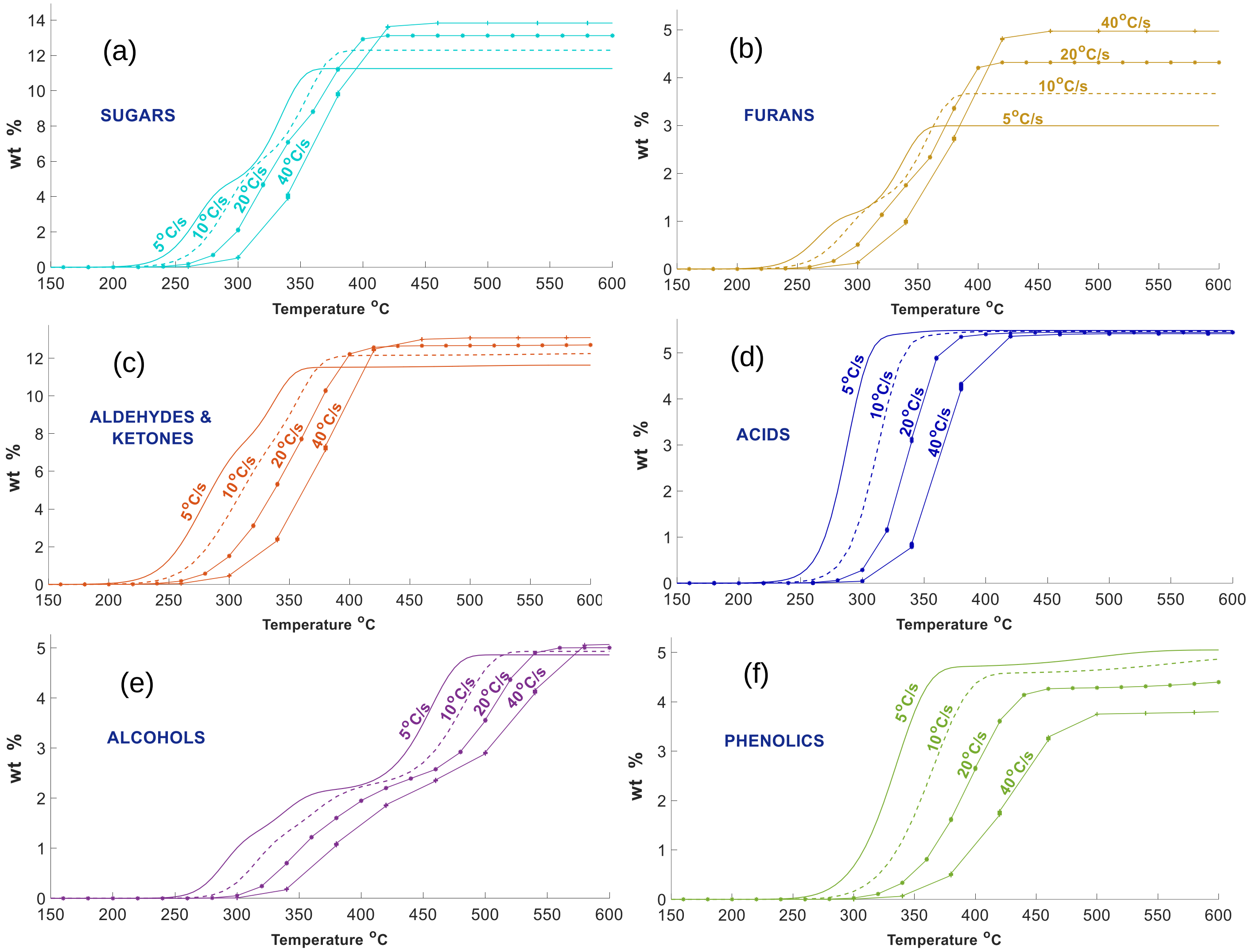

Figure 64. V-heat projections of bio-oil compounds formation from pyrolysis of pre-AD crop at different rates 5ºC/s, 10ºC/s, 20ºC/s and 40ºC/s: (a) sugars, (b) furans, (c) aldehydes & ketones, (d) acids and (e) alcohols and (f) phenolics.

Although these heating rates did not have any effect in final acid yields, there is a significant difference in the 250-350°C range. Alcohol and sugar profiles showed higher production at 40ºC/s. Furans and A&K were produced in greater proportion as heating rates increased, contrary to phenolic profiles which resulted in lower yield at higher heating rates. The projection of the final composition of bio-oils produced at these different heating rates are shown in Table 64.

Compound	5ºC/s	10ºC/s	20ºC/s	40ºC/s
Sugars	11.26	12.29	13.12	13.83
Furans	2.99	3.67	4.32	4.97
Aldehydes and ketones	11.64	12.25	12.71	13.10
Acids	5.49	5.47	5.45	5.42
Alcohols	4.86	4.93	5.01	5.08
Phenolics	5.05	4.87	4.40	3.82

Table 64. Final yields (wt %) of compounds in pyrolysis bio-oil from pre-AD crop at different heating rates at 600ºC.

Sugar concentration in these simulations is higher than the levels measured in experiments. The range of sugars projected was between 11% and almost 14% wt, whereas the maximum recorded from the experiments with pre-AD was around 9% at 530ºC in slow pyrolysis. It is possible that high sugar levels could be found in fast pyrolysis bio-oil if pre-AD crop was used, considering that sugar yield from digestate in fast pyrolysis resulted in 1.3% wt at 460ºC and a maximum of 0.5% wt with slow pyrolysis at 425-485ºC.

Although these projections with the V-heat model showed some differences in yields between digestate and pre-AD due to the variation ash content, yields and chemical composition of bio-oil were not close to experimental measurements. The water for instance, which is one of the key products that could represent secondary reactions during pyrolysis, was produced in large amount in bio-oil yield during the experiments. A comparison of pyrolysis product yields between the model and the experimental results with digestate and pre-AD in pyrolysis technologies is shown in Table 65.

Product	Model (V-heat)	Experiments
Biochar (Digestate)	25-30	30-35
Biochar (Pre-AD)	23-29	22-27
Bio-oil (Digestate)	49-50	36-40
Bio-oil (Pre-AD)	49-52	48-52
Water (Digestate)	*6-10*	*8-11*
Water (Pre-AD)	*6-8*	*5-7*
Organics (Digestate)	*39-43*	*28-37*
Organics (Pre-AD)	*41-46*	*43-47*
Gas (Digestate)	16-18	18-21
Gas (Pre-AD)	20-21	9-15

Table 65. Range of yields resulted from projections with model V-heat and experimental measurements using digestate and pre-AD in fast pyrolysis (Data presented in wt %).

The outcomes from V-heat model showed differences between digestate and pre-AD profiles. Taking the water for instance, the maximum amount produced was 8% from pre-AD crop, whereas with digestate this reached almost 10%. Organics yields also showed differences, with pre-AD this could reach 46% and only 43% with digestate. However, comparing these results with the experimental data, only product yields from pyrolysis of pre-AD had a close approximation. Simulations of final products from pre-AD crop were 49-52% of bio-oil, 6-8% of water, 41-46% of organics and 23-29% wt of biochar, similar results of these products in experiments with 48-52%, 5-7%, 43-47% and 22-27% wt respectively.

On the other hand, yields obtained from pyrolysing digestate contrasted the simulation. Biochar and water were above the range resulted from modelling, the maximum in this estimation was the minimum in experiments. 25-30% biochar was projected from digestate while this was formed in a range of 30-35% wt in experiments. Contrary to organics production, which was much less than predicted with 29-37% and 39-43% wt respectively.

The differences between pyrolysis products from simulations and experimental results showed that the impact of ash in digestate was not fully accounted for in the scheme of reactions. It might be only with a maximum around 4% wt ash, which is the proportion pre-AD crop had. This discrepancy was also found in bio-oil composition. A summary of bio-oil composition resulted from projections and experimental data using both biomasses is presented in Table 66.

Group	Model (V-heat)	Experiments
Sugars (Digestate)	11-12	1-3
Sugars (Pre-AD)	11-14	7-14
Furans (Digestate)	3-5	2-6
Furans (Pre-AD)	3-5	15-20
Aldehydes and ketones (Digestate)	11-14	4- 5
Aldehydes and ketones (Pre-AD)	11-13	13-20
Acids (Digestate)	2-3	6-20
Acids (Pre-AD)	5-6	0-2
Alcohols (Digestate)	3-4	0-1
Alcohols (Pre-AD)	4-5	1-3
Phenolics (Digestate)	6-8	15-22
Phenolics (Pre-AD)	4-5	12-20

Table 66. Range of chemical compounds content in bio-oil resulted from projections with model V-heat and experimental measurements using digestate and pre-AD in fast pyrolysis (Data presented in wt %).

Data presented from the experiments are an average of the samples analysed. The range of sugars, furans and alcohols were in similar proportion between digestate and pre-AD, and aldehydes and ketones; acids and phenolics had just a slight difference between biomass from simulations. Acid yield was higher using pre-AD, resulting in around 5-6%, and 2-3% wt from digestate. Contrasting results were obtained with phenolics, where digestate generated around 6-8% and with pre-AD crop 4-5% wt.

Sugars, acids and phenolics presented the greatest variation between the model outcomes and experimental data. Model predictions show around 11-12% sugars from both biomasses, whereas experiments revealed just 1-3% from digestate and 7-15% wt from pre-AD. Acid yields projected were 2-3% and 4-5% from digestate and pre-AD respectively, and measured 6-20% and only 0-2% wt. Modelling phenolic profiles ended with only 6-8% from digestate and 4-5% from pre-AD material while these were formed in 15-22% and 12-20% wt of the total products in the experiments.

As the scheme of reactions is considerably far from the results obtained with pyrolysing these biomasses, some adjustments were made to the activation energy of some reactions in order to simulate how ash in digestate has a higher impact on pyrolysis product yields and bio-oil composition. This impact can be at least 10 times more than the original scheme considers, and it is described in detail in the next section.

7.2 PYROLYSIS OF DIGESTATE AND PRE-AD CROP AT DIFFERENT RATES WITH HIGHER IMPACT OF ASH CONTENT

Reactions in the original scheme developed by Ranzi et al. [144] consider more biochar and water generation due to ash. However, the ash factor implemented had only a negative impact of around 10%, and just on cellulose and hemicellulose decomposition reactions. Despite that, with the amount of ash in digestate the production of biochar and water should be more favourable. Thus, these specific reactions must have lower values of activation energy because there is competition between sugars, water and biochar from cellulose and hemicellulose thermochemical decomposition.

The kinetic model was adjusted so that the impact of ash was at least ten times higher than in the original scheme. In previous sections it was explained that the effect of ash on lignocellulosic decomposition in the original scheme (see Section 6.4) was included in the reactions with a factor that impacts the activation energy. However, this was included only in three reactions: 2, 4 and 8. The new adjustment consisted of adding this ash factor in six more reactions.

The adjusted scheme has nine reactions impacted by ash content: 2-4 which are related to cellulose decomposition, 7-9 to hemicellulose and 10-15 to lignin. The activation energy of levoglucosan and xylose formation (reaction 3 and 7) resulted in higher value with this modification, leading to a lower activation energy to form water, biochar and other small-molecule compounds. For example, if the ash content of the biomass is 8%, reaction 3 where levoglucosan is formed, the activation energy (E) remains 42 kJ/mol in the original scheme because the ash factor is not integrated. By modifying this reaction, the ash factor increases the E value to around 154 kJ/mol to form levoglucosan, and reaction 5 has a decrease in E from around 131 kJ/mol (original scheme) to 82 kJ/mol, favouring secondary products such as water and biochar.

This model adjusted has been termed VAsh10 as a version with at least 10 times more impact on pyrolysis products due to ash. The results of these simulations are shown in Figure 65.

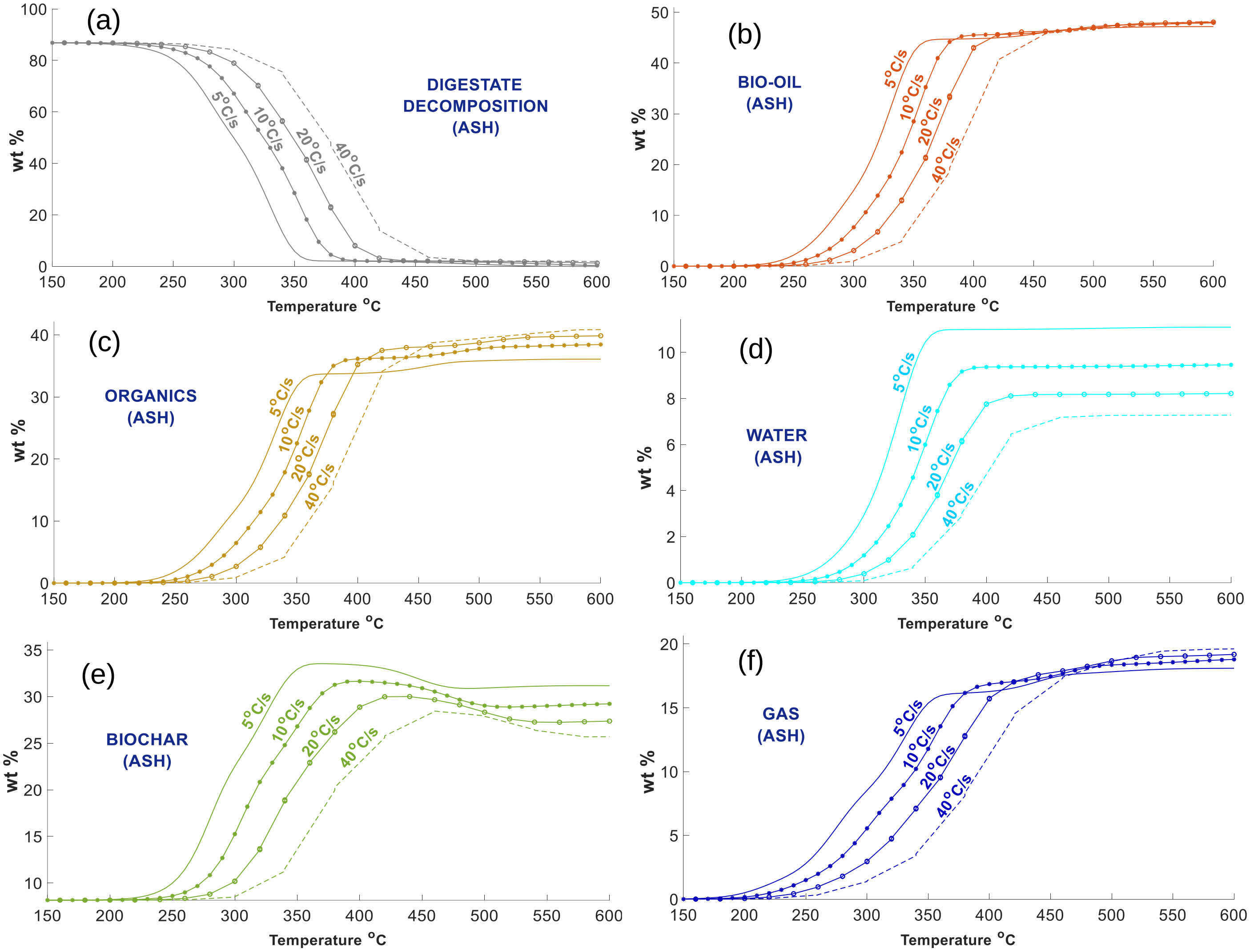

Figure 65. Projections of pyrolysis of digestate with model VAsh10 at different heating rates: 5ºC/s, 10ºC/s, 20ºC/s and 40ºC/s. (a) biomass decomposition, (b) bio-oil, (c) organics, (d) water, (e) biochar, and (f) gas.

These projections were with the same heating rates employed for earlier simulations. Water, biochar and gas yields had an increase with a total of around 11%, 31% and 18% wt at 5ºC/s respectively, whereas using V-heat model these yields were below 10%, 30% and 17% wt. There was a reduction in organics with around 10% in each heating rate. For example at 10ºC/s in earlier projections with V-heat, organics were formed around 43% wt, and VAsh10 simulations showed the organics close to 40% wt. Gas production increased with VAsh10 reaching almost 20% at 40ºC/s, while before this was projected around 18% wt.

Illustrative pyrolysis product distribution using the model VAsh10 and fast pyrolysis products recovered from digestate at different temperatures are presented in Figure 66.

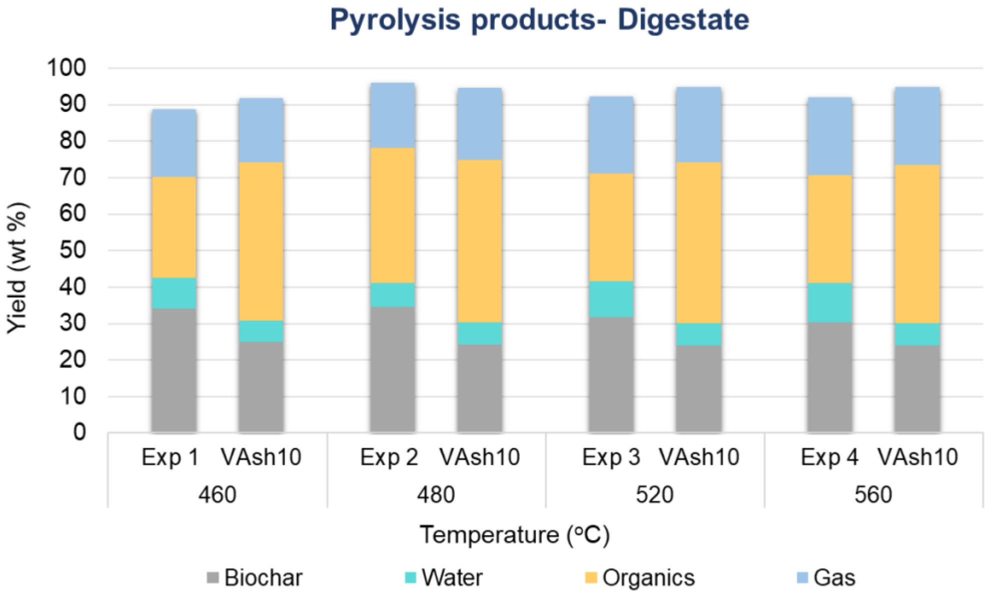

Figure 66. Yields of fast pyrolysis products recovered at different temperature and from projections with model VAsh10 using digestate composition.

These pyrolysis projections had a close approximation to experimental data using digestate. The most noticeable difference was a higher proportion of organics from modelling. Although the adjustments to the kinetics enhance cellulose and hemicellulose decomposition towards more biochar and water generation, lignin is also influenced by this modification, and the reactions that characterise lignin decomposition not only produce biochar and water but large amount of other organics such aldehydes and ketones (A&K). Chemical group outlines in bio-oil from VAsh10 are presented in Figure 67.

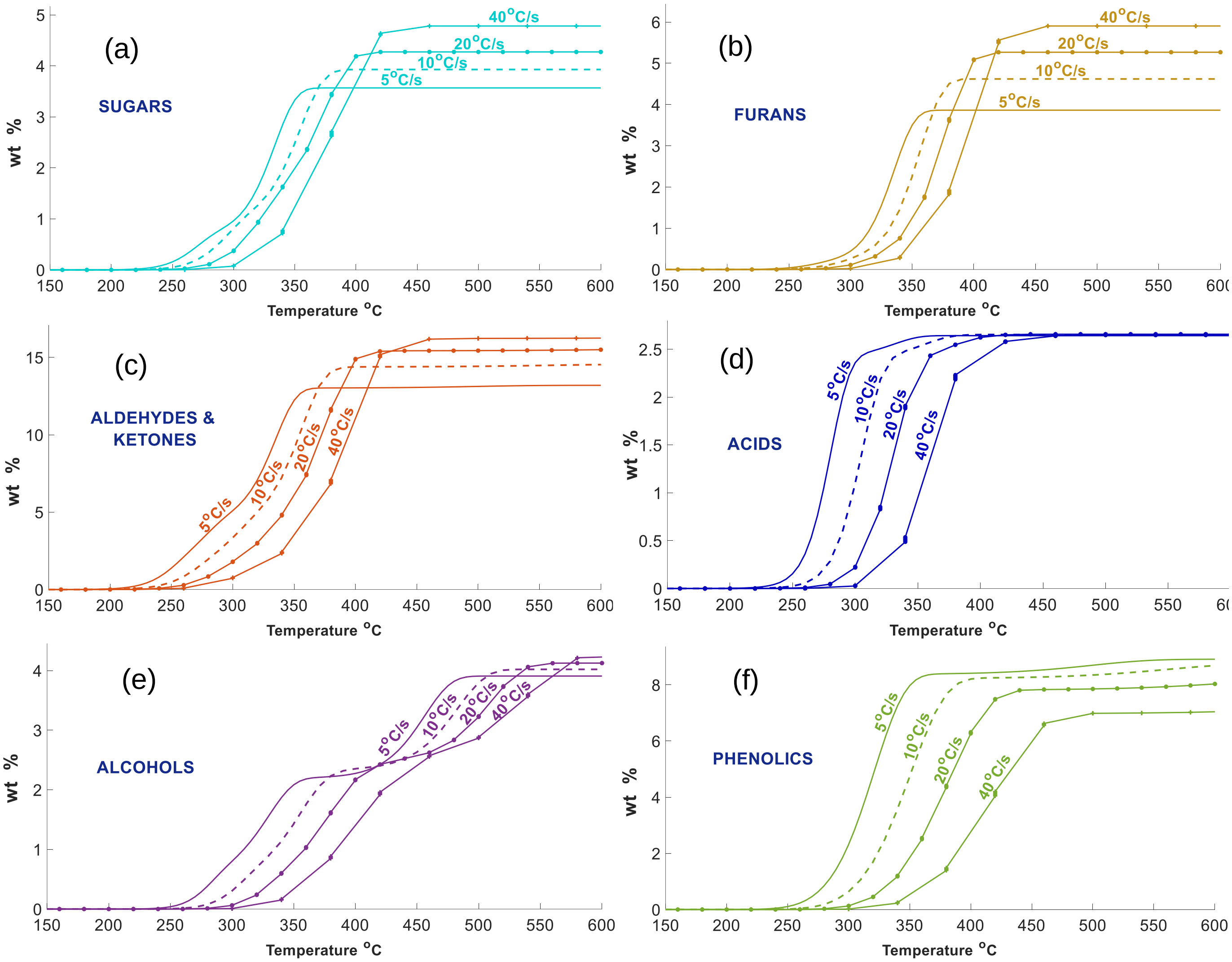

Figure 67. VAsh10 projections of bio-oil compounds formation from pyrolysis of digestate at different heating rates 5ºC/s, 10ºC/s, 20ºC/s and 40ºC/s, with VAsh10 model: (a) sugars. (b) furans, (c) aldehydes & ketones, (d) acids and (e) alcohols and (f) phenolics.

There was a significant reduction in sugar production, yet the other compounds showed an increase with model VAsh10. Sugar profiles were different from earlier projections, where each sugar outline at different heating rate with V-heat finished with almost the same yield at 600ºC, whereas with VAsh10 projections showed an increment linked to heating rates: the lower sugar production was at the lowest heating rate. These yields were from around 12% with V-heat projections to only 4% wt with VAsh10, and with an increase in phenolics. These simulations were also performed with pre-AD crop composition using the 4% wt ash content. The yields of pyrolysis products of pre-AD crop are presented in Table 67.

Product	5ºC/s	10 ºC/s	20 ºC/s	40 ºC/s
Bio-oil	45.70	47.19	48.04	49.28
Organics	*37.18*	*39.66*	*41.32*	*43.15*
Water	*8.52*	*7.53*	*6.73*	*6.14*
Biochar	30.59	29.20	27.41	25.43
Gas	22.95	23.27	23.06	22.63

Table 67. Projections of final yields of pyrolysis products from pre-AD crop at different heating rates from 150ºC to 600ºC, with higher ash impact.

VAsh10 considered a higher impact on pyrolysis products from pre-AD crop despite the fact that this material had much less ash than digestate. The previous model, V-heat, showed pre-AD pyrolytic bio-oil generation with water and organic fractions of 5.78% and 46.23% at 40ºC/s, and 7.85% and 41.29% at 5ºC/s, while VAsh10 projections showed 6.14% water and 43.13% organics at 40ºC/s and 8.52% and 37.18% at 5ºC/s. These outcomes showed a significant reduction in organics formation, similar to what occurs in pyrolysis of lignocellulosic material in the presence of ash.

A compendium of pyrolysis product yields from projections with both models V-heat and VAsh10, and experimental data using both biomasses is shown in Table 68.

Product	Model (V-heat)	Experiments	Model (VAsh10)
Biochar (Digestate)	25-30	30-35	26-32
Biochar (Pre-AD)	23-29	22-27	25-30
Bio-oil (Digestate)	49-50	36-40	47-48
Bio-oil (Pre-AD)	49-52	48-52	46-49
Water (Digestate)	*6-10*	*8-11*	*7-11*
Water (Pre-AD)	*6-8*	*5-7*	*6-8*
Organics (Digestate)	*39-43*	*29-37*	*36-41*
Organics (Pre-AD)	*41-46*	*43-47*	*37-43*
Gas (Digestate)	16-18	18-21	18-20
Gas (Pre-AD)	20-21	13-17	23-24

Table 68. Range of yields resulted from projections with both models and experimental measurements using digestate and pre-AD in fast pyrolysis (Data presented in wt %).

This summary shows the difference between both models and experimental results from pyrolysing pre-AD and digestate. Although bio-oil from digestate was much lower in experiments with a range of 36-40% versus 47-48% wt from the model, yields of bio-oil phases falls into the range of experimental data with 36-41% organics and 7-11% wt water projected, and from experiments these were 29-37% and 8-11% wt respectively. Gas production using digestate also increased from V-heat to VAsh10 projections, with values from 16-18% to 18-20% wt. These last results were equal to yields measured experimentally.

The VAsh10 model gives a much closer alignment with experimental pyrolysis data for digestate. However, the chemical composition of the different phases is also of interest.

The profiles for different compounds through this kinetic model are shown in Figure 68.

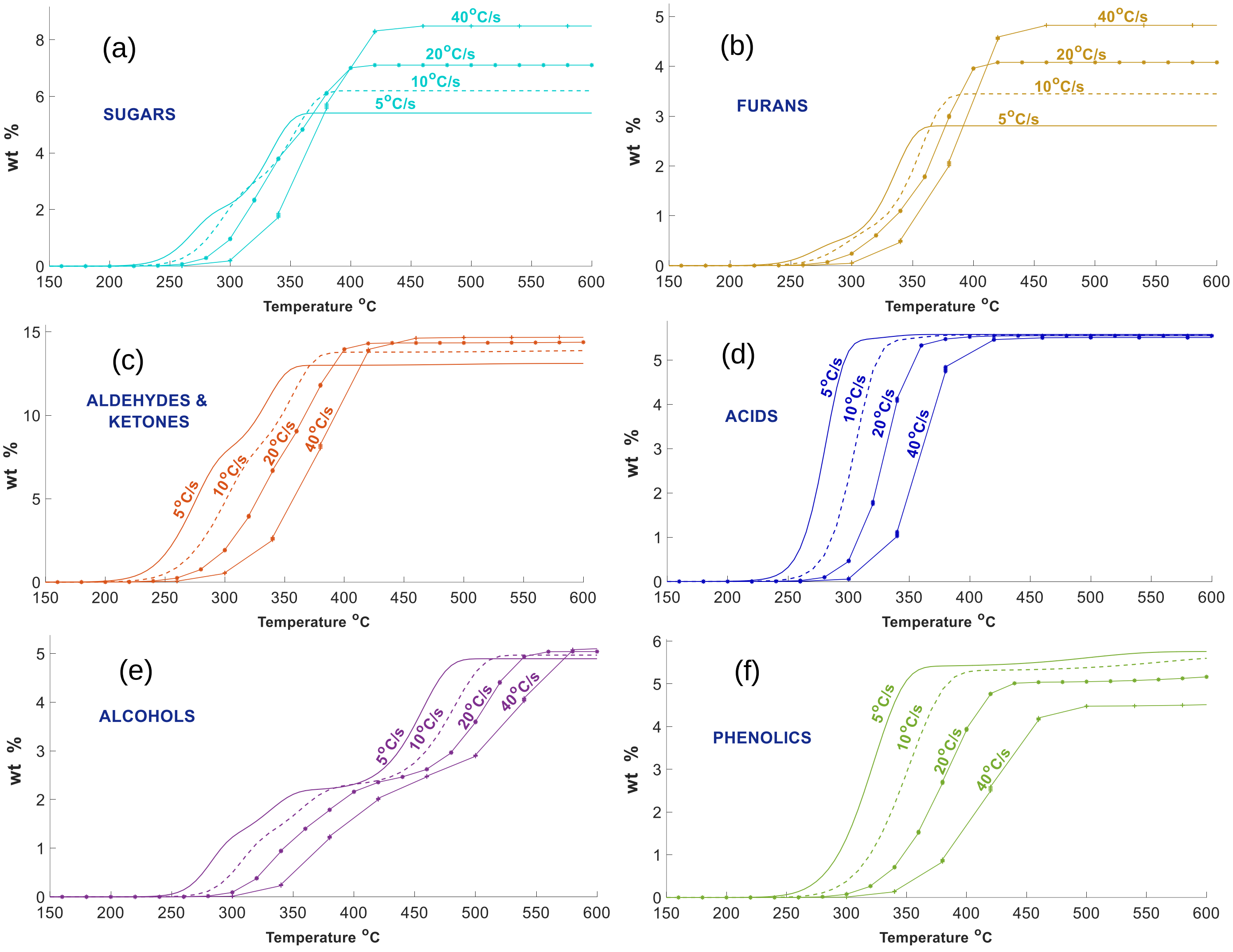

Figure 68. Model projections of bio-oil compounds formation from pyrolysis of pre-AD crop at different heating rates 5ºC/s, 10ºC/s, 20ºC/s and 40ºC/s, with higher impact of ash content: (a) sugars. (b) furans, (c) aldehydes & ketones, (d) acids and (e) alcohols and (f) phenolics.

Although the ash content in pre-AD is only 4% wt, sugars are also the most evident component affected. The variation in sugar production occurs not only as temperature increases, but the final yield is also different between heating rates, while the other compounds have similar profile to previous simulations, but with a slightly increase in Table 69.

Compound	5ºC/s	10ºC/s	20ºC/s	40ºC/s
Sugars	5.36	6.20	7.10	8.49
Furans	2.78	3.45	4.08	4.82
Aldehydes and ketones	12.98	13.88	14.38	14.68
Acids	5.52	5.57	5.55	5.51
Alcohols	4.84	4.97	5.04	5.12
Phenolics	5.70	5.60	5.16	4.53

Table 69. Final yields (wt%) of compounds in pyrolysis bio-oil from pre-AD crop at different heating rates from 150ºC to 600ºC, with higher impact of ash.

Final yields of sugars were much lower with the adjustments made to the kinetic model. V-heat projections showed sugar production of 11.26%, 12.29%, 13.12% and 13.83% wt at 5ºC/s, 10ºC/s, 20ºC/s and 40ºC/s respectively; whereas VAsh10 projected a significant decrease at the same heating rates with 5.36%, 6.2%, 7.10% and 8.49% wt, which is a similar approach of ash effect on sugar productions in pyrolysis.

Summary of bio-oil composition resulted from modelling and experimental data with both biomasses is presented in Table 70.

Group	Model (V-heat)	Experiments	Model (VAsh10)
Sugars (Digestate)	11-12	1-3	3-5
Sugars (Pre-AD)	11-14	7-14	5-9
Furans (Digestate)	3-5	2-6	4-6
Furans (Pre-AD)	3-5	4-20	3-5
Aldehydes and ketones (Digestate)	11-14	4- 5	13-16
Aldehydes and ketones (Pre-AD)	11-13	13-20	13-15
Acids (Digestate)	2-3	6-20	2-3
Acids (Pre-AD)	5-6	0-2	5-6
Alcohols (Digestate)	3-4	0-1	3-4
Alcohols (Pre-AD)	4-5	1-3	4-5
Phenolics (Digestate)	6-8	15-22	7-9
Phenolics (Pre-AD)	4-5	12-20	4-6

Table 70. Range of chemical compounds content in bio-oil resulted from projections with model V-heat, VAsh10 and experimental measurements using digestate and pre-AD in fast pyrolysis (Data presented in wt %)

There are noticeable differences in composition between V-heat and VAsh10 models, especially for sugars and phenolics. Sugars predicted from digestate with V-heat were 11-12% and 3-5% with VAsh10, whereas experimental values were 1-3% wt. Sugar yields from pre-AD also showed a difference; 11-14% from V-heat and 5-9% from VAsh10, but the gap is smaller than for digestate both were within the experimentally observed range of 7-14% wt. The changes made to the kinetics in VAsh10 do not affect the ability of the model to give realistic predictions of sugar yield at relatively low ash content, but they result in a step-change at higher ash content where agreement between model predictions and experimental data is achieved.

Despite the improvements in predictions for sugar yield, the VAsh10 model still under-predicts the yield of phenolic compounds, and cannot give a reliable indication of the total acids. It is important to consider that the scheme of reactions does not include all secondary reactions, where other small-molecule compounds could be formed when primary compounds are decomposed. This was pointed and described in CHAPTER 6. Hexoses such as levoglucosan not only form water, gas and biochar when are subjected to a catalytic decomposition, but compounds such as hydroxyacetaldehyde, glyceraldehyde and acetic acid could be formed [43], and furfural decomposition can lead to forming more acetic acid [175]. Further investigation is needed to assess whether extra kinetic terms for secondary decomposition would make the VAsh10 model more able to predict experimental data for total acids.

The ash content in pre-AD crop and in digestate has a completely different effect from any kinetic reactions proposed in the literature. Additionally, this inorganic material does not have a uniform distribution across the digestate, which has a direct impact on yield and bio-oil composition during pyrolysis processing. This has resulted in more challenging situation to develop a specific kinetic model with detailed composition of pyrolytic bio-oil, biochar and gas. However, VAsh10, the novel kinetic model developed in this work, can not only be implemented at different heating rates but also addresses the ash impact on lignocellulose decomposition, favouring biochar, water and small-molecule compound generation as occurs during pyrolysis of biomass. This results in projections with more precise yields of pyrolytic products from digestate and pre-AD crop. The VAsh10 model may be able to predict generation of pyrolysis products from other digestates, considering this type of waste has a greater amount of ash than other biomasses such as wood.

CHAPTER 8. SCENARIOS FOR THERMAL TREATMENT INTEGRATED TO ANAEROBIC DIGESTION SYSTEMS AND POSSIBLE USES OF PYROLYSIS PRODUCTS

There are several pyrolysis technologies in operation at large scale that could be implemented for the digestate produced at energy sites. The examples in this study are applied for Severn Treat Water plants. Some projections have been performed with examples of industrial-scale reactors to pyrolyse digestate, and on the assumption that the bio-oil formed would have with similar composition to the results of the experimental work of this project.

Drying of digestate prior to pyrolysis has been classified as a very high energy consuming process, which presents a challenge from a techno-economical perspective due to the 80% moisture content in this biomass. On the other hand, through the years some systems have been improved to dry this type of waste at lower temperatures, with less energy input. One advantage of pyrolysing digestate is that the water from drying of digestate could be recovered and recirculated into the anaerobic digestion (AD) system and use it to maintain the temperature required for the digesters. However, the liquid has a high content of ammonia and other compounds such as volatile acids that could affect the AD processing by increasing the concentration in the system. Nitrogen could be recovered from these vapours resulted from drying the digestate through a process known as stripping method in order to obtain ammonium sulphate, or vapours could go through membrane technologies for nutrient concentration [176]. These practices would be implemented with the aim to increase water reutilisation and reduce negative impact on the environment, but it would need to be balanced against the capital and operating costs of the extra process units needed to achieve this.

Other technologies such as hydrothermal carbonisation (HTC) has been seen as a promising route because wet digestate can be directly treated. However, the liquid phase resulting from this process will contain similar compounds to those found in the bio-oils recovered from the pyrolysis experiments carried out in this project [177,178]. This is because there is a thermochemical decomposition of lignocellulose. This liquid cannot be reused, and hydrochar needs to be dewatered, and dried for further use. Thus, this liquid phase would require an additional treatment. Furthermore, recirculating this liquid into the wastewater treatment plant (WWTP) would have a negative impact on wastewater treatment, and is not ideal due to some aromatic hydrocarbons (AHs) and phenolics formation during HTC process, very similar to that identified in slow pyrolysis of digestate. WWTP cannot completely remove all these micropollutants [179], and adding these compounds to a wastewater stream can result in more contamination. The best strategy for this HTC liquid product is that the compounds are recovered for further uses, yet the energy consumption can be similar to that for pyrolysis technologies using dry-basis feedstock. Hydrothermal liquefaction (HTL) could likewise be an alternative option to produce more valuable products in bio-oil formation without drying the digestate first. There have been some studies where ash can be a precursor for more organics HTL [180]. However, the separation of the products needs to be further studied and assessed with more detail.

Each waste collected for this study (Figure 69) has different characteristics, and it cannot be treated with the same technology in expectation of similar results. It is important to consider bio-oil, biochar and gas composition with the purpose of increasing the value of each waste for further generation of usable and valuable products. Following the analysis of these three pyrolysis technologies, it is possible to identify which technology would be most suitable for each waste.

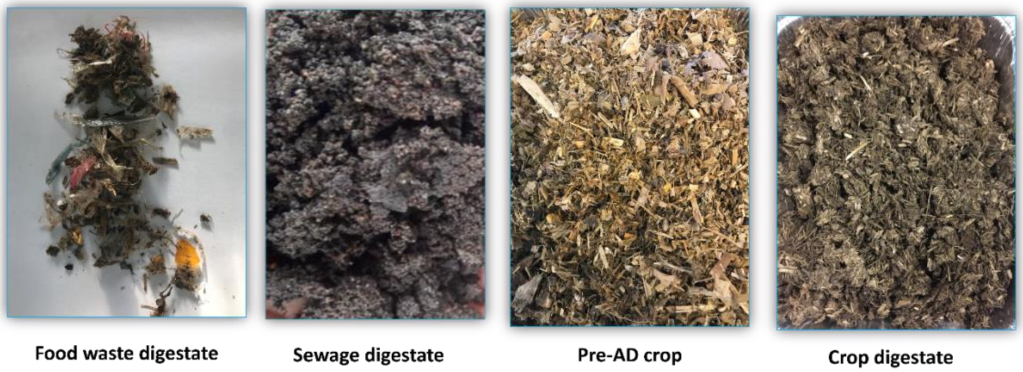

Figure 69. Waste collected from Severn Trent sites.

Several technologies currently in operation were evaluated and selected to run some projections to treat this waste, and some scenarios have been suggested that could be implemented. These include streams of possible uses of the products generated from the systems:

- Scenario 1 consists of thermochemical treatment post AD to convert digestate into pyrolysis products.
- Scenario 2 comprises pyrolysis of pre-AD crop into biochar, bio-oil and gas, without AD process.

- Scenario 3 involves a recovery of high-value compounds from digestate for more biogas production where the depolymerisation of cellulose and hemicellulose occurs in a two-stage process to obtain solutions rich in monosaccharides.

8.1 SCENARIO 1- POST-AD

This section describes each pyrolysis technology integrated into anaerobic digestion systems to treat digestate.

8.1.1 FAST PYROLYSIS POST-AD

Fast pyrolysis was the technology with higher yield of bio-oil. This could be the most convenient for crop digestate due to its lignocellulosic material where more chemical compounds from bio-oil can be recovered. Although the amount of ash this biomass contain has a direct impact on bio-oil composition, aldehydes and ketones and phenolics could have an additional use in production of other biobased products.

Empyro in Hengelo, the Netherlands, is a large-scale pyrolysis facility that can reach a conversion of 60% of pyrolytic bio-oil from woody biomass. Energy outputs consist of 7.4 MW_{th} of steam and 650 kW_e of electricity. This energy could be employed on the sites for operation of the systems or be exported into the grid. Biomass utilised as feedstock is crumbles resulted as a by-product from wood pellets.

This facility has been selected to make some projections of the amount of bio-oil which could be produced in commercial scale from crop digestate. This system was developed by Biomass Technology Group (btg), and their process is shown in Figure 70.

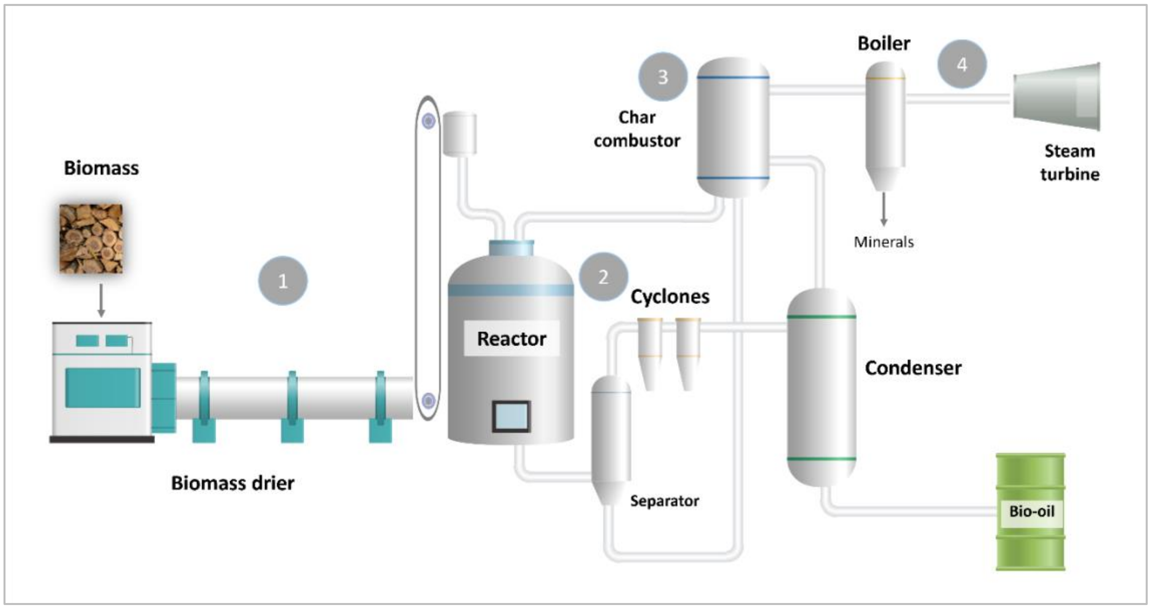

Figure 70. Flow diagram of Empyro pyrolysis process (Modified from BTG bioliquids).

This fast pyrolysis system consists of the following stages:

1. Feedstock is dried to obtain a biomass with 5% moisture content
2. Dry biomass is fed into a fluidised bed reactor
3. Char is recovered with cyclones, and non-condensable gases are separated from the vapours by condensation. Both, biochar and gas are employed in a combustor for energy production as input into the system
4. Bio-oil is stored, and flue gases are used to produce high pressure steam, which can be a source of electricity production through a steam turbine. Low pressure steam is for heat used in the dryer. Finally, high-mineral ash is removed from the flue gases to be utilised as soil fertiliser

The current production of crop digestate in Severn Trent is around 77, 500 tonnes/year. By 2022, this will increase by 40%, resulting in around 107,000 tonnes of crop digestate per year from 122,000 tonnes of crop waste. It is assumed that the Empyro plant can be integrated into this crop-waste AD system with conversions as per the experimental values measured with fast pyrolysis of digestate in the VTT system. The predicted outputs from a fast pyrolysis system for crop digestate are presented in Table 71.

Fast pyrolysis Empyro (digestate)		
5	tonnes biomass/hr (5% moisture)	
2.1	tonnes bio-oil/hr	
7.4	MW$_{th}$ output (steam generation)	
650	kW$_{e}$ output (electricity)	
63	tonnes digestate/day (5% moisture)	
27	**tonnes bio-oil from digestate/day**	
Bio-oil composition		
Acids	4.4	tonnes/day
Aldehydes & ketones	2.9	
Alcohols	0.3	
Furans	4.2	
Sugars	1.2	
Phenolics	11.6	
Others	1.9	

Table 71. Projection of bio-oil composition produced from digestate at 560^{o}C with a current scale-up fast pyrolysis technology, Hengelo, the Netherlands.

There is a drying process called Elodry®, –where waste heat produced from pyrolysis is used to dry sludges at temperatures around 70^{o}C, with a requirement of 70 kWh$_{th}$ per tonne of water. This can be implemented for drying digestate, and the pyrolysis system could supply this thermal energy to reduce reducing external energy input.

Illustrative representation of what would be fast pyrolysis integrated to a crop AD system is shown in Figure 71.

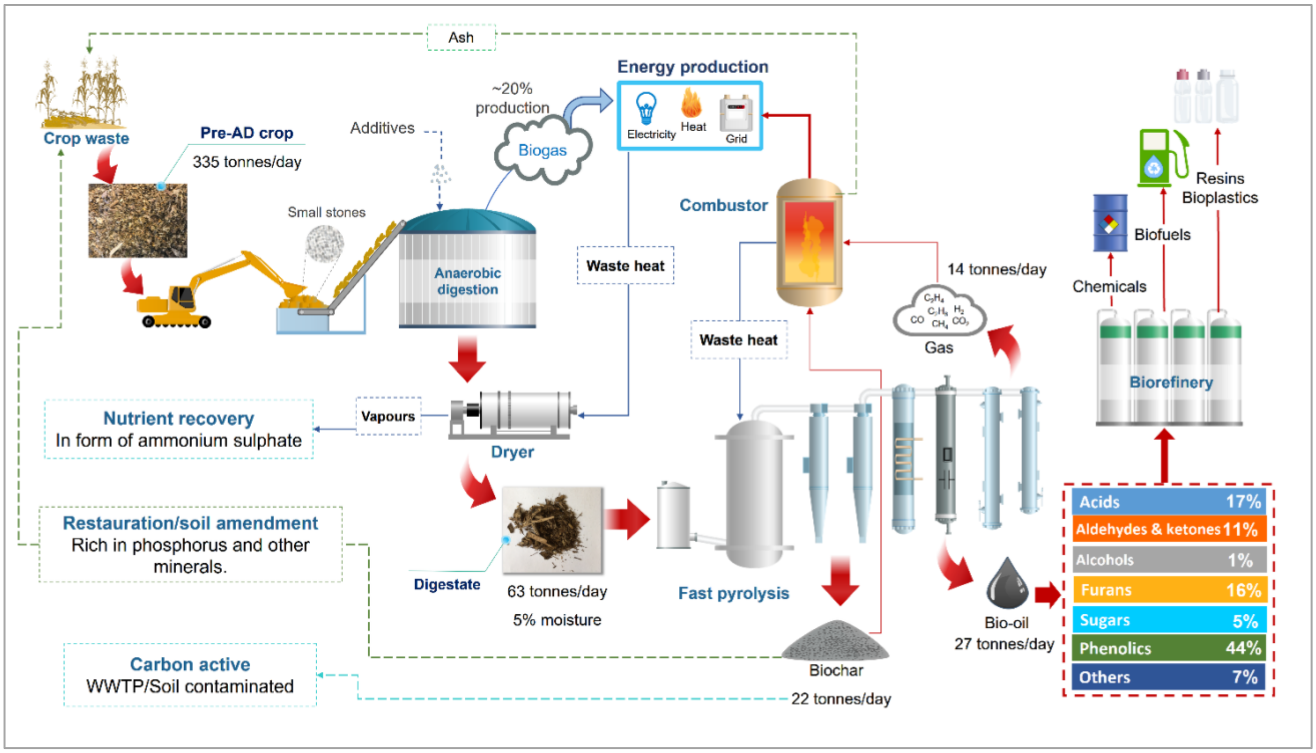
Ash
Energy production
~20%
production
Electricity
Heat
Grid
Biogas
Crop waste
Pre-AD crop
335 tonnes/day
Additives
Small stones
Anaerobic
digestion
Combustor
Waste heat
Waste heat
14 tonnes/day
C_2H_4
C_3H_8
H_2
CO
CH_4
CO_2
Gas
Resins
Bioplastics
Biofuels
Chemicals
Biorefinery
Nutrient recovery
In form of ammonium sulphate
Vapours
Dryer
Restauration/soil amendment
Rich in phosphorus and other
minerals.
Digestate
63 tonnes/day
5% moisture
Fast pyrolysis
Bio-oil
27 tonnes/day
Acids 17%
Aldehydes & ketones 11%
Alcohols 1%
Furans 16%
Sugars 5%
Phenolics 44%
Others 7%
Carbon active
WWTP/Soil contaminated
Biochar
22 tonnes/day

Figure 71. Flow diagram of fast pyrolysis of digestate integrated to crop AD system.

Fast pyrolysis products from digestate of this specific system would consist of approximately 22 tonnes of biochar, 14 tonnes of gas and 27 tonnes of bio-oil per day. Considering the bio-oil analysed from experiments carried out bio-oil generated would have a composition of 17% acids, 11% aldehydes and ketones, 1% alcohol, 16% furans, 5% sugars, 44% phenolics and 7% wt other compounds.

8.1.2 SLOW PYROLYSIS POST-AD

The are no current commercial slow pyrolysis plants in operation where bio-oil is recovered and used for further generation of valuable products. Most of the industrial scale systems are developed to target biochar production, where gases generated, condensable and non-condensable, are employed in a combustion chamber to make this technology almost self-sufficient in terms of energy supply. Some of the energy generated is used to dry the waste and increase the amount of solids from 5-10% to at least 85% wt.

Crop digestate could be converted into more valuable products than just biochar. Lignocellulosic derivatives can be additionally converted into other industrial chemicals or to produce alternative polymers or biofuels.

Evaluating scaled-up systems of slow pyrolysis in the industry, it was found this has been more employed for digestate generated from sewage. The perception of sewage being used as fertiliser is still a stigma due to its origin. Even though this digestate could potentially meet regulations as fertiliser under 86/278/EEC, it ends up mostly incinerated or in landfill. This concept of sewage could change, and it could be thermochemically processed in order to reuse it as a soil improver by converting into a more hygienic material, biochar. Pathogens would be destroyed, and substances considered harmful would be removed.

PYREG GmbH, a pioneer in industrial scale slow pyrolysis systems has some of these technologies in operation for sewage sludge pyrolysis. PYREG's technology includes a drying stage where waste can go from 20-35% dry solids to more than 90%. Elodry®, mentioned in the last section, is a system where the sludges can be dried at 70ºC and use 70 kWh_{th} of energy per tonne of water. This pyrolysis system produces waste heat around 600kW_{th}/unit which available for drying. Some samples of digestate from sewage was collected from Stoke Bardolph., and these contained 80% water at the end of the AD process. This material is sent to agriculture activities has a high transportation cost due to its large volume resulting from the high-water content. Carbonising sludges could lead to a reduction in weight by 90%, and lead to a better quality of soil amendment.

The operation of these system in WWTP would require multiple units for more efficient outcomes. For example, digestate from sewage in Stoke Bardolph has a production of 1200 tonnes/day, and this could be reduced to just 500 tonnes of biochar, which would be transported at lower cost and it could be more manageable due to being a dry solid material.

According to PYREG's information every 100 tonnes of sewage treated produces 46 tonnes of biochar. This information has been used to calculate the conversion of crop digestate through a scaled-up slow pyrolysis system. This estimation considers that condensable gases are recovered as per the Empyro system. The conversion of crop digestate into bio-oil and gas is taken from experiments carried out at 500ºC in this study. This technology is designed with capacity to process around 8 tonnes per day of 85% dry-solid biomass per unit. The projections are based on PYREG's conversion assuming it is possible to scale-up this technology to treat around 67 tonnes of digestate per day with 10% moisture content.

The outcomes of using slow pyrolysis for crop digestate would result in 27 tonnes of bio-oil per day with a composition shown in Table 72.

Slow PYREG PX1500		
2.8	tonnes biomass/hr (10% moisture)	
1.1	tonnes bio-oil/hr	
1.3	biochar/hr	
5000	kW$_{th}$ generation	
67	tonnes digestate/day (10% moisture)	
27.1	**tonnes bio-oil from digestate/day**	
Bio-oil composition		
Acids	2.2	tonnes/day
Aldehydes & ketones	2.1	
Alcohols	0.0	
Furans	5.6	
Sugars	0.2	
Phenolics	15.5	
Others	1.5	

Table 72. Projection of bio-oil composition produced from digestate at around 500ºC with PYREG PX1500 system.

General process of slow pyrolysis integrated to a crop-waste anaerobic digestion system is shown Figure 72.

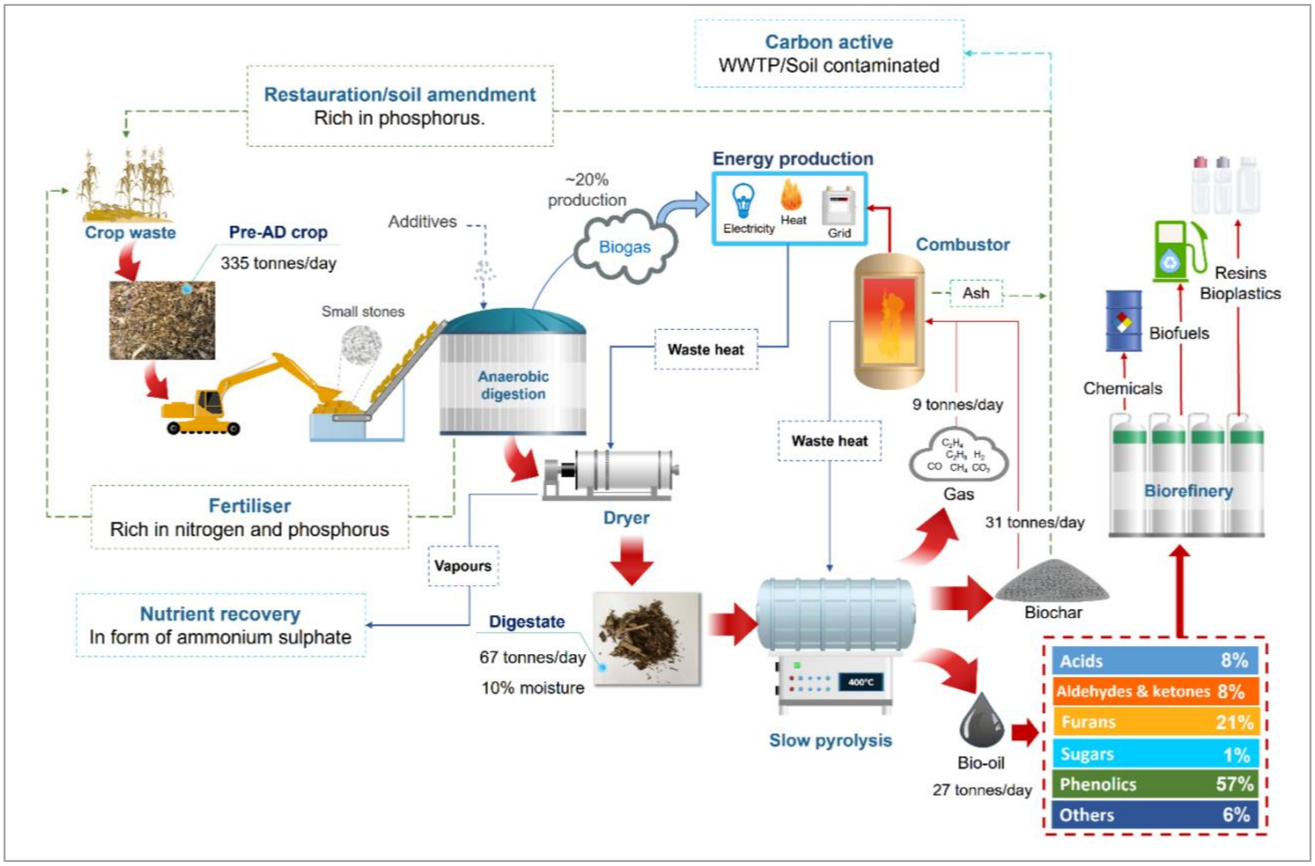
Carbon active
WWTP/Soil contaminated
Restauration/soil amendment
Rich in phosphorus.
Energy production
~20%
production
Electricity
Heat
Grid
Biogas
Additives
Crop waste
Pre-AD crop
335 tonnes/day
Small stones
Anaerobic
digestion
Combustor
Ash
Waste heat
9 tonnes/day
C_2H_4
C_2H_6 H_2
CO CH_4 CO_2
Gas
Waste heat
Resins
Bioplastics
Biofuels
Chemicals
Biorefinery
Fertiliser
Rich in nitrogen and phosphorus
Dryer
Vapours
31 tonnes/day
Biochar
Nutrient recovery
In form of ammonium sulphate
Digestate
67 tonnes/day
10% moisture
400°C
Slow pyrolysis
Bio-oil
27 tonnes/day
Acids 8%
Aldehydes & ketones 8%
Furans 21%
Sugars 1%
Phenolics 57%
Others 6%

Figure 72. Flow diagram of slow pyrolysis of digestate integrated AD system.

Slow pyrolysis products could have the same application as the fast pyrolysis system. 67 tonnes of digestate pyrolysed would result in 31 tonnes of biochar/day, 9 tonnes of gas and 27 tonnes of bio-oil. This pyrolytic bio-oil would contain a larger amount of phenolics, almost 60% wt of the total liquid.

8.1.3 MICROWAVE PYROLYSIS POST-AD

Microwave pyrolysis of digestate did not generate a significant amount of sugars. However, this could change if the biomass is treated differently by using non-ground material, for instance, to avoid surplus energy into the digestate and lead to secondary reactions.

In order to simulate this technology in a scaled-up system, Empyro’s configuration of processing 5 tonnes of digestate/hour was employed. The electricity required to operate microwave pyrolysis would be 20% more than the power input to pyrolyse the biomass. This estimation was based on a conversion of digestate into pyrolysis products for this technology from the experiment carried at around 4kJ/g of energy input with around 27% of bio-oil recovery. The total compounds of bio-oil resulting from 67 tonnes of digestate using microwave pyrolysis are shown in Table 73.

Microwave pyrolysis (digestate)		
5	tonnes biomass/hr (5% moisture)	
6	MW power input for pyrolysis	
7	MW_e, electricity for operation	
1.3	tonnes bio-oil/hr	
67	tonnes digestate/day (5% moisture)	
17	**tonnes bio-oil from digestate/day**	
Bio-oil composition		
Acids	5.29	tonnes/day
Aldehydes & ketones	3.46	
Alcohols	0.00	
Furans	2.34	
Sugars	0.07	
Phenolics	5.42	
Others	0.98	

Table 73. Projection of bio-oil composition produced from digestate generated on site per day with continuous process of microwave pyrolysis.

A diagram of microwave pyrolysis integrated into crop waste anaerobic digestion system is presented in Figure 73.

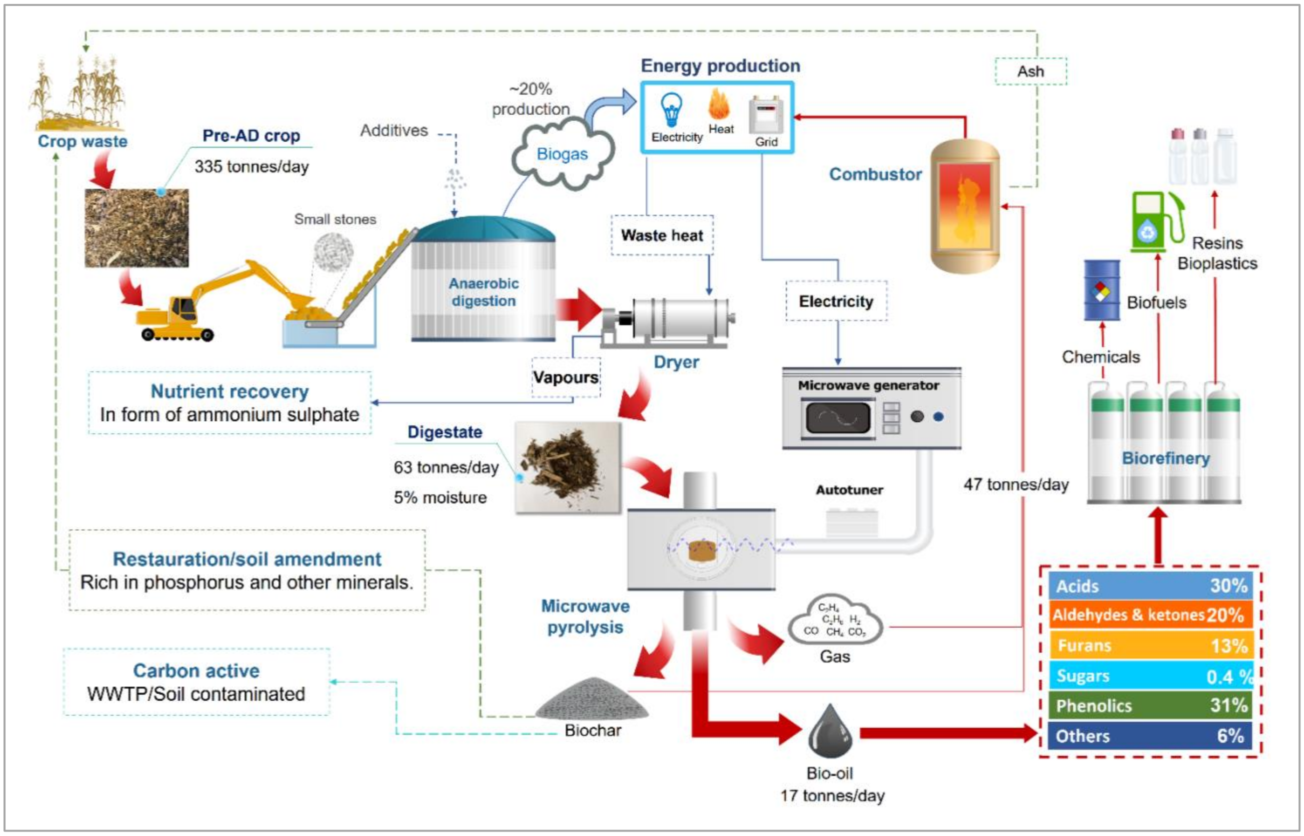
Crop waste
Pre-AD crop
335 tonnes/day
Additives
~20%
production
Biogas
Energy production
Electricity
Heat
Grid
Ash
Combustor
Small stones
Anaerobic
digestion
Waste heat
Electricity
Dryer
Vapours
Nutrient recovery
In form of ammonium sulphate
Digestate
63 tonnes/day
5% moisture
Microwave generator
Autotuner
47 tonnes/day
Resins
Bioplastics
Biofuels
Chemicals
Biorefinery
Restauration/soil amendment
Rich in phosphorus and other minerals.
Microwave
pyrolysis
C_2H_4
C_2H_6 H_2
CO CH_4 CO_2
Gas
Carbon active
WWTP/Soil contaminated
Biochar
Bio-oil
17 tonnes/day
Acids 30%
Aldehydes & ketones 20%
Furans 13%
Sugars 0.4 %
Phenolics 31%
Others 6%

Figure 73. Flow diagram of microwave pyrolysis of digestate integrated AD system.

Approximately 47 tonnes of biochar and gas would be generated from digestate treated with microwave pyrolysis in a scale-up system. This system would produce a bio-oil with 30% acids, 20% aldehydes and ketones, 13% furans, 0.4% sugars, 31% phenolics and 6% wt of other compounds. Due to being a relative new technology to be applied to large scale 30 x 200 kW microwave units would be needed to treat this waste, however microwave pyrolysis could be implemented to target high-value products by processing a smaller amount of digestate.

8.2 SCENARIO 2- PRE-AD

8.2.1 FAST PYROLYSIS PRE-AD

Experimental results of slow pyrolysis where pre-AD crop was used at around 500ºC could be considered as equivalent to the products that will be obtained when using fast pyrolysis. Acids might increase due to grinding and pelletising requirements to obtain the right particle size for optimum fast pyrolysis operation. The possible effects of this pre-treatment was described in Section 5.5 according to experiments performed where there was a noticeable difference between non-ground and ground pre-AD crop. Fast pyrolysis product of pre-AD crop in a larger scale system would result in the figures shown in Table 74.

Fast pyrolysis Empyro (pre-AD)		
5	tonnes biomass/hr (5% moisture)	
2.85	tonnes bio-oil/hr	
7.4	MW_{th} output (steam generation)	
650	kW_{e} output (steam generation)	
130	tonnes digestate/day (5% moisture)	
74	tonnes bio-oil from digestate/day	
Bio-oil composition		
Acids	3.5	tonnes/day
Aldehydes & ketones	17.8	
Alcohols	0.8	
Furans	17.9	
Sugars	8.8	
Phenolics	25.4	
Others	-	

Table 74. Projection of bio-oil composition produced from pre-AD crop generated on site per day with continuous process of pyrolysis based on Empyro production**.**

The amount of bio-oil from an industrial scale of pre-AD crop fast pyrolysis would be 74 tonnes per day. Acid production using pre-AD crop could be at least in 1% of the total bio-oil resulting in 3.5 tonnes/day due to the pre-treatment required. Sugar generation would be in greater amount than using digestate with almost 9 tonnes/day, which could be used for additional biofuel production. Although this waste has less water content than digestate it still contains around 60% moisture, which is high for a pyrolysis process and consequently should be dried. For optimal operation of fast pyrolysis the dry-solids content in biomass should at least 90% [53,54]. The general diagram proposed of fast pyrolysis to treat the pre-AD is presented in Figure 74.

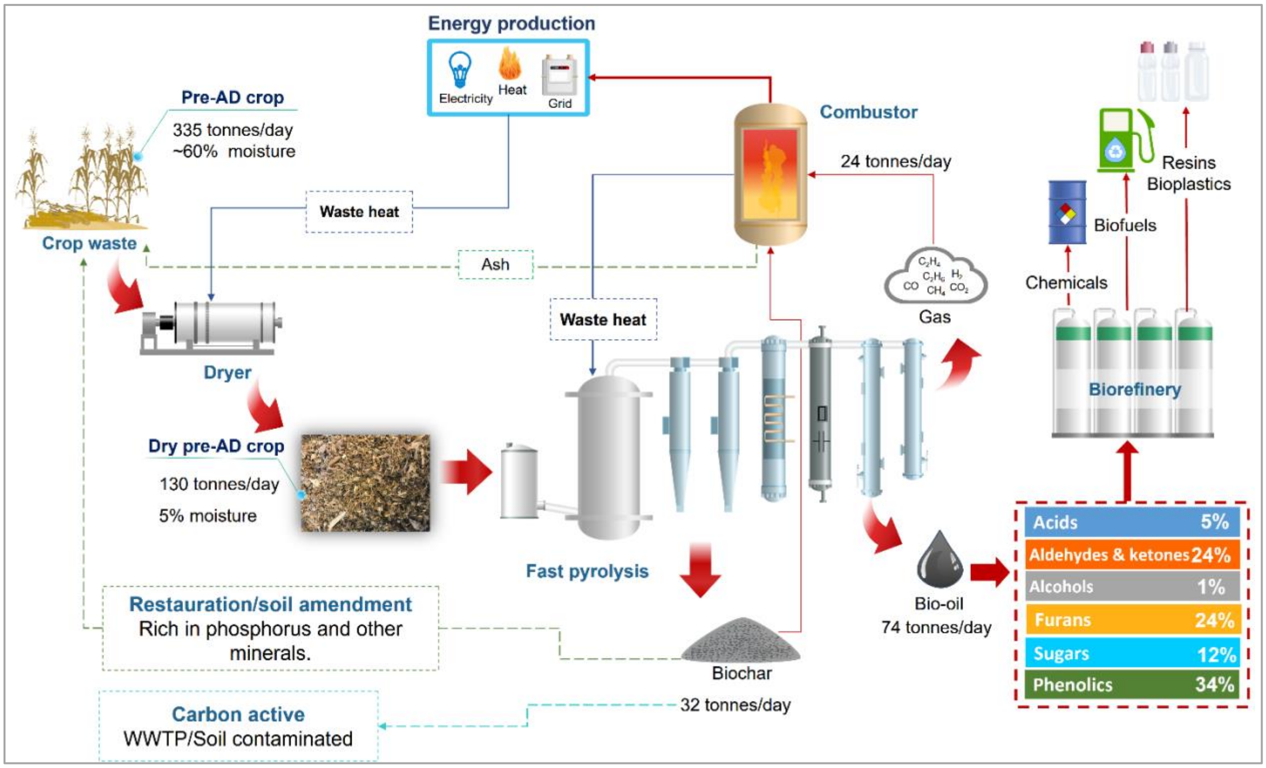
Energy production
Electricity
Heat
Grid
Pre-AD crop
335 tonnes/day
~60% moisture
Crop waste
Waste heat
Ash
Combustor
24 tonnes/day
Gas
C2H4
C2H6
H2
CO
CH4
CO2
Resins
Bioplastics
Biofuels
Chemicals
Biorefinery
Dryer
Waste heat
Dry pre-AD crop
130 tonnes/day
5% moisture
Fast pyrolysis
Bio-oil
74 tonnes/day
Acids 5%
Aldehydes & ketones 24%
Alcohols 1%
Furans 24%
Sugars 12%
Phenolics 34%
Restauration/soil amendment
Rich in phosphorus and other minerals.
Biochar
32 tonnes/day
Carbon active
WWTP/Soil contaminated

Figure 74. Flow diagram of fast pyrolysis of pre-AD.

130 tonnes of pre-AD crop would produce using fast pyrolysis 32 tonnes of biochar and 24 tonnes of gas per day. 74 tons of bio-oil would have a composition that consists of 5% acids, 24% aldehydes and ketones, 1% alcohols, 24% furans, 12% sugars and 31% wt phenolics.

8.2.2 SLOW PYROLYSIS PRE-AD

Slow pyrolysed bio-oil from pre-AD crop had one of the best qualities due to its high sugar content, one of the targets in pyrolysis for further biofuel generation. However, there is no scale-up system that includes condensable gases recovery that can be used to evaluate the amount of bio-oil which could be further processed into a biorefinery step. Beside this, the calculation of this technology to pyrolysed pre-AD crop was based on a similar analysis implemented in Section 8.1.2. This projection was on the basis of PYREG PX1500 conversion to treat 137 tonnes of dry pre-AD crop per day. The results of this estimation are presented in Table 75.

Slow PYREG PX1500		
5.7	tonnes biomass/hr (10% moisture)	
2.3	tonnes bio-oil/hr	
2.6	biochar/hr	
10306	kW$_{th}$ generation	
137	tonnes pre-AD crop /day (10% moisture)	
56	**tonnes bio-oil from pre-AD crop/day**	
Bio-oil composition		
Acids	-	tonnes/day
Aldehydes & ketones	14.1	
Alcohols	0.3	
Furans	14.2	
Sugars	7.0	
Phenolics	20.1	
Others	-	

Table 75. Projection of bio-oil composition produced from pre-AD crop at ~500ºC three units of PYREG PX1500.

Bio-oil would be produced with a composition in which only aldehydes & ketones, alcohols, furans, sugars and phenolics are present if the biomass is used with a pre-treatment that could alter the structure of the material which could lead to a high acid production, something did not occur using slow pyrolysis of pre-AD crop.

A general process that illustrates slow pyrolysis system to process pre-AD crop is shown in Figure 75.

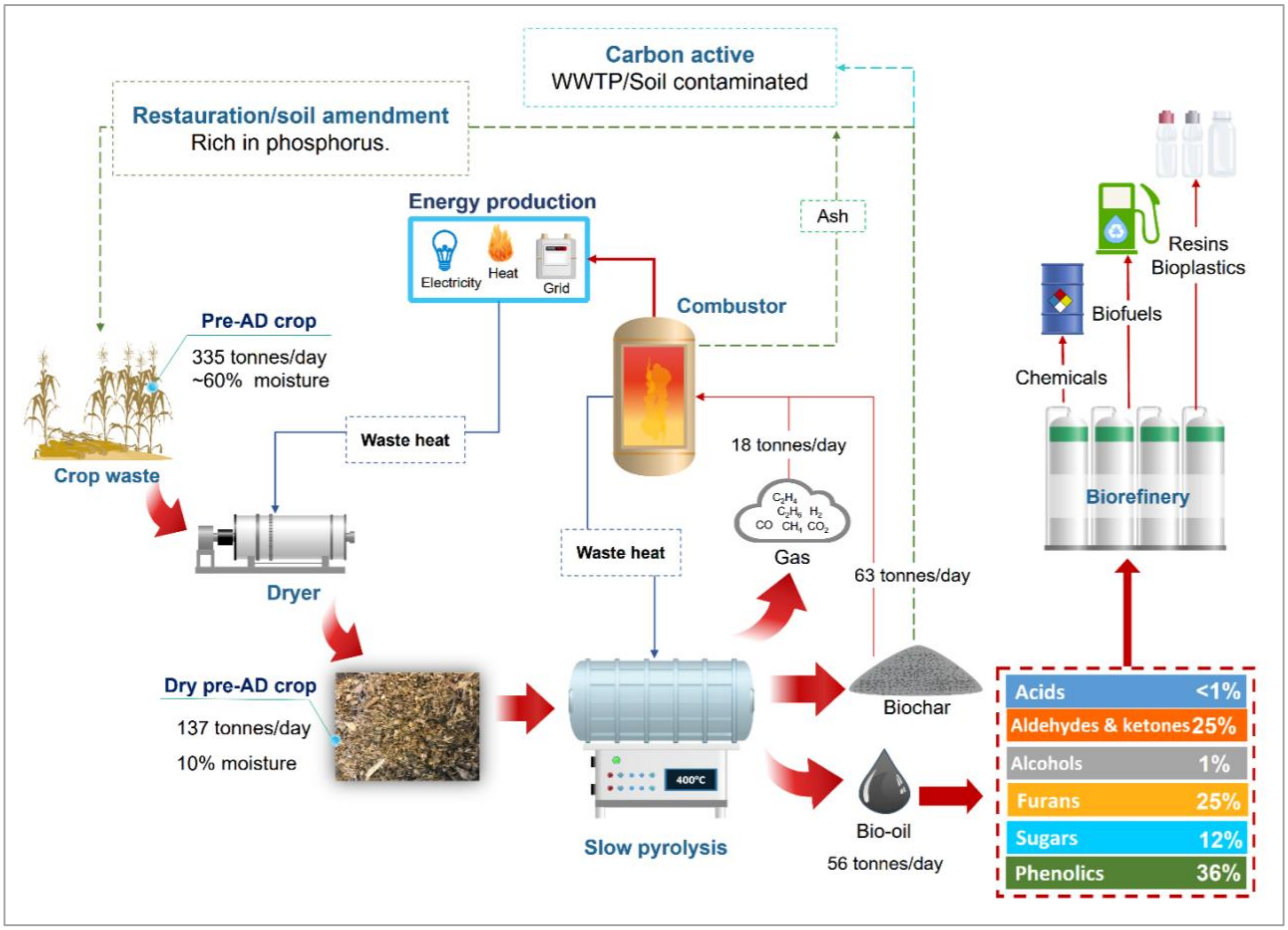
Carbon active
WWTP/Soil contaminated
Restauration/soil amendment
Rich in phosphorus.
Energy production
Electricity
Heat
Grid
Ash
Resins
Bioplastics
Biofuels
Combustor
Pre-AD crop
335 tonnes/day
~60% moisture
Chemicals
Waste heat
18 tonnes/day
Biorefinery
Crop waste
C_2H_4
C_2H_6 H_2
CO CH_4 CO_2
Gas
Waste heat
63 tonnes/day
Dryer
Dry pre-AD crop
137 tonnes/day
10% moisture
400°C
Biochar
Acids <1%
Aldehydes & ketones 25%
Alcohols 1%
Furans 25%
Sugars 12%
Phenolics 36%
Bio-oil
56 tonnes/day
Slow pyrolysis

Figure 75. Flow diagram of slow pyrolysis of pre-AD.

Conversion of pre-AD into pyrolysis products was based on the experimental work performed in slow pyrolysis rig, where 137 tonnes of pre-AD crop per day with 10% water content would produce 63 tonnes of biochar and 18 tonnes of gas. 56 tonnes of bio-oil generated would have a chemical proportion of less than 1% acids, 25% aldehydes and ketones, 1% alcohols, 25% furans, 12% sugar and 36% phenolics.

8.2.3 MICROWAVE PYROLYSIS PRE-AD

The experiments carried out using microwave pyrolysis with pre-AD crop were used to make projections of bio-oil production a larger scale. The evaluation of pyrolysis products with this technology and pre-AD crop used as feedstock is based on the same analysis conducted in Section 8.1.3. The results obtained in lab-runs for pyrolysis with between 3 and 4 kJ/g with bio-oil yield around 40% were used to calculate the proportion of bio-oil composition if the system is scaled-up. These results are shown in Table 76.

Microwave pyrolysis (pre-AD)		
5	tonnes biomass/hr (5% moisture)	
5	MW power input for pyrolysis	
6	MW_e, electricity for operation	
2	tonnes bio-oil/hr	
130	tonnes pre-AD/day (5% moisture)	
53	**tonnes bio-oil from pre-AD/day**	
Bio-oil composition		
Acids	23.3	tonnes/day
Aldehydes & ketones	8.6	
Alcohols	1.0	
Furans	11.7	
Sugars	1.5	
Phenolics	3.1	
Others	3.6	

Table 76. Projection of bio-oil composition produced from pre-AD crop generated on site per day with continuous process of microwave pyrolysis.

Bio-oil resulting in this projection would consist of as major compounds 23 tonnes of acids and almost 12 tonnes of furans per day. Sugars proportion would be low, however, this could increase if pre-AD crop is not ground. Acid production also would change without this pre-treatment and the proportion could be less that the figures projected.

The diagram of microwave pyrolysis of pre-AD crop and the products resulting is displayed in Figure 76.

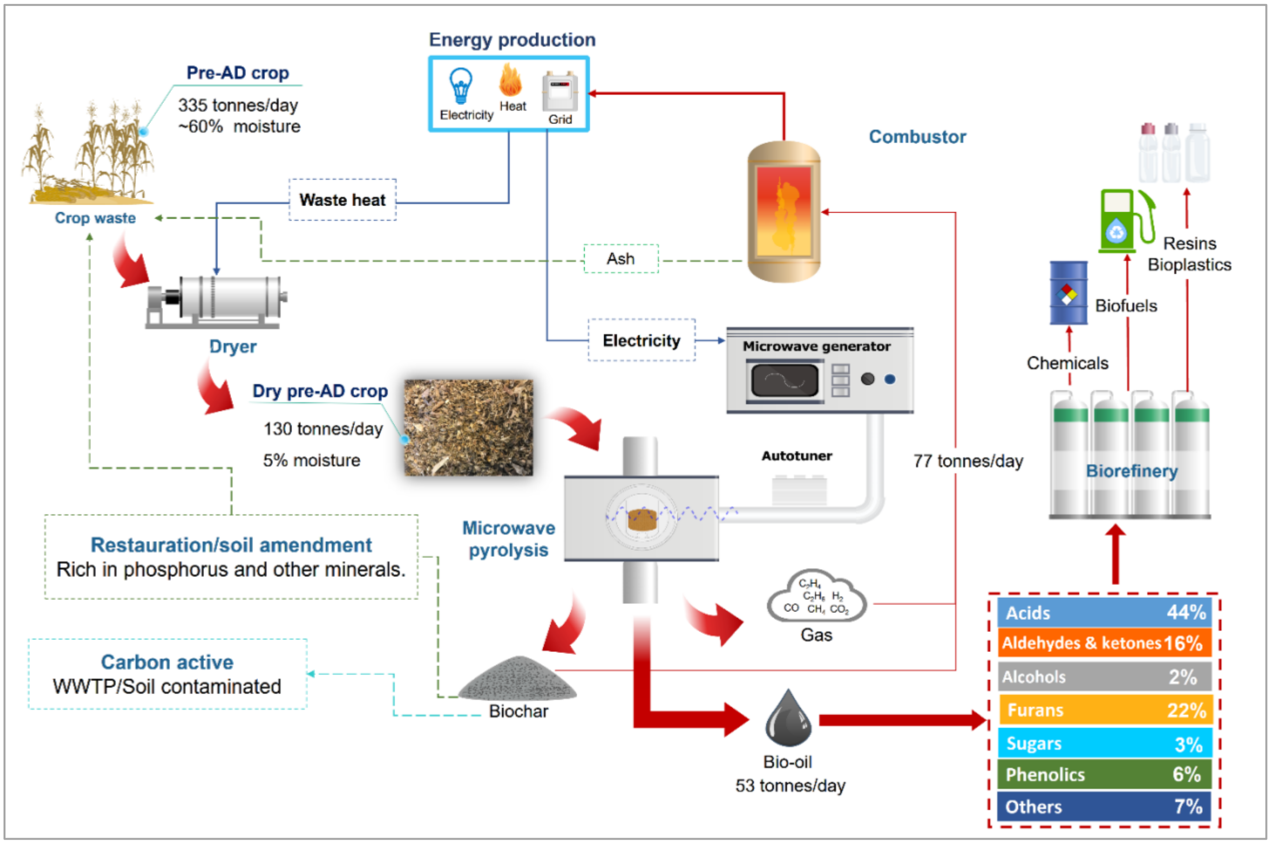
Energy production
Electricity
Heat
Grid
Pre-AD crop
335 tonnes/day
~60% moisture
Combustor
Waste heat
Crop waste
Ash
Resins
Bioplastics
Biofuels
Dryer
Electricity
Microwave generator
Chemicals
Dry pre-AD crop
130 tonnes/day
5% moisture
Autotuner
77 tonnes/day
Biorefinery
Microwave
pyrolysis
Restauration/soil amendment
Rich in phosphorus and other minerals.
C_2H_4
C_2H_6 H_2
CO CH_4 CO_2
Gas
Carbon active
WWTP/Soil contaminated
Biochar
Bio-oil
53 tonnes/day
Acids 44%
Aldehydes & ketones 16%
Alcohols 2%
Furans 22%
Sugars 3%
Phenolics 6%
Others 7%

Figure 76. Flow diagram of microwave pyrolysis of pre-AD crop.

130 tonnes of pre-AD treated through microwave pyrolysis would produce 53 tonnes of bio-oil and 77 tonnes of biochar and gas. Bio-oil composition would contain 44% acids, 16% aldehydes and ketones, 2% alcohols, 22% furans, only 3% and 6% of sugars and phenolics respectively.

Further analysis is needed to determine how these products can be used in a biorefinery, and the amount of gas produced, and its corresponding composition would be required to calculate the possible energy recovered to use it to supply the microwave system.

8.3 SCENARIO 3. DEPOLYMERISATION OF CELLULOSE AND HEMICELLULOSE IN DIGESTATE TO INCREASE BIOGAS PRODUCTION

The anaerobic digestion (AD) system at the crop energy site in Stoke Bardolph has around 20% production of biogas, a similar proportion of the organic compounds which the microorganisms could consume from the AD initial material. Pre-AD crop has a general composition around 16% cellulose, 35% hemicellulose, 15% lignin, 29% starch and 4% ash. The digestate resulting from this crop waste after it goes through the AD system has just under 30% less organic material than the initial crop. The general balance is represented in Figure 77, where the most noticeable change is the amount of starch in post-AD.

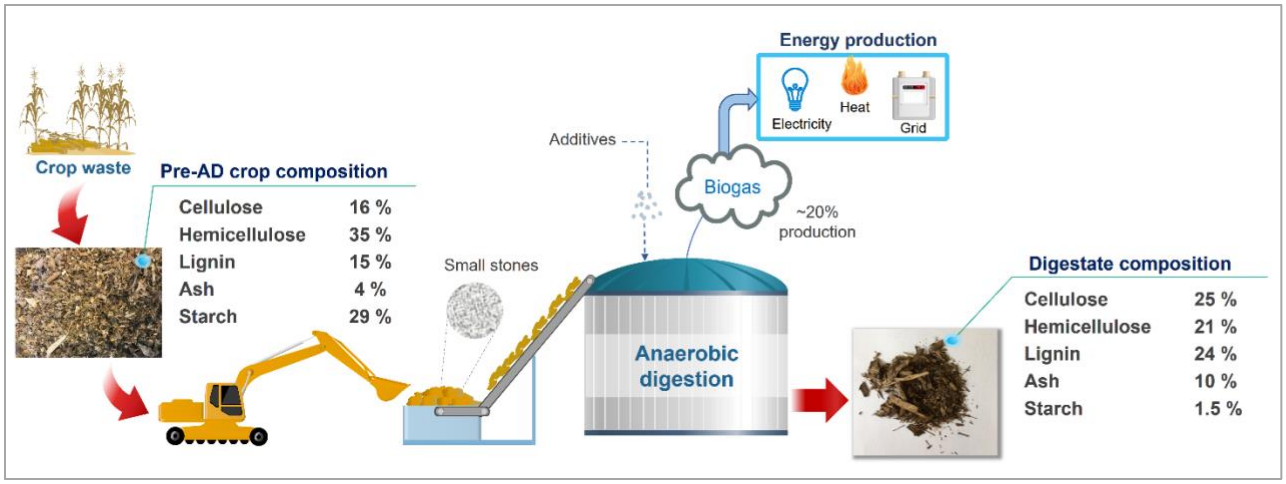
Energy production
Electricity
Heat
Grid
Additives
Biogas
~20% production
Crop waste
Pre-AD crop composition
Cellulose 16 %
Hemicellulose 35 %
Lignin 15 %
Ash 4 %
Starch 29 %
Small stones
Anaerobic digestion
Digestate composition
Cellulose 25 %
Hemicellulose 21 %
Lignin 24 %
Ash 10 %
Starch 1.5 %

Figure 77. General diagram representing pre-AD crop composition and waste crop composition post AD process.

The cellulose composition across the AD process does not change. Some of material the from hemicellulose seems to be easily consumed by microorganisms, but the majority of it was also found in the digestate. If lignocellulosic material content in pre-AD crop was broken down into monosaccharides, the composition would be like the results shown in Table 77, where around 30% of total glucose is starch.

Compound	% wt
Glucose	45
Xylose	17
Arabinose	9
Galactose	9
D-galacturonic acid	3
Lignin	14
Ash	4

Table 77. Pre-AD crop composition broken down into total monosaccharides from cellulose, hemicellulose, and starch.

Around 30% starch, 1% of arabinose, 1% of galactose and 0.4% of D-galacturonic acid were the differences between composition of the initial crop, and the digestate, and these might be the compounds most easily consumed by the microorganisms in the AD system. The illustrative balance of these monosaccharides is presented in Figure 78.

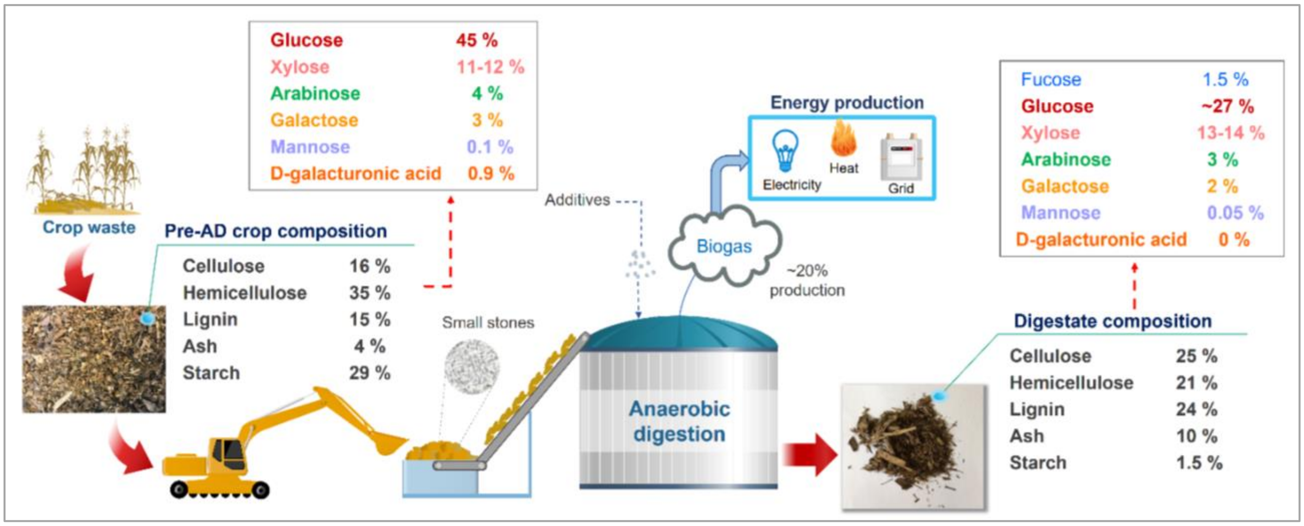

Glucose 45 %
Xylose 11-12 %
Arabinose 4 %
Galactose 3 %
Mannose 0.1 %
D-galacturonic acid 0.9 %
Crop waste
Pre-AD crop composition
Cellulose 16 %
Hemicellulose 35 %
Lignin 15 %
Ash 4 %
Starch 29 %
Additives
Small stones
Energy production
Electricity
Heat
Grid
Biogas
~20% production
Anaerobic digestion
Fucose 1.5 %
Glucose ~27 %
Xylose 13-14 %
Arabinose 3 %
Galactose 2 %
Mannose 0.05 %
D-galacturonic acid 0 %
Digestate composition
Cellulose 25 %
Hemicellulose 21 %
Lignin 24 %
Ash 10 %
Starch 1.5 %

Figure 78. General diagram representing composition of pre-AD crop and digestate in monosaccharides content.

These results presented show that glucose is the main source for biogas generation. If digestate is thermally treated to break down the final lignocellulose content into sugars, then this could be employed to produce more biogas.

This is a proposal for a third scenario to extend the use of digestate, where an intermediate thermal treatment could be an alternative route for more bioenergy production. Additionally, the same AD system set up on site could be used, including the same inoculum, which would consume mainly glucose. Biogas production could increase from around 20% to 30-35% after 60 days with these extra sugars.

There are two possible options for crop and food waste digestate in this third scenario. One is the extraction of sugar by microwave processing, where mainly hemicellulose would be reduced down into xylose, arabinose and galactose. This material requires less energy to be broken down than cellulose which would require and additional treatment if it is also depolymerised. Sugars from hemicellulose could increase the biogas yield from 10% to 20%.

Coleshill food waste plant processes the waste as received, including packaged food. Through a screw conveyor this waste is fed into the AD system for biogas production. Food waste digestate resulting from this AD was collected. It had 50% moisture content, with a large amount of small pieces of plastics, and with remaining organic matter. Examples of the samples collected, and plastics found are shown in Figure 79.

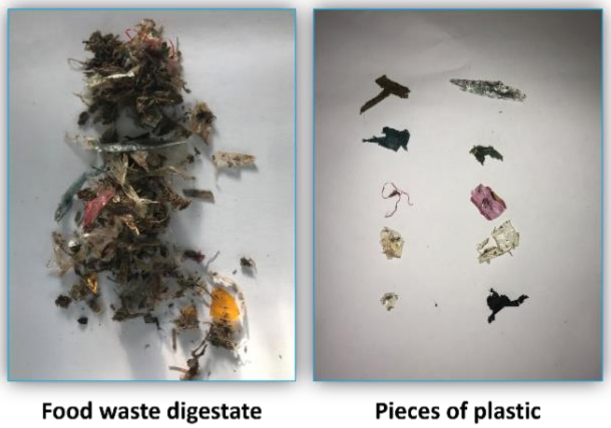

Figure 79.. Food digestate collected from Coleshill site.

These samples were also analysed to determine possible residual monosaccharides the microorganisms did not consume during the AD process. The analysis results revealed that this digestate has approximately 4g of sugars in 30g of sample so this could also be used as a source for more biogas generation. The main sugar analysis in this food digestate was based on glucose, xylose, galactose, and arabinose identification. The quantification of these compounds is presented in Table 78.

Sugar	wt %
Glucose	6.59
Xylose	3.09
Arabinose	1.39
Galactose	1.34
Total sugars	**12.42**

Table 78. Sugar composition of food waste digestate collected from Coleshill energy site.

Despite the fact that this digestate collected contains plastics, it is possible to extract sugars from the organic remains as a source for the microorganisms to convert into biogas. The current system is set to separate solids from the liquid, and this liquid is used as fertiliser under PAS110 regulations, yet this water could be recirculated into the digester after the extraction of the monosaccharides, which are soluble in water. This AD system has a conversion of 10% from organic matter into biogas, where for every 5 tonnes of raw waste added into the AD system 4.5 tonnes of digestate are produced. This might change according to the waste fed.

In both cases, crop and food digestate could be treated using microwave heating whilst still wet to hydrolyse the polysaccharides and produce more sugars l [181]. This liquid can be returned into the digester which would be a sugar-rich recirculation. Additionally, the remaining crop digestate without hemicellulose could then be used as a fertiliser, processed through further hydrothermal treatment or pyrolysed, and more lignin could then be transformed into other valuable products. However, the use might apply solely to crop digestate due to the plastics content in residual food digestate, and combustion may be the only realistic route for this waste in the short term. An illustration of how this digestate treatment could be implemented is presented in Figure 80.

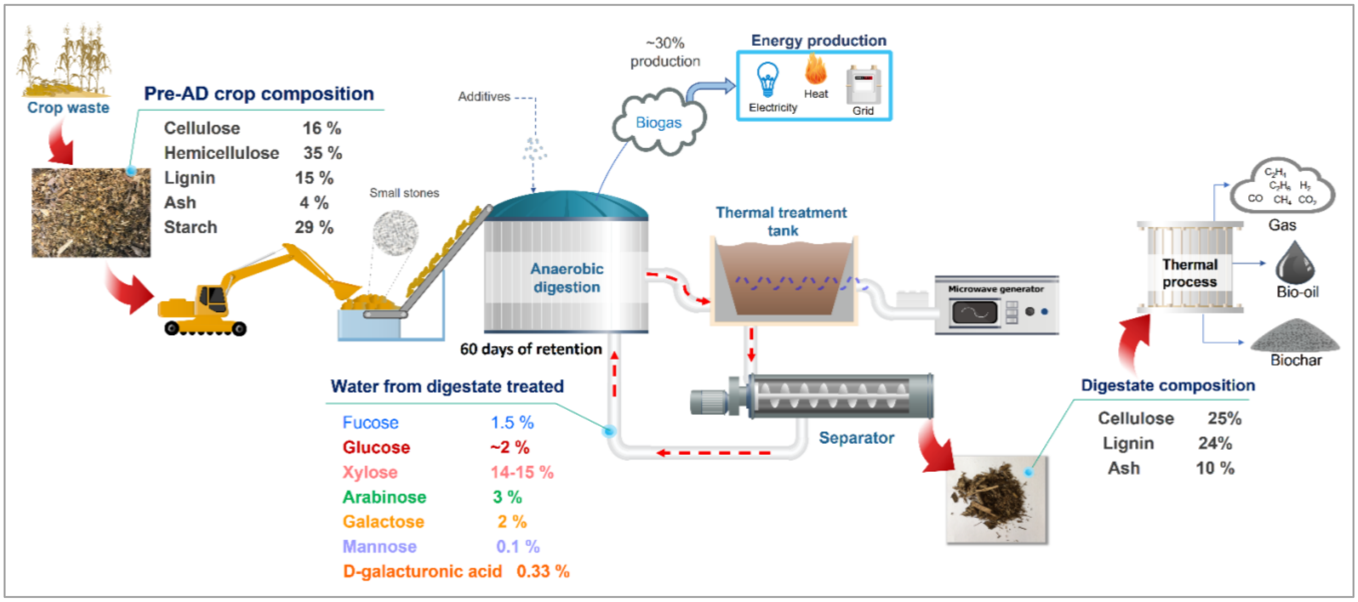
Crop waste
Pre-AD crop composition
Cellulose 16 %
Hemicellulose 35 %
Lignin 15 %
Ash 4 %
Starch 29 %
Small stones
Additives
~30% production
Biogas
Energy production
Electricity
Heat
Grid
Anaerobic digestion
60 days of retention
Thermal treatment tank
Microwave generator
Separator
Water from digestate treated
Fucose 1.5 %
Glucose ~2 %
Xylose 14-15 %
Arabinose 3 %
Galactose 2 %
Mannose 0.1 %
D-galacturonic acid 0.33 %
C_2H_4
C_2H_6 H_2
CO CH_4 CO_2
Gas
Thermal process
Bio-oil
Biochar
Digestate composition
Cellulose 25%
Lignin 24%
Ash 10 %

Figure 80. General diagram representing crop digestate thermal treated to extract additional sugars from hemicellulose and sugar-rich water recirculation into digester for more biogas production. Residual digestate solids could then be processed in thermal technologies.

The second option is a 2-step digestate treatment. Hemicellulose and cellulose are decomposed at different ranges of temperature, and treating them using the same approach would lead to other reactions - xylose for instance, can be converted into furfural if the temperature is higher than required [181]. As a result, the post-AD treatment proposed consists of hemicellulose sugar extraction by microwave hydrolysis, followed by enzymatic depolymerisation of cellulose into glucose. There are current studies of the decomposition of cellulose into simple sugars by enzymes called cellulases, such as Endo-1,4-β-glucanases and β-glucosidases [182,183]. The digestate could be washed out to recover the solution and to return another rich-sugar solution into the AD system. The total conversion from organic material contained in the original crop waste into biogas product would be around 30%, which might be the total sugars consumed by the microorganisms. The residual crop digestate would be then a lignin-rich biomass. According to the experiments performed on pyrolysis of digestate, ash content in waste did not have a negative effect on phenolics production and lignin was easier thermochemical decomposed.

The general process of this proposed system is represented in in Figure 81.

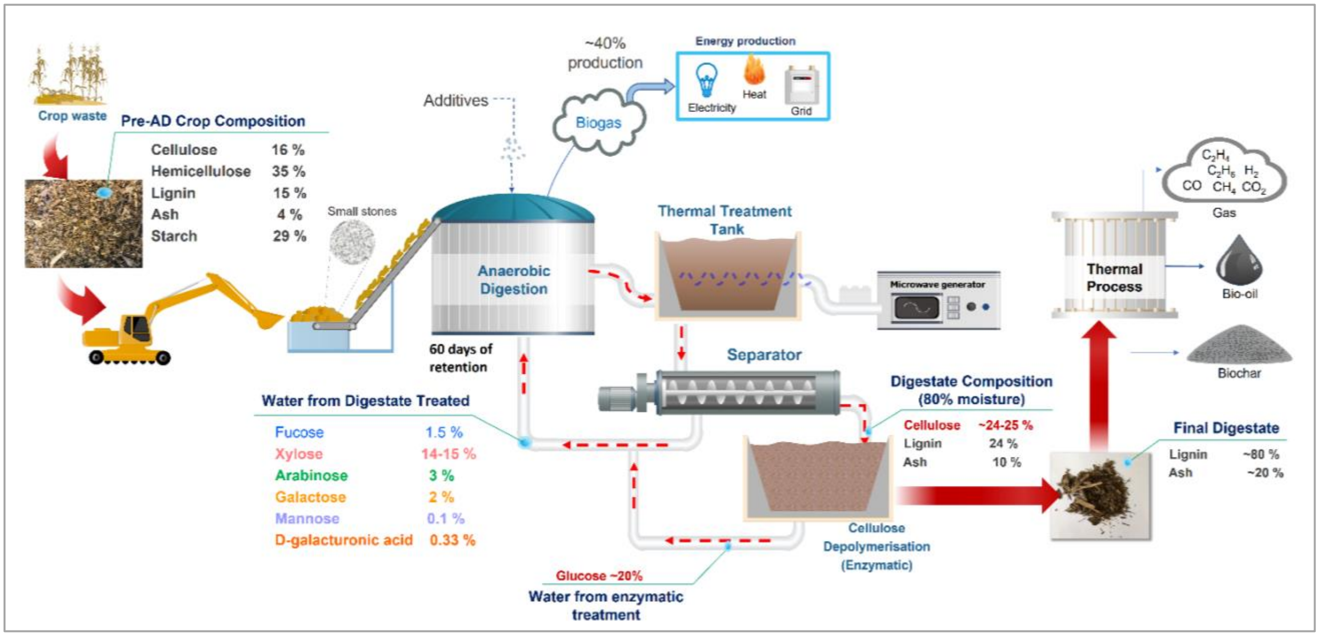
~40%
production
Energy production
Electricity
Heat
Grid
Additives
Biogas
Crop waste
Pre-AD Crop Composition
Cellulose 16 %
Hemicellulose 35 %
Lignin 15 %
Ash 4 %
Starch 29 %
Small stones
Anaerobic Digestion
60 days of retention
Thermal Treatment Tank
Microwave generator
Separator
Water from Digestate Treated
Fucose 1.5 %
Xylose 14-15 %
Arabinose 3 %
Galactose 2 %
Mannose 0.1 %
D-galacturonic acid 0.33 %
Digestate Composition (80% moisture)
Cellulose ~24-25 %
Lignin 24 %
Ash 10 %
Cellulose Depolymerisation (Enzymatic)
Glucose ~20%
Water from enzymatic treatment
C_2H_4 C_2H_6 H_2 CO CH_4 CO_2
Gas
Thermal Process
Bio-oil
Biochar
Final Digestate
Lignin ~80 %
Ash ~20 %

Figure 81. General diagram representing crop digestate 2-step treatment to extract additional sugars from cellulose and hemicellulose and return sugar-rich liquid into the digester for more biogas production. Residual digestate solids could then be processed in thermal technology to produce pyrolytic lignin derivatives.

These digestates derived from food and crop waste are still high-value biomasses due to the large amount of carbohydrates contained within them. The biogas produced from the original waste is not the only green product this waste can produce. Although ash could be an impediment to have large amounts of primary compounds in bio-oil when it is treated through pyrolysis, it will depend on the market pyrolytic products could be used for as sugars are not the only biochemical can be employed for further bio-based products. However, the alternative route of extracting these lignocellulosic compounds could increase the value of both waste. The option presented in this work about the depolymerisation could be a feasible alternative to increase biogas production in AD plants due to most of the infrastructure being already on the site, and rather than only utilise 10% wt and 20% wt of the original food and crop waste respectively, it is possible to recover of the total mass fed into the AD system 20% wt from food waste and almost 60% from crop waste if microbiological methods are implemented. Although, this industrial amount of waste could be challenging to treat to only enrich the sugar content of the liquid product, it might be the case that only some of this waste could be used for further biogas conversion. These types of methods are low energy consumption, and breaking down these biopolymers, including the lignin, can also be useful for other chemical production if it is not implemented into the AD recirculation. Extraction of these polymers for uses could be one of the best routes proposed to increase the circularity of this waste, but also co-processing where some of the waste is treated though pyrolysis and the rest to breakdown biopolymers for green biobased products.

8.4 POSSIBLE USES OF PYROLYSIS PRODUCTS

Biochar and non-condensable gases, for instance, can be employed to generate more energy and be used for the pyrolysis process. Additionally, if there is an excess of heat produced this could be used in the AD system. Most of the anaerobic digestion processes have a set-up to produce energy from biogas and be converted to heat and electricity or supplied to the gas grid.

Pyrolysis needs as initial stage a drying system which results in effluents that can be recovered for further use such as nutrient recovery. Pyrolytic bio-oil could be used in a biorefinery scheme where further chemicals, biofuels and resins could be produced. A brief description of other uses for pyrolysis products is presented in the next Section.

8.4.1 BIOCHAR

Biochar can also be employed as soil amendment and soil structure improver. Studies performed by Yoo et al. [184] showed that soil mixed with biochar improved drainage when excessive water was added, but maintained enough liquid for plants to grow. However, further analysis is needed into whether it can be used as a soil improver, and whether this biochar meets the appropriate regulations to be spread on soil. This pyrolysis product can contain polycyclic aromatic hydrocarbons (PAH) and these could be passed into plants and have a negative impact on the food chain due to carcinogenic characteristics. These aromatics could be produced in any thermochemical conversion of biomass in absence of oxygen [185-187]. Then, in order for char be employed as soil improver, some analyses such as PAH quantification (DIN EN 15527: 2008-9), water holding capacity (DIN EN ISO 14238), trace metals levels (DIN 22022-2 - DIN 22022-7), and others are needed. Consequently, biochar would need further treatment to meet this purpose. In addition, this digestate and others from different waste are currently used as fertiliser and improvement of soil nutrient and meet British Standard Institution PAS 110, which is fundamental for digestate specification as biofertilizer. It is important to evaluate the cost of this treatment in order to balance the total cost of only producing biochar as a target.

Another additional use is as activated carbon. Due to continuous socioeconomic growth, water streams in the world are being negatively impacted with large amounts of contaminants. There are opportunities to improve current conventional waste treatment plants (WWTPs), which are facing challenges. Micropollutants, for instance, cannot be entirely removed from water, but active carbon has properties to absorb these chemicals and improve the quality of water. It has been found that biochar from these pyrolysis technologies requires low costs for activation and it becomes greatly adsorbent [188,189]. This biochar could have an equivalent purpose for contaminated soils as a pollutant remover. There is an additional application, similar to wastewater but to clean gas streams for example as H_2S adsorbent due to physiochemical properties such as pore volume, surface area and alkaline surface [190]. A schematic of possible uses of biochar produced from pyrolysis is presented in Figure 82.

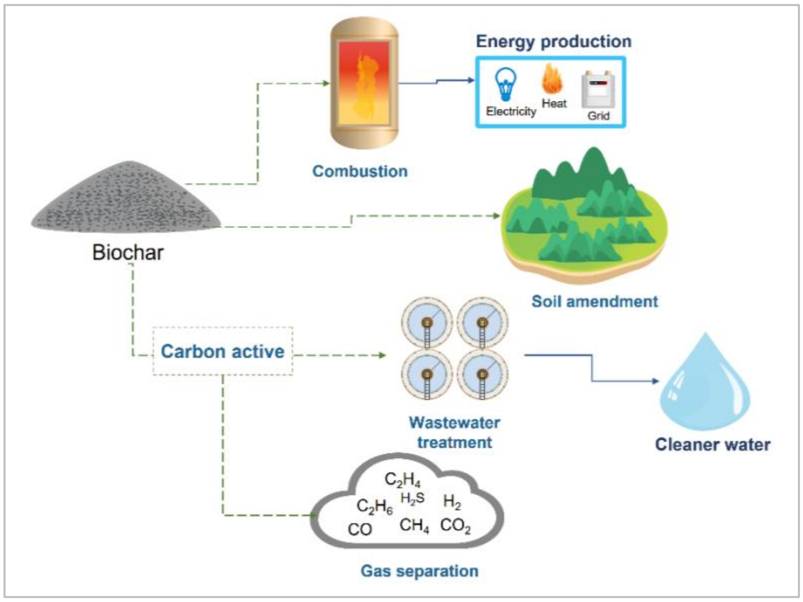
Energy production
Electricity
Heat
Grid
Combustion
Biochar
Soil amendment
Carbon active
Wastewater treatment
Cleaner water
C_2H_4
C_2H_6
H_2S
H_2
CO
CH_4
CO_2
Gas separation

Figure 82. Alternative uses for biochar.

8.4.2 GAS

In AD systems the main target product is the biomethane for energy production. This is produced with others, such as CO_2, some traces of hydrogen sulphide (H_2S), and some water vapour [191-193]. Thus, methane and CH_4 and C2+ gases generated from pyrolysis can be employed in the same way since some energy plants already have systems with this operation to upgrade biogas to biomethane. This can then be integrated into the grid or for energy generation in the site. Although CO_2 and CO are around 90% of this gas, there are other alternatives to use these gases.

If the CO_2 and CO are separated from the other gases, which could be by activated carbon with biochar [194] or membranes [195], these can be a source for biomaterial production through microbes. Studies have been carried with microorganisms that consume CO_2 to produce biopolymers. Cestellos-Blanco et al. [196] proposed 2-step system where electrochemical technologies are combined with microorganisms and CO_2 could be consumed to produce a biopolyester known as poly(3-hydroxybutyrate) (PHB). Sporamusa ovata is used to convert this gas into acetate to then Cupriavidus basilensis use this compound to produce PHB. Other studies consider microalgae a bioprocessing for biohydrogen production using as inorganic carbon CO_2 [197]. A possible scheme of gas uses is presented in Figure 83.

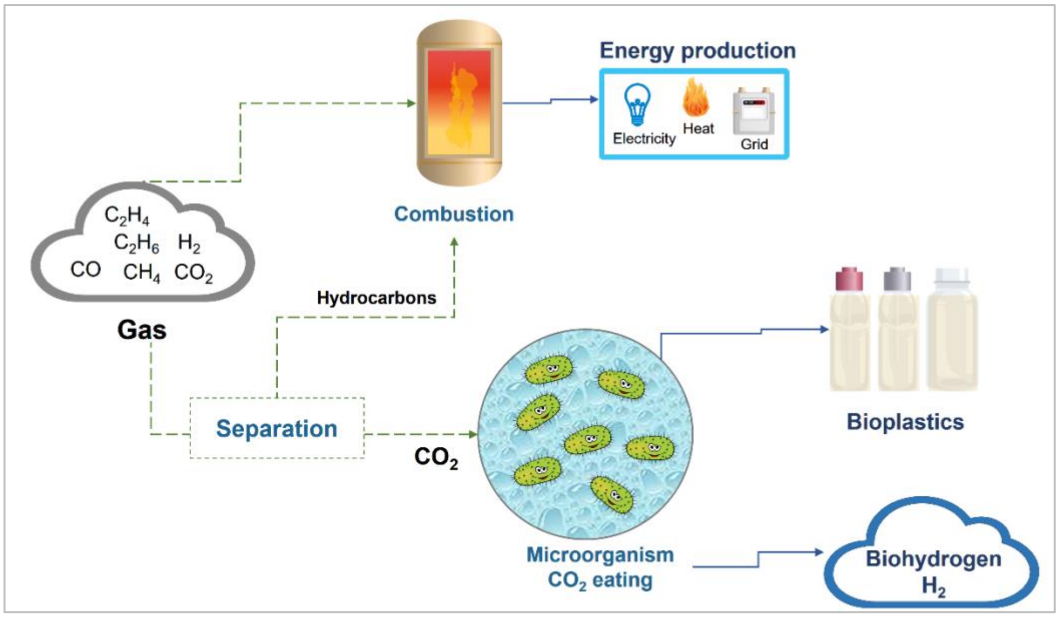
Energy production
Electricity
Heat
Grid
Combustion
C_2H_4
C_2H_6 H_2
CO CH_4 CO_2
Gas
Hydrocarbons
Separation
CO_2
Bioplastics
Microorganism
CO_2 eating
Biohydrogen
H_2

Figure 83. Alternative uses for pyrolytic gas.

These are just alternatives (Figure 83) that could be employed to mitigate some of the CO_2 produced from any pyrolysis technology. Some of these methods are still under research which will take more time to understand if this is possible to implement in large scale.

If hypothetically these non-hydrocarbon gases could be used separately, then hydrocarbons can be employed for energy production or to be integrated into the gas grid. The amount of these gases from pyrolysing 63 tons of digestate/day in a fast pyrolysis system would result in the amount presented in Table 79.

Fast pyrolysis gas				
Compound	**460°C**	**480 °C**	**520 °C**	**560 °C**
Hydrogen, H_2	2.29	3.15	10.89	16.63
Methane, CH_4	61.93	128.30	173.31	171.88
Ethane, C_2H_6	19.07	22.08	36.27	43.15
Ethylene, C_2H_4	10.46	11.32	22.36	32.54
Propane, C_3H_8	3.73	8.74	11.90	13.04
Propylene, C_3H_6	7.88	14.05	25.52	35.55
Acetylene, C_2H_2	0.00	1.00	1.00	1.15
Iso-Butane, I-C_4H_{10}	0.00	0.72	0.86	1.00
Propadiene, C_3H_4	0.00	0.00	0.14	0.14
N-butane, N-C_4H_{10}	0.00	2.15	2.58	2.58
Trans-2-Butene, Trans-2-C_4H_8	0.00	1.58	2.44	3.15
Isobutene, I-C_4H_8	0.00	3.30	4.73	6.02
Isopentane, I-C_5H_{12}	0.00	0.57	0.57	0.57
Pentane, N-C_5H_{12}	0.00	0.57	0.57	0.72
1.3-Butadiene, 1.3-C_4H_6	0.00	1.43	3.73	6.59
1-pentene, 1-C_5H_{10}	0.00	1.15	1.86	2.15
Benzene, C_6H_6	0.00	2.72	59.63	0.14
Toluene, C_7H_8	0.00	3.44	13.91	2.87
C-4	0.00	4.30	7.45	10.46
C-5	0.00	2.58	4.44	6.59
C-6	0.00	12.90	21.79	27.81
C-7	0.00	1.29	2.15	2.58
Total gas (kg/day)	**105.36**	**227.35**	**408.12**	**387.33**

Table 79. Kilograms of hydrogen and hydrocarbon gases per day resulted from scaled-up fast pyrolysis from crop digestate.

Although the amount of these gases seems to be very small compared with CO_2 and CO, they can be used and increase the value of the overall conversion AD waste.

8.4.3 BIO-OIL

The Empyro project has a range of applications for the bio-oil, such as biofuels and biobased products. Due to the characteristics of bio-oil derived from digestate, biobased products could be the best route if this pyrolysis is implemented where the bio-oil can be fractionated in extractives, lignin, pyrolytic sugars, and organic acids. Bio4products, a company which has developed techniques to use bio-oils for further products, has designed a process where phenolics can be used to form resins, including foams. Pyrolytic sugars have also been also employed for PFA (Polyfurfuryl Alcohol) bioresins production by TransFurans Chemicals, company that has been produced some chemicals derived from renewable raw material.

In the third scenario ash content could be considered as positive factor as it promotes lignin depolymerisation, and pyrolysing lignin might require less energy to form phenolics. Pyrolysis of a whole lignocellulosic material to produce bio-oil is a complex thermochemical conversion, and difficult to stabilise. These bio-oils produced from digestate are acid-rich liquids due to the secondary reactions, resulting in less cellulose and hemicellulose primary derivatives. However, recovering sugars from holocellulose final crop digestate would become a rich-lignin biomass and it could be used to produce other products such as bio-asphalt or bio-resins, as it has been found that lignin-derived compounds could increase adhesive properties [198,199]. Possible uses of bio-oil are represented through Figure 84.

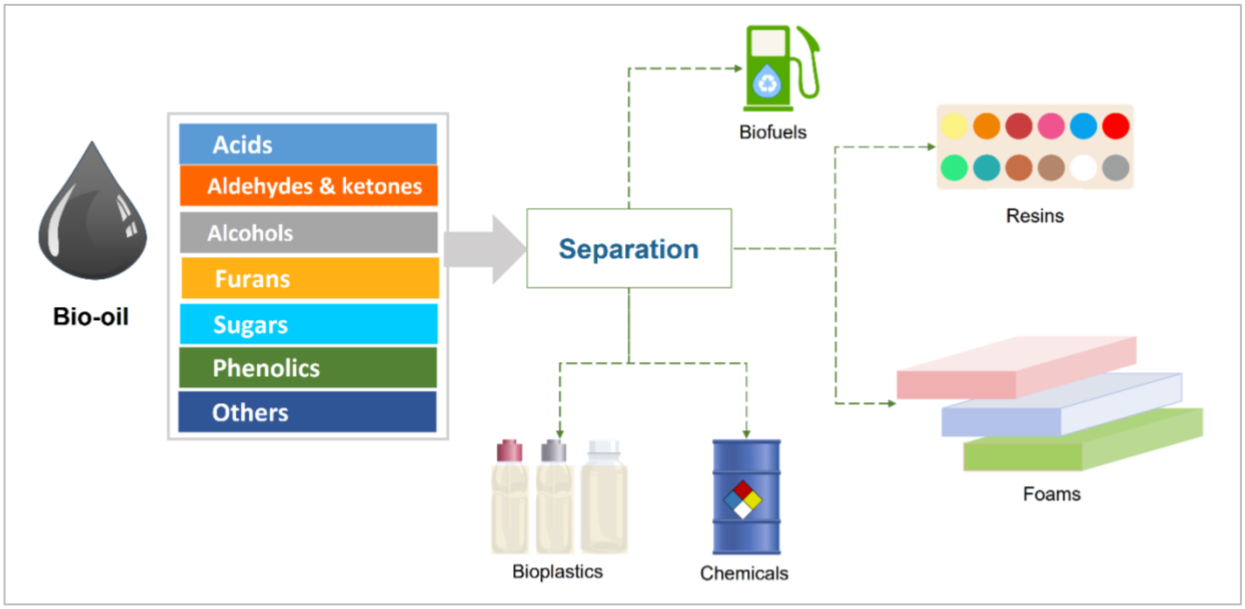

Figure 84. Alternative uses for pyrolytic bio-oil.

These different scenarios proposed for thermochemical conversion of this waste give alternatives to extend its use as full without refuse any stream of the process. Biorefinery concept is still a high-cost implementation, the more steps the process requires the higher the investment will be to obtain pure chemicals for further bioproducts. However, this study is with the purpose to have a general view of what would happen if the amount of pre-AD crop and digestate available are pyrolysed in large scale, and the implications of a high-ash biomass has in these systems.

CHAPTER 9. CONCLUSIONS AND RECOMMENDATIONS

Anaerobic digestion (AD) systems require a large amount of feedstock to produce a relatively small amount of bioenergy product. Systems studied in this work identified that a maximum around 20-30% of typical biomass waste is converted into biogas, resulting in large amounts of digestate remaining. Based on an overall waste characterisation around the AD process it was found that the residual material contained high-value components that can be useful for further treatment to produce more bioenergy or biobased chemicals/biomaterials. Pyrolysis technologies were studied as both additional and alternative process routes to attempt to maximise the value from waste biomass used in AD systems.

Chemical analysis of crop waste (pre-AD) and the resulting digestate revealed both had a high content of biopolymers classified as starch, cellulose, hemicellulose and lignin, making this a high-carbohydrate feedstock. Pre-AD crop contained around 46% D-glucose, 30% derived from starch and 16% from cellulose. Hemicellulose and lignin content were 36% and 15% respectively, and around 4% wt ash was quantified. Dry digestate only contained 2% starch and around 20% hemicellulose, which suggests that the microorganisms use this material as a main source for AD biomethane production. 23% of this digestate was cellulose, 22% lignin and around 10% wt ash. The increase in ash from pre-AD to digestate was as a result of additives going into the digester to maintain the medium in optimum conditions, and not only because of the organic material consumed by the microbes. Ash quantification had a substantial variation across every sample collected, which had a significant effect on the pyrolysis products.

Pyrolysis of digestate showed large differences between different pyrolysis technologies. Slow pyrolysis bio-oil had a considerable amount of water with a range of 13-19% wt of the total products at operating temperatures of 355-530ºC. From the experimental data it is possible to suggest that to obtain higher yield of bio-oil operating temperatures should be higher than 400ºC, as pyrolysis performed below this temperature leads to less bio-oil production and more biochar formation. Chemical composition of bio-oil indicated compounds derived from cellulose and hemicellulose experienced secondary reactions. Although some sugars were identified in bio-oils, levoglucosan and furfural were not detected in this analysis. Other compounds such as 2-Cyclopenten-1-one and 2-Furanmethanol were detected that could result from the decomposition of the primary pyrolysis products. High acetic acid composition in the bio-oil also indicated that secondary decomposition had taken place. Additionally, acetic acid levels were shown to vary significantly between each sample analysed, even at the same process conditions.

These analytical outcomes were also linked with gas composition, where CO_2 and CO levels changed from sample to sample. Due to these findings it is presumed that each batch of digestate loaded into the reactor had a different ash content, which subsequently affected product composition.

Biochar, bio-oil and gas product from fast pyrolysis using digestate showed a consistent distribution across the experiments, but the chemical composition of bio-oil varied from one operating temperature to another. Although the amount of water was small (11%) compared with slow pyrolysis, acids were found in greater amounts from 6% to 24% wt, where acetic acid was the predominant compound. Fast pyrolysis of digestate produced more sugars, where levoglucosan contributed the highest portion quantified, reaching almost 2% wt. However, sugar yields were quite low compared with other tests performed in the same apparatus with low-ash biomasses. Derivative compounds from levoglucosan and furfural were also identified in these bio-oils, which indicated ash had a significant influence in this low-sugar quantification. Phenolics were formed in lower proportion than in slow pyrolysis, but some bio-oils from fast pyrolysis contained up to 19% phenolics. The high levels of phenolics obtained from both slow- and fast pyrolysis suggests that ash enhances lignin decomposition by reducing the activation energies for lignin conversion.

Evaluation of microwave pyrolysis with digestate resulted in different outcome than was expected. Despite several studies about positive results in microwave pyrolysis to form more primary compounds from lignocellulose, dry digestate generated very low levels of levoglucosan and furfural in the bio-oil. Experiments performed with dry and wet digestate showed differences between bio-oils. Larger amounts of aldehydes, ketones, phenolics and even some traces of levoglucosan and furfural were detected when wet biomass was used with lower power input. A highlight of this comparison is that less acetic acid was generated when there was higher moisture levels in the biomass, leading to more primary pyrolysis products in the bio-oil and less evidence of secondary decomposition. Even so, ash had a negative effect on bio-oil from both biomasses. It seems that primary compounds from cellulose and hemicellulose decomposition could have been present in higher concentration, yet due to the heating mechanism of microwaves and the presence of ash these compounds underwent further decomposition. Additionally, the high levels of lignin decomposition observed with slow- and fast pyrolysis of digestate were also observed during microwave pyrolysis. To better understand how the amount of ash impacts on primary lignocellulose derivatives the ash composition of a representative sample should be determined before each experiment, and this is a key recommendation for future work.

Although digestate was one of the main targets to study in this research, the pre-AD crop was also analysed to understand more about pyrolysis behaviour of this waste and to assess whether there are advantages to by-passing the AD process altogether. This crop waste was used as feedstock in slow and microwave pyrolysis at the same conditions the dry digestate was subjected to. This assessment aimed to evaluate if this waste could generate more high-value compound in bio-oil due to it having a lower ash content. Despite the fact this crop had only 4% wt of ash, it had a negative effect on the bio-oil composition in microwave pyrolysis. Different compounds resulted from digestate were found using dry pre-AD crop, such as glycolaldehyde dimer, acetol, levoglucosan and furfural, chemicals which are highlighted in published data as high-value compounds resulting from lignocellulose decomposition. However, they were in very low concentration. Sugar formation was low, not even reaching 1% of the total bio-oil. Additionally, there was high acid generation, where acetic acid was the most prevalent compound. This indicated that most of the starch derivatives underwent secondary decomposition due to the ash, although it should be noted that the microwave energy input may have been excessive for these sample. Bio-oil yield was typically 17-25% wt, with 40% yield achieved in just a single test. For further analysis, different conditions such as longer time and higher moisture content are recommended to increase yields of products.

Product composition from pre-AD using slow pyrolysis had no similarity to other experiments performed with this material. Biochar yield was similar to slow pyrolysis of digestate, but the water was much less across the experiments. Bio-oil recovery was much higher than any other process/feedstock combination performed in this work. Moreover, bio-oil composition showed a considerable production of large-molecule compounds and primary products from lignocellulose. Sugars for instance, researched higher than 8% yield with levoglucosan as the main compound. The maximum furan yield was around 21%, with furfural detected at 2-4% wt. No acetic acid was detected, which revealed that the distribution of ash in pre-AD crop without pre-treatment did not have a significant or negative effect in bio-oil composition when slow pyrolysis was used.

Based on these findings, it can be concluded that not only ash has a negative influence in bio-oil composition, but pre-treatment of feedstock also has a direct effect on how lignocellulose is decomposed during microwave pyrolysis. Pelletising the biomass led to more acid formation, as it is thought that higher internal temperatures are attained when the biomass is in this form.

This project also considered an evaluation of the scheme of reactions of lignocellulose decomposition to validate if a model could be viable as a tool to implement with digestate conversion into pyrolysis products. The only published scheme consists of just 32 compounds derived from cellulose, hemicellulose and lignin, which is far fewer than the total number of individual compounds that have been detected after pyrolysis. However, this scheme was useful to present outputs in yields of biochar, bio-oil and gas, with some chemical groups of bio-oil, not only considering a variation in temperature but also ash content. The published scheme had to be modified in order to correct an error in the stoichiometric balance due to missing products from lignocellulose decomposition. Although this scheme considered ash as a factor to affect cellulose and hemicellulose derivatives, this was not well-supported because lignin is also impacted by this inorganic material, and most of the assumptions were only based on biomasses that have no more than 4-5% wt ash. By computing the scheme as proposed, ash content in pre-AD and digestate showed no effect on water formation, which is one of the key indicators of secondary reactions during pyrolysis of biomass. The kinetic model was improved by adjusting the impact of ash on nine reactions of the scheme and by displaying profiles of biomass decomposition and pyrolysis product formation through heating rate variation. This modification has led to a reduction in the activation energy of biochar, water and small-molecule compounds, giving rise to easier formation in response to ash content.

VAsh10, as the new kinetic model was called, produces a realistic prediction of pyrolysis product distribution from both digestate and pre-AD crop, a feat which is not achievable with current published models. Although phenolic yield is predicted to be low, which differs substantially from experimental quantification, the predicted sugar yield agrees with experimental data obtained from pyrolysing this waste. The reaction schemes associated with lignin decomposition need to be studied and further developed in order to better estimate yields of phenolics, but also acid formation which can also increase as a result of lignin depolymerisation.

Processing digestate through thermal technologies such as pyrolysis involve different chemical composition of bio-oil and gas due to the amount of ash content. Currently, compounds such as levoglucosan, furfural and some specific phenolics have been identified as high-value lignocellulose derivatives to implement as raw material in chemistry industry. Besides the waste having a large amount of carbohydrate-based biopolymers, high inorganic material in digestate results in lowering primary compounds in final products. Nevertheless, an alternative route has been proposed to increase the use of digestate, not only from crop waste but food waste, even if there are plastics contained within.

This study found that lignin-derivatives can be more stable through the pyrolysis process, even in the presence of high amounts of ash. Cellulose- and hemicellulose-derived products were complex to control under these conditions. Food-waste and crop digestate were analysed to determine residual monosaccharides that the microorganisms did not utilise in the AD process. Food-waste digestate analysis revealed that there is 4 g of sugars in 30 g of sample, and around 45% wt of crop digestate has useful sugar for the AD system for more biogas production; however, they need to be depolymerised in order to be consumed. Thermal treatment of the aqueous medium from AD (90% liquid-10%solid) at low temperature using microwave technology could lead to the depolymerisation of hemicellulose and convert this product into a sugar-rich solution for recirculation that could contain fucose, xylose, arabinose, galactose and mannose. The remaining solid digestate after dewatering could potentially be treated with enzymes to obtain more D-glucose and include a second rich-sugar solution in the system and promote more biogas generation. The final solid waste would consist of high-lignin residue that could yield a phenolic-rich liquid product after pyrolysis.

The high ash content in digestate and the initial crop waste appears to preclude their use as an effective pyrolysis feedstock, no matter which pyrolysis technology route is employed. However, it is shown that other options for modifying the process flowsheet could be viable, generating more biogas and conducting pyrolysis on a more concentrated fraction where the ash content has a less pronounced effect.

APPENDIX A. LIST OF COMPONENTS USED IN MODEL

Name	Nomenclature used	Elemental composition
Cellulose	CELL	$C_6H_{10}O_5$
Activated cellulose	CELLA	$C_6H_{10}O_5$
Hemicellulose	HCE	$C_5H_8O_4$
Activated hemicellulose 1	HCEA1	$C_5H_8O_4$
Activated hemicellulose 2	HCEA2	$C_5H_8O_4$
Lignin	LIG	$C_{11}H_{12}O_4$
Lignin rich in Carbon	LIG-C	$C_{15}H_{14}O_4$
Lignin rich in Hydrogen	LIG-H	$C_{22}H_{28}O_9$
Lignin rich in Oxygen	LIG-O	$C_{20}H_{22}O_{10}$
Lignin 2 rich in C	LIG-CC	$C_{15}H_{14}O_4$
Lignin rich in OH	LIG-OH	$C_{19}H_{22}O_8$
Trapped CO_2	G{CO_2}	CO_2
Trapped CO	G{CO}	CO
Trapped COH_2	G{COH_2}	CH_2O
Trapped H_2	G{H_2}	H_2
Biochar	Biochar	C
Hydroxyacetaldehyde (Acetic acid)	HAA	$C_2H_4O_2$
Glyoxal	GLYOX	$C_2H_2O_2$
Propanal (Acetone)	C_3H_6O	C_3H_6O
Propanedial	$C_3H_4O_2$	$C_3H_4O_2$
5-hydroxymethyl-furfural	HMFU	$C_6H_6O_3$
Levoglucosan	LVG	$C_6H_{10}O_5$
Xylose monomer	XYL	$C_5H_8O_4$
Paracoumaryl alcohol	pCOUMARYL	$C_9H_{10}O_2$
Phenol	PHENOL	C_6H_6O
Sinapaldehyde	FE2MACR	$C_{11}H_{12}O_4$
Hydrogen	H_2	H_2
Carbon monoxide	CO	CO
Carbon dioxide	CO_2	CO_2
Methane	CH_4	CH_4
Formaldehyde	CH_2O	CH_2O
Methanol	CH_3OH	CH_4O
Ethylene	C_2H_4	C_2H_4
Acetaldehyde	CH_3CHO	C_2H_4O
Ethanol	ETOH	C_2H_6O
Water vapor	H_2O	H_2O

Table 80. Components used of the model employed for fast pyrolysis of digestate [144].

APPENDIX B. THERMOGRAVIMETRIC ANALYSIS DATA

Batch 1					
Collection:		19-Nov-18	105 ^{o}C		for 24hrs
Porcelain crucibles					
Porcelain crucibles			**1**	**2**	**3**
Crucible weight			139.67	142.59	138.17
Biomass (g)			37.05	33.23	35.87
Weighed dried(g) 24hrs			146.79	148.99	144.97
Dried dry biomass			7.12	6.4	6.8
% Initial moisture			**80.78%**	**80.74%**	**81.04%**
		Mean=	80.86	**SD=**	0.002
TGA-proximate (% wt)					
Run	**Weight (mg)**	**Moisture**	**Volatile matter**	**Fixed carbon**	**Ash**
1	**10.01**	4.569	68.26	18.45	8.74
2	**9.54**	5.271	70.59	18.84	5.30
3	**10.33**	5.151	68.77	19.38	6.71
4	**11.01**	5.257	67.06	19.44	8.25
5	**11.68**	4.959	67.24	19.73	8.07
6	**11.27**	5.19	68	19.96	6.84
Mean=	**10.64**	**5.07**	**68.32**	**19.30**	**7.32**
	SD =	0.3	1.3	0.6	1.3

Table 81. Proximate and Ultimate analysis of batch one of digestate collected used in pyrolysis systems.

Batch 2					
Collection :		29-Nov-18		105 ^{o}C	for 24hrs
Porcelain crucibles					
Porcelain crucibles			**1**	**2**	**3**
Crucibles weight			139.68	142.61	138.2
Biomass (g)			30.81	31.58	31.16
Weighed dried(g) 24hrs			145.35	148.52	143.93
Dried dry biomass			5.67	5.91	5.73
% Initial moisture			**81.60**	**81.29**	**81.61**
		Mean=	81.50	SD=	0.002
TGA-proximate (% wt)					
Run	**Weight (mg)**	**Moisture**	**Volatile matter**	**Fixed Carbon**	**Ash**
1	**10.90**	4.53	67.01	19.69	8.78
2	**11.14**	4.33	66.02	18.98	10.67
3	**10.36**	4.65	66.53	19.7	9.13
4	**11.85**	4.42	67.01	20.09	8.50
5	**11.50**	5.18	67.35	20.12	7.35
6	**11.49**	5.30	67.85	20.41	6.44
Mean=	**11.21**	**4.74**	**66.96**	**19.83**	**8.48**
SD		0.4	0.6	0.5	1.5

Table 82. Proximate and Ultimate analysis of batch two of digestate collected used in pyrolysis systems.

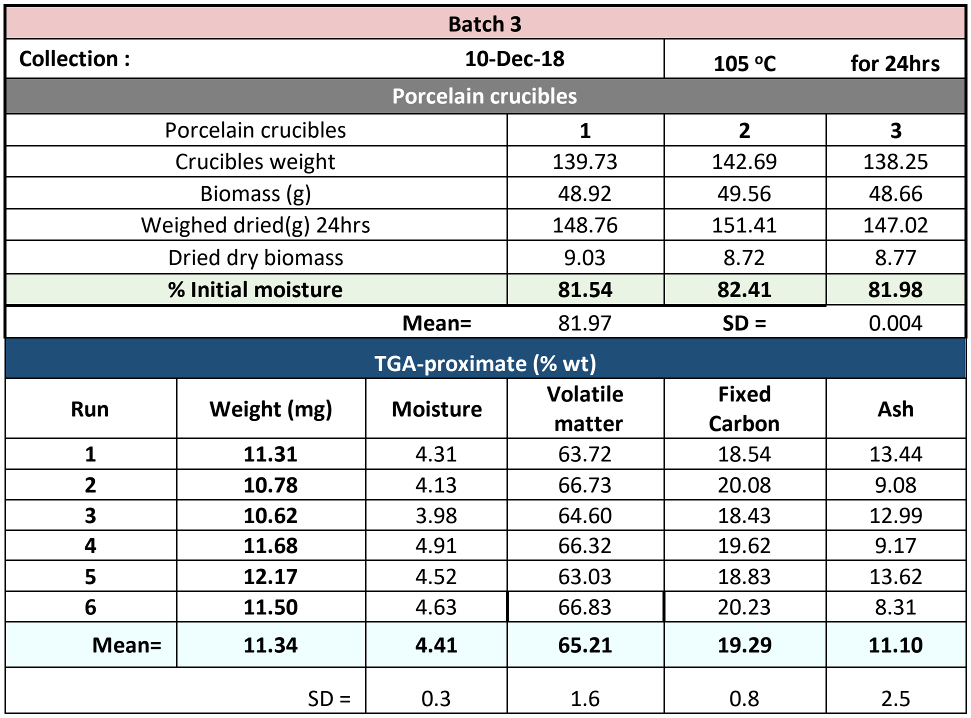

Batch 3			
Collection :	**10-Dec-18**	**105 °C**	**for 24hrs**
Porcelain crucibles			
Porcelain crucibles	**1**	**2**	**3**
Crucibles weight	139.73	142.69	138.25
Biomass (g)	48.92	49.56	48.66
Weighed dried(g) 24hrs	148.76	151.41	147.02
Dried dry biomass	9.03	8.72	8.77
% Initial moisture	**81.54**	**82.41**	**81.98**
Mean=	81.97	**SD =**	0.004

TGA-proximate (% wt)					
Run	**Weight (mg)**	**Moisture**	**Volatile matter**	**Fixed Carbon**	**Ash**
1	**11.31**	4.31	63.72	18.54	13.44
2	**10.78**	4.13	66.73	20.08	9.08
3	**10.62**	3.98	64.60	18.43	12.99
4	**11.68**	4.91	66.32	19.62	9.17
5	**12.17**	4.52	63.03	18.83	13.62
6	**11.50**	4.63	66.83	20.23	8.31
Mean=	**11.34**	**4.41**	**65.21**	**19.29**	**11.10**
	SD =	0.3	1.6	0.8	2.5

Table 83. Proximate and Ultimate analysis of batch three of digestate collected used in pyrolysis systems.

Parameter	19-Nov-18	29-Nov-18	10-Dec-18	20-May-19	3-Jun-19	2-Jul-19	21-Aug-19	9-Sep-19
	Batch 1	**Batch 2**	**Batch 3**	**Batch 4**	**Batch 5**	**Batch 6**	**Batch 7**	**Batch 8**
Initial moisture	80.86 + 0.16	81.50 ± 0.18	81.97 ± 0.43	81.13 ± 0.60	79.65 ± 0.00	78.28 ± 0.01	79.16 ± 0.01	78.77 ± 0.01
Proximate analysis								
Moisture	5.07 + 0.27	4.74 ± 0.41	3.80 ± 1.19	3.80 ± 1.19	4.02 ± 0.17	4.28 ± 0.50	5.12 ± 0.13	3.99 ± 0.30
Volatile matter	68.32 + 1.28	66.96 ± 0.64	65.21 ± 1.64	67.80 ± 0.91	68.51 ± 0.47	67.24 ± 0.59	66.02 ± 1.17	66.08 ± 1.09
Fixed carbon	19.30 + 0.56	19.83 ± 0.50	19.29 ± 0.79	19.02 ± 0.19	19.02 ± 0.19	20.02 ± 0.21	19.26 ± 0.38	19.46 ± 0.29
Ash	7.32 + 1.27	8.48 ± 1.47	11.10 ± 2.49	9.38 ± 0.65	8.43 ± 0.56	8.44 ± 0.84	9.60 ± 1.25	10.48 ± 1.47
Ultimate analysis								
C	44.22 + 0.21	43.86 ± 0.89	44.35 ± 0.66	44.02 ± 0.20	43.84 ± 0.09	43.78 ± 0.12	43.41 ± 0.14	44.20 ± 0.45
H	5.74 + 0.05	5.68 ± 0.13	5.65 ± 0.07	5.85 ± 0.05	5.74 ± 0.00	5.66 ± 0.03	5.88 ± 0.04	5.89 ± 0.02
N	1.52 + 0.13	1.70 ± 0.03	1.77 ± 0.22	2.01 ± 0.02	1.88 ± 0.01	1.99 ± 0.03	1.70 ± 0.04	1.68 ± 0.06
O	48.52 + 0.16	48.76 ± 1.04	48.24 ± 0.51	48.12 ± 0.17	48.54 ± 0.08	48.56 ± 0.14	49.02 ± 0.21	49.02 ± 0.49

Data is the mean ± SD, % weight basis, with at least three replicate measurements.
* Oxygen was obtained by difference

Table 84. Summary of proximate and ultimate analysis of every batch of digestate collected during the 4 seasons to evaluate their variation.

APPENDIX C. LIGNIN COMPOSITION OF SEVERAL BIOMASSES

Biomass	C (wt)	H (wt)	O (wt)	LIG-C		LIG-H		LIG-O	
				wt	mol	wt	mol	wt	mol
Pseudotsuga menziesii	0.648	0.058	0.294	0.6366	0.7447	0.1988	0.1376	0.1646	0.1177
Picea sylvestris	0.64	0.06	0.3	0.5118	0.6372	0.3624	0.267	0.1258	0.0958
Thuja plicata	0.638	0.061	0.301	0.4709	0.5993	0.4377	0.3296	0.0914	0.0711
Picea mariana	0.637	0.063	0.3	0.4201	0.5504	0.5797	0.4494	02	02
Larix occidentalis	0.637	0.061	0.302	0.4610	0.5896	0.4399	0.3329	0.0991	0.0775
Tsuga heterophylla	0.634	0.063	0.303	0.3908	0.5198	0.5855	0.4609	0.0237	0.0193
Picea abies	0.634	0.06	0.306	0.4517	0.5794	0.3762	0.2856	0.1721	0.135
Arachis hypogaea	0.631	0.057	0.312	0.4835	0.6075	0.1711	0.1272	0.3454	0.2653
Metasequoia glyptostroboides	0.629	0.059	0.312	0.4227	0.5494	0.3175	0.2442	0.2597	0.2064
Dalbergia melanoxylon	0.627	0.058	0.315	0.4234	0.5491	0.2520	0.1934	0.3246	0.2574
Dalbergia granadillo	0.625	0.06	0.315	0.3636	0.4881	0.3964	0.3149	0.2400	0.197
Pinus ponderosa	0.625	0.06	0.315	0.3636	0.4881	0.3964	0.3149	0.2400	0.197
Millettia laurentii	0.623	0.057	0.32	0.4044	0.5288	0.1917	0.1483	0.4039	0.3229
Afzelia sp.	0.623	0.056	0.321	0.4247	0.5486	0.1211	0.0926	0.4542	0.3588
Tieghemella heckelii	0.611	0.058	0.331	0.2698	0.3797	0.2904	0.2418	0.4398	0.3785
Manilcara sp.	0.607	0.059	0.334	0.2134	0.3106	0.3676	0.3166	0.4189	0.3728
Entandrophragma cylindricum	0.606	0.058	0.336	0.2233	0.3226	0.3019	0.2581	0.4748	0.4194
Acer macrophyllum	0.604	0.057	0.339	0.2239	0.3228	0.2385	0.2034	0.5376	0.4738
Fagus sylvatica	0.603	0.063	0.334	0.1022	0.16	0.6430	0.5959	0.2549	0.2441
Juglans regia L.	0.604	0.059	0.337	0.1859	0.2749	0.3742	0.3274	0.4399	0.3977
Miscanthus sinensis	0.602	0.058	0.34	0.1866	0.2753	0.3111	0.2716	0.5023	0.4532
Olea sp.	0.601	0.059	0.34	0.1587	0.2384	0.3806	0.3384	0.4607	0.4232
Populus tremuloides	0.6	0.061	0.339	0.1124	0.1743	0.5163	0.4737	0.3713	0.352
Caesaeia paecox	0.6	0.059	0.341	0.1496	0.226	0.3829	0.3422	0.4675	0.4318
Prunus serotina	0.597	0.059	0.344	0.1227	0.1883	0.3893	0.3536	0.4880	0.458
Eucalyptus regnans	0.592	0.063	0.345	0.0059	0.0098	0.6621	0.6522	0.3321	0.338
Liriodendrum tulipifera	0.584	0.058	0.358	0.0266	0.0432	0.3510	0.3378	0.6224	0.619
Liquidambar styraciflua	0.576	0.056	0.368	00	0	0.2358	0.2299	0.7642	0.7701

Table 85. LigniN composition of different biomass analysed Faravelli et al. [147]

APPENDIX D. COMPLEMENTARY DATA - BIO-OIL COMPOSITION

GROUP	SLOW PYROLYSIS													
	Run 1	Run 2	Run 3	Run 4	Run 1	Run 2	Run 3	Run 4	Run 1	Run 2	Run 3	Run 1	Run 2	Run 3
	355°C	355°C	355°C	355°C	425°C	425°C	425°C	425°C	485°C	485°C	485°C	530°C	530°C	530°C
Others	1.75	1.43	1.57	1.39	3.02	2.66	3.37	4.16	3.10	3.06	2.08	2.00	0.87	1.43
Propanoic acid, 2-hydroxy-, methyl ester	0	0	0.05	0	0	0	0	0	0	0	0	0	0	0
Propanoic acid, 2-oxo-, methyl ester	0.18	0.28	0.22	0	0.41	0.26	0.31	0.51	0	0	0	0	0	0
Butanoic acid, 2-oxo-, methyl ester	0.13	0	0	0	0	0	0	0	0	0	0	0	0	0
Pyridine	0.11	0.21	0.22	0.26	0.20	0	0	0.19	0	0	0	0.19	0	0.31
Pyrazine, methyl-	0	0	0.07	0	0	0	0	0	0	0	0	0	0	0.13
Pyrazine, 2,6-dimethyl-	0	0	0.11	0	0	0	0	0	0	0	0	0	0	0
Pyrazine, 2-ethyl-6-methyl-	0.09	0	0	0	0	0	0	0	0	0	0	0	0	0
Acetamide	0.14	0.40	0.29	0.45	0.25	0.20	0.20	0.46	0	0	0	0.21	0	0.47
Naphthalene, 1,2,3,4-tetrahydro-	0.49	0	0	0	0	0	0	0	0	0	0	0	0	0
Naphthalene	0.16	0	0	0	0	0	0	0	0	0	0	0	0	0
4-Pyridinol	0.13	0	0.12	0	0	0	0.19	0.34	0	0	0	0	0	0
Butanoic acid, methyl ester	0	0	0.17	0.33	0.28	0.25	2.21	0.30	0.21	0	0.23	0.25	0.09	0.19
Butanoic acid, propyl ester	0.18	0.36	0.28	0.35	1.30	1.17	0	2.16	1.73	1.26	0.90	1.12	0	0
Benzene, 1,2,3-trimethoxy-5-methyl-	0.15	0.18	0.05	0	0.35	0.42	0.35	0.20	0.58	1.26	0.41	0	0.36	0.18
Hexanamide	0	0	0	0	0	0	0	0	0	0	0	0	0	0
9H-Pyrido[3,4-b]indole, 1-methyl-	0	0	0	0	0	0.17	0	0	0.30	0.29	0.32	0	0.21	0.15
Pyridine, 4-(4-dimethylaminophenyl)-	0	0	0	0	0	0	0	0	0.28	0.24	0.22	0	0	0
Pyridine, 3-(2,4,6-trimethylphenyl)-	0	0	0	0	0.23	0.19	0.11	0	0	0	0	0.22	0.20	0

Table 86. Other compounds identified in bio-oil from slow pyrolysis of digestate at different temperatures.

GROUP	Fast pyrolysis			
	460°C	480°C	520°C	560°C
Others	1.90	1.70	1.85	2.69
Acetic acid, hydroxy-, methyl ester	0	0.09	0	0
Propanoic acid, 2-oxo-, methyl ester	0.55	1.06	0.74	1.09
Pyridine	0	0.16	0.15	0.29
Pyrazine, 2,6-dimethyl-	0	0.10	0	0
Methyl propionate	0	0	0.24	0
Acetamide	0.22	0	0.48	0.49
Methyl 4-hydroxybutanoate	0	0.17	0	0
Indole	0	0	0	0.30
1H-Imidazole, 2,4-dimethyl-	0	0	0	0.22
2-Hydroxy-3-methoxybenzyl alcohol, di(methyl) ether	0.33	0	0	0
Benzene, 1,2,3-trimethoxy-5-methyl-	0	0	0.26	0.19
Hexanamide	0.57	0	0	0
9H-Pyrido[3,4-b]indole, 1-methyl-	0.23	0.13	0.24	0.30

Table 87. Other compounds identified in bio-oil from fast pyrolysis of digestate at different temperatures.

GROUP	Microwave pyrolysis -Digestate									
	1.27 kJ/g	1.88 kJ/g	3.47 kJ/g	3.99 kJ/g	4.07 kJ/g	4.07 kJ/g	4.65 kJ/g	4.75 kJ/g	5.08 kJ/g	6.85 kJ/g
Others	0.63	0.62	0.11	0.93	0.64	0.50	0.13	0.67	0.23	1.08
Acetic acid, hydroxy-, methyl ester	0.04	0	0	0	0	0.06	0	0	0.03	0
Propanoic acid, 2-oxo-, methyl ester	0.02	0	0	0	0	0	0.04	0.04	0.02	0
Pyridine	0.09	0.10	0.01	0.24	0.19	0.21	0.09	0.05	0.05	0.05
Pyrazine, methyl-	0	0	0	0	0	0	0	0	0.01	0
2,2-Dimethoxypropionamide	0	0	0	0	0	0	0	0.03	0	0
Acetamide	0.03	0.05	0.01	0.05	0	0.03	0	0.02	0.03	0.01
4H-1,2,4-Triazol-3-amine, 4-ethyl-	0	0	0	0.11	0	0	0	0	0	0
Butanoic acid, propyl ester	0.15	0.23	0.06	0.26	0.45	0.14	0.06	0.36	0	0.94
Vinyl 2-ethylhexanoate	0	0	0	0	0	0	0	0.02	0	0
Benzene, 1,2,3-trimethoxy-5-methyl-	0.08	0.12	0	0.15	0	0.05	0.07	0.02	0.09	0.07
Hexanamide	0	0	0	0	0	0	0.03	0	0	0
9H-Pyrido[3,4-b]indole, 1-methyl-	0	0	0	0.07	0	0	0	0.03	0	0
9-Octadecenamide, (Z)-	0.22	0.13	0.03	0.07	0	0	0.12	0.09	0	0

Table 88. Other compounds identified in bio-oil from microwave pyrolysis of digestate at different energy input.

GROUPS	MICROWAVE PYROLYSIS- Pre-AD									
	4.07 kJ/g	5.08 kJ/g	4.75 kJ/g	6.85 kJ/g	3.47 kJ/g	4.07 kJ/g	3.99 kJ/g	1.88 kJ/g	4.65 kJ/g	1.27 kJ/g
OTHERS	0.64	0.23	0.67	1.08	0.11	0.50	0.93	0.62	0.13	0.63
Acetic acid, hydroxy-, methyl ester	0	0.03	0	0	0	0.06	0	0	0	0.04
Propanoic acid, 2-oxo-, methyl ester	0	0.02	0.04	0	0	0	0	0	0.04	0.02
Pyridine	0.19	0.05	0.05	0.05	0.01	0.21	0.24	0.10	0.09	0.09
Pyrazine, methyl-	0	0.01	0	0	0	0	0	0	0	0
2,2-Dimethoxypropionamide	0	0	0.03	0	0	0	0	0	0	0
Acetamide	0	0.03	0.02	0.01	0.01	0.03	0.05	0.05	0	0.03
Naphthalene, 1,2,3,4-tetrahydro-	0	0	0	0	0	0	0	0	0	0
Naphthalene	0	0	0	0	0	0	0	0	0	0
4H-1,2,4-Triazol-3-amine, 4-ethyl-	0	0	0	0	0	0	0.11	0	0	0
Butanoic acid, propyl ester	0.45	0	0.36	0.94	0.06	0.14	0.26	0.23	0.06	0.15
Vinyl 2-ethylhexanoate	0	0	0.02	0	0	0	0	0	0	0
Benzene, 1,2,3-trimethoxy-5-methyl-	0	0.09	0.02	0.07	0	0.05	0.15	0.12	0.07	0.08
Hexanamide	0	0	0	0	0	0	0	0	0.03	0
9H-Pyrido[3,4-b]indole, 1-methyl-	0	0	0.03	0	0	0	0.07	0	0	0
9-Octadecenamide, (Z)-	0	0	0.09	0	0.03	0	0.07	0.13	0.12	0.22

Table 89. Other compounds identified in bio-oil from microwave pyrolysis of pre-AD crop at different energy input.

GROUPS	Slow 425°C	Fast 460°C	Microwave 1.88 kJ/g	Slow 530°C	Fast 560°C	Microwave 3.99 kJ/g
Acids	8.2	6.2	4.7	8.3	6.6	7.9
Acetic acid	7.52	5.70	4.49	7.61	6.07	7.43
Propanoic acid	0.73	0.50	0.21	0.68	0.57	0.50
Aldehydes & ketones	3.06	4.03	5.95	3.49	4.41	5.19
2-Propanone, 1-hydroxy-/Acetol	0	0	3.18	0	0	2.71
Acetoin	0	0	0.09	0	0	0
1-Hydroxy-2-butanone	0.08	0	0.48	0	0	0.61
2-Cyclopenten-1-one	0.15	0.18	0.66	0.27	0	0.58
2-Propanone, 1-(acetyloxy)-	0.36	0.34	0.26	0.46	0.30	0.27
2-Cyclopenten-1-one, 2-methyl-	0.11	0.36	0.23	0.32	0.56	0.18
2-Cyclopenten-1-one, 2-hydroxy-	0	0	0.02	0	0	0
Cyclohexanone, 4,4-dimethoxy-	0.58	0	0	0	0	0
2-Cyclopenten-1-one, 3-methyl-	0	0.71	0.19	0	1.00	0
1,2-Cyclopentanedione, 3-methyl-	0.84	0	0.61	1.53	1.77	0.58
2-Cyclopenten-1-one, 2-hydroxy-3-methyl-	0	1.76	0	0	0	0
2-Cyclopenten-1-one, 2-hydroxy-3,4-dimethyl-	0	0	0.03	0	0	0
1,3-Cyclopentanedione, 2,4-dimethyl-	0	0.18	0	0	0.24	0
Cyclohexanone, 4-ethyl-	0.14	0	0	0	0	0.04
2-Cyclopenten-1-one, 3-ethyl-	0	0	0	0	0.25	0
2-Cyclopenten-1-one, 3-ethyl-2-hydroxy-	0.36	0.49	0.16	0.51	0.29	0.18
4-Hexen-3-one, 4,5-dimethyl-	0.16	0	0.04	0.18	0	0
Butanal, 3-hydroxy-	0.14	0	0	0	0	0
Butanal, 2-ethyl-	0	0	0	0.22	0	0
2-Hydroxy-3-propyl-2-cyclopenten-1-one	0.07	0	0	0	0	0
3-Decanone	0.08	0	0	0	0	0
Alcohols	2.33	0.17	0	0.0	0.43	0
1,2-Ethanediol	0	0.17	0	0	0.43	0
1,2-Butanediol	0.09	0	0	0	0	0
Cyclohexanol, 4-methyl-, cis-	1.03	0	0	0	0	0
Cyclohexanol, 4-methyl-	0.98	0	0	0	0	0
3-Hexanol, 5-methyl-	0.08	0	0	0	0	0
1-Octanol, 2-butyl-	0.16	0	0	0	0	0
Furans	5.99	3.46	2.44	6.54	6.31	3.51
Furfural	0	0	0	0	0	0
Furan, 3-methyl-	0	0	0	0	0.24	0
2-Furanmethanol	0.70	0.38	0.51	0.51	0.40	0.87
Ethanone, 1-(2-furanyl)-	0.20	0	0.03	0	0	0.09
Butyrolactone	1.16	0	0.19	0.98	0	0.53
2-Furanmethanol, tetrahydro-	0.66	0	0.08	0.42	0	0.17
2(5H)-Furanone	0	0	0.04	0	0	0
2-Furanone, 2,5-dihydro-3,5-dimethyl	0	0	0	0	0	0.03
2-Hydroxy-gamma-butyrolactone	0	0	0.03	0.12	0	0
Benzofuran, 2,3-dihydro-	2.97	2.86	1.47	4.19	5.48	1.74
5-Hydroxymethyldihydrofuran-2-one	0.30	0.22	0.07	0.32	0.18	0.08
Sugar	0.48	1.28	0.02	0.53	1.86	0.10
1,4:3,6-Dianhydro-.alpha.-d-glucopyranose	0.25	0.16	0.02	0.18	0.31	0.02
DL-Xylose	0.23	0.34	0	0.35	0.36	0.08
d-Mannose	0	0.24	0	0	0.35	0
β.-D-Glucopyranose, 1,6-anhydro-/LVG	0	0.54	0	0	0.84	0

Table 90. Bio-oil comparison between the three pyrolysis technologies from digestate. Proportions of chemical groups are presented in weight basis % of the total bio-oil of one experiment at certain conditions: *temperature, or energy input*.

GROUPS	Slow 425°C	Fast 460°C	Microwave 1.88 kJ/g	Slow 530°C	Fast 560°C	Microwave 3.99 kJ/g
Phenolics	18.12	19.00	6.85	21.94	17.82	8.13
Phenol	1.77	1.68	0.71	2.40	4.03	0.63
Phenol, 2-methoxy-	5.30	2.90	1.49	5.26	1.78	1.74
Phenol, 2-methyl-	0.26	0.54	0.17	0.59	1.03	0.10
Benzene, 1-ethenyl-4-methoxy-	0	0	0	0	0	0
Phenol, 2,5-dimethyl-	0	0	0	0	0.15	0
p-Cresol	0.45	0.90	0.16	0.87	0.95	0.04
Phenol, 3-methyl-	0	0	0	0	0	0.08
Creosol	1.75	0.86	0.52	1.54	0.49	0.44
Phenol, 3,5-dimethyl-	0	0	0.04	0	0.48	0
Phenol, 2,3-dimethyl-	0	0.32	0	0	0.12	0
Phenol, 4-ethyl-	0.61	2.21	0.34	0.86	2.79	0.37
Phenol, 4-ethyl-2-methoxy-	0	1.15	0.58	0	0.43	1.12
Phenol, 4-ethyl-3-methyl-	0	0.13	0	0	0.24	0
Phenol, 2-ethyl-5-methyl-	0	0	0	0.37	0	0
2-Methoxy-4-vinylphenol	1.64	1.58	0.90	2.24	0.88	1.29
Eugenol	0	0.21	0	0	0.30	0
Phenol, 2,6-dimethoxy- / Syringol	4.35	3.01	0.98	5.63	0.98	1.21
Phenol, 4-ethyl-2-methoxy-	0	0	0	0	0.62	0
2-Hydroxy-3-methoxybenzyl alcohol, di(methyl) ether	0	0	0	0	0.45	0
Phenol, 2-methoxy-4-(1-propenyl)-/Isoeugenol	0.15	0.24	0	0	0	0.02
Phenol, 4-(2-propenyl)-	0	0.16	0	0	0.41	0
trans-Isoeugenol	0.39	0.84	0.16	0.53	0.46	0.17
3,5-Dimethoxy-4-hydroxytoluene	0.48	0.52	0.15	0.52	0.27	0.17
Ethanone, 1-(2-hydroxy-4-methoxyphenyl)-	0	0.10	0	0	0	0.03
Ethanone, 1-(3,4-dimethoxyphenyl)-	0	0.31	0	0	0.23	0
3',5'-Dimethoxyacetophenone	0	0	0.28	0.18	0	0
2-Propanone, 1-(4-hydroxy-3-methoxyphenyl)-	0.29	0.25	0.10	0.32	0	0.08
Phenol, 2,6-dimethoxy-4-(2-propenyl)-	0	0	0	0	0.19	0.19
Phenol, 4-(1-methyl-1-phenylethyl)-	0	0.23	0	0	0.18	0.12
Methyl 3-(4-hydroxy-3-methoxyphenyl)propanoate	0.17	0	0	0.17	0	0.05
(E)-2,6-Dimethoxy-4-(prop-1-en-1-yl)phenol	0	0.28	0.20	0	0	0
Ethanone, 1-(4-hydroxy-3,5-dimethoxyphenyl)-	0.24	0.25	0.04	0.26	0	0
2-Pentanone, 1-(2,4,6-trihydroxyphenyl)	0.28	0.14	0.04	0.20	0.16	0.23
others	2.90	1.90	0.62	1.92	2.69	0.04
Propanoic acid, 2-oxo-, methyl ester	0.40	0.55	0	0	1.09	0.04
Butanoic acid, 2-oxo-, methyl ester	0	0	0	0	0	0.93
Pyridine	0.19	0	0.10	0.18	0.29	0
Acetamide	0.24	0.22	0.05	0.21	0.49	0
Butanoic acid, methyl ester	0.27	0	0	0.24	0	0.24
Butanoic acid, propyl ester	1.25	0	0.23	1.08	0	0.05
Indole	0	0	0	0	0.30	0.11
1H-Imidazole, 2,4-dimethyl-	0	0	0	0	0.22	0
2-Hydroxy-3-methoxybenzyl alcohol, di(methyl) ether	0	0.33	0	0	0	0.26
Benzene, 1,2,3-trimethoxy-5-methyl-	0.34	0	0.12	0	0	0
Hexanamide	0	0.57	0	0	0	0
9H-Pyrido[3,4-b]indole, 1-methyl-	0	0.23	0	0	0.30	0
Pyridine, 3-(2,4,6-trimethylphenyl)-	0.22	0	0	0.22	0	0.15
9-Octadecenamide, (Z)-	0	0	0.13	0	0	0

Table 91. Bio-oil comparison between the three pyrolysis technologies from digestate. Proportions of chemical groups are presented in weight basis % of the total bio-oil of one experiment at certain conditions: *temperature, or energy input* (Cont.)

REFERENCES

1. Li, Y., Y. Chen, and J. Wu, *Enhancement of methane production in anaerobic digestion process: A review.* Applied Energy, 2019. 240: p. 120-137.
2. DECC, *Anaerobic Digestion Strategy And Action Plan: A Commitment To Increasing Energy From Waste Through Anaerobic Digestion*, F.a.R.A.D. Department for Environment, Department of Energy and Climate Change (DECC), Editor. 2011: London.
3. USDA, *Biogas Opportunities Roadmap*. 2014, U.S. Department of Agriculture, U.S. Environmental Protection Agency, U.S. Department of Energy. p. 28.
4. Bhada-Tata, D.H.P., *What a Waste. A Global Review of Solid Waste Management*, U.d. series, Editor. 2012, The World Bank: Washington, DC. p. 116.
5. Zhao, Q. and Y. Liu, *Is anaerobic digestion a reliable barrier for deactivation of pathogens in biosludge?* The Science of the total environment, 2019. 668: p. 893-902.
6. Sun, W., et al., *Mechanism and Effect of Temperature on Variations in Antibiotic Resistance Genes during Anaerobic Digestion of Dairy Manure.* Sci Rep, 2016. 6: p. 30237.
7. WRAP, *Driving Innovation in AD Optimisation – Uses for Digestate*. 2012, Wrap: Banbury, Oxon. p. 50.
8. WRAP, *Enhancement and treatment of digestates from anaerobic digestion*. 2012: WRAP. p. 122.
9. Mir, M.A., et al., *Design considerations and operational performance of anaerobic digester: A review.* Cogent Engineering, 2016. 3(1).
10. NNFCC, T.N.N.-F.C.C. *The Official Information Portal on Anaerobic Digestion*. 2016 [cited 2016; Available from: http://www.biogas-info.co.uk/about/digestate/.
11. GMI, G.M.I., *Successful Applications of Anaerobic Digestion from Across the World*. 2013, Global Methane Initiative. p. 24.
12. GMI, G.M.I., *A Global Perspective of Anaerobic Digestion Policies and Incentives*. 2014, Global Methane Initiative. p. 24.
13. Anton Fagerström, et al., *The role of Anaerobic Digestion and Biogas in the Circular Economy*, in *IEA Bioenergy*. 2018, IEA Bioenergy.
14. Pat Howes, et al., *UK and Global bioenergy resources and prices*, D.o.E.a.C.C. (DECC), Editor. 2011: Didcot.
15. Bates, J., *Biomass Feedstock Availability*. 2017, Department for Business, Energy & Industrial Strategy (BEIS). p. 20.
16. BEIS, *Biomass Policy Statement*, in *BIomass strategy*. 2021, Department for Business, Energy & Industrial Strategy (BEIS): London. p. 45.
17. Commision, E. *Closing the loop - An EU action plan for the Circular Economy*. 2015; Available from: https://eur-lex.europa.eu/legal-content/EN/TXT/?uri=CELEX:52015DC0614.
18. Jahirul, M., et al., *Biofuels Production through Biomass Pyrolysis —A Technological Review.* Energies, 2012. 5(12): p. 4952-5001.
19. Rasul, M. and M. Jahirul, *Recent developments in biomass pyrolysis for bio-fuel production: Its potential for commercial applications*. 2012: Rockhampton, Queensland, Australia.
20. Roy, P. and G. Dias, *Prospects for pyrolysis technologies in the bioenergy sector: A review.* Renewable and Sustainable Energy Reviews, 2017. 77: p. 59-69.
21. Monlau, F., et al., *A new concept for enhancing energy recovery from agricultural residues by coupling anaerobic digestion and pyrolysis process.* Applied Energy, 2015. 148: p. 32-38.
22. Opatokun, S.A., V. Strezov, and T. Kan, *Product based evaluation of pyrolysis of food waste and its digestate.* Energy, 2015. 92: p. 349-354.

23. Beneroso, D., et al., *Microwave pyrolysis of biomass for bio-oil production: Scalable processing concepts.* Chemical Engineering Journal, 2017. 316: p. 481-498.

24. Huang, Y.F., et al., *Total recovery of resources and energy from rice straw using microwave-induced pyrolysis.* Bioresour Technol, 2008. 99(17): p. 8252-8.

25. Robinson, J., et al., *Microwave Pyrolysis of Biomass: Control of Process Parameters for High Pyrolysis Oil Yields and Enhanced Oil Quality.* Energy & Fuels, 2015. 29(3): p. 1701-1709.

26. Tekin, K., S. Karagöz, and S. Bektaş, *A review of hydrothermal biomass processing.* Renewable and Sustainable Energy Reviews, 2014. 40: p. 673-687.

27. Berge, N.D., et al., *Hydrothermal Carbonization of Municipal Waste Streams.* Environmental Science & Technology, 2011. 45(13): p. 5696-5703.

28. Elliott, D.C., et al., *Hydrothermal liquefaction of biomass: Developments from batch to continuous process.* Bioresource Technology, 2015. 178: p. 147-156.

29. Nations, U. *The 17 Sustainable Development Goals (SDGs)*. 2015; Available from: https://sdgs.un.org/goals.

30. Department for Environment, F.a.R.A., *UK statistics on waste*, F.a.R.A. Department for Environment, Editor. 2021, Goverment Statistical Service.

31. European_Commision. *A new Circular Economy Action Plan. For a cleaner and more competitive Europe*. 2020; Available from: https://eur-lex.europa.eu/legal-content/EN/TXT/?qid=1583933814386&uri=COM:2020:98:FIN.

32. Liebetrau, J., Kornatz, P., Baier, U., Wall, D., Murphy, J.D., *Integration of Biogas Systems into the Energy System: Technical aspects of flexible plant operation*, in *IEA Bioenergy Task 37*. 2020.

33. Koszel, M. and E. Lorencowicz, *Agricultural Use of Biogas Digestate as a Replacement Fertilizers.* Agriculture and Agricultural Science Procedia, 2015. 7: p. 119-124.

34. Ronga, D., et al., *Using Digestate and Biochar as Fertilizers to Improve Processing Tomato Production Sustainability.* Agronomy, 2020. 10(1).

35. Kataki, S., S. Hazarika, and D.C. Baruah, *Assessment of by-products of bioenergy systems (anaerobic digestion and gasification) as potential crop nutrient.* Waste Manag, 2017. 59: p. 102-117.

36. Department for Environment, F.a.R.A., *Code of Good Agricultural Practice (COGAP) for Reducing Ammonia Emissions*, F.a.R.A. Department for Environment, Editor. 2018, Defra.

37. (EIA), T.U.S.E.I.A. *Energy Explained*. 2021; Available from: https://www.eia.gov/energyexplained/biomass/.

38. Williams, C.L., A. Dahiya, and P. Porter, *Introduction to Bioenergy.* 2015: p. 5-36.

39. Global, S. *Low carbon fuels*. 2021; Available from: https://www.shell.com/energy-and-innovation/new-energies/low-carbon-fuels.html.

40. Bajpai, P., *Structure of Lignocellulosic Biomass*, in *Pretreatment of Lignocellulosic Biomass for Biofuel Production*. 2016, Springer Singapore. p. 7-12.

41. Chen, H., *Chemical Composition and Structure of Natural Lignocellulose*, in *Biotechnology of Lignocellulose. Theory and Practice*. 2014, Springer Netherlands. p. 25-71.

42. Wenger, J., V. Haas, and T. Stern, *Why Can We Make Anything from Lignin Except Money? Towards a Broader Economic Perspective in Lignin Research.* Current Forestry Reports, 2020. 6(4): p. 294-308.

43. Shen, D.K. and S. Gu, *The mechanism for thermal decomposition of cellulose and its main products.* Bioresour Technol, 2009. 100(24): p. 6496-504.

44. Zadeh, Z.E., et al., *Recent Insights into Lignocellulosic Biomass Pyrolysis: A Critical Review on Pretreatment, Characterization, and Products Upgrading.* Processes, 2020. 8(7).

45. Mohan, D., C.U. Pittman, and P.H. Steele, *Pyrolysis of Wood/Biomass for Bio-oil: A Critical Review.* Energy & Fuels, 2006. 20(3): p. 848-889.

46. Nan, L., G. Best, and C. Coelho De Carvalho Neto. *7. The research progress of biomass pyrolysis processes*. Integrated energy systems in China - The cold Northeastern region experience 1994 June 7th 2016]; Available from: http://www.fao.org/3/a-t4470e/t4470e0a.htm#7. the research progress of biomass pyrolysis processes.

47. WRAP, *The case for the PYREG slow pyrolysis process in improving the efficiency and profitability of Anaerobic Digestion plants in the UK*. 2012, WRAP.

48. Peters, J.F., D. Iribarren, and J. Dufour, *Biomass Pyrolysis for Biochar or Energy Applications? A Life Cycle Assessment.* Environmental Science & Technology, 2015. 49(8): p. 5195-5202.

49. Dunnigan, L., et al., *Emission characteristics of a pyrolysis-combustion system for the co-production of biochar and bioenergy from agricultural wastes.* Waste Manag, 2018. 77: p. 59-66.

50. Bridgwater, A.V., *Review of fast pyrolysis of biomass and product upgrading.* Biomass and Bioenergy, 2012. 38: p. 68-94.

51. Shen, Q., et al., *Rapid Pyrolysis of Pulverized Biomass at a High Temperature: The Effect of Particle Size on Char Yield, Retentions of Alkali and Alkaline Earth Metallic Species, and Char Particle Shape.* Energy & Fuels, 2020. 34(6): p. 7140-7148.

52. Zhang, Y., et al., *Chapter 14 - Gasification Technologies and Their Energy Potentials*, in *Sustainable Resource Recovery and Zero Waste Approaches*, M.J. Taherzadeh, et al., Editors. 2019, Elsevier. p. 193-206.

53. Eke, J., J.A. Onwudili, and A.V. Bridgwater, *Influence of Moisture Contents on the Fast Pyrolysis of Trommel Fines in a Bubbling Fluidized Bed Reactor.* Waste and Biomass Valorization, 2020. 11(7): p. 3711-3722.

54. Westerhof, R.J.M., et al., *Controlling the Water Content of Biomass Fast Pyrolysis Oil.* Industrial & Engineering Chemistry Research, 2007. 46(26): p. 9238-9247.

55. Ringer, M., V. Putsche, and J. Scahill, *Large-Scale Pyrolysis Oil: A Technology Assessment and Economic Analysis*. 2006, National Renewable Energy Laboratory: Battelle.

56. Kern, S., et al., *Rotary kiln pyrolysis of straw and fermentation residues in a 3MW pilot plant – Influence of pyrolysis temperature on pyrolysis product performance.* Journal of Analytical and Applied Pyrolysis, 2012. 97: p. 1-10.

57. Li, A.M., et al., *Pyrolysis of solid waste in a rotary kiln: influence of final pyrolysis temperature on the pyrolysis products.* Journal of Analytical and Applied Pyrolysis, 1999. 50(2): p. 149-162.

58. Scott, D.S. and J. Piskorz, *The continuous flash pyrolysis of biomass.* The Canadian Journal of Chemical Engineering, 1984. 62(3): p. 404-412.

59. Elliott, D.C., et al., *Results of the International Energy Agency Round Robin on Fast Pyrolysis Bio-oil Production.* Energy & Fuels, 2017. 31(5): p. 5111-5119.

60. Zmiewski, A.M., et al., *Exploring the Products from Pinewood Pyrolysis in Three Different Reactor Systems.* Energy & Fuels, 2015. 29(9): p. 5857-5864.

61. Westerhof, R.J.M., et al., *Effect of Temperature in Fluidized Bed Fast Pyrolysis of Biomass: Oil Quality Assessment in Test Units.* Industrial & Engineering Chemistry Research, 2010. 49(3): p. 1160-1168.

62. Isahak, W.N.R.W., et al., *A review on bio-oil production from biomass by using pyrolysis method.* Renewable and Sustainable Energy Reviews, 2012. 16(8): p. 5910-5923.

63. DeSisto, W.J., et al., *Fast Pyrolysis of Pine Sawdust in a Fluidized-Bed Reactor.* Energy & Fuels, 2010. 24(4): p. 2642-2651.

64. Branca, C., P. Giudicianni, and C. Di Blasi, *GC/MS Characterization of Liquids Generated from Low-Temperature Pyrolysis of Wood.* Industrial & Engineering Chemistry Research, 2003. 42(14): p. 3190-3202.

65. Singh, S., et al., *Microwave assisted coal conversion.* Fuel, 2015. 140: p. 495-501.

66. Miura, M., et al., *Rapid pyrolysis of wood block by microwave heating.* Journal of Analytical and Applied Pyrolysis, 2004. 71(1): p. 187-199.

67. Adam, M., et al., *Microwave fluidized bed for biomass pyrolysis. Part I: Process design.* Biofuels, Bioproducts and Biorefining, 2017. 11(4): p. 601-612.

68. Martín, M.T., et al., *Microwave-assisted pyrolysis of Mediterranean forest biomass waste: Bioproduct characterization.* Journal of Analytical and Applied Pyrolysis, 2017. 127: p. 278-285.

69. Park, W.C., A. Atreya, and H.R. Baum, *Experimental and theoretical investigation of heat and mass transfer processes during wood pyrolysis.* Combustion and Flame, 2010. 157(3): p. 481-494.

70. Kim, J.-S. and G.-G. Choi, *Chapter 11 - Pyrolysis of Lignocellulosic Biomass for Biochemical Production*, in *Waste Biorefinery*, T. Bhaskar, et al., Editors. 2018, Elsevier. p. 323-348.

71. Oasmaa, A., et al., *Historical Review on VTT Fast Pyrolysis Bio-oil Production and Upgrading.* Energy & Fuels, 2021. 35(7): p. 5683-5695.

72. Guo, X., et al., *Pyrolysis characteristics of bio-oil fractions separated by molecular distillation.* Applied Energy, 2010. 87(9): p. 2892-2898.

73. Lindfors, C., et al., *Fractionation of Bio-Oil.* Energy & Fuels, 2014. 28(9): p. 5785-5791.

74. Giudicianni, P., G. Cardone, and R. Ragucci, *Cellulose, hemicellulose and lignin slow steam pyrolysis: Thermal decomposition of biomass components mixtures.* Journal of Analytical and Applied Pyrolysis, 2013. 100: p. 213-222.

75. Shinde, S.H., A. Hengne, and C.V. Rode, *Lignocellulose-derived platform molecules*, in *Biomass, Biofuels, Biochemicals*. 2020. p. 1-31.

76. Kawamoto, H., *Lignin pyrolysis reactions.* Journal of Wood Science, 2017. 63(2): p. 117-132.

77. Zhou, X., et al., *A mechanistic model of fast pyrolysis of hemicellulose.* Energy & Environmental Science, 2018. 11(5): p. 1240-1260.

78. Zhou, X., et al., *A Critical Review on Hemicellulose Pyrolysis.* Energy Technology, 2016. 5(1): p. 52-79.

79. Patwardhan, P.R., R.C. Brown, and B.H. Shanks, *Product distribution from the fast pyrolysis of hemicellulose.* ChemSusChem, 2011. 4(5): p. 636-43.

80. Supriyanto, et al., *Identifying the primary reactions and products of fast pyrolysis of alkali lignin.* Journal of Analytical and Applied Pyrolysis, 2020. 151.

81. Persson, H. and W. Yang, *Catalytic pyrolysis of demineralized lignocellulosic biomass.* Fuel, 2019. 252: p. 200-209.

82. Oasmaa, A., et al., *Fast Pyrolysis Bio-Oils from Wood and Agricultural Residues.* Energy & Fuels, 2010. 24(2): p. 1380-1388.

83. Oasmaa, A., et al., *Controlling the Phase Stability of Biomass Fast Pyrolysis Bio-oils.* Energy & Fuels, 2015. 29(7): p. 4373-4381.

84. Oasmaa, A., J. Korhonen, and E. Kuoppala, *An Approach for Stability Measurement of Wood-Based Fast Pyrolysis Bio-Oils.* Energy & Fuels, 2011. 25(7): p. 3307-3313.

85. Negahdar, L., et al., *Characterization and Comparison of Fast Pyrolysis Bio-oils from Pinewood, Rapeseed Cake, and Wheat Straw Using 13C NMR and Comprehensive GC × GC.* ACS Sustainable Chemistry & Engineering, 2016. 4(9): p. 4974-4985.

86. Auersvald, M., et al., *Influence of biomass type on the composition of bio-oils from ablative fast pyrolysis.* Journal of Analytical and Applied Pyrolysis, 2020. 150.

87. Bardak, S., G. Nemli, and T. Bardak, *The quality comparison of particleboards produced from heartwood and sapwood of European larch.* Maderas. Ciencia y tecnología, 2019. 21.

88. Guo, X., et al., *Properties of Bio-oil from Fast Pyrolysis of Rice Husk.* Chinese Journal of Chemical Engineering, 2011. 19(1): p. 116-121.

89. Alvarez, J., et al., *Bio-oil production from rice husk fast pyrolysis in a conical spouted bed reactor.* Fuel, 2014. 128: p. 162-169.

90. Kostas, E.T., et al., *Microwave pyrolysis of olive pomace for bio-oil and bio-char production.* Chemical Engineering Journal, 2020. 387.

91. Rios-Del Toro, E.E., et al., *Coupling the biochemical and thermochemical biorefinery platforms to enhance energy and product recovery from Agave tequilana bagasse.* Applied Energy, 2021. 299.

92. Liu, X., et al., *Thermal degradation and stability of starch under different processing conditions.* Starch - Stärke, 2013. 65(1-2): p. 48-60.

93. Piglowska, M., et al., *Kinetics and Thermodynamics of Thermal Degradation of Different Starches and Estimation the OH Group and H2O Content on the Surface by TG/DTG-DTA.* Polymers (Basel), 2020. 12(2).

94. Yang, Z., et al., *Preparation and formation mechanism of levoglucosan from starch using a tubular furnace pyrolysis reactor.* Journal of Analytical and Applied Pyrolysis, 2013. 102: p. 83-88.

95. Zong, P., et al., *Pyrolysis behavior and product distributions of biomass six group components: Starch, cellulose, hemicellulose, lignin, protein and oil.* Energy Conversion and Management, 2020. 216.

96. Ranzi, E., et al., *Chemical Kinetics of Biomass Pyrolysis.* Energy & Fuels, 2008. 22(6): p. 4292-4300.

97. Calonaci, M., et al., *Comprehensive Kinetic Modeling Study of Bio-oil Formation from Fast Pyrolysis of Biomass.* Energy & Fuels, 2010. 24(10): p. 5727-5734.

98. Anca-Couce, A., et al., *Kinetic scheme of biomass pyrolysis considering secondary charring reactions.* Energy Conversion and Management, 2014. 87: p. 687-696.

99. Blondeau, J. and H. Jeanmart, *Biomass pyrolysis at high temperatures: Prediction of gaseous species yields from an anisotropic particle.* Biomass and Bioenergy, 2012. 41: p. 107-121.

100. Ranzi, E., P.E.A. Debiagi, and A. Frassoldati, *Mathematical Modeling of Fast Biomass Pyrolysis and Bio-Oil Formation. Note II: Secondary Gas-Phase Reactions and Bio-Oil Formation.* ACS Sustainable Chemistry & Engineering, 2017. 5(4): p. 2882-2896.

101. Neumann, J., et al., *Production and characterization of a new quality pyrolysis oil, char and syngas from digestate – Introducing the thermo-catalytic reforming process.* Journal of Analytical and Applied Pyrolysis, 2015. 113: p. 137-142.

102. Opatokun, S.A., et al., *Characterization of Food Waste and Its Digestate as Feedstock for Thermochemical Processing.* Energy & Fuels, 2016. 30(3): p. 1589-1597.

103. Brownsort, P., *Biomass Pyrolysis Processes: Review of Scope, Control and Variability.* 2009, UK Biochar Research Centre (UKBRC).

104. Garcia-Perez, M., et al., *Methods for Producing Biochar and Advanced Bio-fuels in Washington State. Part 3: Literature Review of Technologies for Product Collection and Refining*. 2012, Washington State University: Pullman, WA. p. 129.

105. Liu, Y., et al., *Catalytically Upgrading Bio-oil via Esterification.* Energy & Fuels, 2015. 29(6): p. 3691-3698.

106. Hubner, T. and J. Mumme, *Integration of pyrolysis and anaerobic digestion--use of aqueous liquor from digestate pyrolysis for biogas production.* Bioresour Technol, 2015. 183: p. 86-92.

107. Torri, C. and D. Fabbri, *Biochar enables anaerobic digestion of aqueous phase from intermediate pyrolysis of biomass.* Bioresour Technol, 2014. 172: p. 335-341.

108. González, R., et al., *Biochar and Energy Production: Valorizing Swine Manure through Coupling Co-Digestion and Pyrolysis.* C — Journal of Carbon Research, 2020. 6(2).

109. BEIS, *Combined Heat and Power– Technologies- Part 2*, in *Low carbon energy*. 2021, Department for Business, Energy & Industrial Strategy (BEIS). p. 88.

110. Ghysels, S., et al., *Integrating anaerobic digestion and slow pyrolysis improves the product portfolio of a cocoa waste biorefinery.* Sustainable Energy & Fuels, 2020. 4(7): p. 3712-3725.

111. Yildiz, G., et al., *Effect of biomass ash in catalytic fast pyrolysis of pine wood.* Applied Catalysis B: Environmental, 2015. 168-169: p. 203-211.

112. Wang, Y., et al., *CuNi@C catalysts with high activity derived from metal–organic frameworks precursor for conversion of furfural to cyclopentanone.* Chemical Engineering Journal, 2016. 299: p. 104-111.

113. Vassilev, S.V., et al., *An overview of the organic and inorganic phase composition of biomass.* Fuel, 2012. 94: p. 1-33.

114. Shafizadeh, F., et al., *Production of levoglucosan and glucose from pyrolysis of cellulosic materials.* Journal of Applied Polymer Science, 1979. 23(12): p. 3525-3539.

115. Piskorz, J., et al., *Pretreatment of wood and cellulose for production of sugars by fast pyrolysis.* Journal of Analytical and Applied Pyrolysis, 1989. 16(2): p. 127-142.

116. Banks, S.W., D.J. Nowakowski, and A.V. Bridgwater, *Impact of Potassium and Phosphorus in Biomass on the Properties of Fast Pyrolysis Bio-oil.* Energy & Fuels, 2016. 30(10): p. 8009-8018.

117. ASTM-International, *ASTM D7348 - 13 Standard Test Methods for Loss on Ignition (LOI) of Solid Combustion Residues*. 2013, ASTM-International: West Conshohocken, PA.

118. Mayoral, M., et al., *Different approaches to proximate analysis by thermogravimetry analysis*. Vol. 370. 2001. 91-97.

119. ASTM-International, *ASTME1755-01 Standard Test Method for Ash in Biomass*. ASTM International: West Conshohocken, PA.

120. Saeman, J.F., et al., *Techniques for the determination of pulp constituents by quantitiative paper chromatography.* Tappi Journal, 1954. 37: p. 336-343.

121. Tester, R.F., J. Karkalas, and X. Qi, *Starch—composition, fine structure and architecture.* Journal of Cereal Science, 2004. 39(2): p. 151-165.

122. Svihus, B., A.K. Uhlen, and O.M. Harstad, *Effect of starch granule structure, associated components and processing on nutritive value of cereal starch: A review.* Animal Feed Science and Technology, 2005. 122(3-4): p. 303-320.

123. Buléon, A., et al., *Starch granules: structure and biosynthesis.* International Journal of Biological Macromolecules, 1998. 23(2): p. 85-112.

124. Cornejo-Ramírez, Y.I., et al., *The structural characteristics of starches and their functional properties.* CyTA - Journal of Food, 2018. 16(1): p. 1003-1017.

125. Greenwood, C.T., *The Thermal Degradation of Starch*, in *Advances in Carbohydrate Chemistry*, M.L. Wolfrom and R.S. Tipson, Editors. 1967, Academic Press. p. 483-515.

126. Pulp, T.A.o.t. and P. Industry, *Acid-soluble Lignin in Wood and Pulp*. 2011: TAPPI.

127. TAPPI, U., *250. Acid-soluble lignin in wood and pulp.* 1991 TAPPI useful methods, 1991.

128. Analysis, A.A.M.o., *TOTAL STARCH ASSAY PROCEDURE*, in *AOAC Method 996.11*

AACC Method 76.13. 2019.

129. Diebold, J.P., *A review of the chemical and physical mechanisms of the storage stability of fast pyrolysis bio-oils*. 1999: United States.

130. Luder, W.F., *Ideal gas definition.* Journal of Chemical Education, 1968. 45(5): p. 351.

131. Lindfors, C., et al., *Standard liquid fuel for industrial boilers from used wood.* Biomass and Bioenergy, 2019. 127.

132. Oasmaa, A. and C. Peacocke, *A Guide to Physical Property Characterisation of Biomassderived Fast Pyrolysis Liquids.* 2001.

133. Kostas, E.T., et al., *Microwave pyrolysis of Laminaria digitata to produce unique seaweed-derived bio-oils.* Biomass and Bioenergy, 2019. 125: p. 41-49.

134. Mott, R. and C. Spooner, *The calorific value of carbon in coal: the Dulong relationship.* Fuel, 1940. 19(226-231): p. 242-251.

135. Muley, P.D., et al., *A critical comparison of pyrolysis of cellulose, lignin, and pine sawdust using an induction heating reactor.* Energy Conversion and Management, 2016. 117: p. 273-280.

136. Scholze, B. and D. Meier, *Characterization of the water-insoluble fraction from pyrolysis oil (pyrolytic lignin). Part I. PY–GC/MS, FTIR, and functional groups.* Journal of Analytical and Applied Pyrolysis, 2001. 60(1): p. 41-54.

137. Yang, H., et al., *Estimation of Enthalpy of Bio-Oil Vapor and Heat Required for Pyrolysis of Biomass.* Energy & Fuels, 2013. 27(5): p. 2675-2686.

138. Brocks, J.J., *Millimeter-scale concentration gradients of hydrocarbons in Archean shales: Live-oil escape or fingerprint of contamination?* Geochimica et Cosmochimica Acta, 2011. 75(11): p. 3196-3213.

139. Brocks, J.J. and J.M. Hope, *Tailing of chromatographic peaks in GC-MS caused by interaction of halogenated solvents with the ion source.* J Chromatogr Sci, 2014. 52(6): p. 471-5.

140. Christensen, E., et al., *Quantification of Semi-Volatile Oxygenated Components of Pyrolysis Bio-Oil by Gas Chromatography/Mass Spectrometry (GC/MS). Laboratory Analytical Procedure (LAP)*. 2016: United States.

141. EPA., U.S., *Method 8270E (SW-846): Semivolatile Organic Compounds by Gas Chromatography/ Mass Spectrometry (GC/MS)*. 2014, EPA: Washington, DC.

142. ASTM-International, *ASTM D95-13(2018) Standard Test Method for Water in Petroleum Products and Bituminous Materials by Distillation*. 2018, ASTM-International: West Conshohocken, PA.

143. ASTM-International, *ASTM D7833-14 Standard Test Method for Determination of Hydrocarbons and Non-Hydrocarbon Gases in Gaseous Mixtures by Gas Chromatography*. ASTM International: West Conshohocken, PA.

144. Ranzi, E., P.E.A. Debiagi, and A. Frassoldati, *Mathematical Modeling of Fast Biomass Pyrolysis and Bio-Oil Formation. Note I: Kinetic Mechanism of Biomass Pyrolysis.* ACS Sustainable Chemistry & Engineering, 2017. 5(4): p. 2867-2881.

145. Diaz Perez, N., *Fast Pyrolysis as a Thermal Treatment for Post-Digested Sludges of Crop Waste to Recover Energy*, in *Faculty of Engineering*. 2016, University of Nottingham: Nottingham, UK. p. 72.

146. Kostas, E.T., et al., *Selection of yeast strains for bioethanol production from UK seaweeds.* J Appl Phycol, 2016. 28: p. 1427-1441.

147. Faravelli, T., et al., *Detailed kinetic modeling of the thermal degradation of lignins.* Biomass and Bioenergy, 2010. 34(3): p. 290-301.

148. Rangarajan, B., *Modeling of waste to energy processes in an engineering environment*, in *Mechanical Engineering*. 2014, Delft University of Technology. p. 63.

149. Ranzi, E., et al., *Kinetic modeling of the thermal degradation and combustion of biomass.* Chemical Engineering Science, 2014. 110: p. 2-12.

150. Vassilev, S.V., et al., *An overview of the chemical composition of biomass.* Fuel, 2010. 89(5): p. 913-933.

151. Houston, P.L., *Chemical Kinetics and Reaction Dynamics*. 2001, Mineola, New York: Dover Publications.

152. Wang, X., et al., *Biomass Pyrolysis in a Fluidized Bed Reactor. Part 2: Experimental Validation of Model Results.* Industrial & Engineering Chemistry Research, 2005. 44(23): p. 8786-8795.

153. Zaini, I.N., et al., *Characterization of pyrolysis products of high-ash excavated-waste and its char gasification reactivity and kinetics under a steam atmosphere.* Waste Manag, 2019. 97: p. 149-163.

154. Miles, T.R., et al., *Alkali deposits found in biomass power plants: A preliminary investigation of their extent and nature. Volume 1*. 1995: United States. p. Medium: ED; Size: 131 p.

155. Tomczyk, A., Z. Sokołowska, and P. Boguta, *Biochar physicochemical properties: pyrolysis temperature and feedstock kind effects.* Reviews in Environmental Science and Bio/Technology, 2020. 19(1): p. 191-215.

156. Demirbas, A., *Effects of temperature and particle size on bio-char yield from pyrolysis of agricultural residues.* Journal of Analytical and Applied Pyrolysis, 2004. 72(2): p. 243-248.

157. Moldoveanu, S.C., *Chapter 9. Analytical pyrolysis of lignins*, in *Techniques and Instrumentation in Analytical Chemistry*, S.C. Moldoveanu, Editor. 1998, Elsevier. p. 327-351.

158. Kim, Y.M., et al., *Investigation into the lignin decomposition mechanism by analysis of the pyrolysis product of Pinus radiata.* Bioresour Technol, 2016. 219: p. 371-377.

159. Shao, S., et al., *Comparison of Catalytic Characteristics of Biomass Derivates with Different Structures Over ZSM-5.* BioEnergy Research, 2013. 6(4): p. 1173-1182.

160. Gancedo, J., L. Faba, and S. Ordóñez, *Benzofuran as deactivation precursor molecule: Improving the stability of acid zeolites in biomass pyrolysis by co-feeding propylene.* Applied Catalysis A: General, 2021. 611.

161. Usino, D.O., et al., *Primary interactions of biomass components during fast pyrolysis.* Journal of Analytical and Applied Pyrolysis, 2021. 159.

162. Yu, Y., Y.W. Chua, and H. Wu, *Characterization of Pyrolytic Sugars in Bio-Oil Produced from Biomass Fast Pyrolysis.* Energy & Fuels, 2016. 30(5): p. 4145-4149.

163. Beneroso, D., et al., *Integrated microwave drying, pyrolysis and gasification for valorisation of organic wastes to syngas.* Fuel, 2014. 132: p. 20-26.

164. Wang, X., et al., *The Influence of Microwave Drying on Biomass Pyrolysis.* Energy & Fuels, 2008. 22(1): p. 67-74.

165. Salema, A.A., et al., *Dielectric properties and microwave heating of oil palm biomass and biochar.* Industrial Crops and Products, 2013. 50: p. 366-374.

166. Robinson, J., et al., *Unravelling the mechanisms of microwave pyrolysis of biomass.* Chemical Engineering Journal, 2022. 430.

167. Lin, F., et al., *Relationships between biomass composition and liquid products formed via pyrolysis.* Frontiers in Energy Research, 2015. 3.

168. Li, C., et al., *Catalytic Transformation of Lignin for the Production of Chemicals and Fuels.* Chem Rev, 2015. 115(21): p. 11559-624.

169. Shen, D.K., et al., *The pyrolytic degradation of wood-derived lignin from pulping process.* Bioresour Technol, 2010. 101(15): p. 6136-46.

170. Liu, C., et al., *Catalytic fast pyrolysis of lignocellulosic biomass.* Chem Soc Rev, 2014. 43(22): p. 7594-623.

171. Pino, N., D. Lopez, and J.F. Espinal, *Thermochemistry and kinetic analysis for the conversion of furfural to valuable added products.* J Mol Model, 2019. 25(1): p. 26.

172. Mariscal, R., et al., *Furfural: a renewable and versatile platform molecule for the synthesis of chemicals and fuels.* Energy & Environmental Science, 2016. 9(4): p. 1144-1189.

173. Cui, Y., W. Wang, and J. Chang, *Study on the Product Characteristics of Pyrolysis Lignin with Calcium Salt Additives.* Materials (Basel), 2019. 12(10).

174. Patwardhan, P.R., R.C. Brown, and B.H. Shanks, *Understanding the fast pyrolysis of lignin.* ChemSusChem, 2011. 4(11): p. 1629-36.

175. Casoni, A.I., et al., *Catalytic conversion of furfural from pyrolysis of sunflower seed hulls for producing bio-based furfuryl alcohol.* Journal of Cleaner Production, 2018. 178: p. 237-246.

176. Bernhard Drosg, et al., *Nutrient Recovery by Biogas Digestate Processing*, in *IEA Bioenergy*. 2015, IEA Bioenergy.

177. Urbanowska, A., et al., *Treatment of Liquid By-Products of Hydrothermal Carbonization (HTC) of Agricultural Digestate Using Membrane Separation.* Energies, 2020. 13(1).

178. Broch, A., et al., *Analysis of Solid and Aqueous Phase Products from Hydrothermal Carbonization of Whole and Lipid-Extracted Algae.* Energies, 2013. 7(1): p. 62-79.

179. Guillossou, R., et al., *Organic micropollutants in a large wastewater treatment plant: What are the benefits of an advanced treatment by activated carbon adsorption in comparison to conventional treatment?* Chemosphere, 2019. 218: p. 1050-1060.

180. Chen, W.-T., et al., *Effect of ash on hydrothermal liquefaction of high-ash content algal biomass.* Algal Research, 2017. 25: p. 297-306.

181. Li, H., et al., *Functional relationship of furfural yields and the hemicellulose-derived sugars in the hydrolysates from corncob by microwave-assisted hydrothermal pretreatment.* Biotechnol Biofuels, 2015. 8: p. 127.

182. Houfani, A.A., et al., *Insights from enzymatic degradation of cellulose and hemicellulose to fermentable sugars– a review.* Biomass and Bioenergy, 2020. 134.

183. Langston James, A., et al., *Oxidoreductive Cellulose Depolymerization by the Enzymes Cellobiose Dehydrogenase and Glycoside Hydrolase 61.* Applied and Environmental Microbiology, 2011. 77(19): p. 7007-7015.

184. Yoo, S.Y., Y.J. Kim, and G. Yoo, *Understanding the role of biochar in mitigating soil water stress in simulated urban roadside soil.* Sci Total Environ, 2020. 738: p. 139798.

185. Lang, Q., et al., *Formation and toxicity of polycyclic aromatic hydrocarbons during CaO assisted hydrothermal carbonization of swine manure.* Waste Manag, 2019. 100: p. 84-90.

186. Weidemann, E., et al., *Influence of pyrolysis temperature and production unit on formation of selected PAHs, oxy-PAHs, N-PACs, PCDDs, and PCDFs in biochar—a screening study.* Environmental Science and Pollution Research, 2018. 25(4): p. 3933-3940.

187. Liu, T., et al., *Distribution and toxicity of polycyclic aromatic hydrocarbons during CaO-assisted hydrothermal carbonization of sewage sludge.* Waste Manag, 2021. 120: p. 616-625.

188. Thompson, K.A., et al., *Environmental Comparison of Biochar and Activated Carbon for Tertiary Wastewater Treatment.* Environ Sci Technol, 2016. 50(20): p. 11253-11262.

189. Tong, Y., B.K. Mayer, and P.J. McNamara, *Adsorption of organic micropollutants to biosolids-derived biochar: estimation of thermodynamic parameters.* Environmental Science: Water Research & Technology, 2019. 5(6): p. 1132-1144.

190. Liu, Z., et al., *Hydrochar and pyrochar for sorption of pollutants in wastewater and exhaust gas: A critical review.* Environ Pollut, 2021. 268(Pt B): p. 115910.

191. Esposito, E., et al., *Simultaneous production of biomethane and food grade CO2 from biogas: an industrial case study.* Energy & Environmental Science, 2019. 12(1): p. 281-289.

192. Adnan, A.I., et al., *Technologies for Biogas Upgrading to Biomethane: A Review.* Bioengineering (Basel), 2019. 6(4).

193. Angelidaki, I., et al., *Biogas upgrading and utilization: Current status and perspectives.* Biotechnology Advances, 2018. 36(2): p. 452-466.

194. Sethupathi, S., et al., *Biochars as Potential Adsorbers of CH4, CO2 and H2S.* Sustainability, 2017. 9(1).

195. Lei, L., et al., *Carbon membranes for CO2 removal: Status and perspectives from materials to processes.* Chemical Engineering Journal, 2020. 401.

196. Cestellos-Blanco, S., et al., *Production of PHB From CO2-Derived Acetate With Minimal Processing Assessed for Space Biomanufacturing.* Front Microbiol, 2021. 12: p. 700010.

197. Wang, J. and Y. Yin, *Fermentative hydrogen production using pretreated microalgal biomass as feedstock.* Microb Cell Fact, 2018. 17(1): p. 22.

198. Fayzrakhmanova, G.M., et al., *A study of the properties of a composite asphalt binder using liquid products of wood fast pyrolysis.* Polymer Science Series D, 2016. 9(2): p. 181-184.

199. Mante, O.D., D.C. Dayton, and M. Soukri, *Production and distillative recovery of valuable lignin-derived products from biocrude.* RSC Advances, 2016. 6(96): p. 94247-94255.